SIMULATIONS ON LÉVY SUBORDINATORS AND LÉVY DRIVEN CONTAGION MODELS

Yan Qu

Department of Statistics

The London School of Economics and Political Science

A thesis submitted for the degree of

Doctor of Philosophy

July 2019

Declaration

I certify that the thesis I have presented for examination for the PhD degree of the London School of Economics and Political Science is solely my own work other than where I have clearly indicated that it is the work of others (in which case the extent of any work carried out jointly by me and any other person is clearly identified in it). The copyright of this thesis rests with the author. Quotation from it is permitted, provided that full acknowledgement is made.This thesis may not be reproduced without my prior written consent. I warrant that this authorisation does not, to the best of my belief, infringe the rights of any third party.

Statement of conjoint work

I confirm that parts of Chapter 3 were adapted into a paper entitled "Exact Simulation of Generalised Vervaat Perpetuities" jointly co-authored with Prof Angelos Dassios and Dr Jia Wei Lim, and is published in *Journal of Applied Probability*.

I confirm that Chapter 5 were adapted into a paper entitled "Efficient Simulation of Lévy driven Point Processes" jointly co-authored with Prof Angelos Dassios and Dr Hongbiao Zhao, and is published in *Advances in Applied Probability*.

Acknowledgments

First and foremost, I would like to thank my supervisor Prof Angelos Dassios. My PhD journey would not have been such pleasant and enjoyable without his support, guidance, patience, and encouragement over the years. His profound insights, enthusiasm and perseverance towards research have always given me momentum to progress. I really appreciate all his contributions of time for numerous discussions to make my work productive and stimulating, and for that I owe him many thanks.

I am grateful to my second supervisor Dr Erik Baurdoux for introducing me to the field of Lévy processes. His important suggestions and advice are invaluable. My thanks also goes to my examiners Prof Kostas Kardaras and Prof Andreas Kyprianou for giving me helpful comments to improve my thesis. I would like to extend my sincerest thanks to Dr Jia Wei Lim and Dr Hongbiao Zhao for many enlightening discussions and helpful suggestions during my PhD studies. I feel privileged and lucky to get the opportunity to work with them together.

I would like to thank the Department of Statistics at London School of Economics and Political Science for providing such a friendly working and teaching environment. Special thanks to my office mates Andy Ho, Haziq Jamil, Pheonix Feng, Luting Li, Filippo Pellegrino, Alice Pignatelli Di Cerchiara, Ragvir Sabharwal, Tayfun Terzi, and Xiaolin Zhu for all the fruitful chats and enjoyable moments we have shared together.

Finally I would like to thank my beloved parents for their unconditional love, support and understanding.

Abstract

Lévy subordinators have become a fundamental component to be used to construct many useful stochastic processes, which have numerous applications in finance, insurance and many other fields. However, as many applications of Lévy based stochastic models use fairly complicated analytical and probabilistic tools, it has been challenging to implement in practice. Hence, simulation-based study becomes more desirable. In this thesis, we deal with exact simulation on Lévy subordinators and Lévy driven stochastic models. In the first part, we focus on developing more efficient exact simulation schemes for Lévy subordinators with existing simulation algorithms in the literature. Besides, we also introduce a new type of Lévy subordinators, i.e. truncated Lévy subordinators. We study the path properties, develop exact simulation algorithms based on marked renewal representations, and provide relevant applications in finance and insurance. The associated results in this part are later used in the sequel. The second part of this thesis proposes a new type of point processes by generalising the classical self-exciting Hawkes processes and doubly stochastic Poisson processes with Lévy driven Ornstein-Uhlenbeck type intensities. These resulting models are analytically tractable, and intrinsically inherit the great flexibility as well as desirable features from the two original processes, including skewness, leptokurtosis, mean-reverting dynamics, and more importantly, the contagion or feedback effects. These newly constructed processes would then substantially enrich continuous-time models tailored for quantifying the contagion of event arrivals in finance, economics, insurance, queueing and many other fields. In turn, we characterise the distributional properties of this new class of point processes and design an exact simulation algorithm to generate sample paths. This is done by applying the exact distributional decomposition technique. We carry out extensive numerical implementations and tests to demonstrate the accuracy and effectiveness of our scheme and give examples of some financial applications to credit portfolio risk to show the applicability and flexibility of our new model.

Contents

Chapter 1

Introduction

Doubly stochastic Poisson processes or *Cox processes* (Cox, 1955, 1972) have now been widely applied as survival or event timing models in many areas. They are more capable than Poisson process to capture event arrivals with complex dynamics structures. However, in reality, except for the impact from external factors, event arrivals may often present contagion, clustering, or feedback effects, such as social media sharing online, trade transactions in market microstructure, defaults in the credit market, jumps in investment returns, and loss claims in insurance businesses to name a few. Das et al. (2007) and Duffie et al. (2009) provided evidence that, Cox models, which are based on conditional independence assumption, can not fully capture credit contagion. The phenomena of contagion became more evident in the credit market during the global financial crisis of *2007-09* and European debt crisis since the end of *2009* (Giesecke et al., 2011). A seminal framework tailored for modelling event contagion is *Hawkes process* (Hawkes, 1971a,b). It is a self-exciting point process where each arrival of events would trigger a simultaneous jump in its own intensity and hence more events follow. Empirical evidence and econometric analysis can be viewed from Bowsher (2007), Large (2007), Crane and Sornette (2008), Errais et al. (2010), Embrechts et al. (2011), Bacry et al. (2013), Aït-Sahalia et al. (2014, 2015) and Azizpour et al. (2018). Recently, it has been extended in the literature by being combined with Cox processes to enrich the model eligibility, in the sense that both internal and external impacts can be facilitated in one single framework, see Brémaud and Massoulié (1996, 2002) and Dassios and Zhao (2011, 2017).

Meanwhile, from a micro perspective, it becomes more apparent that real financial data exhibits deviations from normality with the availability of high-frequency data[1]. Barndorff-Nielsen and Shephard (2001a,b) proposed a new class of stochastic processes, namely *non-Gaussian Ornstein-Uhlenbeck (OU) models*, which have gained extensive popularity for modelling the non-normality

[1] See a pioneering investigation into the high-frequency financial data by Gençay et al. (2001).

presented in finance and economics. They could offer greater flexibility and possess many crucial features, such as skewness, leptokurtosis and mean-reverting dynamics, which are often observed from financial markets[2]. Moreover, this generality does not hinder their analytical tractability. In particular, they become extremely popular for modelling stochastic volatilities, see Barndorff-Nielsen et al. (1998), Barndorff-Nielsen and Shephard (2001a,b, 2002, 2003a,b) and Carr et al. (2003). These stochastic volatility models have further led to other applications such as derivative pricing and risk analysis, see Nicolato and Venardos (2003) and Li and Linetsky (2014). On the other hand, these processes can serve as stochastic intensity models for event arrivals. For instance, they have been used to model irregularly-spaced trade-by-trade intraday data, mortality rates in insurance, and default intensities for credit risk in finance, see Rydberg and Shephard (2000), Centanni and Minozzo (2006), Hainaut and Devolder (2008) and Schoutens and Cariboni (2010). In particular, for credit risk modelling, a mean-reverting OU intensity could be particularly useful to capture business cycle effects on average industrial defaults, as obviously default rates would increase in a recession and decrease in a boom (Elsinger et al., 2006, p.1306). This is similar as the environment of interest rates, so, defaults and the associated losses in the credit market often present a mean-reverting pattern, see detailed analysis and evidence in Giesecke et al. (2011) from a long-term historical perspective. Duffie et al. (2009) also found a mean-reverting frailty that would influence U.S. non-financial defaults. Moreover, empirical evidence shows that, the tails of Gaussian distributions are often too thin to capture risk in the credit market, and fluctuations are often sudden and jump-like, which are driven by unexpected news announcements. The distribution of default rates is highly skewed towards large values (Giesecke et al., 2011, p.236-239). Therefore, macroeconomic shocks powered by a Lévy driven non-Gaussian process rather than a Gaussian one may be more appropriate to capture the dynamic structure of default intensities in reality.

It is then natural for us to put these main streamlines above in the literature together to form a unified and consistent framework. We construct a new large family of Lévy driven point processes, termed *self-exciting jump process with non-Gaussian OU intensity*, or, *Lévy driven contagion process*, see Qu et al. (2019). It is fundamentally powered by a *Lévy subordinator*. More precisely, its stochastic intensity is a positive non-Gaussian process with additional self-exciting jumps. It can be also defined as a *branching process* through the cluster process representation. Accordingly, the resulting models are analytically tractable, and intrinsically inherit the great flexibility as well as the desirable features from the two original processes, including skewness, leptokurtosis, mean-reverting dynamics, and more importantly, the contagion or feedback effects. These newly constructed processes would then substantially enrich continuous-time models tailored for quanti-

[2]See empirical evidences from Poterba and Summers (1988) and Cont (2001).

fying the contagion of event arrivals in finance, economics, insurance, queueing and many other fields.

Simulation plays a crucial role in the implementation, simulation-based statistical inference and empirical studies for new models. For instance, for modelling credit risk in practice, events of extreme losses and defaults are rare, and data are scarce. The key quantities at the center of financial risk management, such as the value at risk of an aggregate loss distribution for a heterogeneous portfolio, are often lack of closed-form formulas. The simulation-based approach then becomes a standard technique. In particular, the *exact simulation* scheme is highly desirable as it has the primary advantage of generating sample paths according to the underlying process law exactly (Broadie and Kaya, 2006; Chen and Huang, 2013), no procedure of truncation or discretisation is required. Moreover, there is no numerical inversion for the cumulative distribution function (CDF) or Laplace (Fourier) transform. We propose a general sampling framework based on *distributional decomposition technique*. The processes can be break into several types of basic components. These components consist of compound Poisson processes and underlying Lévy subordinators, each of which requires an exact simulation scheme in order to simulate the contagion processes.

For the compound Poisson process, it can be simulated either directly, or via an *acceptance-rejection (AR) scheme*. For the underlying Lévy subordinator, there are simulation algorithms available in the literature for some typical specifications of Lévy subordinators. However, the available examples of Lévy subordinators are very limited and there associated simulation algorithms are not always efficient. Therefore, in this thesis, we carry out additional research on simulation of Lévy subordinators. On one hand, we focus on developing more efficient exact simulation schemes for those Lévy subordinators with existing simulation algorithms in the literature. On the other hand, we construct new Lévy subordinators and develop exact simulation algorithms accordingly to expand the family of underlying Lévy subordinators.

The thesis is organised as follows:

Chapter 2: We briefly review the definitions, properties and exact simulation algorithms for typical Lévy subordinators, i.e. *the compound Poisson process, the gamma process, the tempered stable process*. In addition, we develop an alternative exact simulation algorithm for the tempered stable process based on *two-dimensional single rejection* scheme, which is more efficient than all the existing algorithms in the literature.

Chapter 3: We introduce a new type of Lévy subordinators, namely truncated Lévy subordinators. We derive key distributional results, establish a marked renewal representation for this type of processes and develop exact simulation schemes. We also provide several applications of the truncated Lévy subordinators in finance and insurance.

Chapter 4: We focus on the Lévy driven *Ornstein-Uhlenbeck(OU)* processes. We provide the preliminaries, including formal mathematical definitions and introductions for this class of processes. The theoretical results for Laplace transform have been derived. Simulation algorithms have also been provided for future study on self-excited point processes with Lévy driven OU intensities.

Chapter 5: We introduce the Lévy driven contagion processes, derive distributional properties, such as the Laplace transforms of the intensities, the joint Laplace transforms of the intensities and pre-jump intensities, and develop a distributional decomposition scheme to establish exact simulation schemes. Numerical examples and corresponding applications are also presented.

Part I

Exact Simulation on Lévy Subordinators

Chapter 2

Lévy Subordinators

This chapter serves mainly two purposes. First, we give an overview of Lévy subordinators and illustrate several typical Lévy subordinators, i.e. *the compound Poisson process*, *the gamma process*, *the tempered stable process*. Second, we provide exact simulation algorithms to sample these typical Lévy subordinators, which will be used in the sequel. In particular, for the tempered stable process, we develop a more efficient uniformly bounded simulation algorithm in Section 2.4. This method is later used for the implementation of the tempered stable based stochastic model problem. Our scheme is based on *two-dimensional single rejection* (SR). For our two-dimensional SR scheme, its complexity is uniformly bounded over all ranges of parameters. This new algorithm outperforms all existing schemes. In particular, it is much more efficient than the well-known *double rejection* (DR) scheme suggested in Devroye (2009), which is the only algorithm with uniformly bounded complexity that we can find in the current literature. Our algorithms are straightforward to implement, and numerical experiments and tests are conducted to demonstrate the accuracy and efficiency.

2.1 Definitions

Lévy processes have many interesting properties and play an important role in finance and insurance. An overview of Lévy processes and their applications are available in Bertoin (1998); Sato (1999); Kyprianou (2006); Barndorff-Nielsen et al. (2012). Meanwhile, Lévy subordinators, which are real-valued Lévy processes with non-decreasing sample paths, have also been widely used for financial modelling, see Barndorff-Nielsen (1998); Madan et al. (1998); Carr et al. (2003), etc. Let us first establish some common notation and some properties of Lévy processes and Lévy subordinators.

Definition 2.1.1. *A stochastic process* $\{X_t\}_{t\geq 0}$ *such that* $X_0 = 0$ *is called a Lévy process if it processes the following properties:*

1. *Independent increments: for every increasing sequence of times $t_0, ..., t_n$, the random variables X_{t_0}, $X_{t_1} - X_{t_0}$, ..., $X_{t_n} - X_{t_{n-1}}$ are independent.*

2. *Stationary increments: for every $s > 0$, the law of $X_{t+s} - X_t$ does not depend on t.*

The law of a Lévy process is completely identified by its characteristic function, i.e. for all $t \geq 0$,

$$\mathbb{E}\left[e^{\mathrm{i}vX_t}\right] = \exp\left(t\Psi(v)\right), \qquad v \in \mathbb{R},$$

where the characteristic exponent Ψ is of the form

$$\Psi(v) = \mathrm{i}vc - \frac{v^2 b}{2} + \int_{\mathbb{R}} \left[e^{\mathrm{i}vx} - 1 - \mathrm{i}vx\mathbf{1}_{\{|x|<1\}}\right] \nu(x)\mathrm{d}x,$$

with $c \in \mathbb{R}$, $b \in \mathbb{R}^+$ and ν being the Lévy measure on $\mathbb{R}$ satisfying

$$\int_{\mathbb{R}} \min\{1, x^2\}\nu(x)\mathrm{d}x < \infty,$$

which characterizes the size and frequency of the jumps.

Definition 2.1.2. *A Lévy subordinator is a real-valued Lévy process with non-decreasing sample paths. It can be characterised via its Laplace transform, i.e.*

$$\mathbb{E}\left[e^{-vX_t}\right] = \exp\left(-t\Phi(v)\right), \qquad v \in \mathbb{R}^+,$$

where Φ is Laplace exponent of the form

$$\Phi(v) = \int_0^\infty (1 - e^{-vx})\nu(x)\mathrm{d}x,$$

with ν being the Lévy measure that satisfies the following condition

$$\int_0^\infty \min\{1, x\}\nu(x)\mathrm{d}x < \infty.$$

It follows that every subordinator is of bounded variation. When $\int_0^\infty \nu(x)\mathrm{d}x < \infty$, X_t is of finite activity. Otherwise, X_t is an infinite activity process as it has an infinite number of small jumps in finite time interval.

We now illustrate some examples of Lévy subordinators to which we refer throughout the thesis.

2.2 Compound Poisson Process

Let N be a Poisson random variable with parameter $\lambda > 0$ and $\{J_i\}_{i=1,2,\dots}$ be a sequence of independent and identical distributed (i.i.d) random variables with density f. For any $v \in \mathbb{R}^+$, we have

$$\mathbb{E}\left[e^{-v\sum_{i=1}^{N} J_i}\right] = \exp\left(-\lambda \int_0^\infty \left(1 - e^{-vx}\right) f(x)\mathrm{d}x\right).$$

Now let N_t be a Poisson process with intensity $\lambda > 0$, then a compound Poisson process X_t is defined by

$$X_t = \sum_{i=1}^{N_t} J_i, \qquad t > 0.$$

As N_t has stationary independent increments and $\{J_i\}_{i=1,2,\dots}$ are i.i.d random variables, it is clear that the increments of X_t are stationary and independent. And right-continuity and left limits of the Poisson process N_t also ensure right-continuity and left limits of the compound Poisson process. Hence, compound Poisson processes are indeed Lévy processes. The Laplace transform of the compound Poisson process X_t is given as

$$\mathbb{E}\left[e^{-vX_t}\right] = \exp\left(-\lambda t \int_0^\infty \left(1 - e^{-vx}\right) f(x)\mathrm{d}x\right).$$

The Lévy measure $\nu(x) = f(x)$ is always finite.

Simulation of compound Poisson process at time t is straightforward. We interpret X_t at time t as a compound Poisson variable with Poisson rate λt and jump distribution $f(x)$.

2.3 Gamma Process

The gamma distribution with shape parameter α and rate parameter β, denoted by $\Gamma(\alpha, \beta)$, has the density function

$$f_{\Gamma(\alpha,\beta)}(x) = \frac{\beta^\alpha}{\Gamma(\alpha)} x^{\alpha-1} e^{-\beta x}, \quad \alpha, \beta > 0,$$

where $\Gamma(\cdot)$ is the *gamma function*, i.e. $\Gamma(u) := \int_0^\infty s^{u-1} e^{-s}\mathrm{d}s$. The associated gamma process $\{X_t, t \geq 0\}$ is a pure-jump increasing Lévy process with independently gamma distributed increments satisfying $X_1 \sim \Gamma(\alpha, \beta)$, $X_0 = 0$, and it has Lévy measure

$$\nu(x) = \frac{\alpha e^{-\beta x}}{x}, \tag{2.3.1}$$

where $\alpha, \beta > 0$, is called a gamma process. The Laplace transform follows that

$$\mathbb{E}\left[e^{-vX_t}\right] = \left(1 + \frac{v}{\beta}\right)^{\alpha t}. \tag{2.3.2}$$

Gamma process is simple and highly mathematically tractable, which has been used as a very popular representative for Lévy processes in the literature, see Barndorff-Nielsen and Shephard (2001a,b, 2003a), Schoutens (2003), Cont and Tankov (2004), Kyprianou (2006) and Schoutens and Cariboni (2010). It has been used to model stochastic volatilities (Barndorff-Nielsen and Shephard, 2003a; Brockwell et al., 2007; Granelli and Veraart, 2016), human mortality rates, actuarial valuations (Hainaut and Devolder, 2008) and instantaneous short rates of interest (Norberg, 2004; Eberlein et al., 2013). Barndorff-Nielsen and Shephard (2001b, 2002, 2003a,b) used the gamma based stochastic processes to model the stochastic volatility of stock prices, see also Roberts et al. (2004), Jongbloed et al. (2005), Griffin and Steel (2006), Creal (2008) and Frühwirth-Schnatter and Sögner (2009). Moreover, Nicolato and Venardos (2003) further applied these type of stochastic volatility models to pricing European options. Schoutens and Cariboni (2010) and Bianchi and Fabozzi (2015) also adopted the gamma based stochastic process as a stochastic intensity process for modelling credit default risk and pricing credit default swaps (CDSs). Cartea et al. (2015, p.220) used it for modelling the stochastic mean-reverting volume rate of trading, see also Cartea and Jaimungal (2016).

Simulation of the gamma process at time t is achieved by sampling a gamma variable with shape αt and rate β.

2.4 Tempered Stable Process

The tempered stable process was initially proposed by Tweedie (1984) and Hougaard (1986). It is closely related with the stable process, which is a type of Lévy processes whose characteristic exponents correspond to stable distributions. The Lévy measure of stable process is of the form

$$\nu(x) = \frac{\theta}{x^{\alpha+1}},$$

with stability parameter $\alpha \in (0,1)$, and scale parameter $\theta > 0$. In this case, the Laplace transform is

$$\mathbb{E}\left[e^{-vX_t}\right] = \exp\left(-\frac{t\theta\Gamma(1-\alpha)}{\alpha}v^{\alpha}\right).$$

The tempered stable (TS) process, abbreviated as $TS(\alpha, \beta, \theta)$, is defined by its Lévy measure

$$\nu(x) = \frac{\theta}{x^{\alpha+1}} e^{-\beta x}, \qquad y \geq 0, \qquad \alpha \in (0,1), \quad \beta, \theta \in \mathbb{R}^+, \tag{2.4.1}$$

where β is the tilting parameter. The associated Laplace transform of tempered stable process is of the form

$$\mathbb{E}\left[e^{-vX_t}\right] = \exp\left(-\frac{t\theta\Gamma(1-\alpha)}{\alpha}\left[(\beta+v)^\alpha - \beta^\alpha\right]\right). \tag{2.4.2}$$

The stable index α determines the importance of small jumps for the process trajectories, the intensity parameter θ controls the intensity of jumps, and the tilting parameter β determines the decay rate of large jumps. In particular, if $\alpha = \frac{1}{2}$, it reduces to a very important distribution, the *inverse Gaussian* (IG) distribution, which can be interpreted as the distribution of the first passage time of a Brownian motion to an absorbing barrier. So, this family of tempered stable subordinator also covers the *inverse Gaussian (IG) subordinator* as an important special case (Barndorff-Nielsen, 1997, 1998). Conventionally, the inverse Gaussian distribution is denoted by $IG\left(\mu_{IG}, \lambda_{IG}\right)$ where μ_{IG} is the *mean parameter* and λ_{IG} is the *rate parameter*, see a detailed introduction for inverse Gaussian distributions in Chhikara and Folks (1988). The inverse Gaussian subordinator is a special tempered stable subordinator such that $X_t \sim IG\left(\frac{t}{c}, t^2\right)$ for any $c, t \in \mathbb{R}^+$, i.e.,

$$IG\left(\frac{t}{c},\, t^2\right) \overset{\mathcal{D}}{=} TS\left(\frac{1}{2},\, \frac{c^2}{2},\, \frac{t}{\sqrt{2\pi}}\right).$$

The family of tempered stable process plays a key role in mathematical statistics, as a model for randomness used by Bayesians, and in economic models (Devroye, 2009). Furthermore, this family has become a fundamental component to be used to construct many useful stochastic processes, which have numerous applications in finance and many other fields. For example, Ornstein-Uhlenbeck processes driven by tempered stable are used for modelling stochastic volatilities of asset prices (Barndorff-Nielsen and Shephard, 2002, 2003a; Andrieu et al., 2010; Todorov, 2015). More recently, tempered stable processes have been adopted for modelling the stochastic-time clocks in a series of time-changed models proposed by Li and Linetsky (2013, 2014, 2015) and Mendoza-Arriaga and Linetsky (2014, 2016).

The simulation design for exactly sampling tempered stable without bias has been recently brought to the attention in the literature. The most widely used and trivial algorithm probably is the *simple stable rejection* (SSR) scheme, which is developed by a simple combination of the well known *Zolotarev's integral representation* (Zolotarev, 1964) and an acceptance-rejection (A/R) scheme; see Brix (1999). Hofert (2011a,b) suggested a *fast rejection* (FR) algorithm to enhance

the SSR scheme. However, the complexities of SSR and FR are unbounded, which obviously limit their applicability as they would become extremely inefficient for some parameter choices. To overcome this problem, Devroye (2009) developed a novel scheme based on *double rejection* (DR) such that the complexity is uniformly bounded. To further reduce the computational costs, we design a very efficient new scheme based on *two-dimensional single rejection* (SR)[1]. The complexity of our SR scheme is also uniformly bounded, and remarkably, it outperforms all existing schemes for all ranges of parameters. More precisely, the complexity of our SR scheme is roughly bounded by 2.6 over all parameters, which is much smaller than the one for the DR scheme.

To establish the simulation algorithm for tempered stable, first, we provide preliminaries for tempered stable distribution and the general two-dimensional SR framework in Section 2.4.1.

Remark 2.4.1. The term "complexity" in here and the other part of this thesis stands for the expected number of iterations before halting. For acceptance-rejection scheme, the complexity of the scheme is exactly the associated A/R constant.

2.4.1 Tempered Stable Distributions

Let S_α be a stable random variable with the stability index $\alpha \in (0,1)$ with Laplace transform

$$\mathbb{E}\left[e^{-vS_\alpha}\right] = e^{-v^\alpha}, \qquad v \in \mathbb{R}^+.$$

The density function of S_α has the well-known integral representation (Zolotarev, 1986),

$$f_\alpha(s) = \frac{1}{\pi}\int_0^\pi \frac{\alpha}{1-\alpha} B(u)^{\frac{1}{1-\alpha}} s^{-\frac{1}{1-\alpha}} e^{-B(u)^{\frac{1}{1-\alpha}} s^{-\frac{\alpha}{1-\alpha}}} \mathrm{d}u, \tag{2.4.3}$$

where $B(u)$ is defined as

$$B(u) := \frac{\sin^\alpha(\alpha u)\sin^{1-\alpha}\left((1-\alpha)u\right)}{\sin u}.$$

The associated tempered stable random variable $S_{\alpha,\beta}$ is defined through exponentially tilting the distribution of S_α with tilting parameter $\beta \in \mathbb{R}^+$. The Laplace transform of $S_{\alpha,\beta}$ therefore is

$$\mathbb{E}\left[e^{-vS_{\alpha,\beta}}\right] = e^{\beta^\alpha - (\beta+v)^\alpha}, \tag{2.4.4}$$

[1]This idea originates from Dassios et al. (2018b) where they tailored efficient simulation algorithms for some special TS classes.

and the density function of $S_{\alpha,\beta}$ is given by

$$f_{\alpha,\beta}(s) = e^{\beta^\alpha - \beta s} f_\alpha(s) = \int_0^\pi f(s,u)\mathrm{d}u, \tag{2.4.5}$$

where $f(s,u)$ is the bivariate density function of (S,U) in (s,u) on $[0,\infty)\times[0,\pi]$, i.e.

$$f(s,u) = \frac{\alpha e^{\beta^\alpha}}{(1-\alpha)\pi} B(u)^{\frac{1}{1-\alpha}} s^{-\frac{1}{1-\alpha}} e^{-B(u)^{\frac{1}{1-\alpha}} s^{-\frac{\alpha}{1-\alpha}} - \beta s}. \tag{2.4.6}$$

Remark 2.4.2. For a tempered process X_t with Laplace transform (2.4.2), we have

$$X_t \overset{\mathcal{D}}{=} \hat{t} S_{\alpha,\beta\hat{t}},$$

with $\hat{t} = [t\theta\Gamma(1-\alpha)/\alpha]^{\frac{1}{\alpha}}$, see Devroye (2009). Hence, without loss of generality, we set $\hat{t} = 1$, i.e. $\theta = \frac{\alpha}{t\Gamma(1-\alpha)}$ in (2.4.1) for simplicity.

This $S_{\alpha,\beta}$ can not easily be simulated directly due to the Zolotarev's integral representation (2.4.3). However, we can use two-dimensional A/R scheme, namely *two-dimensional single rejection* scheme to sample (S,U) and return S to sample $S_{\alpha,\beta}$ instead.

2.4.2 Two-Dimensional Single Rejection Scheme

Given a bivariate variable (S,U) with density $f(s,u)$, we can use the two-dimensional A/R scheme to sample (S,U) by choosing an appropriate bivariate envelop (S',U') with density $g(s,u)$. Therefore, we can use the following general simulation framework, Algorithm 2.4.1, to sample the associated marginal variate S.

Algorithm 2.4.1 (Two-Dimensional Single Rejection Framework)**.** *The simulation framework for two-dimensional single rejection scheme is given as follows:*

1. *Set* $C = \max_{s,u}\{f(s,u)/g(s,u)\}$,
2. *Generate* (S,U) *with density* $g(s,u)$,
3. *Generate* $V \sim \mathcal{U}(0,1)$, *if*
$$V \le \frac{f(S,U)}{Cg(S,U)},$$
then, accept (S,U)*; Otherwise, reject this candidate and go back to Step 2,*
4. *Return* S.

For (S, U) with joint density (2.4.6), if we can find an appropriate bivariate envelop with low rejection rate, then this method is more suitable than the *double rejection* (DR) method used in Devroye (2009), as there is only one rejection procedure is involved within entire simulation instead of two.

2.4.3 Exact Simulation Scheme

Several exact algorithms for simulating tempered stable have been proposed in the literature, i.e. *simple stable rejection* (SSR) scheme (Brix, 1999), *double rejection* (DR) scheme (Devroye, 2009) and *fast rejection* (FR) scheme (Hofert, 2011b). These algorithms are exact which can produce very accurate samples. However, each of them has its own advantages and limitations. For the SSR scheme, since the expected complexity is exponentially increasing, the algorithm has a very poor acceptance rate for a large value of tilting parameter β. For the DR scheme, although the complexity is uniformly bounded, the upper bound is still large. In particular, when α is close to 0, the simulation becomes less efficient. As also pointed out by Hofert (2011b), comparing with the SSR scheme, the DR scheme is more difficult for a practitioner to implement as the procedure is rather complicated. For the FR scheme, it works well for a small value of α, but its complexity is $\mathcal{O}(\beta^\alpha)$ which is clearly unbounded. In this section, we aim to develop a simpler and more efficient algorithm with lower uniformly bounded complexity for all $\alpha \in (0,1)$ and $\beta \in \mathbb{R}^+$ based on *two-dimensional single rejection* (SR) framework.

According to (2.4.3) and (2.4.5), for $X = \beta S_{\alpha,\beta}$, the density of X is specified by

$$f_X(x) = \frac{1}{\pi}\int_0^\pi \frac{\alpha e^{\beta^\alpha}}{1-\alpha} B(u)^{\frac{1}{1-\alpha}} \beta^{\frac{\alpha}{1-\alpha}} x^{-\frac{1}{1-\alpha}} e^{-B(u)^{\frac{1}{1-\alpha}} \beta^{\frac{\alpha}{1-\alpha}} x^{-\frac{\alpha}{1-\alpha}} - x} \mathrm{d}u,$$

which is the marginal density of bivariate variable (X, U) on $[0,\infty) \times [0,\pi]$ with density

$$f(x,u) = \frac{\alpha e^{\beta^\alpha}}{\pi(1-\alpha)} B(u)^{\frac{1}{1-\alpha}} \beta^{\frac{\alpha}{1-\alpha}} x^{-\frac{1}{1-\alpha}} e^{-B(u)^{\frac{1}{1-\alpha}} \beta^{\frac{\alpha}{1-\alpha}} x^{-\frac{\alpha}{1-\alpha}} - x}. \tag{2.4.7}$$

To sample $S_{\alpha,\beta}$, first, we sample (X, U) by applying the two-dimensional SR scheme in Algorithm 2.4.1, and then return $S_{\alpha,\beta} = X/\beta$. Hence, to simulate (X, U) with density (2.4.7), we could choose a Gamma-Uniform bivariate envelope (X', U') with density

$$g(x,u) = \frac{1}{\pi}\frac{1}{\Gamma(m)} x^{m-1} e^{-x}. \tag{2.4.8}$$

for some $m \in \mathbb{R}^+$. The details of the simulation procedure are provided as follows.

Algorithm 2.4.2 (Exact Simulation of $S_{\alpha,\beta}$ with Gamma-Uniform Envelope)**.** *The simulation scheme for $S_{\alpha,\beta}$ with Gamma-Uniform envelope is given as follows:*

1. *Set* $C_1 = (\alpha\beta^\alpha)^{-\beta^\alpha} e^{\alpha\beta^\alpha - 1}\Gamma(\alpha\beta^\alpha)\left(\frac{\alpha}{1-\alpha} + \alpha\beta^\alpha\right)^{\beta^\alpha(1-\alpha)+1}$,

2. *Generate* $U \sim \mathcal{U}[0,\pi]$, $X \sim \Gamma(\alpha\beta^\alpha, 1)$,

3. *Set* $B(U) = \sin^\alpha(\alpha U)\sin^{1-\alpha}\big((1-\alpha)U\big)/\sin U$,

4. *Generate* $V \sim \mathcal{U}[0,1]$, *if*

$$V \le \frac{\alpha e^{\beta^\alpha}\Gamma(\alpha\beta^\alpha)}{C_1(1-\alpha)} B(U)^{\frac{1}{1-\alpha}} \beta^{\frac{\alpha}{1-\alpha}} X^{-\frac{\alpha}{1-\alpha}} e^{-\alpha\beta^\alpha - B(U)^{\frac{1}{1-\alpha}}\beta^{\frac{\alpha}{1-\alpha}} X^{-\frac{\alpha}{1-\alpha}}},$$

   then, accept (X,U) *and go to Step 5; Otherwise, reject this candidate and go back to Step 2,*

5. *Return* X/β.

Proof. Given $f(x,u)$ for (X,U) in (2.4.7) and $g(x,u)$ for (X',U') in (2.4.8), we have

$$\begin{aligned}
\frac{f(x,u)}{g(x,u)} &= \frac{\alpha e^{\beta^\alpha}\Gamma(m)}{1-\alpha} B(u)^{\frac{1}{1-\alpha}}\beta^{\frac{\alpha}{1-\alpha}} x^{-\frac{\alpha}{1-\alpha}-m} e^{-B(u)^{\frac{1}{1-\alpha}}\beta^{\frac{\alpha}{1-\alpha}} x^{-\frac{\alpha}{1-\alpha}}} \\
&\le \frac{\alpha e^{\beta^\alpha}\Gamma(m)}{1-\alpha} B(u)^{\frac{1}{1-\alpha}}\beta^{\frac{\alpha}{1-\alpha}} \left[\frac{\frac{\alpha}{1-\alpha} B(u)^{\frac{1}{1-\alpha}}\beta^{\frac{\alpha}{1-\alpha}}}{\frac{\alpha}{1-\alpha}+m}\right]^{-\frac{(1-\alpha)m+\alpha}{\alpha}} e^{-B(u)^{\frac{1}{1-\alpha}}\beta^{\frac{\alpha}{1-\alpha}}\left[\frac{\alpha B(u)^{\frac{1}{1-\alpha}}\beta^{\frac{\alpha}{1-\alpha}}}{\alpha+(1-\alpha)m}\right]^{-1}} \\
&= \left(\frac{\alpha}{1-\alpha}\right)^{-\frac{m(1-\alpha)}{\alpha}} \beta^{-m}\Gamma(m)\left(\frac{\alpha}{1-\alpha}+m\right)^{\frac{m(1-\alpha)+\alpha}{\alpha}} e^{-\frac{m(1-\alpha)+\alpha}{\alpha}+\beta^\alpha} B(u)^{-\frac{m}{\alpha}} \\
&\le \left(\frac{\alpha}{1-\alpha}\right)^{-\frac{m(1-\alpha)}{\alpha}} \beta^{-m}\Gamma(m)\left(\frac{\alpha}{1-\alpha}+m\right)^{\frac{m(1-\alpha)+\alpha}{\alpha}} e^{-\frac{m(1-\alpha)+\alpha}{\alpha}+\beta^\alpha} B(0)^{-\frac{m}{\alpha}} \\
&= \left(\frac{\alpha}{1-\alpha}\right)^{-\frac{m(1-\alpha)}{\alpha}} \beta^{-m}\Gamma(m)\left(\frac{\alpha}{1-\alpha}+m\right)^{\frac{m(1-\alpha)+\alpha}{\alpha}} e^{-\frac{m(1-\alpha)+\alpha}{\alpha}+\beta^\alpha}\left[(1-\alpha)^{1-\alpha}\alpha^\alpha\right]^{-\frac{m}{\alpha}} \\
&= C_1(m,\alpha,\beta),
\end{aligned}$$

where $B(u)$ is a monotone increasing function with

$$\min_{0\le u\le\infty}\{B(u)\} = B(0) = (1-\alpha)^{1-\alpha}\alpha^\alpha. \tag{2.4.9}$$

The A/R constant $C_1(m,\alpha,\beta)$ can be further minimised over m. The optimal value m^* satisfies

$$\frac{\alpha}{1-\alpha}\psi^{(0)}(m^*) + \ln\left(\frac{\alpha}{1-\alpha}+m^*\right) = \ln\left(\alpha^{\frac{1}{1-\alpha}}\beta^{\frac{\alpha}{1-\alpha}}\right), \qquad \text{for } \psi^{(0)}(m) = \frac{\mathrm{d}\Gamma(m)}{\mathrm{d}m}. \tag{2.4.10}$$

Hence, by approximating the LHS of (2.4.10), the optimal rate m^* for the gamma-distributed en-

velope is chosen by setting[2]

$$m^* = \alpha\beta^\alpha.$$

The A/R decision therefore follows

$$V \leq \frac{f(X', U')}{C_1 g(X', U')},$$

with

$$C_1 = C_1\left(\alpha\beta^\alpha\right) = \left(\alpha\beta^\alpha\right)^{-\beta^\alpha} e^{\alpha\beta^\alpha - 1}\Gamma\left(\alpha\beta^\alpha\right)\left(\frac{\alpha}{1-\alpha} + \alpha\beta^\alpha\right)^{\beta^\alpha(1-\alpha)+1}.$$

where C_1 is the associated A/R constant. □

Remark 2.4.3. According to Stirling's approximation for large x,

$$\Gamma(x+1) \sim x^{x+\frac{1}{2}} e^{-x+1}, \tag{2.4.11}$$

the following holds for very large β,

$$\begin{aligned} C_1 &= \left(\alpha\beta^\alpha\right)^{-\beta^\alpha - 1} e^{\alpha\beta^\alpha - 1}\Gamma(\alpha\beta^\alpha + 1)\left(\frac{\alpha}{1-\alpha} + \alpha\beta^\alpha\right)^{\beta^\alpha(1-\alpha)+1} \\ &\leq \left(\alpha\beta^\alpha\right)^{\frac{1}{2}-\beta^\alpha(1-\alpha)-1}\left(\alpha\beta^\alpha + \frac{\alpha}{(1-\alpha)}\right)^{1+\beta^\alpha(1-\alpha)} \\ &\leq e\sqrt{\alpha}\left(1 + \frac{1}{(1-\alpha)\beta^\alpha}\right)\beta^{\frac{\alpha}{2}}. \end{aligned}$$

We can see that the complexity C_1 is unbounded and the order of C_1 for large β is less than $\mathcal{O}\left(\beta^{\frac{\alpha}{2}}\right)$.

Algorithm 2.4.2 has a better performance for a small α, since the A/R constant is relative small and does not increase fast against the tilting parameter β. However, when α is large, this algorithm becomes inefficient due to the low acceptance rate.

In order to improve the performance for a large α, we develop an enhanced algorithm based on the new transformation

$$Z = B(U)^{\frac{1}{1-\alpha}} S_{\alpha,\beta}^{-\frac{\alpha}{1-\alpha}}. \tag{2.4.12}$$

Hence, according to (2.4.6), by changing the variables of the joint distribution function from (S, U) to (Z, U), we have

$$f(z, u) = \frac{e^{\beta^\alpha}}{\pi}\exp\left(-z - \beta B(u)^{\frac{1}{\alpha}} z^{-\frac{1-\alpha}{\alpha}}\right). \tag{2.4.13}$$

[2] Alternatively, m^* can also be obtained via numerical optimisation.

To sample $S_{\alpha,\beta}$, we could sample (Z,U) first, and then return $S_{\alpha,\beta} = B(U)^{\frac{1}{\alpha}} Z^{-\frac{1-\alpha}{\alpha}}$. A Gamma-Uniform bivariate variate is also a suitable envelope to use to implement the two-dimensional SR to sample (Z,U). The associated details are presented in Algorithm 2.4.3.

Algorithm 2.4.3 (Enhanced Exact Simulation of $S_{\alpha,\beta}$ with Gamma-Uniform Envelope)**.** *The enhanced simulation scheme for $S_{\alpha,\beta}$ with Gamma-Uniform envelope is given as follows:*

1. *Set* $C_2 = \beta^{-\alpha(1-\alpha)\beta^\alpha} e^{(1-\alpha)\beta^\alpha} \Gamma\big((1-\alpha)\beta^\alpha + 1\big)(1-\alpha)^{-(1-\alpha)\beta^\alpha}$,

2. *Generate* $U \sim \mathcal{U}[0,\pi]$, $Z \sim \Gamma\big((1-\alpha)\beta^\alpha + 1, 1\big)$,

3. *Set* $B(U) = \sin^\alpha(\alpha U) \sin^{1-\alpha}\big((1-\alpha)U\big)/\sin U$,

4. *Generate* $V \sim \mathcal{U}[0,1]$, *if*

$$V \le e^{\beta^\alpha} \Gamma\left((1-\alpha)\beta^\alpha + 1\right) Z^{-(1-\alpha)\beta^\alpha} e^{-\beta B(U)^{\frac{1}{\alpha}} Z^{-\frac{1-\alpha}{\alpha}}} / C_2,$$

   then, accept (Z,U) and go to Step 5; Otherwise, reject this candidate and go back to Step 2,

5. *Return* $B(U)^{\frac{1}{\alpha}} Z^{-\frac{1-\alpha}{\alpha}}$.

Proof. We choose an envelope (Z',U') with joint density function

$$g(z,u) = \frac{1}{\pi} \frac{1}{\Gamma(r+1)} z^r e^{-z},$$

according to (2.4.9), we have

$$\begin{aligned}
\frac{f(z,u)}{g(z,u)} &= e^{\beta^\alpha} \Gamma(r+1) z^{-r} e^{-\beta B(u)^{\frac{1}{\alpha}} z^{-\frac{1-\alpha}{\alpha}}} \\
&\le e^{\beta^\alpha} \Gamma(r+1) z^{-r} e^{-\beta\alpha(1-\alpha)^{\frac{1-\alpha}{\alpha}} z^{-\frac{1-\alpha}{\alpha}}} \\
&\le \left(\frac{\alpha r}{(1-\alpha)\beta}\right)^{\frac{r\alpha}{1-\alpha}} e^{-\frac{r\alpha}{1-\alpha} + \beta^\alpha} \Gamma(r+1) \left[(1-\alpha)\alpha^{\frac{\alpha}{1-\alpha}}\right]^{-r} = C_2(r),
\end{aligned}$$

where $C_2(r)$ can be minimised over r. The optimal value r^* satisfies

$$\psi^{(0)}(r^*+1) = \frac{\alpha}{1-\alpha} \ln\left(\frac{\beta(1-\alpha)^{\frac{1}{\alpha}}}{r^*}\right), \qquad \text{for } \psi^{(0)}(r) = \frac{\mathrm{d}\Gamma(r)}{\mathrm{d}r}. \tag{2.4.14}$$

By approximating the LHS of (2.4.14), the optimal rate r^* is chosen by setting

$$r^* = (1-\alpha)\beta^\alpha.$$

Hence, the associated A/R constant with r^* is given by

$$C_2 = C_2\big((1-\alpha)\beta^\alpha\big) = \beta^{-\alpha(1-\alpha)\beta^\alpha} e^{(1-\alpha)\beta^\alpha} \Gamma\big((1-\alpha)\beta^\alpha + 1\big)(1-\alpha)^{-(1-\alpha)\beta^\alpha}.$$

where C_2 is the associated A/R constant. □

Remark 2.4.4. For large value of β, applying Stirling approximation in (2.4.11), we have

$$C_2 \leq e\sqrt{1-\alpha}\beta^{\frac{\alpha}{2}},$$

The complexity C_2 is unbounded and the order is also less than $\mathcal{O}\left(\beta^{\frac{\alpha}{2}}\right)$.

Although the complexity of Algorithm 2.4.3 is unbounded, there is still a massive improvement for the acceptance rate for a large α. For small α, Algorithm 2.4.3 performs better than 2.4.2, whereas for large α, the out-performance of Algorithm 2.4.3 is more substantial. In general, Algorithm 2.4.3 is more favorable for $C_2 < C_1$.

Clearly, Algorithm 2.4.2 and 2.4.3 have better performance than the fast rejection (FR) scheme (Hofert, 2011b), as the complexity of FR scheme is of order $\mathcal{O}\left(\beta^\alpha\right)$ which is growing faster than the complexity of order $\mathcal{O}\left(\beta^{\frac{\alpha}{2}}\right)$. Comparing with DR scheme, Algorithm 2.4.2 and 2.4.3 are much simpler to implement, but both complexities are unbounded. Therefore, the next task for us is to design enhanced algorithms based on those bivariate envelopes used in Algorithm 2.4.2, 2.4.3 in order to obtain uniformly bounded complexities over all parameter ranges.

Let us first consider the case when α is small. For Algorithm 2.4.2, we sample (X, U) with density (2.4.7) by choosing an envelope (X', U') such that $X' \sim \Gamma\left(\alpha\beta^\alpha, 1\right), U' \sim \mathcal{U}[0, \pi]$. Instead of a uniform-distributed envelope for U', we use a truncated normal with domain $(0, \pi)$. The associated joint density of this Gamma and truncated normal bivariate variate $(\bar{X}, \bar{U})$ is of the form

$$h(x,u) = \frac{x^{\alpha\beta^\alpha - 1}e^{-x}}{\Gamma\left(\alpha\beta^\alpha\right)} \frac{\sqrt{2\alpha(1-\alpha)\beta^\alpha}/\sqrt{\pi}}{\mathrm{Erf}\left(\pi\sqrt{\alpha(1-\alpha)\beta^\alpha/2}\right)} e^{-\frac{\alpha(1-\alpha)\beta^\alpha u^2}{2}}, \tag{2.4.15}$$

In fact, this alternative bivariate envelope will significantly improve the efficiency of Algorithm 2.4.2. The details are given in Algorithm 2.4.4 below.

Algorithm 2.4.4 (Exact Simulation of $S_{\alpha,\beta}$ with Gamma and Truncated-Normal Envelope)**.** *The simulation scheme for $S_{\alpha,\beta}$ with Gamma and Truncated-Normal envelope is given as follows:*

1. *Set* $C_3 = \frac{\Gamma(\alpha\beta^\alpha+1)\beta^{-\alpha^2\beta^\alpha} e^{-1+\alpha\beta^\alpha} \alpha^{-\alpha\beta^\alpha}(1-\alpha)^{-1-(1-\alpha)\beta^\alpha}}{\sqrt{2\pi\alpha(1-\alpha)\beta^\alpha}} \left(\frac{1}{\beta^\alpha} + (1-\alpha)\right)^{1+(1-\alpha)\beta^\alpha}$,

2. *Generate* $U \sim \mathcal{N}\left(\mu = 0, \sigma^2 = [\alpha(1-\alpha)\beta^\alpha]^{-1}, lb = 0, ub = \pi\right)$,

3. *Set* $B(U) = \sin^\alpha(\alpha U)\sin^{1-\alpha}\left((1-\alpha)U\right)/\sin U$,

4. *Generate* $X \sim \Gamma(\alpha\beta^\alpha, 1)$,

5. *Generate* $V \sim \mathcal{U}[0,1]$, *if*

$$V \leq \frac{\text{Erf}\left(\sqrt{\alpha(1-\alpha)\beta^\alpha\pi^2/2}\right)\alpha e^{\beta^\alpha}\Gamma(\alpha\beta^\alpha)\beta^{\frac{\alpha}{1-\alpha}}B(U)^{\frac{1}{1-\alpha}}}{C_3(1-\alpha)\sqrt{2\pi\alpha(1-\alpha)\beta^\alpha}X^{\frac{\alpha}{1-\alpha}+\alpha\beta^\alpha}}e^{-\left(\beta B(u)^{\frac{1}{\alpha}}X^{-1}\right)^{\frac{\alpha}{1-\alpha}}+\frac{\alpha(1-\alpha)\beta^\alpha U^2}{2}},$$

then, accept (X, U) *and go to Step 6; Otherwise, reject this candidate and go back to Step 2,*

6. *Return* X/β.

Proof. Instead of simulating (X, U) with density in (2.4.7) with envelope (X', U') such that $X' \sim \Gamma(\alpha\beta^\alpha, 1)$ and $U' \sim \mathcal{U}[0,\pi]$, we consider a new envelope $(\bar{X}, \bar{U})$ such that $\bar{X} \sim \Gamma(\alpha\beta^\alpha, 1)$ and $\bar{U} \sim \mathcal{N}\left(\mu = 0, \sigma^2 = [\alpha(1-\alpha)\beta^\alpha]^{-1}, \text{lb} = 0, \text{ub} = \pi\right)$[3], which is a truncated normal variable with mean $\mu = 0$ and variance $\sigma^2 = \frac{1}{\alpha(1-\alpha)\beta^\alpha}$ within the domain $(0,\pi)$. Given the joint density of (X, U) in (2.4.7) and joint density of $(\bar{X}, \bar{U})$ in (2.4.15), first, by maximising $f(x,u)/g(x,u)$ with respect to x, we have

$$\begin{aligned}
\frac{f(x,u)}{h(x,u)} &= \frac{\text{Erf}\left(\pi\sqrt{\alpha(1-\alpha)\beta^\alpha/2}\right)\alpha e^{\beta^\alpha}\Gamma(\alpha\beta^\alpha)}{(1-\alpha)\sqrt{2\pi\alpha(1-\alpha)\beta^\alpha}}B(u)^{\frac{1}{1-\alpha}}\beta^{\frac{\alpha}{1-\alpha}}x^{-\frac{\alpha}{1-\alpha}-\alpha\beta^\alpha} \\
&\quad \times \exp\left(-B(u)^{\frac{1}{1-\alpha}}\beta^{\frac{\alpha}{1-\alpha}}x^{-\frac{\alpha}{1-\alpha}} + \frac{\alpha(1-\alpha)\beta^\alpha u^2}{2}\right) \\
&\leq \frac{\text{Erf}\left(\pi\sqrt{\alpha(1-\alpha)\beta^\alpha/2}\right)\alpha e^{\beta^\alpha}\Gamma(\alpha\beta^\alpha)}{(1-\alpha)\sqrt{2\pi\alpha(1-\alpha)\beta^\alpha}}\beta^{-\alpha\beta^\alpha}B(u)^{-\beta^\alpha}e^{\frac{\alpha(1-\alpha)\beta^\alpha u^2}{2}} \\
&\quad \times\left(1+(1-\alpha)\beta^\alpha\right)^{1+(1-\alpha)\beta^\alpha}e^{-(1+(1-\alpha)\beta^\alpha)}.
\end{aligned}$$

According to Devroye (2009), we have the inequality

$$B(u)^{-\beta^\alpha} \leq B(0)^{-\beta^\alpha}e^{-\frac{\alpha(1-\alpha)\beta^\alpha u^2}{2}} = \left[\alpha^\alpha(1-\alpha)^{1-\alpha}\right]^{-\beta^\alpha}e^{-\frac{\alpha(1-\alpha)\beta^\alpha u^2}{2}}. \tag{2.4.16}$$

Hence, by (2.4.16), we then have

$$\frac{f(x,u)}{h(x,u)} \leq \frac{\text{Erf}\left(\pi\sqrt{\alpha(1-\alpha)\beta^\alpha/2}\right)\Gamma(\alpha\beta^\alpha+1)\beta^{-\alpha^2\beta^\alpha}e^{-1+\alpha\beta^\alpha}\alpha^{-\alpha\beta^\alpha}(1-\alpha)^{-1-(1-\alpha)\beta^\alpha}}{\sqrt{2\pi\alpha(1-\alpha)\beta^\alpha}\left(\frac{1}{\beta^\alpha}+(1-\alpha)\right)^{-1-(1-\alpha)\beta^\alpha}}$$

[3] "lb" stands for lower bound and "ub" stands for upper bound.

$$\leq \frac{\Gamma(\alpha\beta^\alpha+1)\beta^{-\alpha^2\beta^\alpha}e^{-1+\alpha\beta^\alpha}\alpha^{-\alpha\beta^\alpha}(1-\alpha)^{-1-(1-\alpha)\beta^\alpha}}{\sqrt{2\pi\alpha(1-\alpha)\beta^\alpha}}\left(\frac{1}{\beta^\alpha}+(1-\alpha)\right)^{1+(1-\alpha)\beta^\alpha} = C_3,$$

where C_3 is the associated A/R constant. □

Remark 2.4.5. For a small α, the complexity of Algorithm 2.4.4 is uniformly bounded in terms of β. In particular, with large value of β, we have

$$\begin{aligned} C_3 &\leq \frac{1}{\sqrt{2\pi(1-\alpha)}}\left(\frac{1}{\beta^\alpha}+(1-\alpha)\right)^{1+(1-\alpha)\beta^\alpha}(1-\alpha)^{-1-(1-\alpha)\beta^\alpha} \\ &\leq \frac{e}{\sqrt{2\pi(1-\alpha)}}\left(1+\frac{1}{(1-\alpha)\beta^\alpha}\right), \end{aligned}$$

and it goes to $e/\sqrt{2\pi(1-\alpha)}$ when β goes to infinity.

For a large α, in particular when α is close to 1, Algorithm 2.4.4 is no longer suitable, we develop an enhanced simulation scheme in Algorithm 2.4.5 based on the transformation in (2.4.12) using the Gamma and truncated-normal bivariate envelope.

Algorithm 2.4.5 (Enhanced Exact Simulation of $S_{\alpha,\beta}$ with Gamma and Truncated-Normal Envelope)**.** *The enhanced simulation scheme for $S_{\alpha,\beta}$ with Gamma and Truncated-Normal envelope is given as follows:*

1. *Set* $C_4 = \frac{e^{(1-\alpha)\beta^\alpha}\Gamma((1-\alpha)\beta^\alpha+1)}{\sqrt{2\pi\alpha(1-\alpha)\beta^\alpha}}(1-\alpha)^{-(1-\alpha)\beta^\alpha}\beta^{-\alpha(1-\alpha)\beta^\alpha}$,
2. *Generate* $U \sim \mathcal{N}\left(\mu=0, \sigma^2=[\alpha(1-\alpha)\beta^\alpha]^{-1}, lb=0, ub=\pi\right)$,
3. *Set* $B(U) = \sin^\alpha(\alpha U)\sin^{1-\alpha}\left((1-\alpha)U\right)/\sin U$,
4. *Generate* $Z \sim \Gamma\left((1-\alpha)\beta^\alpha+1, 1\right)$,
5. *Generate* $V \sim \mathcal{U}[0,1]$, *if*

$$V \leq \frac{\text{Erf}\left(\sqrt{\alpha(1-\alpha)\beta^\alpha\pi^2/2}\right)e^{\beta^\alpha}\Gamma\left((1-\alpha)\beta^\alpha+1\right)}{C_4\sqrt{2\pi\alpha(1-\alpha)\beta^\alpha}Z^{(1-\alpha)\beta^\alpha}}e^{-\beta B(U)^{\frac{1}{\alpha}}Z^{-\frac{1-\alpha}{\alpha}}+\frac{\alpha(1-\alpha)\beta^\alpha U^2}{2}},$$

   then, accept (Z,U) *and go to Step 6; Otherwise, reject this candidate and go back to Step 2,*

6. *Return* $B(U)^{\frac{1}{\alpha}}Z^{-\frac{1-\alpha}{\alpha}}$.

Proof. We consider a new envelope $(\bar{Z},\bar{U})$ for (Z,U) with density (2.4.13), such that $\bar{Z} \sim \Gamma((1-\alpha)\beta^\alpha+1,1)$ and $\bar{U} \sim \mathcal{N}\left(\mu=0,\sigma^2=[\alpha(1-\alpha)\beta^\alpha]^{-1}, \text{lb}=0, \text{ub}=\pi\right)$, the joint density is

given as

$$h(z,u) = \frac{z^{(1-\alpha)\beta^\alpha} e^{-z}}{\Gamma((1-\alpha)\beta^\alpha + 1)} \frac{\sqrt{2\alpha(1-\alpha)\beta^\alpha}/\sqrt{\pi}}{\text{Erf}\left(\pi\sqrt{\alpha(1-\alpha)\beta^\alpha/2}\right)} e^{-\frac{\alpha(1-\alpha)\beta^\alpha u^2}{2}}.$$

Then, by maximising $f(z,u)/h(z,u)$ with respect to z and applying inequality (2.4.16), we have

$$\begin{aligned}
\frac{f(z,u)}{h(z,u)} &= \frac{\text{Erf}\left(\pi\sqrt{\alpha(1-\alpha)\beta^\alpha/2}\right) e^{\beta^\alpha}\Gamma((1-\alpha)\beta^\alpha+1)}{\sqrt{2\pi\alpha(1-\alpha)\beta^\alpha}} z^{-(1-\alpha)\beta^\alpha} e^{-\beta B(u)^{\frac{1}{\alpha}} z^{-\frac{1-\alpha}{\alpha}} + \frac{\alpha(1-\alpha)\beta^\alpha u^2}{2}} \\
&\leq \frac{\text{Erf}\left(\pi\sqrt{\alpha(1-\alpha)\beta^\alpha/2}\right) e^{(1-\alpha)\beta^\alpha}\Gamma((1-\alpha)\beta^\alpha+1)}{\sqrt{2\pi\alpha(1-\alpha)\beta^\alpha}} (1-\alpha)^{-(1-\alpha)\beta^\alpha} \beta^{-\alpha(1-\alpha)\beta^\alpha} \\
&\leq \frac{e^{(1-\alpha)\beta^\alpha}\Gamma((1-\alpha)\beta^\alpha+1)}{\sqrt{2\pi\alpha(1-\alpha)\beta^\alpha}} (1-\alpha)^{-(1-\alpha)\beta^\alpha} \beta^{-\alpha(1-\alpha)\beta^\alpha} = C_4,
\end{aligned}$$

where C_4 is the associated A/R constant. □

Remark 2.4.6. For a large α, the complexity therefore is uniformly bounded. In particular, for large value of β, we have $C_4 \leq e/\sqrt{2\pi\alpha}$. It is reasonably small when α close to 1.

Since the complexity of Algorithm 2.4.4 is bounded for a small α and the complexity of Algorithm 2.4.5 is bounded for a large α, a combination of Algorithm 2.4.4 and 2.4.5 therefore has a bounded complexity over the whole range of α and β. In particular, given α and β with $C_4 > C_3$, then Algorithm 2.4.5 outperforms Algorithm 2.4.4 much more substantially.

In general, each of Algorithm 2.4.2, 2.4.3, 2.4.4 and 2.4.5 has its own advantages for different pairs of α and β, one could optimally combine all of them and implement the most efficient scheme by choosing the scheme with the smallest complexity to sample the exponential tilted stable $S_{\alpha,\beta}$. The details are presented in Algorithm 2.4.6. The overall complexity C is given by $C = \min\{C_1,\ C_2,\ C_3,\ C_4\}$, which is uniformly bounded. The trend of this complexity in terms of α and β is presented in Figure 2.1. Apparently, the complexity is uniformly bounded, which is much smaller than the complexity of DR scheme (Devroye, 2009).

Algorithm 2.4.6 (Two-Dimensional Single Rejection Algorithm for $S_{\alpha,\beta}$)**.** *The general simulation scheme for $S_{\alpha,\beta}$ is given as follows:*

1. **set** $C_1 = \frac{e^{\alpha\beta^\alpha - 1}\Gamma(\alpha\beta^\alpha)}{(\alpha\beta^\alpha)^{\beta^\alpha}} \left(\frac{\alpha+\alpha(1-\alpha)\beta^\alpha}{1-\alpha}\right)^{\beta^\alpha(1-\alpha)+1}$, $C_2 = \frac{e^{(1-\alpha)\beta^\alpha}\Gamma((1-\alpha)\beta^\alpha+1)}{(1-a)^{(1-\alpha)\beta^\alpha}\beta^{\alpha(1-\alpha)\beta^\alpha}}$,
   $C_3 = \frac{\Gamma(\alpha\beta^\alpha+1)\beta^{-\alpha^2\beta^\alpha} e^{-1+\alpha\beta^\alpha}\alpha^{-\alpha\beta^\alpha}(1-\alpha)^{-1-(1-\alpha)\beta^\alpha}}{\sqrt{2\pi\alpha(1-\alpha)\beta^\alpha}(1/\beta^\alpha+(1-\alpha))^{-1-(1-\alpha)\beta^\alpha}}$, $C_4 = \frac{e^{(1-\alpha)\beta^\alpha}\Gamma((1-\alpha)\beta^\alpha+1)}{\sqrt{2\pi\alpha(1-\alpha)\beta^\alpha}((1-\alpha)\beta^\alpha)^{(1-\alpha)\beta^\alpha}}$
2. **if** $(C_1 = \min\{C_1,\ C_2,\ C_3,\ C_4\})$ **{**
3. **repeat{**

4. **sample** $U \sim \mathcal{U}[0,\pi]$, $X \sim \Gamma(\alpha\beta^{\alpha},1)$, $V \sim \mathcal{U}[0,1]$

5. **set** $B(U) = \sin^{\alpha}(\alpha U)\sin^{1-\alpha}\big((1-\alpha)U\big)/\sin U$, $S = X/\beta$

6. **if** $\big(V \leq \frac{\alpha e^{\beta^{\alpha}}\Gamma(\alpha\beta^{\alpha})}{1-\alpha} B(U)^{\frac{1}{1-\alpha}} \beta^{\frac{\alpha}{1-\alpha}} X^{-\frac{\alpha}{1-\alpha}-\alpha\beta^{\alpha}} e^{-B(U)^{\frac{1}{1-\alpha}}\beta^{\frac{\alpha}{1-\alpha}}X^{-\frac{\alpha}{1-\alpha}}}/C_1\big)$ **break**

7. **}**

8. **}**

9. **if** $\big(C_3 = \min\{C_1,\ C_2,\ C_3,\ C_4\}\big)$**{**

10. **repeat{**

11. **sample** $U \sim \mathcal{N}\left(\mu = 0, \sigma^2 = [\alpha(1-\alpha)\beta^{\alpha}]^{-1}, lb = 0, ub = \pi\right)$

12. **set** $B(U) = \sin^{\alpha}(\alpha U)\sin^{1-\alpha}\big((1-\alpha)U\big)/\sin U$

13. **sample** $X \sim \Gamma(\alpha\beta^{\alpha},1)$, $V \sim \mathcal{U}[0,1]$; **set** $S = X/\beta$

14. **if** $\big(V \leq \frac{\mathrm{Erf}\left(\sqrt{\alpha(1-\alpha)\beta^{\alpha}\pi^2/2}\right)\alpha e^{\beta^{\alpha}}\Gamma(\alpha\beta^{\alpha})\beta^{\frac{\alpha}{1-\alpha}}B(U)^{\frac{1}{1-\alpha}}}{C_3(1-\alpha)\sqrt{2\pi\alpha(1-\alpha)\beta^{\alpha}}X^{\frac{\alpha}{1-\alpha}+\alpha\beta^{\alpha}}} e^{-\left(\beta B(u)^{\frac{1}{\alpha}}X^{-1}\right)^{\frac{\alpha}{1-\alpha}}+\frac{\alpha(1-\alpha)\beta^{\alpha}U^2}{2}}\big)$ **break**

15. **}**

16. **}**

17. **if** $\big(C_2 = \min\{C_1,\ C_2,\ C_3,\ C_4\}\big)$**{**

18. **repeat{**

19. **sample** $U \sim \mathcal{U}[0,\pi]$, $Z \sim \Gamma\big((1-\alpha)\beta^{\alpha}+1,1\big)$, $V \sim \mathcal{U}[0,1]$

20. **set** $B(U) = \sin^{\alpha}(\alpha U)\sin^{1-\alpha}\big((1-\alpha)U\big)/\sin U$, $S = B(U)^{\frac{1}{\alpha}}Z^{-\frac{1-\alpha}{\alpha}}$

21. **if** $\big(V \leq e^{\beta^{\alpha}}\Gamma((1-\alpha)\beta^{\alpha}+1)Z^{-(1-\alpha)\beta^{\alpha}}e^{-\beta B(U)^{\frac{1}{\alpha}}Z^{-\frac{1-\alpha}{\alpha}}}/C_2\big)$ **break**

22. **}**

23. **}**

24. **if** $\big(C_4 = \min\{C_1,\ C_2,\ C_3,\ C_4\}\big)$**{**

25. **repeat{**

26. **sample** $U \sim \mathcal{N}\left(\mu = 0, \sigma^2 = [\alpha(1-\alpha)\beta^{\alpha}]^{-1}, lb = 0, ub = \pi\right)$

27. **set** $B(U) = \sin^{\alpha}(\alpha U)\sin^{1-\alpha}\big((1-\alpha)U\big)/\sin U$,

28. **sample** $Z \sim \Gamma\big((1-\alpha)\beta^{\alpha}+1,1\big)$, $V \sim \mathcal{U}[0,1]$; **set** $S = B(U)^{\frac{1}{\alpha}}Z^{-\frac{1-\alpha}{\alpha}}$

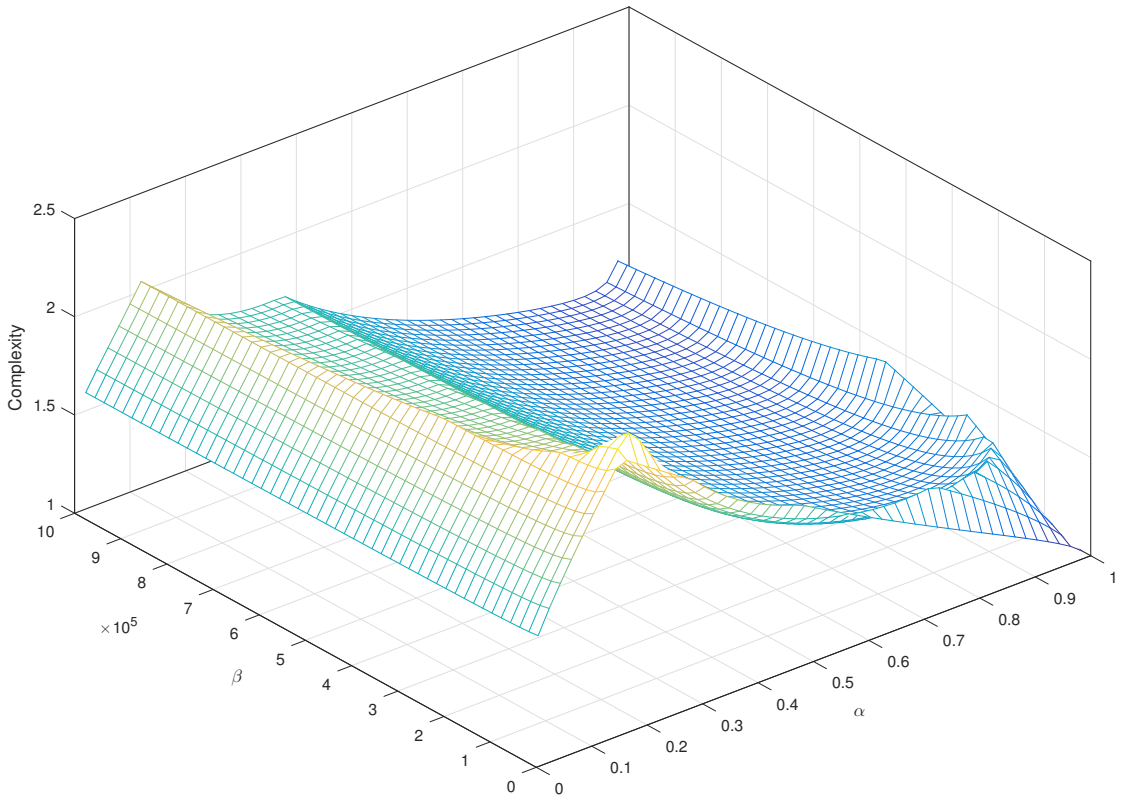

Figure 2.1: The complexity of Algorithm 2.4.6 for $\alpha \in (0,1)$ and $\beta \in \mathbb{R}^+$.

29. **if** $($ $V \leq \frac{\mathrm{Erf}\left(\sqrt{\alpha(1-\alpha)\beta^\alpha \pi^2/2}\right) e^{\beta^\alpha} \Gamma((1-\alpha)\beta^\alpha+1)}{C_4\sqrt{2\pi\alpha(1-\alpha)\beta^\alpha} Z^{(1-\alpha)\beta^\alpha}} e^{-\beta B(U)^{\frac{1}{\alpha}} Z^{-\frac{1-\alpha}{\alpha}} + \frac{\alpha(1-\alpha)\beta^\alpha U^2}{2}}$ $)$ **break**

30. **}**

31. **}**

32. **return** S

2.4.4 Numerical Experiments

We provide numerical examples for sampling tempered stable variables. The simulation experiments are all conducted on a normal laptop with the Intel Core i7-6500U CPU@2.50GHz processor, 8.00GB RAM, Windows 10 Home and 64-bit Operating System. The algorithms are coded and performed in R.3.4.2, and computing time is measured by the elapsed *CPU time* in seconds in here and the other parts of this thesis.

Numerical validation and tests for the tempered stable algorithm are based on the probability density function (PDF) and cumulative distribution function (CDF) of $S_{\alpha,\beta}$, for which can be obtained by inverting Laplace transform (2.4.4) numerically.

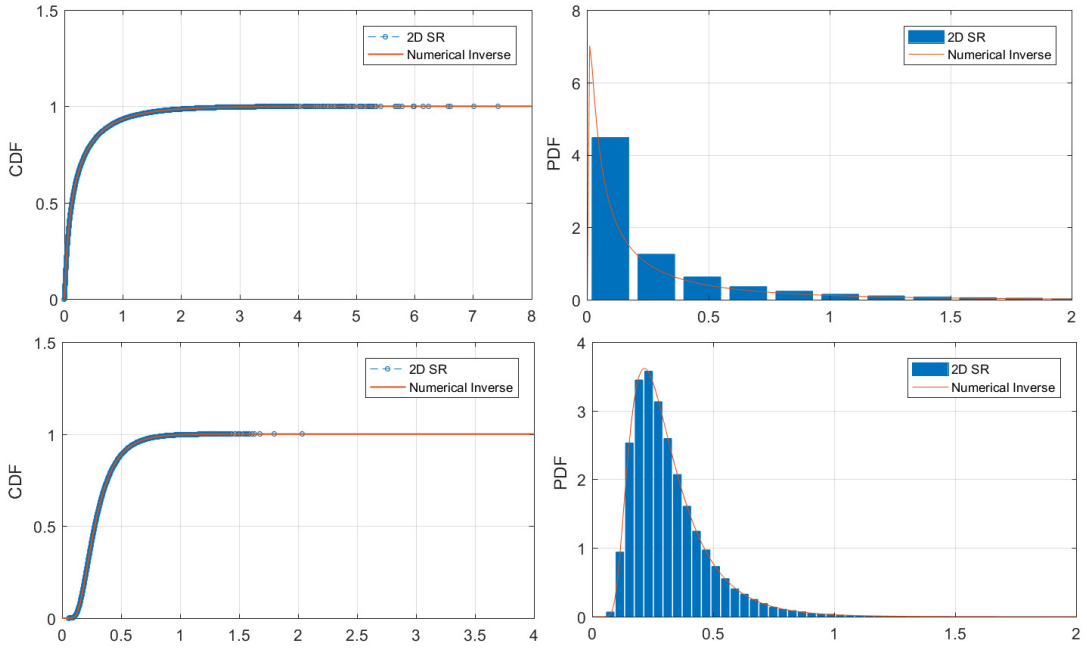

Figure 2.2: Comparison of the empirical CDF/PDF for SR scheme (via Algorithm 2.4.6) of $S_{\alpha,\beta}$ with the CDF/PDF obtained via numerical inverse using parameter settings $\alpha = 0.3, 0.6$, $\beta = 1.0, 5.0$, respectively.

For Algorithm 2.4.6, the plots of CDFs and PDFs under parameter settings $\alpha = 0.3, 0.6$, $\beta = 1.0, 5.0$ are provided in Figure 2.2 . We can see that our algorithm can achieve a very high level of accuracy, the simulated CDFs and PDFs are fitted pretty well to the associated numerical inversions. There are a variety of available algorithms for numerically inverting Laplace transforms with high accuracy in the literature, such as Gaver (1966), Stehfest (1970), Abate and Whitt (1992, 1995, 2006) to name a few. Here, we adopt the classical Euler scheme as described in Abate and Whitt (2006, Section 5, p.415-416).

To investigate the performance of our SR scheme, we made a comparison of CPU time for Algorithm 2.4.6 against the DR scheme for simulating $100,000$ replications under parameter settings $\alpha \in \{0.05, 0.1, ..., 0.9, 0.99\}$ and $\beta \in \{0.01, 0.1, ..., 10^6\}$. The numerical results are reported in Table 2.1. We can see that our SR scheme performances well for all combinations of α and β. The out-performance of our algorithm would even become much more substantial when α is close to 0. For example, it is about 8 times faster than the DR scheme when $\alpha = 0.05$. In addition, Algorithm 2.4.6 is also very fast when the tilting parameter β is not very large, which clearly indicates that the acceptance rate of Algorithm 2.4.6 is much higher than the DR scheme (Devroye, 2009) for a small tilting parameter β.

Table 2.1: Comparison of CPU time for the SR scheme (via Algorithm 2.4.6) against the DR scheme (Devroye, 2009) based on parameter settings $\alpha \in \{0.05, 0.1, ..., 0.9, 0.99\}$ and $\beta \in \{0.01, 0.1, ..., 10^6\}$; each value in the table is produced from $100,000$ replications.

α \ β	0.01		0.10		1.00		10		100		1,000		10,000		100,000		1,000,000	
	SR	DR	SR	DR	SR	DR	SR	DR	SR	DR	SR	DR	SR	DR	SR	DR	SR	DR
0.05	2.58	18.35	2.33	18.80	2.36	19.05	2.42	19.24	2.23	18.62	2.22	19.09	2.47	18.79	2.32	18.59	2.45	18.16
0.10	2.51	19.36	2.67	18.92	2.56	18.36	2.47	18.14	2.62	18.08	4.44	17.98	3.96	17.71	4.08	17.3	3.44	16.78
0.20	2.33	18.72	2.53	20.44	5.22	18.26	4.51	17.16	3.86	16.31	3.50	15.43	3.58	9.43	3.22	6.91	3.05	5.18
0.30	2.02	19.23	2.36	18.16	4.45	17.54	4.50	15.93	3.95	14.14	3.21	6.84	3.30	4.98	3.21	4.39	2.69	4.07
0.40	1.93	18.69	2.35	18.29	4.03	18.61	3.86	14.97	3.69	7.19	3.78	4.69	3.47	4.64	3.19	4.12	2.76	4.21
0.50	1.73	19.55	1.94	18.53	3.59	17.08	3.50	13.73	3.22	5.14	3.11	4.46	3.36	4.23	3.53	3.95	3.69	4.02
0.60	1.56	18.66	1.97	19.05	3.65	18.47	3.28	13.97	3.39	4.75	3.19	4.22	3.00	4.19	3.49	4.03	3.17	4.03
0.70	1.61	18.50	1.76	18.81	3.46	17.88	3.17	9.28	3.01	4.50	3.11	4.32	3.19	4.23	3.34	3.97	3.25	4.08
0.80	1.84	18.53	1.83	18.49	3.45	18.42	2.94	9.33	2.92	4.52	2.38	4.47	3.17	4.81	3.31	3.92	3.07	4.24
0.90	1.78	18.45	1.59	18.96	1.70	18.62	2.90	14.73	2.76	4.46	2.39	4.55	2.84	4.78	2.94	4.00	2.86	4.97
0.99	1.50	17.81	1.54	18.00	1.62	18.86	1.88	18.44	3.14	13.94	2.28	4.41	2.64	4.69	3.02	4.06	2.83	4.21

2.5 Conclusion

In this chapter, we provide definitions of Lévy subordinators, discuss several classical Lévy subordinators, i.e. the compound Poisson process, the gamma process and the tempered stable process, and illustrate exact simulation algorithms for these processes. In particular, we develop a new efficient simulation scheme for the tempered stable process based on two-dimensional single rejection, which is very different from other existing schemes in the literature. The complexity of our new algorithm is uniformly bounded over all range of parameters. Remarkably, it beats all other existing algorithms. At a number of points later on, we will use these processes and their simulation algorithms to deal with more complicated Lévy based stochastic models.

Chapter 3

Truncated Lévy Subordintors

In this chapter, we propose a new type of Lévy subordinators, namely the truncated Lévy subordinators, which is obtained by restricting the size of each jump. The truncated Lévy subordinator is defined through the Lévy measure with the limitation that the jump sizes do not exceed a certain truncation level. We study the path properties of truncated Lévy subordinator and develop exact simulation algorithm based on marked renewal process. In particular, we study several examples of truncated Lévy subordinators, such as *the Dickman process, the truncated gamma process, the truncated stable process, the truncated inverse Gaussian process*, in details. This type of Lévy subordinators has various applications in finance and insurance. First, we could use these processes to model aggregate claims distributions as individual claim sizes are often bounded from above. We also discover that the value of truncated Lévy subordinator at time t is the value of a perpetuity with stochastic discounting. Besides, we observe that the process has a duality relationship with the Parisian stopping time of diffusion processes. Hence our algorithms provide alternative methods for pricing Parisian options and bonds.

3.1 Preliminaries

Definition 3.1.1. *A truncated Lévy subordinator Z_t is defined by restringing the Lévy measure ν with an upper bound b. The Laplace transform of Z_t is given as*

$$\mathbb{E}\left[e^{-vZ_t}\right] = \exp\left(-t\int_0^b (1-e^{-vz})\nu(z)\mathrm{d}z\right), \qquad v \in \mathbb{R}^+.$$

Z_t preserves most properties of the original Lévy subordinator. It is a non-decreasing process with bounded variation and infinite activity, i.e, there are infinite number of jumps over a compact interval. The only difference is that the sizes of those infinite number of jumps are not allowed

to exceed a certain level b. This is illustrated in Figure 3.1, where we plot the sample paths of a truncated Lévy subordinator Z_t for three different truncation levels b.

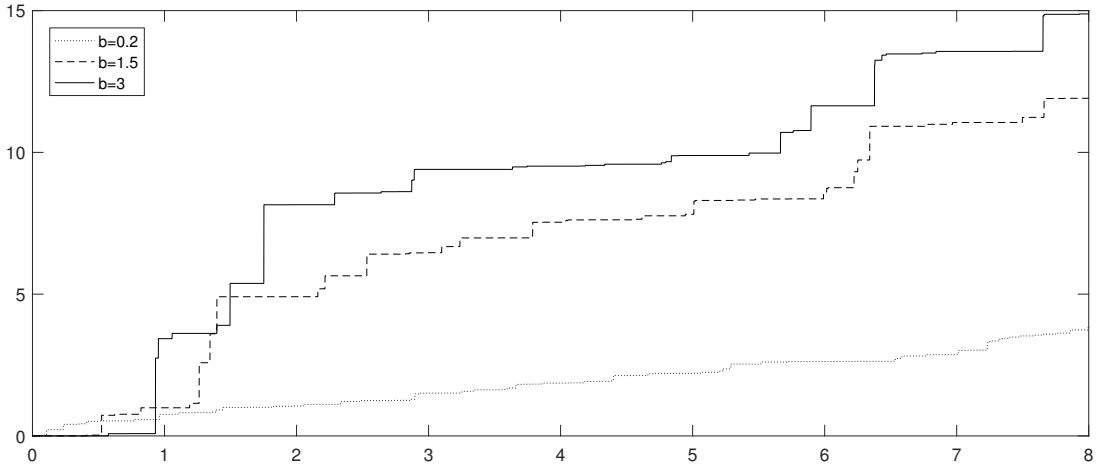

Figure 3.1: Sample paths of a truncated Lévy Subordinator with $b = 0.2, 1.5, 3$, respectively.

The original non-truncated Lévy subordinator X_t is thus equivalent to

$$X_t \stackrel{\mathcal{D}}{=} Z_t + R_t,$$

where Z_t is the truncated Lévy subordinator with Lévy measure restricted to $(0, b)$, and R_t is a compound Poisson process with mean $t\int_b^\infty \nu(x)\mathrm{d}x$, independent from Z_t, and the density of its jump sizes is

$$f(x) = \frac{\nu(x)}{\int_b^\infty \nu(x)\mathrm{d}x}, \qquad b \leq x < \infty.$$

This allows us to consider subordinators whose Lévy measure is discontinuous at b, and thus jump sizes are not characterised by a single continuous distribution. More generally, R_t can be replaced by any compound Poisson process with an arbitrary Poisson rate and jump distribution.

The paths of the truncated Lévy subordinator Z_t can be characterised via hitting times and associated overshoots. The definitions for hitting time and corresponding overshoot are provided as below,

Definition 3.1.2. *Let T be the first hitting time of level b of the truncated Lévy subordinator Z_t, and W be the associated overshoot at time T, i.e.*

$$T := \inf\{t > 0 | Z_t > b\}, \tag{3.1.1}$$

$$W := Z_T - b. \tag{3.1.2}$$

3.2 Distributional Properties

The general representation of the joint distribution of the first passage time and the associated overshoot is formulated in Theorem 3.2.1.

Theorem 3.2.1. *Let T be the first hitting time of level b of Z_t with Lévy measure ν, and W be the overshoot at time T. Then the joint distribution of (T, W) is given by*

$$f_{T,W}(t,w) = \int_w^b f(y,t)\nu(b+w-y)\mathrm{d}y, \tag{3.2.1}$$

where $t \in (0,\infty)$, $w \in (0,b)$, and $f(\cdot,t)$ denotes the density of Z_t within $(0,b)$. In particular, we have

$$f(\cdot,t) = e^{\bar{\nu}(b)t} f_{X_t}(\cdot,t)\mathbf{1}_{\{0<x<b\}}, \tag{3.2.2}$$

where $\bar{\nu}(s) := \int_s^\infty \nu(x)\mathrm{d}x$, and $f_{X_t}(\cdot,t)$ is the density of X_t with Laplace transform

$$\mathbb{E}\left[e^{-vX_t}\right] = \exp\left(-t\int_0^\infty \left(1-e^{-vx}\right)\nu(x)\mathrm{d}x\right). \tag{3.2.3}$$

Proof. Using the strong Markov property of Lévy processes, we have

$$\begin{aligned} P\left(T \in \mathrm{d}t, W > w\right) &= \lim_{\epsilon\to 0}\frac{1}{\epsilon}P\left(Z_{t-\epsilon} \le b, Z_t > b+w\right) \\ &= \lim_{\epsilon\to 0}\frac{1}{\epsilon}\int_0^b P(Z_{t-\epsilon}\in \mathrm{d}y)P(Z_\epsilon > b+w-y) \\ &= \int_0^b f(y,t)\int_{b+w-y}^\infty \nu(u)\mathrm{d}u\mathrm{d}y, \end{aligned} \tag{3.2.4}$$

Differentiating (3.2.4) with respect to w, the joint density of (T,W) directly follows (3.2.1). The density of Z_t within $(0,b)$ can be derived though its Laplace transform, we have

$$\begin{aligned} f(x,t) &= \mathcal{L}^{-1}\left\{\mathbb{E}\left[e^{-vZ_t}\right]\right\}\mathbf{1}_{\{0<x<b\}} \\ &= \mathcal{L}^{-1}\left\{\exp\left(-t\int_0^\infty \left(1-e^{-vx}\right)\nu(x)\mathrm{d}x\right)\exp\left(t\int_b^\infty \left(1-e^{-vx}\right)\nu(x)\mathrm{d}x\right)\right\}\mathbf{1}_{\{0<x<b\}} \\ &= \mathcal{L}^{-1}\left\{\exp\left(-t\int_0^\infty \left(1-e^{-vx}\right)\nu(x)\mathrm{d}x\right)\exp\left(t\int_b^\infty \nu(x)\mathrm{d}x\right)\exp\left(-t\int_b^\infty e^{-vx}\nu(x)\mathrm{d}x\right)\right\}\mathbf{1}_{\{0<x<b\}} \end{aligned}$$

$$= \mathcal{L}^{-1}\left\{\int_0^\infty e^{-vx} f_{X_t}(x,t)\mathrm{d}x \exp\left(t\int_b^\infty \nu(x)\mathrm{d}x\right)\sum_{k=0}^\infty \frac{(-t)^k}{k!}\left(\int_b^\infty e^{-vs}\nu(x)\mathrm{d}x\right)^k\right\}\mathbf{1}_{\{0<x<b\}}$$
$$= e^{\bar{\nu}(b)t} f_{X_t}(x,t)\mathbf{1}_{\{0<x<b\}}.$$

where $f_{X_t}(\cdot,t)$ denotes the density of X_t with Laplace transform (3.2.3). □

Under the circumstance that the first passage time of Z_t hits level b is greater than t, the distribution of the truncated process Z_t is characterised via its density within $(0,b)$. The details are illustrated in Theorem 3.2.2.

Theorem 3.2.2. *Given the time t, the density of* $\{Z_t|Z_t < b\}$ *is given by*

$$f_{Z_t|Z_t<b}(x|t) = \frac{f_{X_t}(x,t)}{\int_0^b f_{X_t}(x,t)\mathrm{d}x}, \qquad 0 < x < b, \tag{3.2.5}$$

where $f_{X_t}(\cdot,t)$ *denotes the density of* X_t *with Laplace transform* (3.2.3)*.*

Proof. The density immediately follows (3.2.5) by truncating the density of X_t. □

3.3 Marked Renewal Representation

The paths of the truncated subordinator Z_t can be characterised by a marked renewal process. First, we define a sequence of hitting times $T_1, T_2, T_3, ...$, and denoting $S_i = \sum_{j=1}^{i} T_j$, let

$$T_i := \inf\{t > S_{i-1}|Z_t > Z_{S_{i-1}} + b\}, \qquad i = 2,3,..., \tag{3.3.1}$$

These $T_1, T_2, ...$ are treated as the holding times for the events $\{T_{i-1} < t < T_i|Z_t - Z_{T_{i-1}} < b\}$, for $i = 2,3,....$ We further define $W_1, W_2, ...$ to be the overshoots at time $S_1, S_2, ...$, i.e.

$$W_i := Z_{S_i} - Z_{S_{i-1}} - b. \tag{3.3.2}$$

Hence, at time S_i the process will automatically increase by $(b + W_i)$ units for all i. Since the process Z_t has independent and stationary increments, each pair of (T_i, W_i) are independent and identically distributed with joint density given in Theorem 3.2.1. In addition, W_i will be bounded by 0 and b for all i as the jump sizes of the process is restricted with an upper bound b. The value of the process at time S_n will be $Z_{S_n} = \sum_{i=1}^{n}(b + W_i)$. The position of the process Z_t at time t

therefore can be expressed as using a marked renewal process as follows,

$$Z_t = \sum_{i=1}^{N_t}(b + W_i) + \left(Z_t - Z_{S_{N_t}} \mid S_{N_t} < t < S_{N_t} + T_{n+1}; Z_t - Z_{S_{N_t}} < b + W_{n+1}\right), \quad (3.3.3)$$

where $N_t = \sum_{i=1}^{\infty} \mathbf{1}_{\{S_i \le t\}}$ is determined via (3.3.1) such that $t \in [S_{N_t}, S_{N_t} + T_{n+1})$. We also use Figure 3.2 to illustrate the marked renewal idea graphically. The first part in (3.3.3) represents the

Figure 3.2: Graphical illustration of a sample path of X_t

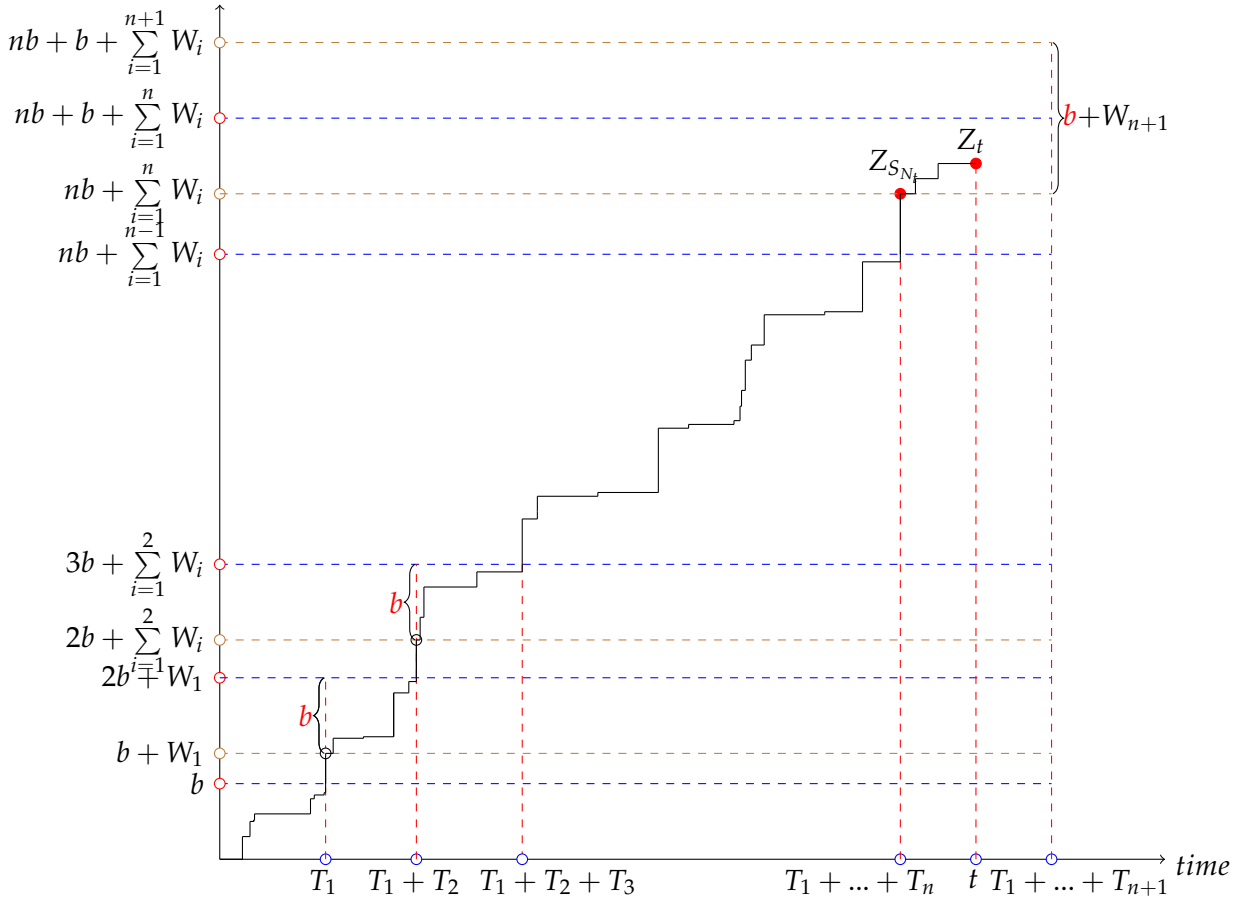

position of the truncated process at time S_{N_t} before reaches t. The second term in (3.3.3) represents the movement of the process within the time $t - S_{N_t}$. As $\{t - S_{N_t} < T_{n+1}\} \overset{\mathcal{D}}{=} \{Z_{t-S_{N_t}} < b\}$, we have

$$\begin{aligned}
& \{Z_t - Z_{S_{N_t}} \mid S_{N_t} < t < S_{N_t} + T_{n+1}, Z_t - Z_{S_{N_t}} < b + W_{n+1}\} \\
\overset{\mathcal{D}}{=} \; & \{Z_{t-S_{N_t}} | t - S_{N_t} < T_{n+1}, Z_{t-S_{N_t}} < b + W_{n+1}\} \\
\overset{\mathcal{D}}{=} \; & \{Z_{t-S_{N_t}} | Z_{t-S_{N_t}} < b, Z_{t-S_{N_t}} < b + W_{n+1}\} \\
\overset{\mathcal{D}}{=} \; & \{Z_{t-S_{N_t}} | Z_{t-S_{N_t}} < b\}. \qquad (3.3.4)
\end{aligned}$$

Conditioning on $t - S_{N_t} < T_{n+1}$ and $Z_{t-S_{N_t}} < b + W_{n+1}$, the distribution of $Z_{t-S_{N_t}}$ satisfies (3.2.5) in Theorem 3.2.2. Thus, Z_t can be simulated by generating pairs of hitting time and overshoot (T_i, W_i), stopping when the sum of T_i that have been generated, say $S_{N_t} + T_{n+1}$, becomes larger than the input t. We then generate the part $\{Z_{t-S_{N_t}} | Z_{t-S_{N_t}} < b\}$ and return to (3.3.3). We give the details of the exact simulation method in Algorithm 3.3.1. In particular, we show how to emphasis the marked renewal procedure using a recursive loop.

Algorithm 3.3.1 (Marked Renewal Simulation Framework)**.** *The truncated Lévy subordinator Z_t can be simulated via the following steps:*

1. *Set $S = 0$,*
2. *Generate (T, W) from the distribution $f_{T,W}(t, w)$ in (3.2.1); If $t < T$, go to step 3; Otherwise, go to step 4,*
3. *Generate Z from the distribution $f_{Z_t|Z_t<b}(x|t)$ in (3.2.5), then go to step 5,*
4. *Set $S = S + b + W$ and $t = t - T$, then go back to step 2,*
5. *Return $S + Z$.*

For implementation, one needs to specify the Lévy measure in explicit form in order to identify the joint distribution of (T, W) and distribution of $\{Z_t | Z_t < b\}$. In the following sections, we consider several typical examples of truncated Lévy subordinators and develop associated simulation algorithms based on Algorithm 3.3.1.

3.4 Dickman and Truncated Gamma Process

Dickman processes (Dickman, 1930; Arratia, 1998; Penrose and Wade, 2004; Caravenna et al., 2018) and truncated gamma processes are well-defined truncated Lévy subordinators. In this section, we provide key results concerning the densities of hitting time and overshoot of these processes and develop corresponding exact simulation algorithms.

3.4.1 Definitions and Distributional Properties

Definition 3.4.1. *Let Z_t be a Lévy subordinator with the following Laplace transform* [1]

$$\mathbb{E}\left[e^{-vZ_t}\right] = \exp\left(-t\int_0^1 (1 - e^{-vz})\frac{1}{z}e^{-\mu z}\mathrm{d}z\right),$$

[1] Without loss of generality, we set the truncation level $b = 1$ to simplify notation.

where $\mu \in \mathbb{R}^+$ is the scaling parameter that controls the jump size. When $\mu > 0$, Z_t is a truncated gamma process with parameter μ with Lévy measure $\frac{e^{-\mu z}}{z}\mathbf{1}_{\{z<1\}}$. When $\mu = 0$, the associated Laplace transform is given as

$$\mathbb{E}\left[e^{-vZ_t}\right] = \exp\left(-t\int_0^1 \frac{1-e^{-vz}}{z}\mathrm{d}z\right),$$

which is the Laplace transform of a generalised Dickman distribution with parameter t. This is also a Lévy process Z_t with Lévy measure $\frac{1}{z}\mathbf{1}_{\{z<1\}}$, and hence we coin it the Dickman process.

Now, we obtain analytical joint distributions of the first hitting times and overshoots of the truncated gamma process and the Dickman process. This is given in the following Lemma 3.4.1.

Lemma 3.4.1. *Let T be the first hitting time of level 1 of a truncated gamma process Z_t with $\mu \geq 0$, and W be the associated overshoot. Then the joint distribution of (T, W) is given by*

$$f_{T,W}(t,w) = \int_w^1 \frac{e^{\Gamma(0,\mu)t}\mu^t}{\Gamma(t)} y^{t-1}\frac{e^{-\mu(1+w)}}{1+w-y}\mathrm{d}y, \qquad \text{for } \mu > 0, \tag{3.4.1}$$

where $t \in (0,\infty)$, $w \in (0,1)$.
For the Dickman process, the joint density of (T, W) is the limit of (3.4.1) as $\mu \to 0$,

$$f_{T,W}(t,w) = \int_w^1 \frac{e^{-\gamma t}}{\Gamma(t)}\frac{y^{t-1}}{1+w-y}\mathrm{d}y, \tag{3.4.2}$$

where γ is the Euler–Mascheroni constant, $t \in (0,\infty)$, and $w \in (0,1)$.

Proof. Let $f(x,t)$ denote the density of Z_t. For $\mu > 0$, according to Theorem 3.2.1, we have

$$\begin{aligned}
f(x,t) &= \mathcal{L}^{-1}\left\{\mathbb{E}\left[e^{-vZ_t}\right]\right\}\mathbf{1}_{\{0<x<1\}} \\
&= \mathcal{L}^{-1}\left\{\exp\left(-t\int_0^\infty \left(1-e^{-vs}\right)s^{-1}e^{-\mu s}\mathrm{d}s\right)\exp\left(t\int_1^\infty \left(1-e^{-vs}\right)s^{-1}e^{-\mu s}\mathrm{d}s\right)\right\}\mathbf{1}_{\{0<x<1\}} \\
&= \mathcal{L}^{-1}\left\{\left(1+\frac{v}{\mu}\right)^{-t}\exp\left(t\int_1^\infty s^{-1}e^{-\mu s}\mathrm{d}s\right)\sum_{k=0}^\infty \frac{(-t)^k}{k!}\left(\int_1^\infty e^{-vs}s^{-1}e^{-\mu s}\mathrm{d}s\right)^k\right\}\mathbf{1}_{\{0<x<1\}} \\
&= \mathcal{L}^{-1}\left\{e^{t\Gamma(0,\mu)}\left(1+\frac{v}{\mu}\right)^{-t} + e^{t\Gamma(0,\mu)}\left(1+\frac{v}{\mu}\right)^{-t}\sum_{k=1}^\infty \frac{(-t)^k}{k!}\left(\int_1^\infty e^{-vs}s^{-1}e^{-\mu s}\mathrm{d}s\right)^k\right\}\mathbf{1}_{\{0<x<1\}} \\
&= \mathcal{L}^{-1}\left\{e^{t\Gamma(0,\mu)}\left(1+\frac{v}{\mu}\right)^{-t}\right\}\mathbf{1}_{\{0<x<1\}} \\
&= \frac{e^{\Gamma(0,\mu)t}\mu^t}{\Gamma(t)}x^{t-1}e^{-\mu x}\mathbf{1}_{\{0<x<1\}}.
\end{aligned} \tag{3.4.3}$$

According to Theorem 3.2.1, we have

$$P\left(T \in dt, W > w\right) \quad = \quad \int_0^1 \frac{e^{\Gamma(0,\mu)t}\mu^t}{\Gamma(t)} y^{t-1} e^{-\mu y} \int_{1+w-y}^{\infty} z^{-1} e^{-\mu z} \mathrm{d}z\mathrm{d}y, \tag{3.4.4}$$

Differentiating (3.4.4) with respect to w, the joint density of (T, W) in (3.4.1) directly follows. For the Dickman process, we take the limit as $\mu \to 0$. The density of Z_t within $(0,1)$ is obtain by taking limit of (3.4.3), i.e.

$$f(x,t) = \lim_{\mu \to 0} \frac{e^{[\Gamma(0,\mu)+\log(\mu)]t}}{\Gamma(t)} x^{t-1} e^{-\mu x} = \frac{e^{-\gamma t}}{\Gamma(t)} x^{t-1}, \qquad 0 < x < 1, \tag{3.4.5}$$

with γ being the Euler–Mascheroni constant. Hence, associated distribution of (T, W) directly follows (3.4.2). □

Given that the first passage time of Z_t hitting level 1 is greater than t, the distribution of the truncated process Z_t is characterised via its density within $(0,1)$. The details are in Lemma 3.4.2.

Lemma 3.4.2. *The density of* $\{Z_t | Z_t < 1\}$ *is given by*

$$f_{Z_t|Z_t<1}(x|t) = \begin{cases} \frac{\mu^t}{\Gamma(t,\mu)} x^{t-1} e^{-\mu x}, & \mu > 0, \\ t x^{t-1}, & \mu = 0, \end{cases} \tag{3.4.6}$$

where $0 < x < 1$.

Proof. Results in (3.4.6) immediately follows Theorem 3.2.2. □

3.4.2 Exact Simulation Scheme

The first simulation method to sample the Dickman process is based on a density approximation given in Devroye (2001). Later, Fill and Huber (2010) and Devroye and Fawzi (2010) using a dominated coupling from the past procedure for Markov chains. Cloud and Huber (2017) proposed an improvement by running both an upper and lower bound on the Markov chain. Chi (2012) suggested an alternative approach based on a rejection sampling procedure. However, these algorithms are efficient only for the Dickman distribution, where the parameter $t = 1$, and their speed slows down considerably when t gets larger than 1. In this section, based on the marked renewal framework and choosing suitable acceptance-rejection (A/R) envelopes for $f_{T,W}(t,w)$ and $f_{Z_t|Z_t<1}(x|t)$, we develop an alternative simulation algorithm for the Dickman process, which outperforms all the existing simulation algorithms, especially for $t > 1$.

Algorithm 3.4.1 (Exact Simulation of Dickman Process)**.** *The Dickman process can be simulated via the following steps:*

1. *Set* $S = 0$, $\gamma = -digamma(1)$,
2. *Generate* (T, W) *via the following steps:*
   (a) *Generate* $U_1 \sim \mathcal{U}[0,1]$, *and set* $T = -\frac{1}{0.8}\log U_1$,
   (b) *Generate* $Y \sim Beta(T, 0.5)$, $U_2 \sim \mathcal{U}[0,1]$, *and set*
   $$W = Y - 1 + (1-Y)\exp\left(-U_2 \log(1-Y)\right),$$
   (c) *Generate* $V \sim \mathcal{U}[0,1]$, *if*
   $$V \leq \frac{1}{2.35}\frac{\Gamma(0.5)e^{-(\gamma-0.8)T}}{0.8\Gamma(T+0.5)}\frac{(-\log(1-Y))}{(1-Y)^{-0.5}},$$
   then, accept (T, W)*; Otherwise, reject this candidate and go back to Step 2(a),*
3. *If* $t < T$, *go to Step 4; Otherwise, set* $S = S + 1 + W$, $t = t - T$, *and go back to Step 2,*
4. *Generate* $U \sim \mathcal{U}[0,1]$, *and set* $Z = U^{\frac{1}{t}}$,
5. *Return* $S + Z$.

Proof. For the joint density $f_{T,W}(t,w)$, we simulate (T, W, Y) jointly from the integral in (3.4.2),

$$f(t,w,y) = \frac{e^{-\gamma t}y^{t-1}}{\Gamma(t)}\frac{1}{1+w-y},$$

for $t \in (0,\infty)$, $0 < w < y < 1$. The A/R envelope chosen is

$$g(t,w,y) = \sigma e^{-\sigma t}\frac{\Gamma(t+\eta)}{\Gamma(t)\Gamma(\eta)}y^{t-1}(1-y)^{\eta-1}\frac{\frac{1}{1+w-y}}{(-\log(1-y))},$$

where $\sigma = 0.8$ and $\eta = 0.5$ are chosen numerically via two-dimensional optimisation. Furthermore, $f_{Z_t|Z_t<1}(x|t)$ can be simulated directly via inverse transformation resulting in Step 4. □

For the truncated gamma process, we propose the following algorithm based on the marked renewal framework to sample truncated gamma process.

Algorithm 3.4.2 (Exact Simulation of Truncated Gamma Process)**.** *The truncated gamma process can be simulated via the following steps:*

1. *Set* $S = 0$,

2. *Generate* (T, W) *via the following steps:*

   (a) *Numerically minimise*

   $$C(\vartheta, \delta) = \frac{\Gamma(\delta)e^{-\mu}}{\vartheta(1-\delta)e} \frac{e^{\Gamma(0,\mu)\exp(\Gamma(0,\mu)+\vartheta+\log(\mu))}\mu^{\exp(\Gamma(0,\mu)+\vartheta+\log(\mu))}e^{\vartheta\exp(\Gamma(0,\mu)+\vartheta+\log(\mu))}}{\Gamma(\exp(\Gamma(0,\mu)+\vartheta+\log(\mu))+\delta)},$$

   record the optimal value ϑ^* *and* δ^* *and set* $C = C(\vartheta^*, \delta^*)$,

   (b) *Generate* $U_1 \sim \mathcal{U}[0,1]$ *and set* $T = -\frac{1}{\vartheta^*}\log(U_1)$,

   (c) *Generate* $Y \sim Beta(T, \delta^*)$, $U_2 \sim \mathcal{U}[0,1]$ *and set*

   $$W = Y - 1 + (1-Y)\exp\left(-U_2\log(1-Y)\right),$$

   (d) *Generate* $V_1 \sim \mathcal{U}[0,1]$, *if*

   $$V_1 \leq \frac{1}{C}\frac{\Gamma(\delta^*)}{\vartheta^*}\frac{e^{\Gamma(0,\mu)T}\mu^T e^{\vartheta^* T}}{\Gamma(T+\delta^*)}\frac{-\log(1-Y)}{(1-Y)^{\delta^*-1}}e^{-\mu(1+W)},$$

   then, accept (T, W)*; Otherwise, reject this candidate and go back to Step 2(b),*

3. *If* $t < T$, *go to Step 4; Otherwise, set* $S = S + 1 + W$, $t = t - T$ *and go back to Step 2,*

4. *Generate* Z *via the following steps:*

   (a) *Generate* $U_3 \sim \mathcal{U}[0,1]$ *and set* $Z = U_3^{\frac{1}{t}}$.

   (b) *Generate* $V_2 \sim \mathcal{U}[0,1]$, *if*

   $$V_2 \leq \exp(-\mu Z),$$

   then, accept Z*; Otherwise, reject this candidate and go back to Step 4(a),*

5. *Return* $S + Z$.

Proof. For the joint density $f_{T,W}(t,w)$, we simulate (T, W, Y) jointly from the integral in (3.4.1)

,

$$f(t,w,y) = \frac{e^{\Gamma(0,\mu)t}\mu^t}{\Gamma(t)}y^{t-1}\frac{e^{-\mu(1+w)}}{1+w-y},$$

where $t \in (0,\infty)$, $0 < w < y < 1$. We choose the envelope with density of the following form,

$$g(t,w,y) = \vartheta e^{-\vartheta t}\frac{\Gamma(t+\delta)}{\Gamma(t)\Gamma(\delta)}y^{t-1}(1-y)^{\delta-1}\frac{\frac{1}{1+w-y}}{[-\log(1-y)]}.$$

The ratio of the densities is bounded by

$$\frac{f(t,w,y)}{g(t,w,y)} \leq \frac{\Gamma(\delta)e^{-\mu}}{\alpha(1-\delta)e}\frac{e^{\Gamma(0,\mu)t^*}\mu^{t^*}e^{\alpha t^*}}{\Gamma(t^*+\delta)} := C(\vartheta,\delta),$$

where we obtained by maximising the ratio with respect to t,

$$t^* = \exp\left(\Gamma(0,\mu) + \alpha + \log(\mu) + \mathcal{O}\left(\frac{1}{t^*}\right)\right) \approx \exp\left(\Gamma(0,\mu) + \alpha + \log(\mu)\right).$$

We then minimise $C(\vartheta,\delta)$ with respect to ϑ and δ via two dimensional numerical optimisation. Finally, $\{Z_t|Z_t < 1\}$ can be simulated directly via A/R scheme by choosing an envelope with density $g(x,t) = \frac{x^{t-1}}{t}\mathbf{1}_{\{0<x<1\}}$. □

Remark 3.4.1. The numerical optimisation in here and the other parts of this thesis is only carried once before entering the loop. Hence, the optimisation will not slow down the entire simulation procedure.

3.5 Truncated Stable Process

Truncated stable processes and truncated tempered stable processes retain most properties of stable processes and tempered stable processes. In this section, we analyse distributional properties of these processes and develop corresponding exact simulation algorithms based on marked renewal framework.

3.5.1 Definitions and Distributional Properties

Definition 3.5.1. *Let Z_t be a Lévy subordinator with Lévy measure*

$$\nu(z) = \frac{\alpha z^{-\alpha-1}e^{-\mu z}}{\Gamma(1-\alpha)}\mathbf{1}_{\{0<z<1\}}, \tag{3.5.1}$$

where $\alpha \in (0,1)$ is the stability parameter and $\mu \in \mathbb{R}$ is the tilting parameter. The associated Laplace transform is given as

$$\mathbb{E}\left[e^{-vZ_t}\right] = \exp\left(-\frac{\alpha t}{\Gamma(1-\alpha)}\int_0^1 (1-e^{-vz})z^{-\alpha-1}e^{-\mu z}\mathrm{d}z\right), \qquad v \in \mathbb{R}^+.$$

For $\mu = 0$, Z_t is a truncated stable process with stability α. For $\mu > 0$, Z_t is a truncated tempered stable process. For $\mu < 0$, Z_t is also a well-defined Lévy subordinator.

For $\mu = 0$, Z_t is a truncated stable process with stability α. As the density of a stable process can be expressed using an integral representation of Zolotarev (1964), see Kanter (1975), Zolotarev (1986), we can easily obtain analytical expression for the joint distribution (T,W) and the distribution of $\{Z_t|Z_t < 1\}$ based on Theorem 3.2.1 and 3.2.2.

Lemma 3.5.1. *For a truncated stable process Z_t the joint distribution of (T, W) is given by*

$$f_{T,W}(t,w) = \int_w^1 \int_0^\pi \frac{\alpha e^{\frac{t}{\Gamma(1-\alpha)}}}{\pi\Gamma(1-\alpha)} \frac{\alpha}{1-\alpha} A(u) y^{-\frac{1}{1-\alpha}} t^{\frac{1}{1-\alpha}} e^{-A(u)y^{-\frac{\alpha}{1-\alpha}} t^{\frac{1}{1-\alpha}}} \frac{1}{(1+w-y)^{\alpha+1}} \mathrm{d}u\mathrm{d}y, \tag{3.5.2}$$

and

$$A(u) := \left[\frac{\sin(\alpha u)^\alpha \sin((1-\alpha)u)^{1-\alpha}}{\sin u}\right]^{\frac{1}{1-\alpha}}. \tag{3.5.3}$$

In addition, given the hitting time T, the density of $\{Z_t | Z_t < 1\}$ is given by

$$f_{Z_t|Z_t<1}(x|t) = \int_0^\pi \frac{1}{B\pi} \frac{\alpha}{1-\alpha} A(u) x^{-\frac{1}{1-\alpha}} t^{\frac{1}{1-\alpha}} e^{-A(u)x^{-\frac{\alpha}{1-\alpha}} t^{\frac{1}{1-\alpha}}} \mathrm{d}u, \qquad 0 < x < 1, \tag{3.5.4}$$

where

$$B = \int_0^\pi \frac{1}{\pi} e^{-A(u)t^{\frac{1}{1-\alpha}}} \mathrm{d}u.$$

Proof. For a stable process S_t with Laplace transform

$$\mathbb{E}\left[e^{-S_t}\right] = e^{-tv^\alpha},$$

the density of S_t is of the form

$$\begin{aligned} f_\alpha(x,t) &= t^{-\frac{1}{\alpha}} f_\alpha(t^{-\frac{1}{\alpha}}x, 1) \\ &= \frac{1}{\pi}\int_0^\pi \frac{\alpha}{1-\alpha} A(u) x^{-\frac{1}{1-\alpha}} t^{\frac{1}{1-\alpha}} e^{-A(u)x^{-\frac{\alpha}{1-\alpha}} t^{\frac{1}{1-\alpha}}} \mathrm{d}u, \end{aligned} \tag{3.5.5}$$

with $A(u)$ defined in (3.5.3) (Devroye, 2009). Hence, the density of Z_t within $(0,1)$ is given by

$$\begin{aligned} f(x,t) &= \exp\left(\frac{t\alpha}{\Gamma(1-\alpha)} \int_1^\infty x^{-\alpha-1}\mathrm{d}x\right) f_\alpha(x,t) \\ &= \frac{e^{\frac{t}{\Gamma(1-\alpha)}}}{\pi}\int_0^\pi \frac{\alpha}{1-\alpha} A(u) x^{-\frac{1}{1-\alpha}} t^{\frac{1}{1-\alpha}} e^{-A(u)x^{-\frac{\alpha}{1-\alpha}} t^{\frac{1}{1-\alpha}}} \mathrm{d}u. \end{aligned} \tag{3.5.6}$$

The joint distribution of the hitting time and overshoot (T, W) therefore directly follows (3.5.2).

□

For truncated tempered stable process, the joint distribution of (T, W) and the distribution of $\{Z_t | Z_t < 1\}$ depends on the density of the associated tempered stable process. The details are

given below in Lemma 3.5.2.

Lemma 3.5.2. *For a truncated tempered stable process Z_t with Lévy measure (3.5.1) for $\mu > 0$, the density of Z_t within $(0,1)$ is given as*

$$f(x,t;\mu) = \frac{e^{\frac{t}{\Gamma(1-\alpha)}(e^{-\mu}+\mu^{\alpha}\gamma(1-\alpha,\mu))}}{\pi} \int_0^{\pi} \frac{\alpha}{1-\alpha} A(u) x^{-\frac{1}{1-\alpha}} t^{\frac{1}{1-\alpha}} e^{-A(u)x^{-\frac{\alpha}{1-\alpha}} t^{\frac{1}{1-\alpha}} - \mu x} \mathrm{d}u \tag{3.5.7}$$

with $A(u)$ defined in (3.5.3) and $\gamma(\cdot,\cdot)$ is the lower incomplete gamma function such that

$$\gamma(s,x) = \int_0^x y^{s-1} e^{-y} \mathrm{d}y.$$

Proof. For a general tempered stable process S_t with Laplace transform

$$\mathbb{E}\left[e^{-vS_t}\right] = \exp\left(-t\left[(\mu+v)^{\alpha} - \mu^{\alpha}\right]\right)$$

The density of S_t is of the following form

$$f_{\alpha,\mu}(x,t) = e^{\mu^{\alpha}t - \mu x} t^{-\frac{1}{\alpha}} f_{\alpha}(t^{-\frac{1}{\alpha}}x, 1).$$

where $f_{\alpha}(\cdot,1)$ is the associated density of stable distribution with stability α. Hence we obtain (3.5.7) based on the Zolotarev integral representation and Theorem 3.2.1. □

Lemma 3.5.3. *For a truncated tempered stable process X_t, the joint distribution of (T,W) is of the form*

$$f_{T,W}(t,w) = \int_w^1 \int_0^{\pi} \frac{\alpha e^{\frac{(e^{-\mu}+\mu^{\alpha}\gamma(1-\alpha,\mu))t}{\Gamma(1-\alpha)}}}{\pi\Gamma(1-\alpha)} \frac{\alpha}{1-\alpha} A(u) y^{-\frac{1}{1-\alpha}} t^{\frac{1}{1-\alpha}} e^{-A(u)y^{-\frac{\alpha}{1-\alpha}} t^{\frac{1}{1-\alpha}}} \frac{e^{-\mu(1+w)}}{(1+w-y)^{\alpha+1}} \mathrm{d}u\mathrm{d}y. \tag{3.5.8}$$

In addition, given the hitting, the distribution of $\{Z_t | Z_t < 1\}$ is given by

$$f(x,t) = \int_0^{\pi} \frac{1}{D\pi} \frac{\alpha}{1-\alpha} A(u) x^{-\frac{1}{1-\alpha}} t^{\frac{1}{1-\alpha}} e^{-A(u)x^{-\frac{\alpha}{1-\alpha}} t^{\frac{1}{1-\alpha}} - \mu x} \mathrm{d}u, \tag{3.5.9}$$

where

$$D = \int_0^1 \int_0^{\pi} \frac{\alpha}{\pi(1-\alpha)} A(u) x^{-\frac{1}{1-\alpha}} t^{\frac{1}{1-\alpha}} e^{-A(u)x^{-\frac{\alpha}{1-\alpha}} t^{\frac{1}{1-\alpha}} - \mu x} \mathrm{d}u\mathrm{d}x.$$

Proof. (3.5.8) and (3.5.9) are derived directly based on Theorem 3.2.1, 3.2.2 and Lemma 3.5.2. □

3.5.2 Exact Simulation Scheme

For $\mu = 0$, with analytical expressions for the joint distribution (T, W) and the distribution of $\{Z_t | Z_t < 1\}$ in Lemma 3.5.1, we can develop simulation algorithms to sample (T, W) and $\{Z_t | Z_t < 1\}$ accordingly. The details are provided in the following Algorithm 3.5.1 and 3.5.2.

Algorithm 3.5.1 (Exact Simulation of (T, W))**.** *The hitting time and overshoot (T, W) can be simulated via the following steps:*

1. *Set $\zeta = \Gamma(1-\alpha)^{-1}$, and $A_0 = (1-\alpha)\alpha^{\frac{\alpha}{1-\alpha}}$,*
2. *Numerical minimise*

$$C(\lambda) = A_0 e^{\zeta \frac{1}{\alpha} \lambda^{1-\frac{1}{\alpha}} \alpha (1-\alpha)^{\frac{1}{\alpha}-1}} (A_0 - \lambda)^{\alpha-2},$$

   record the optimal value λ^* and set $C = C(\lambda^*)$,

3. *Generate $U \sim \mathcal{U}[0, \pi]$, $U_1 \sim \mathcal{U}[0, 1]$,*
4. *Set $Y = 1 - U_1^{\frac{1}{1-\alpha}}$, $A_U = \left[\sin^\alpha(\alpha U) \sin^{1-\alpha}((1-\alpha)U)/\sin(U)\right]^{\frac{1}{1-\alpha}}$,*
5. *Generate $R \sim \Gamma(2-\alpha, A_U - \lambda)$,*
6. *Generate $V \sim \mathcal{U}[0, 1]$, if*

$$V \leq A_U e^{\zeta R^{1-\alpha} Y^\alpha} e^{-\lambda^* R} (A_U - \lambda^*)^{\alpha-2} Y^{\alpha-1} (1 - (1-Y)^\alpha)/C,$$

   then, accept (R, Y, U) and go to Step 7; Otherwise, reject this candidate and go back to Step 3,

7. *Generate $U_2 \sim \mathcal{U}[0, 1]$,*
8. *Set $T = R^{1-\alpha} Y^\alpha$, and $W = Y - 1 + \left[(1-Y)^{-\alpha} - U_2\left((1-Y)^{-\alpha} - 1\right)\right]^{-\frac{1}{\alpha}}$,*
9. *Return (T, W).*

Proof. The simulation algorithm for (T, W) is developed based on an multi-dimensional A/R scheme. The joint distribution of the hitting time and overshoot is given by

$$f_{T,W}(t, w) = \int_w^1 \int_0^\pi f(t, y, u) f(w|y) \mathrm{d}u \mathrm{d}y,$$

where

$$f(t, y, u) = \frac{\alpha\zeta}{\pi(1-\alpha)} A(u) y^{-\frac{1}{1-\alpha}} t^{\frac{1}{1-\alpha}} e^{-A(u) y^{-\frac{\alpha}{1-\alpha}} t^{\frac{1}{1-\alpha}} + \zeta t} \left((1-y)^{-\alpha} - 1\right),$$

for $t \in (0,\infty)$, $y \in (0,1)$, $u \in (0,\pi)$, and

$$f(w|y) = \frac{\frac{1}{(1+w-y)^{\alpha+1}}}{\frac{1}{\alpha}\left((1-y)^{-\alpha}-1\right)}, \qquad 0 < w < y.$$

with $\zeta = \frac{1}{\Gamma(1-\alpha)}$. We then make a transformation by setting $r = y^{-\frac{\alpha}{1-\alpha}} t^{\frac{1}{1-\alpha}}$, the density of (R, Y, U) is of the form

$$f(r,y,u) = \frac{\alpha\zeta e^{\zeta r^{1-\alpha} y^{\alpha}}}{\pi} A(u) r^{(1-\alpha)} y^{-(1-\alpha)} e^{-A(u)r} (1-y)^{-\alpha} \left(1-(1-y)^{\alpha}\right),$$

for $r \in (0,\infty)$, $y \in (0,1)$, $u \in (0,\pi)$.

To simulate (R, Y, U), we choose an envelope with density

$$g(r,y,u) = \frac{1}{\pi} \frac{(A(u)-\lambda)^{2-\alpha} r^{1-\alpha} e^{-(A(u)-\lambda)r}}{\Gamma(2-\alpha)} (1-\alpha)(1-y)^{-\alpha}.$$

Hence, the ratio of these two densities is given as

$$\begin{aligned} \frac{f(r,y,u)}{g(r,y,u)} &= \frac{\alpha\zeta\Gamma(2-\alpha)A(u)}{(1-\alpha)(A(u)-\lambda)^{2-\alpha}} e^{\zeta r^{1-\alpha} y^{\alpha}} e^{-\lambda r} y^{\alpha-1} (1-(1-y)^{\alpha}) \\ &\leq \frac{\alpha\zeta\Gamma(2-\alpha)A_0}{(1-\alpha)(A_0-\lambda)^{2-\alpha}} e^{\zeta r^{1-\alpha} y^{\alpha}} e^{-\lambda r} y^{\alpha-1} (1-(1-y)^{\alpha}) \\ &\leq \frac{\alpha\zeta\Gamma(2-\alpha)A_0}{(1-\alpha)(A_0-\lambda)^{2-\alpha}} e^{\zeta^{\frac{1}{\alpha}} \lambda^{1-\frac{1}{\alpha}} \alpha(1-\alpha)^{\frac{1}{\alpha}-1}} = C(\lambda), \end{aligned} \tag{3.5.10}$$

where $A_0 = (1-\alpha)\alpha^{\frac{\alpha}{1-\alpha}}$. Note that $C(\lambda)$ can be further minimised over λ via numerical optimisation.

Given Y, we can directly simulate W via inverse transformation as the CDF of $\{W|Y\}$ is given as

$$F(w|y) = \frac{1}{\left((1-y)^{-\alpha}-1\right)} \left[(1-y)^{-\alpha} - (1+w-y)^{-\alpha}\right], \qquad 0 < w < y,$$

which can be inverted explicitly and thus simulated via inverse transformation. □

Algorithm 3.5.2 (Exact Simulation of $\{Z_t|Z_t<1\}$)**.** *The simulation Scheme for* $\{Z_t|Z_t<1\}$ *is given as follows:*

1. *Generate* $U_1 \sim \mathcal{U}[0,\pi]$*, and set*

$$A_{U_1} = \left[\frac{\sin^{\alpha}(\alpha U_1)\sin^{1-\alpha}((1-\alpha)U_1)}{\sin(U_1)}\right]^{\frac{1}{1-\alpha}},$$

2. *Generate* $U_2 \sim \mathcal{U}[0, \pi]$, *and set*

$$Z = \left[-\frac{\log(U_2)}{A_{U_1} t^{\frac{1}{1-\alpha}}} \right]^{-\frac{\alpha}{1-\alpha}}, \tag{3.5.11}$$

if $Z < 1$, *then, accept* Z*; Otherwise, reject this candidate and go back to Step 1.*

Proof. To generate $\{Z_t | Z_t < 1\}$, we can generate the stable process S_t with the density

$$f(x) = \int_0^\pi \frac{1}{\pi} \frac{\alpha}{1-\alpha} A(u) x^{-\frac{1}{1-\alpha}} t^{\frac{1}{1-\alpha}} e^{-A(u) x^{-\frac{\alpha}{1-\alpha}} t^{\frac{1}{1-\alpha}}} \mathrm{d}u, \qquad 0 < x < \infty,$$

If $S_t < 1$, then we accept the candidate. S_t can be simulated via inverse transformation, the CDF is given as

$$F_{S_t}(x) = \int_0^\pi \frac{1}{\pi} e^{-A(u) x^{-\frac{\alpha}{1-\alpha}} t^{\frac{1}{1-\alpha}}} \mathrm{d}u, \qquad 0 < x < \infty,$$

Hence, we first sample a uniform variable uniform variable with domain $(0, \pi)$ and then sample S_t via (3.5.11) through inverse transformation. □

Hence, to generate a truncated stable sample Z_t, we implement the following simulation scheme.

Algorithm 3.5.3 (Exact Simulation of Truncated Stable Process)**.** *The truncated stable* Z_t *can be simulated via Algorithm 3.3.1, by simulating* (T, W) *via Algorithm 3.5.1, and simulating* $\{Z_t | Z_t < 1\}$ *via Algorithm 3.5.2.*

For $\mu > 0$, the truncated tempered stable process Z_t can be simulated either via the marked renewal approach or via simple rejection method based on truncated stable process. Although we can use the marked renewal approach to generate this truncated tempered stable Z_t, due to the complexity of the analytical distribution of (T, W), we therefore design an alternative simulation scheme based on the simulation algorithm for truncated stable process. As the density for the truncated stable is obtained by tempering exponential function to the truncated stable process, we can use an A/R scheme after generating the truncated stable sample. The procedures are illustrated in Algorithm 3.5.4.

Algorithm 3.5.4 (Exact Simulation of Truncated Tempered Stable Process)**.** *The truncated tempered stable* Z_t *with* $\mu > 0$ *can be simulated via the following steps:*

1. *Generate a truncated stable process* Z_t *with stability* α *via Algorithm 3.5.3,*

2. *Generate* $V \sim \mathcal{U}[0,1]$, *if*

$$V \leq \exp(-\mu Z_t),$$

then, accept Z_t*; Otherwise, reject this candidate and go back to step 1.*

This algorithm relies on the fact that the density of the truncated tempered stable process is obtained by multiplying an exponential function to the density of the truncated stable process. The algorithm only works efficiently for smaller tilting parameter μ. As the complexity of the algorithm is given by $\exp(\mu)$, the computation costs will increase rapidly when the tilting parameter increases. In order to improve the efficiency and reduce simulation time, we develop the following simulation algorithm to generate truncated tempered stable process.

Algorithm 3.5.5 (Enhanced Exact Simulation of Truncated Tempered Stable Process)**.** *Given* $\mu > 0$ *and a constant* $b \in (0,1)$*, the simulation scheme for truncated tempered stable process* Z_t *is given as follows:*

1. *Generate a truncated tempered stable* Y_t *with stability* α*, skewness* $M = \mu b$*, and scale* $\frac{\alpha}{b^\alpha \Gamma(1-\alpha)}$ *via Algorithm 3.5.4,*
2. *Generate* $N_t \sim$ *Poisson* $\left(\frac{t}{\Gamma(1-\alpha)}\left[\left(b^{-\alpha}e^{-b\mu} - e^{-\mu}\right) + \mu^\alpha\left(\Gamma(1-\alpha,\mu) - \Gamma(1-\alpha,\mu b)\right)\right]\right)$,
3. *Generate* $\{J_i\}_{i=1,2,\ldots,N_t}$ *using an A/R scheme via the following steps,*
   (a) *Numerical minimise*

$$C(\kappa) = \frac{\alpha\left(e^{-(\kappa+\mu)b} - e^{-(\kappa+\mu)}\right)\max\left\{e^{\kappa}, \frac{e^{\kappa b}}{b^{\alpha+1}}\right\}}{(\kappa+\mu)\left[\left(b^{-\alpha}e^{-b\mu} - e^{-\mu}\right) + \mu^\alpha\left(\Gamma(1-\alpha,\mu) - \Gamma(1-\alpha,\mu b)\right)\right]}, \quad (3.5.12)$$

   record the optimal value κ^**,*
   (b) *Generate* J_i *by setting*

$$J_i = \frac{1}{(\kappa^*+\mu)}\ln\left(e^{-(\kappa^*+\mu)b} - (e^{-(\kappa^*+\mu)b} - e^{-(\kappa^*+\mu)})U\right), \qquad U \sim \mathcal{U}[0,1],$$

   (c) *Generate* $V \sim \mathcal{U}[0,1]$, *if*

$$V \leq \frac{1}{\max\left\{e^{\kappa^*}, \frac{e^{\kappa^* b}}{b^{\alpha+1}}\right\} {J_i}^{\alpha+1}} e^{\kappa^* J_i}, \quad (3.5.13)$$

   then, accept J_i*; Otherwise, reject this candidate and go back to Step 3(b),*
4. *Return* $b \times Y_t + \sum_{i=1}^{N_t} J_i$.

Proof. For a truncated tempered stable process Z_t with $\mu > 0$, the Laplace transform is of the following form

$$\begin{aligned}
&\mathbb{E}\left[e^{-vZ_t}\right] \\
= \;& \exp\left(-\frac{\alpha t}{\Gamma(1-\alpha)}\int_0^1 (1-e^{-vz})z^{-\alpha-1}e^{-\mu z}\mathrm{d}z\right) \\
= \;& \exp\left(-\frac{\alpha t}{\Gamma(1-\alpha)}\int_0^b (1-e^{-vz})\frac{e^{-\mu z}}{z^{\alpha+1}}\mathrm{d}z\right)\exp\left(-\frac{\alpha t}{\Gamma(1-\alpha)}\int_b^1 (1-e^{-vz})\frac{e^{-\mu z}}{z^{\alpha+1}}\mathrm{d}z\right) \\
= \;& \exp\left(-\frac{\alpha t}{b^\alpha\Gamma(1-\alpha)}\int_0^1 (1-e^{-vbz})\frac{e^{-\mu bz}}{z^{\alpha+1}}\mathrm{d}z\right)\exp\left(-\frac{\alpha t}{\Gamma(1-\alpha)}\int_b^1 (1-e^{-vz})\frac{e^{-\mu z}}{z^{\alpha+1}}\mathrm{d}z\right),
\end{aligned}$$

where $b < 1$. Hence, we have

$$Z_t \overset{\mathcal{D}}{=} b \times Y_t + \sum_{i=1}^{N_t} J_i,$$

where

- Y_t is a truncated tempered stable process with Lévy measure

$$\nu(\mathrm{d}y) = \frac{\alpha}{b^\alpha\Gamma(1-\alpha)}\frac{e^{-My}}{y^{\alpha+1}}, \qquad \text{for} \quad M = \mu b;$$

- $\sum_{i=1}^{N_t} J_i$ is a compound Poisson process with
  - N_t is a Poisson process with rate

$$\frac{t}{\Gamma(1-\alpha)}\left[\left(b^{-\alpha}e^{-b\mu} - e^{-\mu}\right) + \mu^\alpha\left(\Gamma(1-\alpha,\mu) - \Gamma(1-\alpha,\mu b)\right)\right];$$

  - $\{J_i\}_{i=1,2,\ldots}$ are i.i.d jumps with density

$$f_{J_i}(x) = \frac{\alpha x^{-\alpha-1}e^{-\mu x}}{\left[\left(b^{-\alpha}e^{-b\mu} - e^{-\mu}\right) + \mu^\alpha\left(\Gamma(1-\alpha,\mu) - \Gamma(1-\alpha,\mu b)\right)\right]},$$

    for $x \in (b, 1)$.

These i.i.d jumps can be simulated via A/R scheme, we choose an envelope with density

$$g(x) = \frac{(\kappa+\mu)e^{-(\kappa+\mu)x}}{e^{-(\kappa+\mu)b} - e^{-(\kappa+\mu)}}.$$

The A/R constant is given as $C(\kappa^*)$ in (3.5.12), where κ^* is the critical value that minimises $C(\kappa)$.

□

Since we break the truncated tempered stable process into a truncated tempered process with a smaller tilting parameter and a compound Poisson process, the computation costs will be reduced for the truncated tempered stable process with smaller tilting parameter, but there will be extra costs to generate the compound Poisson process. Therefore, we also need to consider the efficiency to generate the compound Poisson process to choose an optimal b to decompose the process.

Finally, for $\mu < 0$, we could follow Algorithm 3.5.6 to simulate Z_t.

Algorithm 3.5.6 (Exact Simulation of Z_t with $\mu < 0$)**.** *The simulation scheme for $\mu < 0$ is given as follows:*

1. *Generate a truncated stable Y_t via Algorithm 3.5.3,*
2. *Generate $N_t \sim$ Poisson $\left(\frac{t\alpha F}{\Gamma(1-\alpha)}\right)$, where*

$$F = \int_0^1 (e^{|\mu|x} - 1)x^{-\alpha-1}\mathrm{d}x, \tag{3.5.14}$$

3. *Generate $\{J_i\}_{i=1,2,\ldots,N_t}$ using an A/R scheme via the following steps,*

   (1) Numerical minimise

$$C(\xi) = \frac{e^{\xi} - 1}{F\xi(1-\alpha)} \max\left\{(e^{|\mu|} - 1)e^{-\xi}, |\mu|\right\},$$

   record the optimal value ξ^*,

   (2) Generate J_i by setting

$$J_i = \left[\frac{1}{\xi^*}\log\left(U\left(e^{\xi^*} - 1\right) + 1\right)\right]^{\frac{1}{1-\alpha}}, \qquad U \sim \mathcal{U}[0,1],$$

   (3) Generate $V \sim \mathcal{U}[0,1]$, if

$$V \leq \frac{(e^{|\mu|J_i} - 1)e^{-\xi^* J_i^{1-\alpha}}}{J_i \max\left\{(e^{|\mu|} - 1)e^{-\xi^*}, |\mu|\right\}},$$

   then, accept J_i; Otherwise, reject this candidate and go back to Step (2),

4. *Return $Y_t + \sum_{i=0}^{N_t} J_i$.*

Proof. For $\mu < 0$, Z_t can be decomposed into a truncated stable process Y_t with Lévy measure in (3.5.1) with $\mu = 0$ and a compound Poisson process with poisson rate $\frac{t\alpha F}{\Gamma(1-\alpha)}$ for F in (3.5.14).

The density of i.i.d jumps $\{J_i\}_{i=1,2,...}$ is given as

$$f_{J_i}(x) = \frac{1}{F}\frac{e^{|\mu|x}-1}{x^{\alpha+1}}, \qquad 0 < x < 1.$$

We simulate J_i using an A/R scheme by choosing an envelope J_i' with density

$$g_{J_i'}(x) = \frac{\xi(1-\alpha)}{e^{\xi}-1}\frac{e^{\xi x^{1-\alpha}}}{x^{\alpha}}, \qquad 0 < x < 1,$$

the CDF is given by

$$G_{J_i'}(x) = \frac{e^{\xi x^{1-\alpha}}-1}{e^{\xi}-1}, \qquad 0 < x < 1,$$

which can be inverted explicitly and thus J_i' can be simulated via inverse transformation. To find the A/R constant, we have

$$\begin{aligned}\frac{f_{J_i}(x)}{g_{J_i'}(x)} &= \frac{e^{\xi}-1}{F\xi(1-\alpha)}\frac{(e^{|\mu|x}-1)e^{-\xi x^{1-\alpha}}}{x} \\ &\leq \frac{e^{\xi}-1}{F\xi(1-\alpha)}\max\left\{(e^{|\mu|}-1)e^{-\xi}, |\mu|\right\} \qquad (3.5.15)\end{aligned}$$

The A/R constant depends on the input μ, in order to obtain high acceptance rate, we use numerical optimization to find the optimal ξ^* that minimises (3.5.15). □

3.5.3 Special Case: Truncated Inverse Gaussian Processes

In this section, we consider specifically the truncated inverse Gaussian Z_t associated with Lévy measure

$$\nu(z) = \frac{1}{\sqrt{2\pi z^3}}e^{-\mu z}\mathbf{1}_{\{0<z<1\}}, \quad \mu \in \mathbb{R}.$$

For $\mu > 0$, Z_t is a truncated inverse Gaussian process. We provide the joint density of the hitting time and overshoot as below in Proposition 3.5.1.

Proposition 3.5.1. *For a truncated inverse Gaussian Z_t with $\mu \in \mathbb{R}^+$, the joint distribution of the hitting time T and overshoot W is given by*

$$\begin{aligned}f_{T,W}(t,w) &= \frac{e^{t\left(\sqrt{\frac{2}{\pi}}e^{-\mu}+\sqrt{2\mu}\,\mathrm{Erf}(\sqrt{\mu})\right)}e^{-\mu(1+w)}e^{-\frac{t^2}{2(1+w)}}}{\sqrt{2\pi}(1+w)^{\frac{3}{2}}} \\ &\quad\times\left(1-\frac{t^2}{1+w}\right)\left(Erf\left(\frac{t}{\sqrt{2w(1+w)}}\right)-Erf\left(\frac{t\sqrt{w}}{\sqrt{2(1+w)}}\right)\right) \\ &\quad+\frac{te^{t\left(\sqrt{\frac{2}{\pi}}e^{-\mu}+\sqrt{2\mu}\,\mathrm{Erf}(\sqrt{\mu})\right)}e^{-\mu(1+w)}}{\pi\sqrt{w}(1+w)^2}\left(e^{-\frac{t^2}{2}}-we^{-\frac{t^2}{2w}}\right), \qquad (3.5.16)\end{aligned}$$

for $t \in \mathbb{R}^+$ *and* $w \in (0,1)$.

Proof. According to Theorem 3.2.1, the joint distribution of (T, W) satisfies (3.2.1). First, one can derive the density of Z_t within $(0,1)$ through its Laplace transform,

$$
\begin{aligned}
& f(y,t) \\
= \;& \mathcal{L}^{-1}\left\{\mathbb{E}\left[e^{-vZ_t}\right]\right\} 1_{\{0<y<1\}} \\
= \;& \mathcal{L}^{-1}\left\{\exp\left(-t\int_0^1 \left(1-e^{-vy}\right)\frac{1}{\sqrt{2\pi y^3}}e^{-\frac{(\sqrt{2\mu})^2 y}{2}}\mathrm{d}y\right)\right\}\mathbf{1}_{\{0<y<1\}} \\
= \;& \mathcal{L}^{-1}\left\{\int_0^\infty e^{-vy}\frac{te^{-\frac{(\sqrt{2\mu}y-t)^2}{2y}}}{\sqrt{2\pi y^3}}\mathrm{d}y \exp\left(t\int_1^\infty \frac{e^{-\mu y}}{\sqrt{2\pi y^3}}\mathrm{d}y\right)\exp\left(-t\int_1^\infty \frac{e^{-vy}}{\sqrt{2\pi y^3}}e^{-\frac{(\sqrt{2\mu})^2 y}{2}}\mathrm{d}y\right)\right\}\mathbf{1}_{\{0<y<1\}} \\
= \;& \mathcal{L}^{-1}\left\{e^{-t(\sqrt{2v+2\mu}-2\mu)}\exp\left(t\int_1^\infty \frac{e^{-\mu y}}{\sqrt{2\pi y^3}}\mathrm{d}y\right)\sum_{k=0}^\infty \frac{(-t)^k}{k!}\left(\int_1^\infty \frac{e^{-vy}e^{-\mu y}}{\sqrt{2\pi y^3}}\mathrm{d}y\right)^k\right\}\mathbf{1}_{\{0<y<1\}} \\
= \;& \frac{t}{\sqrt{2\pi y^3}}e^{-\frac{(\sqrt{2\mu}y-t)^2}{2y}}\exp\left(t\int_1^\infty \frac{e^{-\mu y}}{\sqrt{2\pi y^3}}\mathrm{d}y\right) \\
= \;& \frac{t}{\sqrt{2\pi y^3}}e^{-\frac{(\sqrt{2\mu}y-t)^2}{2y}}e^{t\left(\sqrt{\frac{2}{\pi}}e^{-\mu}-\sqrt{2\mu}\,\mathrm{Erfc}(\sqrt{\mu})\right)}.
\end{aligned}
$$

The joint distribution of the hitting time and overshoot (T, W) is therefore

$$
\begin{aligned}
& f_{T,W}(t,w) \\
= \;& \int_0^1 f(y,t)\nu(1+w-y)\mathrm{d}y \\
= \;& \int_w^1 \frac{t}{\sqrt{2\pi y^3}}e^{-\frac{(\sqrt{2\mu}y-t)^2}{2y}}e^{t\left(\sqrt{\frac{2}{\pi}}e^{-\mu}-\sqrt{2\mu}\,\mathrm{Erfc}(\sqrt{\mu})\right)}\frac{e^{-\mu(1+w-y)}}{\sqrt{2\pi(1+w-y)^3}}\mathrm{d}y \\
= \;& \frac{te^{t\left(\sqrt{\frac{2}{\pi}}e^{-\mu}+\sqrt{2\mu}\,\mathrm{Erf}(\sqrt{\mu})\right)}e^{-\mu(1+w)}}{2\pi}\int_w^1 \frac{1}{\sqrt{y^3(1+w-y)^3}}e^{-\frac{t^2}{2y}}\mathrm{d}y \\
= \;& \frac{te^{t\left(\sqrt{\frac{2}{\pi}}e^{-\mu}+\sqrt{2\mu}\,\mathrm{Erf}(\sqrt{\mu})\right)}e^{-\mu(1+w)}}{2\pi}\int_1^{\frac{1}{w}} \frac{u}{\sqrt{[(1+w)u-1]^3}}e^{-\frac{t^2 u}{2}}\mathrm{d}u \\
= \;& \frac{te^{t\left(\sqrt{\frac{2}{\pi}}e^{-\mu}+\sqrt{2\mu}\,\mathrm{Erf}(\sqrt{\mu})\right)}e^{-\mu(1+w)}e^{-\frac{t^2}{2(1+w)}}}{2\pi(1+w)^2}\int_w^{\frac{1}{w}} \frac{v+1}{\sqrt{v^3}}e^{-\frac{t^2 v}{2(1+w)}}\mathrm{d}v \\
= \;& \frac{te^{t\left(\sqrt{\frac{2}{\pi}}e^{-\mu}+\sqrt{2\mu}\,\mathrm{Erf}(\sqrt{\mu})\right)}e^{-\mu(1+w)}e^{-\frac{t^2}{2(1+w)}}}{2\pi(1+w)^2}\left[\int_w^{\frac{1}{w}} \frac{1}{\sqrt{v}}e^{-\frac{t^2 v}{2(1+w)}}\mathrm{d}v + \int_w^{\frac{1}{w}} \frac{1}{\sqrt{v^3}}e^{-\frac{t^2 v}{2(1+w)}}\mathrm{d}v\right].
\end{aligned}
\tag{3.5.17}
$$

We also have

$$\begin{aligned}
&\int_w^{\frac{1}{w}} \frac{1}{\sqrt{v}} e^{-\frac{t^2 v}{2(1+w)}} \mathrm{d}v \\
&= \left[\frac{\sqrt{2\pi}\sqrt{1+w}}{t} \mathrm{Erf}\left(\frac{t\sqrt{v}}{\sqrt{2(1+w)}} \right) \right]_w^{\frac{1}{w}} \\
&= \frac{\sqrt{2\pi}\sqrt{1+w}}{t} \left[\mathrm{Erf}\left(\frac{t}{\sqrt{2w(1+w)}} \right) - \mathrm{Erf}\left(\frac{t\sqrt{w}}{\sqrt{2(1+w)}} \right) \right],
\end{aligned} \tag{3.5.18}$$

and

$$\begin{aligned}
&\int_w^{\frac{1}{w}} \frac{1}{\sqrt{v^3}} e^{-\frac{t^2 v}{2(1+w)}} \mathrm{d}v \\
&= \left[-\frac{2}{\sqrt{v}} e^{-\frac{t^2 v}{2(1+w)}} - \frac{\sqrt{2\pi}t}{\sqrt{1+w}} \mathrm{Erf}\left(\frac{t\sqrt{v}}{\sqrt{2(1+w)}} \right) \right]_w^{\frac{1}{w}} \\
&= \left(\frac{2}{\sqrt{w}} e^{-\frac{t^2 w}{2(1+w)}} - 2\sqrt{w} e^{-\frac{t^2}{2w(1+w)}} \right) - \frac{\sqrt{2\pi}t}{\sqrt{1+w}} \left[\mathrm{Erf}\left(\frac{t}{\sqrt{2w(1+w)}} \right) - \mathrm{Erf}\left(\frac{t\sqrt{w}}{\sqrt{2(1+w)}} \right) \right].
\end{aligned} \tag{3.5.19}$$

Combining (3.5.17), (3.5.18) and (3.5.19), the joint density of (T, W) immediately follows (3.5.16).

□

The closed form marginal distribution of the hitting time therefore can be derived by integrating the joint distribution of the hitting time and overshoot. The details are provided in Corollary 3.5.1.

Corollary 3.5.1. *The marginal distribution of the hitting time T for X_t is given by*

$$\begin{aligned}
&f_T(t) \\
&= e^{t\left(\sqrt{\frac{2}{\pi}} e^{-\mu} + \sqrt{2\mu}\,\mathrm{Erf}(\sqrt{\mu})\right)} \left(\sqrt{\frac{2}{\pi}} e^{-\mu} e^{-\frac{t^2}{2}} - \frac{1}{2} e^{\sqrt{2\mu}t} \left(1 - \mathrm{Erf}\left(\sqrt{\mu} + \frac{t}{\sqrt{2}} \right) \right) \right. \\
&\times \left[\sqrt{\frac{2}{\pi}} e^{-\mu} + \sqrt{2\mu}\,\mathrm{Erfc}(-\sqrt{\mu}) \right] - \frac{1}{2} e^{\sqrt{2\mu}t} \left(1 + \mathrm{Erf}\left(\sqrt{\mu} - \frac{t}{\sqrt{2}} \right) \right) \\
&\left. \times \left[\sqrt{\frac{2}{\pi}} e^{-\mu} - \sqrt{2\mu}\,\mathrm{Erfc}(\sqrt{\mu}) \right] \right),
\end{aligned} \tag{3.5.20}$$

for $t \in \mathbb{R}^+$.

Proof. Since

$$\begin{aligned}\int_0^y \frac{e^{-\mu(1+w-y)}}{\sqrt{2\pi(1+w-y)^3}}\mathrm{d}w &= \int_{1-y}^1 \frac{e^{-\mu z}}{\sqrt{2\pi z^3}}\mathrm{d}z \\ &= \sqrt{\frac{2}{\pi}}\left[\frac{e^{-\mu(1-y)}}{\sqrt{1-y}} - e^{-\mu}\right] - \sqrt{2\mu}\left[\mathrm{Erf}(\sqrt{\mu}) - \mathrm{Erf}(\sqrt{(1-y)\mu})\right],\end{aligned}$$

therefore, the marginal density of T is given by

$$\begin{aligned}f_T(t) &= \int_0^1 \frac{te^{t\left(\sqrt{\frac{2}{\pi}}e^{-\mu}+\sqrt{2\mu}\,\mathrm{Erf}(\sqrt{\mu})\right)}}{\sqrt{2\pi y^3}} e^{-\frac{t^2}{2y}-\mu y}\Bigg(\left(\sqrt{\frac{2}{\pi}}\frac{e^{-\mu(1-y)}}{\sqrt{1-y}} + \sqrt{2\mu}\,\mathrm{Erf}(\sqrt{(1-y)\mu})\right) \\ &\quad - \left(\sqrt{\frac{2}{\pi}}e^{-\mu} + \sqrt{2\mu}\,\mathrm{Erf}(\sqrt{\mu})\right)\Bigg)\mathrm{d}y. \qquad (3.5.21)\end{aligned}$$

First of all, we have

$$\int_0^1 \frac{e^{-\frac{t^2}{2y}}e^{-\mu y}}{y^{3/2}}\mathrm{d}y = \frac{\sqrt{2\pi}}{2t}\left(e^{\sqrt{2\mu}t}\left(1-\mathrm{Erf}\left(\sqrt{\mu}+\frac{t}{\sqrt{2}}\right)\right) + e^{-\sqrt{2\mu}t}\left(1+\mathrm{Erf}\left(\sqrt{\mu}-\frac{t}{\sqrt{2}}\right)\right)\right), \qquad (3.5.22)$$

and

$$\int_0^1 \frac{e^{-\frac{t^2}{2y}}}{y^{3/2}\sqrt{1-y}}\mathrm{d}y = \left[-\frac{\sqrt{2\pi}e^{-\frac{t^2}{2}}\,\mathrm{Erf}\left(\frac{t\sqrt{1-y}}{\sqrt{2y}}\right)}{t}\right]_0^1 = \frac{\sqrt{2\pi}}{t}e^{-\frac{t^2}{2}}. \qquad (3.5.23)$$

In addition, we have

$$\int_0^1 \frac{e^{-\frac{t^2}{2y}}e^{-\mu y}}{y^{3/2}}\,\mathrm{Erf}\left(\sqrt{(1-y)\mu}\right)\mathrm{d}y = \int_0^1 \frac{e^{-\frac{t^2}{2y}}e^{-\mu y}}{y^{3/2}}\left(1-2\int_{\sqrt{2\mu(1-y)}}^\infty \frac{1}{\sqrt{2\pi}}e^{-\frac{x^2}{2}}dx\right)\mathrm{d}y, \qquad (3.5.24)$$

and

$$\begin{aligned}&\sqrt{\frac{2}{\pi}}\int_0^1 \frac{e^{-\frac{t^2}{2y}}e^{-\mu y}}{y^{3/2}}\int_{\sqrt{2\mu(1-y)}}^\infty e^{-\frac{x^2}{2}}\mathrm{d}x\mathrm{d}y \\ =\ &\sqrt{\frac{2}{\pi}}\int_0^1 \frac{e^{-\frac{t^2}{2y}}e^{-\mu y}}{y^{3/2}}\int_0^\infty e^{-\frac{x^2}{4\mu(1-y)}}e^{-x}e^{-\mu(1-y)}\frac{1}{\sqrt{2\mu(1-y)}}\mathrm{d}x\mathrm{d}y \\ =\ &\sqrt{\frac{2}{\pi}}\int_0^\infty e^{-\sqrt{2\mu}x}\int_0^1 \frac{e^{-\frac{t^2}{2y}}}{y^{3/2}}e^{-\mu}e^{-\frac{x^2}{2(1-y)}}\frac{1}{\sqrt{1-y}}\mathrm{d}y\mathrm{d}x\end{aligned}$$

$$
\begin{aligned}
&= \sqrt{\frac{2}{\pi}} \int_0^\infty e^{-\mu} e^{-\sqrt{2\mu}x} \frac{\sqrt{2\pi}}{t} e^{-\frac{(x+t)^2}{2}} \mathrm{d}x \\
&= \frac{\sqrt{2\pi}}{t} e^{\sqrt{2\mu}t} \left(1 - \mathrm{Erf}\left(\sqrt{\mu} + \frac{t}{\sqrt{2}}\right)\right). \qquad (3.5.25)
\end{aligned}
$$

Substituting (3.5.22), (3.5.23), (3.5.24), and (3.5.25) into (3.5.21), the density of T directly follows (3.5.20). □

Proposition 3.5.2. *Given the hitting time T, the density of $\{Z_t | Z_t < 1\}$ is given by*

$$
f_{Z_t|Z_t<1}(x|t) = \frac{\frac{t}{\sqrt{2\pi x^3}} e^{-\frac{t^2}{2x} - \mu x}}{\frac{1}{2}\left(e^{-t\sqrt{2\mu}} \mathrm{Erfc}\left(\frac{t}{\sqrt{2}} - \sqrt{\mu}\right) + e^{t\sqrt{2\mu}} \mathrm{Erfc}\left(\frac{t}{\sqrt{2}} + \sqrt{\mu}\right)\right)}, \qquad 0 < x < 1. \qquad (3.5.26)
$$

Proof. According to Theorem 3.2.2, we have

$$
\begin{aligned}
f_{Z_t|Z_t<1}(x|t) &= \frac{\frac{t}{\sqrt{2\pi x^3}} e^{-\frac{(\sqrt{2\mu}x - t)^2}{2x}} e^{t\left(\sqrt{\frac{2}{\pi}} e^{-\mu} - \sqrt{2\mu}\,\mathrm{Erfc}(\sqrt{\mu})\right)}}{\int_0^1 \frac{t}{\sqrt{2\pi x^3}} e^{-\frac{(\sqrt{2\mu}x - t)^2}{2x}} e^{t\left(\sqrt{\frac{2}{\pi}} e^{-\mu} - \sqrt{2\mu}\,\mathrm{Erfc}(\sqrt{\mu})\right)} \mathrm{d}x} \\
&= \frac{1}{D} \frac{t}{\sqrt{2\pi x^3}} e^{-\frac{t^2}{2x} - \mu x},
\end{aligned}
$$

where

$$
\begin{aligned}
D &= \int_0^1 \frac{t}{\sqrt{2\pi x^3}} e^{-\frac{t^2}{2x} - \mu x} \mathrm{d}x \\
&= \frac{1}{2}\left(e^{-t\sqrt{2\mu}} \mathrm{Erfc}\left(\frac{t}{\sqrt{2}} - \sqrt{\mu}\right) + e^{t\sqrt{2\mu}} \mathrm{Erfc}\left(\frac{t}{\sqrt{2}} + \sqrt{\mu}\right)\right). \qquad (3.5.27)
\end{aligned}
$$

Given T, the conditional density $f_{Z_t|Z_t<1}$ is a proper density function as $f_{Z_t|Z_t<1}(x|t) > 0$ for all $x \in (0,1)$ and $\int_0^\infty f_{Z_t|Z_t<1}(x|t)\mathrm{d}x = 1$. □

For μ equal to 0, Z_t is a truncated stable process with stability index $\alpha = 1/2$, this has obvious connections with the Parisian stopping time or drawdown stopping time of Brownian motion, see Dassios and Lim (2018). The joint distribution of its first passage time and the overshoot, the marginal distribution of the first passage time and the conditional distribution of the truncated process given the hitting time have simpler expressions which allow us to develop enhanced simulation algorithms. The relevant results are listed in Corollary 3.5.2 below.

Corollary 3.5.2. *Let $f_{T,W}(t,w)$ denote the joint density of the hitting time T and the overshoot W*

at the time of a truncated stable process Z_t with Lévy measure

$$\nu(z) = \frac{1}{\sqrt{2\pi}} z^{-\frac{3}{2}} \mathbf{1}_{\{0<z<1\}},$$

let $f_T(t)$ denote the density of T, and $f_{Z_t|Z_t<1}(x|t)$ denote the conditional density of $Z_t|Z_t < 1$. Then we have the following results:

$$\begin{aligned} f_{T,W}(t,w) &= \frac{e^{\sqrt{\frac{2}{\pi}}t} e^{-\frac{t^2}{2(w+1)}}}{\sqrt{2\pi}(w+1)^{3/2}} \left(1 - \frac{t^2}{w+1}\right) \left(\text{Erf}\left(\frac{t}{\sqrt{2w(w+1)}}\right) - \text{Erf}\left(t\sqrt{\frac{w}{2(w+1)}}\right)\right) \\ &\quad + \frac{te^{\sqrt{\frac{2}{\pi}}t}}{\pi\sqrt{w}(w+1)^2} \left(e^{-\frac{t^2}{2}} - we^{-\frac{t^2}{2w}}\right), \qquad (3.5.28) \\ f_T(t) &= \sqrt{\frac{2}{\pi}} e^{\sqrt{\frac{2}{\pi}}t} \left(e^{-\frac{t^2}{2}} - \text{Erfc}\left(\frac{t}{\sqrt{2}}\right)\right), \qquad (3.5.29) \\ f_{Z_t|Z_t<1}(x|t) &= \frac{1}{\text{Erfc}\left(\frac{t}{\sqrt{2}}\right)} \frac{t}{\sqrt{2\pi x^3}} e^{-\frac{t^2}{2x}}, \qquad 0 < x < 1. \qquad (3.5.30) \end{aligned}$$

Proof. These formulas directly follow (3.5.16), (3.5.20) and (3.5.26) with $\mu = 0$. □

Since the analytical joint distribution of hitting time and overshoot and conditional distribution of $\{Z_t|Z_t < 1\}$ for the truncated stable with index $1/2$ and inverse Gaussian processes are available, we, therefore, develop more efficient simulation algorithm to sample these processes. First, let us consider the simulation algorithm for the truncated stable process with stability index $1/2$.

Algorithm 3.5.7 (Exact Simulation of Truncated Stable $1/2$)**.** *The simulation scheme for truncated stable with stability $1/2$ is given as follows:*

1. *Set $S = 0$,*

2. *Generate (T, W) via the following steps:*

   (1) Generate T by setting

   $$T = \sqrt{-\log(U_1)}/0.33, \qquad U_1 \sim \mathcal{U}[0,1],$$

   (2) Generate W by setting

   $$W = 2 - U_2 - \sqrt{1 - U_2} \qquad U_2 \sim \mathcal{U}[0,1],$$

(3) Generate $V_1 \sim \mathcal{U}[0,1]$, if

$$V_1 \leq \frac{\frac{e^T\sqrt{\frac{2}{\pi}}-\frac{T^2}{2(1+W)}}{\sqrt{2\pi}(1+W)^{\frac{3}{2}}}\left(1-\frac{T^2}{1+W}\right)\left(Erf\left(\frac{T}{\sqrt{2W(1+W)}}\right)-Erf\left(\frac{T\sqrt{W}}{\sqrt{2(1+W)}}\right)\right)+\frac{Te^T\sqrt{\frac{2}{\pi}}\left(e^{-\frac{T^2}{2}}-We^{-\frac{T^2}{2W}}\right)}{\pi\sqrt{W}(1+W)^2}}{1.21\times 0.66Te^{-0.33T^2}\left(\frac{1}{\sqrt{W}}-1\right)},$$

then, accept (T,W); Otherwise, go back to Step (1),

With the accepted (T,W), if $t<T$, go to step 3; Otherwise, go to step 4,

3. *Generate Z via the following steps,*

   (I) Generate Z by setting

$$Z = t^2/\left[t^2 - 2\ln(U_3)\right], \qquad U_3 \sim \mathcal{U}[0,1], \tag{3.5.31}$$

   (II) Generate $V_2 \sim \mathcal{U}[0,1]$, if

$$V_2 \leq \sqrt{Z}, \tag{3.5.32}$$

   then, accept Z; Otherwise, go back to Step 3(I),

   With the accepted Z, then go to step 5,

4. *Set $S = S + 1 + W$ and $t = t - T$ then go back to step 2,*

5. *Return $S + Z$.*

Proof. The simulation algorithms for (T,W) and $\{Z_t|Z_t < 1\}$ are developed based on A/R schemes using the densities given in Corollary 3.5.2. To generate (T,W), we choose an envelope (T',W') with density function

$$g(t,w) = 2\alpha t e^{-\alpha t^2}\left(\frac{1}{\sqrt{w}}-1\right), \qquad \alpha > 0,$$

so that (T',W') can be simulated jointly and directly via explicit inverse transformation. The A/R constant is given by

$$\begin{aligned}
&\frac{f_{T,W}(t,w)}{g(t,w)}\\
=\ &\frac{\frac{e^t\sqrt{\frac{2}{\pi}}e^{-\frac{t^2}{2(1+w)}}}{\sqrt{2\pi}(1+w)^{\frac{3}{2}}}\left(1-\frac{t^2}{1+w}\right)\left(\mathrm{Erf}\left(\frac{t}{\sqrt{2w(1+w)}}\right)-\mathrm{Erf}\left(\frac{t\sqrt{w}}{\sqrt{2(1+w)}}\right)\right)}{2\alpha t e^{-\alpha t^2}\left(\frac{1}{\sqrt{w}}-1\right)}+\frac{\frac{te^t\sqrt{\frac{2}{\pi}}}{\pi\sqrt{w}(1+w)^2}\left(e^{-\frac{t^2}{2}}-we^{-\frac{t^2}{2w}}\right)}{2\alpha t e^{-\alpha t^2}\left(\frac{1}{\sqrt{w}}-1\right)}\\
\leq\ &C(\alpha).
\end{aligned}$$

Based on numerical approximation, we discovered that the optimal value α^* that minimises $C(\alpha)$ is 0.33 and that $C(\alpha^*) = 1.21$. Hence, the expected number of iterations required for each sample of (T, W) is 1.21.

To generate $\{Z_t | Z_t < 1\}$, we choose an envelope Z' with density

$$f_{Z'}(x|t) = e^{\frac{t^2}{2}} \frac{t^2}{2x^2} e^{-\frac{t^2}{2x}}, \qquad 0 < x < 1,$$

the CDF is given by

$$F_{Z'}(x) = 1 - e^{\frac{t^2}{2}} e^{-\frac{t^2}{2x}}, \qquad 0 < x < 1,$$

which can be inverted explicitly and generated via (3.5.31). The A/R constant is given by

$$\frac{f_{Z_t|Z_t<1}(x|t)}{f_{Z'}(x|t)} \leq \frac{\sqrt{2} e^{-\frac{t^2}{2}}}{\sqrt{\pi}\, \mathrm{Erfc}\left(\frac{t}{\sqrt{2}}\right) t}.$$

We then follow the A/R decision (3.5.32) to generate $\{Z_t | Z_t < 1\}$. Using these A/R algorithms to generate (T, W) and $\{Z_t | Z_t < 1\}$, we then follow the recursive procedure to simulate the truncated stable process Z_t with stability index $\frac{1}{2}$. □

To generate the truncated inverse Gaussian process, as the analytical joint distribution of the hitting time and overshoot (T, W) and the conditional distribution of $\{Z_t | Z_t < 1\}$, we could develop an exact simulation scheme for truncated inverse Gaussian process via marked renewal approach. Unlike Algorithm 3.5.4, this alternative algorithms reduce the complexity for large value of μ. The details are provided in Algorithm 3.5.8 below.

Algorithm 3.5.8 (Exact Simulation of Truncated Inverse Gaussian Process)**.** *The truncated inverse Gaussian process can be simulated via the following steps:*

1. *Set* $S = 0$,

2. *Generate* (T, W) *via the following steps,*

   (1) Set

$$\begin{aligned} \alpha^* &= \frac{1}{8}\left(4 + \left(\sqrt{\frac{2}{\pi}} e^{-\mu} + \sqrt{2\mu}\, \mathrm{Erf}(\sqrt{\mu})\right)^2 \right. \\ &\quad \left. - \left(\sqrt{\frac{2}{\pi}} e^{-\mu} + \sqrt{2\mu}\, \mathrm{Erf}(\sqrt{\mu})\right) \sqrt{8 + \left(\sqrt{\frac{2}{\pi}} e^{-\mu} + \sqrt{2\mu}\, \mathrm{Erf}(\sqrt{\mu})\right)^2}\right), \end{aligned} \tag{3.5.33}$$

(2) Generate T by setting $T = \sqrt{-\log(U_1)/\alpha^*}$ with $U_1 \sim \mathcal{U}[0,1]$,

(3) Generate W by setting $W = 2 - U_2 - \sqrt{1-U_2}$ with $U_2 \sim \mathcal{U}[0,1]$,

(4) Generate $V_1 \sim \mathcal{U}[0,1]$, if

$$V_1 \leq \frac{e^{T\left(\sqrt{\frac{2}{\pi}}e^{-\mu}+\sqrt{2\mu}\,\mathrm{Erf}(\sqrt{\mu})\right)}\left(1-\frac{T^2}{1+W}\right)\left(Erf\left(\frac{T}{\sqrt{2W(1+W)}}\right)-Erf\left(\frac{t\sqrt{W}}{\sqrt{2(1+W)}}\right)\right)}{2C_1\alpha^* Te^{-\alpha^* T^2}\left(\frac{1}{\sqrt{W}}-1\right)} \times\frac{e^{-\mu(1+W)}e^{-\frac{T^2}{2(1+W)}}}{\sqrt{2\pi}(1+W)^{\frac{3}{2}}}+\frac{\frac{Te^{T\left(\sqrt{\frac{2}{\pi}}e^{-\mu}+\sqrt{2\mu}\,\mathrm{Erf}(\sqrt{\mu})\right)}e^{-\mu(1+W)}}{\pi\sqrt{W}(1+W)^2}\left(e^{-\frac{T^2}{2}}-We^{-\frac{t^2}{2W}}\right)}{2C_1\alpha^* Te^{-\alpha^* T^2}\left(\frac{1}{\sqrt{W}}-1\right)}, \tag{3.5.34}$$

with

$$C_1 = 1.8\times\mathbf{1}_{\{\mu<1\}}+\frac{\mathbf{1}_{\{\mu\geq 1\}}}{2\alpha^*\pi}\exp\left(-\mu+\left(\frac{1}{2}-\alpha^*\right)\frac{\left(\sqrt{\frac{2}{\pi}}e^{-\mu}+\sqrt{2\mu}\,\mathrm{Erf}(\sqrt{\mu})\right)^2}{(1-2\alpha^*)^2}\right),$$

then, accept (T,W); Otherwise, reject this candidate and go back to step 2(2),

With the accepted (T,W), if $t < T$, go to step 3; Otherwise, go to step 4,

3. *Generate Z via the following steps,*

   (I) Generate Z by setting $Z = t^2/\left[t^2 - 2\ln(U_3)\right]$ with $U_3 \sim \mathcal{U}[0,1]$,

   (II) Generate $V_2 \sim \mathcal{U}[0,1]$, if $V_2 \leq \frac{1}{C_2}\sqrt{Z}e^{-\mu Z}$, where

$$C_2 = \begin{cases} \exp(-\mu), & \text{for } \mu \leq \frac{1}{2}, \\ \frac{1}{\sqrt{2\pi e}}, & \text{for } \mu > \frac{1}{2}, \end{cases}$$

   then, accept Z; Otherwise, reject this candidate and go back to Step 3(I),

   With the accepted Z, then go to step 5,

4. *Set $S = S + 1 + W$ and $t = t - T$ then go back to step 2,*

5. *Return $S + Z$.*

Proof. For $\mu > 0$, given the joint density of (T,W) of the form (3.5.16), we choose an envelope (T',W') with density

$$g(t,w) = 2\alpha t e^{-\alpha t^2}\left(\frac{1}{\sqrt{w}}-1\right).$$

Hence, the A/R constant is derived by finding the maximum of the ratio $\frac{f_{T,W}(t,w)}{g(t,w)}$ in terms of t and w, details are given as follow,

$$\begin{aligned}
\frac{f_{T,W}(t,w)}{g(t,w)} &= \frac{\frac{e^{t\left(\sqrt{\frac{2}{\pi}}e^{-\mu}+\sqrt{2\mu}\,\mathrm{Erf}(\sqrt{\mu})\right)}e^{-\mu(1+w)}e^{-\frac{t^2}{2(1+w)}}}{\sqrt{2\pi}(1+w)^{\frac{3}{2}}}\left(1-\frac{t^2}{1+w}\right)\left(\mathrm{Erf}\left(\frac{t}{\sqrt{2w(1+w)}}\right)-\mathrm{Erf}\left(\frac{t\sqrt{w}}{\sqrt{2(1+w)}}\right)\right)}{2\alpha t e^{-\alpha t^2}\left(\frac{1}{\sqrt{w}}-1\right)} \\
&\quad + \frac{\frac{te^{t\left(\sqrt{\frac{2}{\pi}}e^{-\mu}+\sqrt{2\mu}\,\mathrm{Erf}(\sqrt{\mu})\right)}e^{-\mu(1+w)}}{\pi\sqrt{w}(1+w)^2}\left(e^{-\frac{t^2}{2}}-we^{-\frac{t^2}{2w}}\right)}{2\alpha t e^{-\alpha t^2}\left(\frac{1}{\sqrt{w}}-1\right)} \\
&\leq \bar{C}\times\mathbf{1}_{\{\mu<a\}}+\frac{e^{t\left(\sqrt{\frac{2}{\pi}}e^{-\mu}+\sqrt{2\mu}\,\mathrm{Erf}(\sqrt{\mu})\right)}e^{-\mu}e^{\alpha t^2-\frac{t^2}{2}}}{2\alpha\pi}\times\mathbf{1}_{\{\mu\geq a\}} \\
&\leq \bar{C}\times\mathbf{1}_{\{\mu<a\}}+\frac{\mathbf{1}_{\{\mu\geq a\}}}{2\alpha\pi}\exp\left(-\mu+\left(\frac{1}{2}-\alpha\right)\frac{\left(\sqrt{\frac{2}{\pi}}e^{-\mu}+\sqrt{2\mu}\,\mathrm{Erf}(\sqrt{\mu})\right)^2}{(1-2\alpha)^2}\right) \\
&= C(\mu,\alpha).
\end{aligned}$$

We notice that for $\mu > 1$, the maximum occurs at $w = 0$ and $t = \frac{\sqrt{\frac{2}{\pi}}e^{-\mu}+\sqrt{2\mu}\,\mathrm{Erf}(\sqrt{mu})}{1-2\alpha}$, and for $\mu < 1$, the maximum of the ratio does not exceed 1.8. Hence we have a choice of $\bar{C} = 1.8$ and $a = 1$. Then with the A/R constant, the next task is to find the optimal α^* such that $C(\mu,\alpha^*) \leq C(\mu,\alpha)$ for all α. As the derivative of $C(\mu,\alpha)$ with respect to α satisfies the following

$$\frac{\partial C(\mu,\alpha)}{\partial\alpha} = \frac{4\alpha^2-4\alpha-\left(\sqrt{\frac{2}{\pi}}e^{-\mu}+\sqrt{2\mu}\,\mathrm{Erf}(\sqrt{\mu})\right)^2\alpha+1}{2\pi(1-2\alpha)^2\alpha^2}e^{-\mu+\left(\frac{1}{2}-\alpha\right)\frac{\left(\sqrt{\frac{2}{\pi}}e^{-\mu}+\sqrt{2\mu}\,\mathrm{Erf}(\sqrt{\mu})\right)^2}{(1-2\alpha)^2}},$$

the optimal α^* satisfies the following equation

$$4\alpha^{*2}-4\alpha^*-\left(\sqrt{\frac{2}{\pi}}e^{-\mu}+\sqrt{2\mu}\,\mathrm{Erf}(\sqrt{\mu})\right)^2\alpha^*+1=0.$$

Hence, we can express the optimal α^* in (3.5.33) in terms of μ. This α^* indeed is the critical value that minimises $C(\mu,\alpha)$ as

$$\left.\frac{\partial C(\mu,\alpha)}{\partial\alpha}\right|_{\alpha=\alpha^*}=0, \qquad \text{and} \qquad \left.\frac{\partial^2 C(\mu,\alpha)}{\partial\alpha^2}\right|_{\alpha=\alpha^*}>0.$$

Then the two-dimensional A/R scheme to generate (T,W) is to choose an envelope with density $g(t,w)$ and the A/R decision directly follows (3.5.34). The expected number of iterations of this A/R scheme is $C_1 = C(\mu,\alpha^*)$.

To simulate $\{Z_t|Z_t < 1\}$, we use the same envelope that was used in Algorithm 3.5.7. The A/R constant is given by

$$\frac{f_{Z_t|Z_t<1}(x|t)}{f_{Z'}(x|t)} = \frac{2e^{-\frac{t^2}{2}}}{Dt\sqrt{2\pi}}\sqrt{x}e^{-\mu x} \leq \begin{cases} \frac{2e^{-\frac{t^2}{2}}e^{-\mu}}{Dt\sqrt{2\pi}}, & \text{for } \mu \leq \frac{1}{2}, \\ \frac{e^{-\frac{t^2}{2}}}{Dt\sqrt{\pi e}}, & \text{for } \mu > \frac{1}{2}. \end{cases}$$

where D satisfies (3.5.27). The recursive procedure to simulate the truncated inverse Gaussian process follows. □

3.6 Numerical Experiments

In this section, we present some numerical results of the exact simulation methods developed in Algorithm 3.4.1, 3.4.2, 3.5.3, 3.5.4, 3.5.5, 3.5.6, 3.5.7 and 3.5.8. Numerical validation and tests for our simulation algorithms are all based on the true mean. The associated errors from the true values are reported via the following three standard measures:

1. *difference* = estimated value - true value;
2. *relative error (error %)* = $\frac{\text{estimated value-true value}}{\text{true value}}$;
3. *root mean square error (RMSE)* = $\sqrt{\text{bias}^2 + \text{SE}^2}$, where SE is the standard error of the simulation output. The bias is conventionally set to zero as the algorithms we developed are all exact simulation algorithms.

The detailed numerical results are reported in Table 3.1, 3.2, 3.3 . We can see that each algorithm can achieve a very high level of accuracy, which is reflected by the difference in the theoretical mean and associated percentage errors.

For the Dickman process, we implement a comparison between Algorithm 3.4.1 against the algorithms suggested by Devroye and Fawzi (2010), Fill and Huber (2010), Chi (2012), and Cloud and Huber (2017). The detailed numerical results based on different parameter settings against t are reported in Table 3.4. In addition, we also compared the computation time to generate $100,000$ samples using these five algorithms for different values of t, and details are presented in Table 3.5. We can see that sampling based on Algorithm 3.4.1 is much faster than algorithms in Devroye and Fawzi (2010), Fill and Huber (2010), Chi (2012), and Cloud and Huber (2017). For instance, when $t = 3$, Algorithm 3.4.1 is 4 times faster than Devroye and Fawzi (2010), 50 times faster than Fill and Huber (2010), 25 times faster than Chi (2012), and 7 times faster than Cloud and Huber (2017). Compared with the other algorithms, the main advantage of Algorithm 3.4.1 is that the incremental

Table 3.1: Comparison between the true means and the associated simulation results for Algorithm 3.4.1, 3.4.2 based on the parameter setting $t = 0.5, 1, 2.5, 3$, $\mu = 0, 0.5, 1$, respectively.

Paths	True	Simulation	Diff	Error%	RMSE	Time	True	Simulation	Diff	Error%	RMSE	Time
Algorithm 3.4.1			$t = 0.5$	$\mu = 0$					$t = 2.5$	$\mu = 0$		
1,000	0.5000	0.4879	-0.0121	-2.47%	0.0155	0.11	2.5000	2.4421	-0.0579	-2.37%	0.0343	0.08
4,000	0.5000	0.5057	0.0057	1.12%	0.0079	0.13	2.5000	2.5148	0.0148	0.59%	0.0178	0.11
16,000	0.5000	0.5011	0.0011	0.22%	0.0040	0.38	2.5000	2.5073	0.0073	0.29%	0.0089	0.36
64,000	0.5000	0.5008	0.0008	0.16%	0.0020	1.09	2.5000	2.4975	-0.0025	-0.10%	0.0044	1.17
256,000	0.5000	0.5002	0.0002	0.05%	0.0010	4.35	2.5000	2.5058	0.0058	0.23%	0.0022	4.43
1,024,000	0.5000	0.5009	0.0009	0.19%	0.0005	16.63	2.5000	2.5003	0.0003	0.01%	0.0011	17.19
Algorithm 3.4.2			$t = 1$	$\mu = 0.5$					$t = 1$	$\mu = 1$		
1,000	0.7869	0.7890	0.0020	0.25%	0.0183	0.14	0.6321	0.6426	0.0105	1.63%	0.0165	0.19
4,000	0.7869	0.7909	0.0039	0.49%	0.0095	0.28	0.6321	0.6318	-0.0003	-0.04%	0.0081	0.28
16,000	0.7869	0.7809	-0.0060	-0.76%	0.0047	0.66	0.6321	0.6338	0.0017	0.26%	0.0041	0.83
64,000	0.7869	0.7891	0.0021	0.26%	0.0024	2.12	0.6321	0.6304	-0.0017	-0.27%	0.0020	2.18
256,000	0.7869	0.7855	-0.0014	-0.18%	0.0012	8.38	0.6321	0.6324	0.0002	0.03%	0.0010	8.55
1,024,000	0.7869	0.7865	-0.0004	-0.05%	0.0006	33.09	0.6321	0.6327	0.0005	0.08%	0.0005	31.48
Algorithm 3.4.2			$t = 3$	$\mu = 0.5$					$t = 3$	$\mu = 1$		
1,000	2.3608	2.3699	0.0091	0.38%	0.0326	0.17	1.8964	1.9056	0.0092	0.48%	0.0289	0.16
4,000	2.3608	2.3431	-0.0177	-0.75%	0.0163	0.30	1.8964	1.8995	0.0031	0.16%	0.0139	0.17
16,000	2.3608	2.3731	0.0123	0.51%	0.0083	0.75	1.8964	1.8964	0.0000	0.00%	0.0070	0.50
64,000	2.3608	2.3629	0.0020	0.08%	0.0041	2.12	1.8964	1.8965	0.0002	0.01%	0.0035	1.94
256,000	2.3608	2.3608	0.0000	0.00%	0.0021	8.76	1.8964	1.8977	0.0013	0.06%	0.0018	6.98
1,024,000	2.3608	2.3579	-0.0029	-0.12%	0.0010	32.33	1.8964	1.8960	-0.0003	-0.01%	0.0009	31.60

Table 3.2: Comparison between the true means and the associated simulation results for Algorithm 3.5.3, 3.5.4, 3.5.5, and 3.5.6 based on parameter setting $t = 0.5, 1, 4$, $\alpha = 0.3, 0.5, 0.8$, and $\mu = 0, \pm 0.5, \pm 1$, respectively.

Paths	True	Simulation	Diff	Error%	RMSE	Time	True	Simulation	Diff	Error%	RMSE	Time
Algorithm 3.5.3			$\alpha = 0.3$	$t = 0.5$	$\mu = 0$				$\alpha = 0.3$	$t = 1$	$\mu = 0$	
1,000	0.1651	0.1602	-0.0049	-3.03%	0.0081	0.45	0.3302	0.3187	-0.0115	-3.60%	0.0112	0.37
4,000	0.1651	0.1619	-0.0032	-1.98%	0.0041	0.37	0.3302	0.3418	0.0116	3.40%	0.0062	0.57
16,000	0.1651	0.1651	0.0001	0.03%	0.0021	0.78	0.3302	0.3318	0.0016	0.50%	0.0029	1.09
64,000	0.1651	0.1661	0.0010	0.61%	0.0010	3.27	0.3302	0.3294	-0.0007	-0.22%	0.0015	3.71
256,000	0.1651	0.1647	-0.0004	-0.23%	0.0005	11.35	0.3302	0.3314	0.0012	0.37%	0.0007	12.62
1,024,000	0.1651	0.1652	0.0001	0.08%	0.0003	43.49	0.3302	0.3303	0.0002	0.05%	0.0004	44.38
Algorithm 3.5.3			$\alpha = 0.8$	$t = 0.5$	$\mu = 0$				$\alpha = 0.8$	$t = 1$	$\mu = 0$	
1,000	0.4356	0.4289	-0.0067	-1.57%	0.0087	0.27	0.8713	0.8780	0.0067	0.76%	0.0118	0.42
4,000	0.4356	0.4315	-0.0041	-0.95%	0.0041	0.41	0.8713	0.8726	0.0013	0.15%	0.0061	0.39
16,000	0.4356	0.4345	-0.0011	-0.26%	0.0021	0.78	0.8713	0.8665	-0.0048	-0.56%	0.0030	0.69
64,000	0.4356	0.4361	0.0005	0.11%	0.0011	1.64	0.8713	0.8692	-0.0021	-0.24%	0.0015	2.20
256,000	0.4356	0.4359	0.0003	0.06%	0.0005	5.28	0.8713	0.8707	-0.0006	-0.07%	0.0008	7.59
1,024,000	0.4356	0.4352	-0.0005	-0.11%	0.0003	22.05	0.8713	0.8711	-0.0002	-0.02%	0.0004	26.09
Algorithm 3.5.4			$\alpha = 0.5$	$t = 0.5$	$\mu = 1$				$\alpha = 0.5$	$t = 4$	$\mu = 1$	
1,000	0.2107	0.2111	0.0004	0.19%	0.0087	0.15	1.6854	1.6924	0.0070	0.40%	0.0250	0.14
4,000	0.2107	0.2069	-0.0038	-1.78%	0.0043	0.56	1.6854	1.6834	-0.0021	-0.12%	0.0122	0.61
16,000	0.2107	0.2129	0.0023	1.06%	0.0022	2.08	1.6854	1.6854	0.0000	0.00%	0.0062	2.73
64,000	0.2107	0.2093	-0.0013	-0.63%	0.0011	7.47	1.6854	1.6849	-0.0005	-0.02%	0.0030	10.67
256,000	0.2107	0.2102	-0.0005	-0.22%	0.0005	28.41	1.6854	1.6859	0.0005	0.03%	0.0015	43.81
1,024,000	0.2107	0.2108	0.0002	0.08%	0.0003	117.74	1.6854	1.6846	-0.0008	-0.04%	0.0007	167.59
Algorithm 3.5.5			$\alpha = 0.5$	$t = 0.5$	$\mu = 1$				$\alpha = 0.5$	$t = 4$	$\mu = 1$	
1,000	0.2107	0.2127	0.0020	0.94%	0.0084	0.11	1.6854	1.6897	0.0043	0.25%	0.0243	0.12
4,000	0.2107	0.2059	-0.0048	-2.25%	0.0042	0.45	1.6854	1.6751	-0.0104	-0.61%	0.0124	0.40
16,000	0.2107	0.2098	-0.0009	-0.41%	0.0022	1.73	1.6854	1.6863	0.0009	0.05%	0.0062	1.75
64,000	0.2107	0.2114	0.0008	0.36%	0.0011	6.14	1.6854	1.6893	0.0039	0.23%	0.0031	7.45
256,000	0.2107	0.2111	0.0004	0.19%	0.0005	24.31	1.6854	1.6871	0.0017	0.10%	0.0015	30.41
1,024,000	0.2107	0.2107	0.0000	0.00%	0.0003	98.69	1.6854	1.6857	0.0003	0.01%	0.0008	110.74
Algorithm 3.5.6			$\alpha = 0.5$	$t = 0.5$	$\mu = -0.5$				$\alpha = 0.5$	$t = 1$	$\mu = -1$	
1,000	0.3371	0.3298	-0.0073	-2.16%	0.0131	0.13	0.8252	0.7990	-0.0262	-3.17%	0.0220	0.33
4,000	0.3371	0.3362	-0.0009	-0.27%	0.0067	0.28	0.8252	0.8297	0.0045	0.54%	0.0111	0.48
16,000	0.3371	0.3345	-0.0026	-0.77%	0.0033	1.40	0.8252	0.8299	0.0047	0.56%	0.0056	1.94
64,000	0.3371	0.3356	-0.0015	-0.45%	0.0017	5.71	0.8252	0.8256	0.0004	0.04%	0.0028	7.52
256,000	0.3371	0.3370	-0.0001	-0.02%	0.0008	19.72	0.8252	0.8247	-0.0005	-0.06%	0.0014	30.31
1,024,000	0.3371	0.3373	0.0002	0.05%	0.0004	90.09	0.8252	0.8239	-0.0014	-0.16%	0.0007	152.13

Table 3.3: Comparison between the true means and the associated simulation results for Algorithm 3.5.7 and 3.5.8 based on the parameter setting $t = 1, 3$ and $\mu = 0, \pm 0.5, \pm 1$, respectively.

Paths	True	Simulation	Diff	Error%	RMSE	Time	True	Simulation	Diff	Error%	RMSE	Time
Algorithm 3.5.7			$t=1$	$\mu=0$					$t=3$	$\mu=0$		
1,000	0.7979	0.8498	0.0519	6.50%	0.0171	0.07	2.3937	2.4404	0.0467	1.95%	0.0286	0.07
4,000	0.7979	0.8085	0.0106	1.33%	0.0083	0.27	2.3937	2.3856	-0.0081	-0.34%	0.0140	0.28
16,000	0.7979	0.8011	0.0032	0.41%	0.0041	1.08	2.3937	2.3935	-0.0001	0.00%	0.0070	1.57
64,000	0.7979	0.7971	-0.0008	-0.10%	0.0020	3.96	2.3937	2.3939	0.0002	0.01%	0.0035	4.88
256,000	0.7979	0.7970	-0.0009	-0.12%	0.0010	21.46	2.3937	2.3909	-0.0027	-0.11%	0.0018	19.07
1,024,000	0.7979	0.7983	0.0004	0.06%	0.0005	65.19	2.3937	2.3937	0.0000	0.00%	0.0009	90.81
Algorithm 3.5.8			$t=1$	$\mu=0.5$					$t=3$	$\mu=1$		
1,000	0.6827	0.6889	0.0063	0.92%	0.0145	0.2	1.7876	1.7834	-0.0043	-0.24%	0.0216	0.14
4,000	0.6827	0.6848	0.0021	0.31%	0.0072	0.32	1.7876	1.7803	-0.0074	-0.41%	0.0105	0.45
16,000	0.6827	0.6789	-0.0038	-0.55%	0.0035	1.32	1.7876	1.7813	-0.0064	-0.36%	0.0053	1.95
64,000	0.6827	0.6831	0.0004	0.06%	0.0018	5.63	1.7876	1.7932	0.0055	0.31%	0.0027	8.38
256,000	0.6827	0.6836	0.0009	0.13%	0.0009	24.05	1.7876	1.7880	0.0004	0.02%	0.0013	30.37
1,024,000	0.6827	0.6822	-0.0005	-0.08%	0.0004	106.21	1.7876	1.7863	-0.0013	-0.07%	0.0007	126.28

Table 3.4: Comparison for Algorithm 3.4.1 and Algorithms suggested in Devroye and Fawzi (2010), Fill and Huber (2010), Chi (2012), and Cloud and Huber (2017) based on the parameter setting $t = 1, 3$ respectively.

Paths	True	Simulation	Diff	Error%	RMSE	Time	True	Simulation	Diff	Error%	RMSE	Time
Algorithm 3.4.1			$t=1$						$t=3$			
1,000	1.0000	0.9813	-0.0187	-1.91%	0.0218	0.07	3.0000	3.0031	0.0031	0.10%	0.0379	0.09
4,000	1.0000	1.0057	0.0057	0.57%	0.0114	0.17	3.0000	3.0030	0.0030	0.10%	0.0192	0.14
16,000	1.0000	1.0043	0.0043	0.43%	0.0056	0.28	3.0000	2.9979	-0.0021	-0.07%	0.0096	0.41
64,000	1.0000	0.9997	-0.0003	-0.03%	0.0028	0.97	3.0000	2.9967	-0.0033	-0.11%	0.0048	1.19
256,000	1.0000	0.9985	-0.0015	-0.15%	0.0014	4.30	3.0000	3.0041	0.0041	0.14%	0.0024	4.51
1,024,000	1.0000	0.9994	-0.0006	-0.06%	0.0007	16.69	3.0000	2.9978	-0.0022	-0.07%	0.0012	18.84
Devroye and Fawzi (2010)			$t=1$						$t=3$			
1,000	1.0000	0.9923	-0.0077	-0.77%	0.0221	0.03	3.0000	2.9731	-0.0269	-0.90%	0.0038	0.14
4,000	1.0000	0.9977	-0.0023	-0.22%	0.0113	0.13	3.0000	3.0006	0.0006	0.02%	0.0192	0.61
16,000	1.0000	1.0011	0.0011	0.11%	0.0056	0.57	3.0000	2.9935	-0.0065	-0.21%	0.0097	2.00
64,000	1.0000	1.0057	0.0057	0.56%	0.0028	1.95	3.0000	2.9951	-0.0049	-0.16%	0.0048	5.54
256,000	1.0000	1.0034	0.0034	0.33%	0.0014	7.99	3.0000	3.0014	0.0014	0.04%	0.0024	23.93
1,024,000	1.0000	0.9993	-0.0007	-0.07%	0.0007	37.51	3.0000	3.0014	0.0014	0.04%	0.0012	101.61
Fill and Huber (2010)			$t=1$						$t=3$			
1,000	1.0000	0.9851	-0.0149	-1.50%	0.0027	0.10	3.0000	2.9516	-0.0484	-1.64%	0.0398	1.31
4,000	1.0000	0.9977	-0.0023	-0.23%	0.0113	0.28	3.0000	2.9444	-0.0556	-1.88%	0.0195	4.56
16,000	1.0000	1.0004	0.0004	0.04%	0.0056	1.09	3.0000	3.0175	0.0175	0.58%	0.0099	18.69
64,000	1.0000	0.9968	-0.0032	-0.32%	0.0028	2.67	3.0000	2.9995	-0.0005	-0.02%	0.0049	75.23
256,000	1.0000	0.9977	-0.0023	-0.23%	0.0013	11.14	3.0000	2.9969	-0.0031	-0.10%	0.0025	325.37
1,024,000	1.0000	0.9994	-0.0006	-0.06%	0.0006	57.37	3.0000	3.0131	0.0131	0.43%	0.0012	1358.24
Chi (2012)			$t=1$						$t=3$			
1,000	1.0000	1.0070	0.0070	0.70%	0.0233	0.33	3.0000	3.0109	0.0109	0.36%	0.0392	0.62
4,000	1.0000	1.0100	0.0100	0.99%	0.0115	0.78	3.0000	3.0208	0.0208	0.69%	0.0197	2.19
16,000	1.0000	0.9955	-0.0045	-0.45%	0.0057	2.83	3.0000	3.0107	0.0107	0.35%	0.0099	8.44
64,000	1.0000	1.0026	0.0026	0.26%	0.0029	12.24	3.0000	3.0027	0.0027	0.09%	0.0050	31.16
256,000	1.0000	1.0018	0.0018	0.18%	0.0014	46.27	3.0000	3.0016	0.0016	0.05%	0.0025	132.28
1,024,000	1.0000	1.0036	0.0036	0.36%	0.0007	193.00	3.0000	2.9978	-0.0002	-0.01%	0.0012	514.12
Cloud and Huber (2017)			$t=1$						$t=3$			
1,000	1.0000	0.9832	-0.0168	-1.71%	0.0220	0.09	3.0000	2.9376	-0.0624	-2.12%	0.0379	0.28
4,000	1.0000	1.0153	0.0153	1.50%	0.0113	0.33	3.0000	2.9986	-0.0014	-0.05%	0.0195	0.92
16,000	1.0000	1.0059	0.0059	0.58%	0.0056	0.84	3.0000	3.0108	0.0108	0.36%	0.0096	2.31
64,000	1.0000	1.0076	0.0076	0.75%	0.0028	3.07	3.0000	3.0014	0.0014	0.05%	0.0048	8.61
256,000	1.0000	1.0013	0.0013	0.13%	0.0014	12.51	3.0000	3.0021	0.0021	0.07%	0.0024	36.47
1,024,000	1.0000	1.0017	0.0017	0.17%	0.0007	58.19	3.0000	3.0038	0.0038	0.13%	0.0012	155.93

random variables $(T_i, W_i)_{i\geq 0}$ are i.i.d pairs, and this means that we can employ vectorisation to reduce total computation time, especially for large values of t. Although the expected simulation time is unbounded for Algorithm 3.4.1, the simulation idea based on the marked renewal approach still outperforms the dominated coupling approach and rejection sampling approach, and even more so when t is large.

Table 3.5: Comparison CPU time (sec) for Algorithms suggested in Devroye and Fawzi (2010), Fill and Huber (2010), Chi (2012) and Cloud and Huber (2017) with Algorithm 3.4.1 for 100,000 replications.

Input t	0.40	0.60	0.80	1.00	1.20	1.40	1.60	1.80	2.00	2.20	2.40	2.60	2.80	3.00	3.20	3.40
Algorithm 3.4.1	1.85	1.81	1.68	1.60	1.71	1.79	1.82	1.83	1.78	2.03	1.72	1.77	1.83	2.02	1.83	1.95
Devroye and Fawzi (2010)	3.02	2.23	3.19	3.94	5.66	5.47	5.23	5.31	5.93	8.48	7.22	7.51	7.97	8.47	10.88	11.50
Fill and Huber (2010)	1.87	2.53	3.14	4.12	5.68	7.34	10.33	13.64	18.28	20.76	36.78	51.22	70.23	100.75	140.91	200.04
Chi (2012)	3.92	6.28	9.62	18.52	21.25	23.53	27.45	31.80	34.78	36.92	38.41	41.57	55.31	50.54	55.83	59.23
Cloud and Huber (2017)	2.45	3.09	3.93	4.71	5.66	6.71	7.57	9.70	11.16	11.82	13.45	13.72	14.71	15.54	16.99	17.25

For truncated stable process and truncated tempered stable process, we have implemented the exact simulation algorithms for Algorithm 3.5.3, 3.5.4, 3.5.5, and 3.5.6 based on parameter setting $t = 0.5, 1, 4$, $\alpha = 0.3, 0.5, 0.8$, and $\mu = 0, \pm 0.5, \pm 1$, respectively. Convergence analysis for these four algorithms based on the increasing numbers of samples is reported in Table 3.2. We can see that Algorithm 3.5.3 is more efficient for large stability parameter α as $C(\lambda)$ in (3.5.10) is smaller for large α. Larger t also requires more computation time as one has to generate more hitting times to break the marked renewal routine. Meanwhile, we carry out a comparison between Algorithm 3.5.4 and 3.5.5. We can see that when μ and t are small, the time needed for two algorithms are more or less the same. However, when μ and t are larger, Algorithm 3.5.5 outperforms Algorithm 3.5.4 in terms of computation time. The out-performance becomes even more substantial when μ and t increase.

For truncated inverse Gaussian process, we carry out the standard convergence analysis for the Algorithms 3.5.7 and 3.5.8 with the parameter settings $t = 1, 3$, and $\mu = 0, \pm 0.5, \pm 1$. The detailed numerical results are reported in Table 3.3. The sample path of the truncated process Z_t is provided in Figure 3.3. We also plot histograms of the truncated process at time t for different values of μ. The histograms and sample paths clearly demonstrate that the process increases faster for smaller μ , especially when μ is negative. This is due to the fact that the mean of the first passage time to level 1 decreases as μ decreases. This implies that the process with smaller tilting parameter μ will on average hit the level 1 faster than the process with larger tilting parameter. For μ being negative, the jump size is still restricted to $(0, 1)$, but the process jumps more frequently compared with the truncated process with positive μ.

3.7 Applications in Finance and Insurance

3.7.1 Exact Simulation of Generalised Vervaat Perpetuities

A stochastic perpetuity is a random variable which takes the form

$$X = Y_1 W_1 + Y_2 W_1 W_2 + Y_3 W_1 W_2 W_3 + ... + Y_n W_1 W_2 ... W_n + ..., \tag{3.7.1}$$

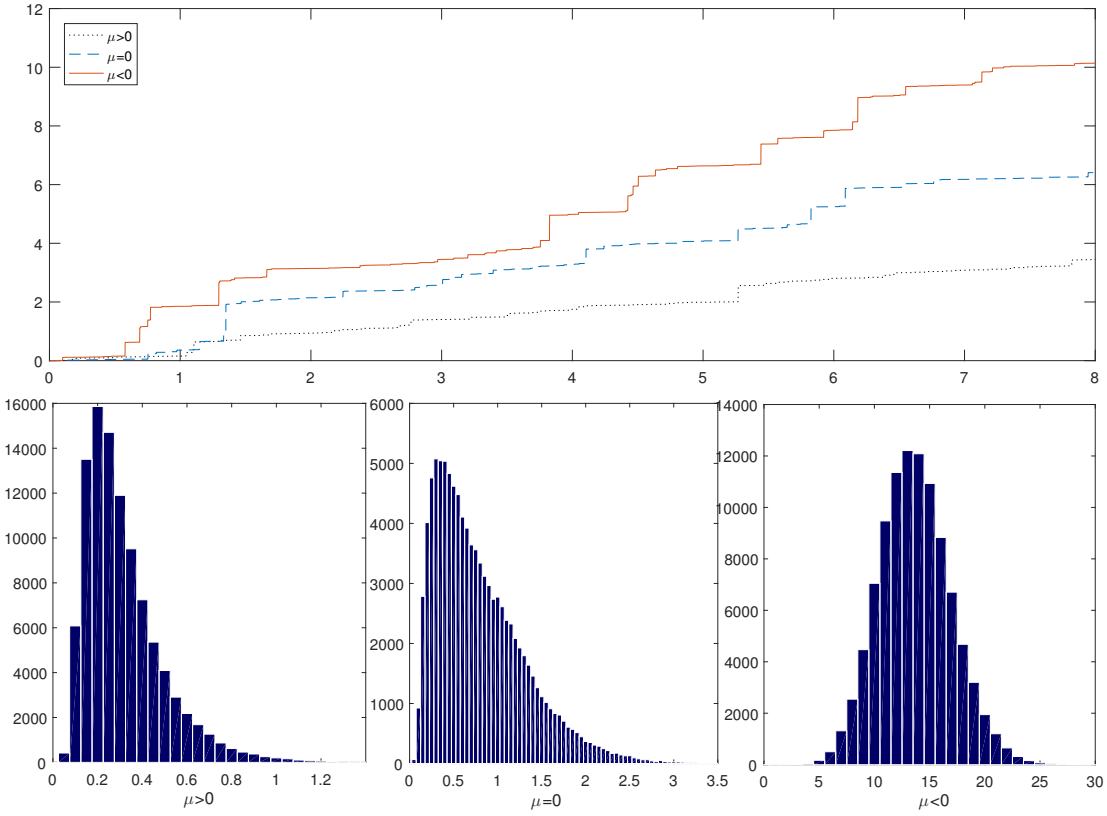

Figure 3.3: Sample Paths and Histograms of truncated IG with $\mu > 0$, $\mu = 0$ and $\mu < 0$, respectively.

where the W_i and Y_i are i.i.d random variables independent of each other. Perpetuities arise in a diverse range of fields such as economics (Embrechts et al., 1996), insurance mathematics (Nyrhinen, 2001), astrophysics (Chandrasekhar and Münch, 1950), analytic number theory (De Bruijn, 1951), and in the analysis of Hoare's selection algorithm (Mahmoud et al., 1995). We refer to Vervaat (1979) and Embrechts and Goldie (1994) for a huge variety of references and examples of applications, ranging from the brightness of the Milky Way to ARCH processes of financial modelling. In the context of economics, the quantity Y_i represents a random cashflow at time i and W_i represents the discount rate from time i to time $i-1$. The random variable X then represents the net present value of the stochastic cashflows.

When $W_i \overset{\mathcal{D}}{=} U^{1/t}$, for $U \sim \mathcal{U}[0,1]$ and $t \in \mathbb{R}^+$, the random variable X is known as a generalised Vervaat perpetuity. It was shown in Vervaat (1979) that the series converges if and only if $\mathbb{E}\left(\log^+ |Y_i|\right) < \infty$, and it satisfies the distributional identity

$$X \overset{\mathcal{D}}{=} W(X+Y), \tag{3.7.2}$$

where W and Y represent random variables distributed like W_i and Y_i respectively. Under the mild condition

$$\lim_{y\to 0} \frac{\mathbb{P}(Y < y)}{y} < \infty, \tag{3.7.3}$$

X turns out to be a Lévy process with Lévy measure proportional to $\frac{1}{y}\mathbb{P}(Y > y)$, see Dassios et al. (2019). There is also no loss of generality to consider only the case when $Y > 0$, as it can be shown that a two-sided perpetuity can be split into the difference of two one-sided perpetuities. Goldie and Grübel (1996) and Grübel and Rösler (1996) studied the tails of these perpetuities. Random variables of this type also appear as the limit of shot noise processes (Takács, 1954, 1955).

In the simplest case when $Y_i = 1$ almost surely, X reduces to the Dickman process. When $Y_i \sim V$, where $V \sim Exp(\mu)$, we obtain the Gamma process with parameter μ, when $Y_i \sim V \wedge 1$, we obtain the truncated Gamma process. To simulate more general Vervaat perpetuities, we develop a decomposition scheme to break the Vervaat perpetuity X into the sum of a Gamma process (or truncated Gamma process), and compound Poisson processes. The details are provided in the following Lemma 3.7.1.

Lemma 3.7.1. *Consider a perpetuity X defined in (3.7.1), with $Y \in \mathbb{R}^+$. If the density of Y satisfies (3.7.3), then there exists $k \in \mathbb{R}^+$ and $b \in \mathbb{R}^+$ such that $\mathbb{P}(Y > y) \geq e^{-ky}$ for all $y < b$. We then have the following two cases:*

1. ***Case 1:** There exists $k \in \mathbb{R}^+$ such that $\mathbb{P}(Y > y) \geq e^{-ky}$ for all $y \in \mathbb{R}^+$. Then we have*

$$B = \int_0^\infty \frac{\mathbb{P}(Y > y) - e^{-ky}}{y} \mathrm{d}y < \infty, \tag{3.7.4}$$

and thus

$$X \overset{\mathcal{D}}{=} \Gamma_t + \sum_{i=1}^{N_t} J_i, \tag{3.7.5}$$

where

- *Γ_t is a Gamma process such that $\Gamma_t \sim \Gamma(t, k)$;*
- *$\sum_{i=1}^{N_t} J_i$ is a compound Poisson process such that*
  - *N_t is a poisson process with rate tB,*
  - *$\{J_i\}_{i=1,2,\ldots}$ are i.i.d jumps with density*

$$g_{J_i}(y) = \frac{\mathbb{P}(Y \geq y) - e^{-ky}}{By}, \qquad y \in \mathbb{R}^+.$$

2. ***Case 2:** Otherwise, for the case that there only exists $k \in \mathbb{R}^+$ such that $\mathbb{P}(Y > y) \geq e^{-ky}$*

for $y < b$. We have

$$D = \int_0^b \frac{\mathbb{P}(Y > y) - e^{-ky}}{y} \mathrm{d}y < \infty, \tag{3.7.6}$$

and thus

$$X \overset{\mathcal{D}}{=} Z_t + \sum_{i=1}^{N_t^1} J_i^{(1)} + \sum_{k=1}^{N_t^2} J_k^{(2)}, \tag{3.7.7}$$

where

- *Z_t is a truncated Gamma process with Lévy measure*

$$\nu(z) = z^{-1} e^{-kz} \mathbf{1}_{\{0<z<b\}};$$

- *$\sum_{i=1}^{N_t^1} J_i^{(1)}$ is a compound Poisson process such that*
  - *N_t^1 is a poisson process with rate tD,*
  - *$\{J_i^{(1)}\}_{i=1,2,\ldots}$ are i.i.d jumps with density*

$$g_{J_i^{(1)}}(y) = \frac{\mathbb{P}(Y \geq y) - e^{-ky}}{Dy}, \qquad y \in (0, b).$$

- *$\sum_{k=1}^{N_t^2} J_k^{(2)}$ is a compound Poisson process such that*
  - *N_t^2 is a poisson process with rate tE, where*

$$E = \int_b^\infty \frac{\mathbb{P}(Y \geq y)}{y} \mathrm{d}y \tag{3.7.8}$$

  - *$\{J_k^{(2)}\}_{i=1,2,\ldots}$ are i.i.d jumps with density*

$$g_{J_k^{(2)}}(y) = \frac{\mathbb{P}(Y \geq y)}{Ey}, \qquad y \in (b, \infty).$$

Proof. If the density of Y satisfies (3.7.3), then $g(0) < \infty$. Hence, the survival function of Y, $\mathbb{P}(Y > y)$, decays at an exponential rate or slower at 0. This implies that there exists a $k \in \mathbb{R}^+$ such that $\mathbb{P}(Y > y) \geq e^{-ky}$ for all $y < b$, for some $b \in \mathbb{R}^+$.

1. **Case 1:** If, furthermore, there exists such $k \in \mathbb{R}^+$ so that $\mathbb{P}(Y > y) \geq e^{-ky}$ holds for all $y \in \mathbb{R}^+$, then for B defined as in (3.7.4), we have that the integral B is finite since

$$\int_0^\infty \frac{\mathbb{P}(Y > y) - e^{-ky}}{y} \mathrm{d}y = \int_0^1 \frac{\mathbb{P}(Y > y) - e^{-ky}}{y} \mathrm{d}y + \int_1^\infty \frac{\mathbb{P}(Y > y) - e^{-ky}}{y} \mathrm{d}y.$$

The second term is finite since we have assumed that the mean of Y exists, and we also have

that

$$\begin{aligned}
&\int_0^1 \frac{\mathbb{P}(Y>y)-e^{-ky}}{y}\mathrm{d}y \\
= \;& \left[\log y\left(\mathbb{P}(Y>y)-e^{-ky}\right)\right]_0^1 + \int_0^1 \log y\left(g(y)-\frac{e^{-ky}}{k}\right)\mathrm{d}y \\
= \;& \int_0^1 \log y\left(g(y)-\frac{e^{-ky}}{k}\right)\mathrm{d}y < \infty,
\end{aligned}$$

since $g(0) < \infty$. Hence, the Laplace transform of X can be expressed as

$$\begin{aligned}
\mathbb{E}\left[e^{-\beta X}\right] &= \exp\left(-t\int_0^\infty (1-e^{-\beta y})\frac{e^{-ky}}{y}\mathrm{d}y\right) \\
&\quad \times \exp\left(-tB\int_0^\infty (1-e^{-\beta y})\frac{\mathbb{P}(Y>y)-e^{-ky}}{By}\mathrm{d}y\right) \\
&= \mathbb{E}\left[e^{-\beta\Gamma_t}\right]\mathbb{E}\left[e^{-\beta\sum_{i=1}^{N_t} J_i}\right], \qquad (3.7.9)
\end{aligned}$$

and we have the distributional decomposition result given in (3.7.5).

2. **Case 2:** In the case where we only have $\mathbb{P}(Y>y) \geq e^{-ky}$ for $y < b$ for some $b \in \mathbb{R}^+$, we define the integral D as in (3.7.6) and E as in (3.7.8). A similar argument as above would show that they are finite, and we thus have

$$\begin{aligned}
\mathbb{E}\left[e^{-\beta X}\right] &= \exp\left(-t\int_0^b (1-e^{-\beta y})\frac{\mathbb{P}(Y>y)}{y}\mathrm{d}y\right) \\
&\quad \times \exp\left(-t\int_b^\infty (1-e^{-\beta y})\frac{\mathbb{P}(Y>y)}{y}\mathrm{d}y\right) \\
&= \exp\left(-t\int_0^b (1-e^{-\beta y})\frac{e^{-ky}}{y}\mathrm{d}y\right) \\
&\quad \times \exp\left(-tD\int_0^b (1-e^{-\beta y})\frac{\mathbb{P}(Y>y)-e^{-ky}}{Dy}\mathrm{d}y\right) \\
&\quad \times \exp\left(-tE\int_b^\infty (1-e^{-\beta y})\frac{\mathbb{P}(Y>y)}{Ey}\mathrm{d}y\right) \\
&= \mathbb{E}\left[e^{-\beta Z_t}\right]\mathbb{E}\left[e^{-\beta\sum_{i=1}^{N_t^1} J_i^{(1)}}\right]\mathbb{E}\left[e^{-\beta\sum_{k=1}^{N_t^2} J_k^{(2)}}\right]. \qquad (3.7.10)
\end{aligned}$$

The distributional decomposition result (3.7.7) thus follows. □

Here, we provide some examples to demonstrate the methodology.

Example 1: $Y \sim Pareto(\alpha, \sigma)$. The Laplace transform of X is

$$E\left[e^{-\beta X}\right] = \exp\left(-t\int_0^\sigma \frac{1-e^{-\beta y}}{y}\mathrm{d}y\right)\exp\left(-t\int_\sigma^\infty \frac{1-e^{-\beta y}}{y}\left(\frac{\sigma}{y}\right)^\alpha \mathrm{d}y\right). \qquad (3.7.11)$$

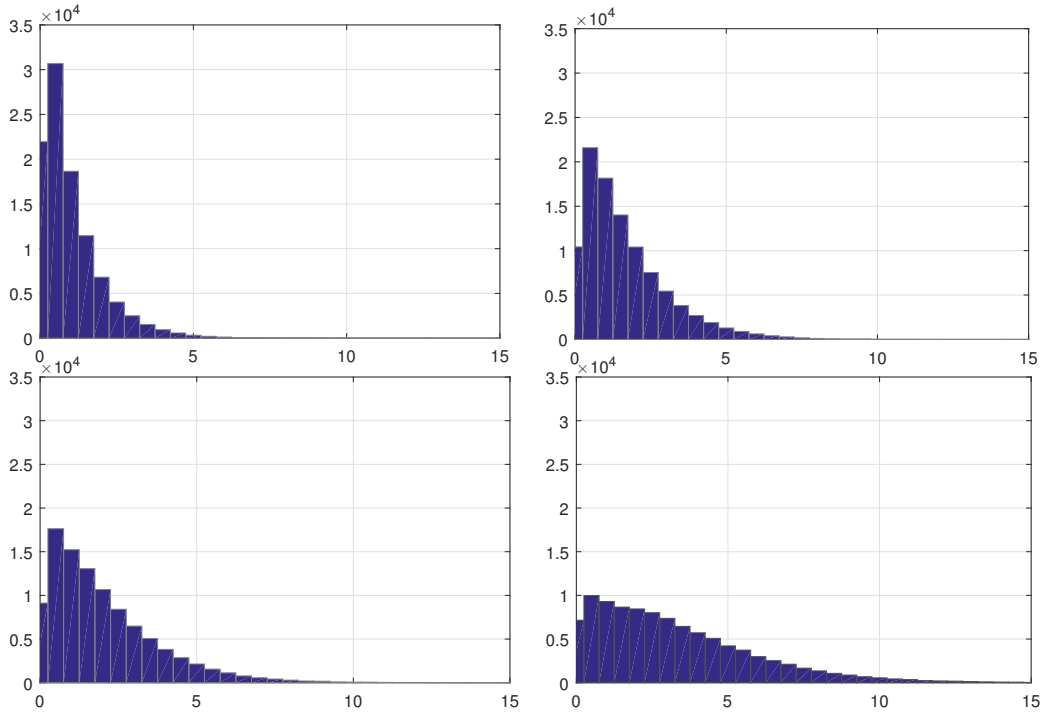

Figure 3.4: Histograms of perpetuity X with $Y \sim \Gamma(\alpha, \beta)$ under the parameter setting $\alpha = 1, 1.5, 2, 2.5$ and $\beta = 1$.

Hence, $X \overset{\mathcal{D}}{=} Z_t + CP$, where $Z_t \sim$ Dickman process, and CP is a Compound Poisson process, independent of each other. The Dickman process can be generated using Algorithm 3.4.1, and the Compound Poisson process can be generated easily via an A/R scheme.

Example 2: $Y \sim Gamma(\alpha, \beta)$. Since $g(0) < \infty$[2] for all $\alpha \geq 1$, we can simulate all Gamma perpetuities with $\alpha \geq 1$ and all values of β. Furthermore, for all $\alpha \geq 1$, there exists a k such that $\mathbb{P}(Y > y) \geq e^{-ky}$ for all y, thus the Gamma perpetuity X can be split into $X \overset{\mathcal{D}}{=} Z_t + CP$, where Z_t is a Gamma process, and CP is a Compound Poisson process independent of Z_t. Figure 3.4 shows the histograms of the Vervaat perpetuity X for $Y \sim \Gamma(\alpha, \beta)$ with different shape parameters α.

Example 3: $Y \sim Weibull(\kappa, \lambda)$. Since $g(0) < \infty$ for all $\kappa \geq 1$, we can simulate all Weibull perpetuities with $\kappa \geq 1$ and all values of λ. Furthermore, there only exists a k such that $\mathbb{P}(Y > y) \geq e^{-ky}$ for $y \in (0, b)$ for some $b \in \mathbb{R}^+$. The perpetuity can be split into $X \overset{\mathcal{D}}{=} Z_t + CP_1 + CP_2$, where Z_t is a truncated Gamma process, CP_1 and CP_2 are Compound Poisson processes, independent of each other and Z_t. The truncated Gamma process can be generated using Algorithm 3.4.2 and the two compound Poisson processes can be easily generated via A/R schemes.

[2]For simplicity, we assume Y has a continuous density g.

Example 4: $Y \sim Beta(\alpha, \beta)$. Since $g(0) < \infty$ for all $\alpha \geq 1$, we can simulate all Beta perpetuities with $\alpha \geq 1$ and all values of β. Furthermore, since the distribution has a finite support, there only exists a k such that $\mathbb{P}(Y > y) \geq e^{-ky}$ for $y \in (0, b)$ for some $b \in \mathbb{R}^+$. Hence, the Lévy measure needs to be truncated. The Beta perpetuity can be split into $X \overset{\mathcal{D}}{=} Z_t + CP_1 + CP_2$, where Z_t is a truncated Gamma process, and CP_1 and CP_2 are two compound Poisson processes, independent of each other and Z_t.

Example 5: $Y \sim Normal(\mu, \sigma^2)$. The Normal perpetuity X is two-sided. One could sample independent X_1 and X_2, each of which are half-normal perpetuities, and the difference $X_1 - X_2$ is the realisation of the two-sided perpetuity X.

For a half-normal perpetuity X_i, where $Y_i \sim$ *Half-Normal*(μ, σ), there only exists a k such that $\mathbb{P}(Y > y) \geq e^{-ky}$ for $y \in (0, b)$ for some $b \in \mathbb{R}^+$. Hence, the perpetuity X_i falls into Case 2 and can be split into a truncated Gamma process and two compound Poisson processes. The truncated Gamma process can be generated via Algorithm 3.4.2 and the two compound Poisson processes can be easily generated via A/R schemes. Figure 3.5 illustrates a sample density plot for the perpetuity X_i with $Y_i \sim$ Half-Normal$(0, 1)$. Figure 3.6 compares the distribution of X_i under different parameter settings.

Now, we can simulate the Normal perpetuity X by generating two independent half-normal perpetuities X_1 and X_2 and taking the difference $X \overset{\mathcal{D}}{=} X_1 - X_2$. Figure 3.7 and 3.8 demonstrate the distribution behaviour of the two sided perpetuity X via its histogram and density plot. We can also obtain other variations of the Normal perpetuities by introducing a new variable $B \sim Bernoulli(p)$ and setting $\hat{X} \overset{\mathcal{D}}{=} pX_1 - (1-p)X_2$. When $p = \frac{1}{2}$ and $X_i \sim Normal(0, 1)$, this is identical to the $Normal(0, 1)$ perpetuity. Figure 3.9 illustrates the differences of the perpetuity $\hat{X}$ and X in terms of their histograms.

3.7.2 Loss distributions with excess of loss reinsurance

We can use the truncated Lévy subordinator to model loss distribution of an insurer with the excess of loss reinsurance with retention level b. Without loss of generality, we use truncated inverse Gaussian as an example to illustrate the idea. Suppose the aggregate claims process follows an inverse Gaussian process. For each claim larger than size b, the insurer only retains b and the excess is ceded to the reinsurer. Denote the claims process of the insurer by C_t^I, and that of the reinsurer by C_t^R. Then the joint Laplace transform of C_t^I and C_t^R is

$$\mathbb{E}\left[e^{-\beta C_t^I - \gamma C_t^R}\right]$$

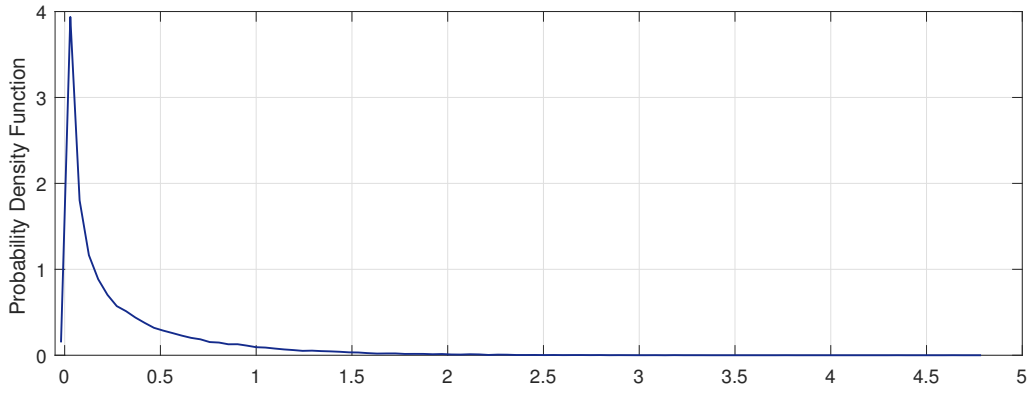

Figure 3.5: Probability density function of Perpetuity X_i with $Y_i \sim$ Half-Normal$(0,1)$.

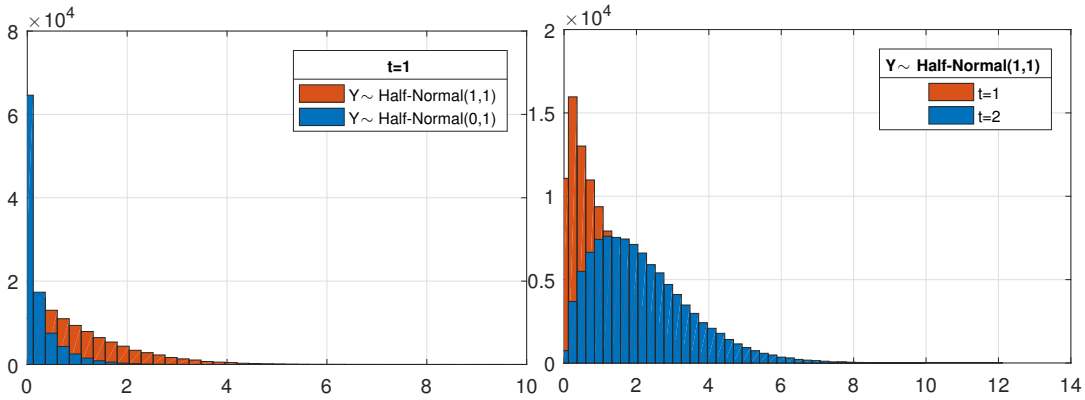

Figure 3.6: Histograms of Perpetuity X_i with $Y_i \sim$ Half-Normal$(0,1)$ and $Y_i \sim$ Half-Normal$(1,1)$ with $t = 1, 2$, respectively.

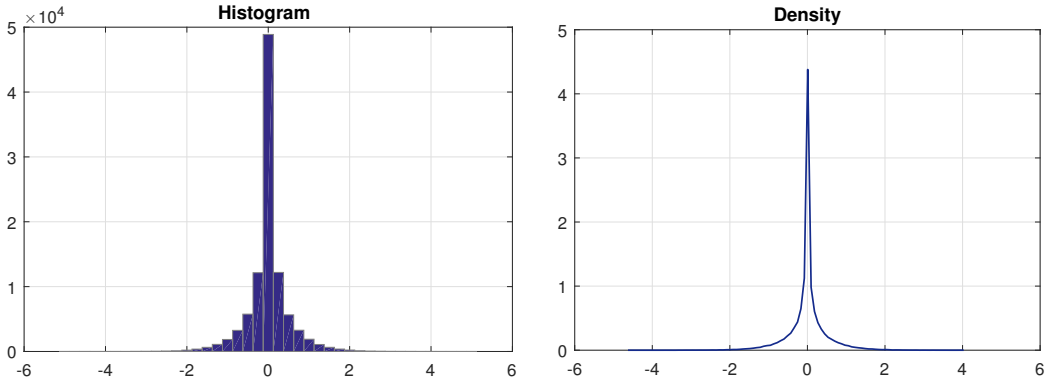

Figure 3.7: Histogram and Density Plot of Perpetuity X with $Y \sim$ Normal$(0,1)$.

$$= \exp\left(-t\int_0^b (1-e^{-\beta x})\frac{e^{-\mu x}}{\sqrt{2\pi x^3}}\mathrm{d}x - t\int_b^\infty (1-e^{-\beta b}e^{-\gamma(x-b)})\frac{e^{-\mu x}}{\sqrt{2\pi x^3}}\mathrm{d}x\right)$$

$$= \exp\left(-t\int_0^b (1-e^{-\beta x})\frac{e^{-\mu x}}{\sqrt{2\pi x^3}}\mathrm{d}x - t\lambda\int_0^\infty (1-e^{-\beta b}e^{-\gamma x})\frac{e^{-\mu(x+b)}}{\lambda\sqrt{2\pi(x+b)^3}}\mathrm{d}x\right).$$

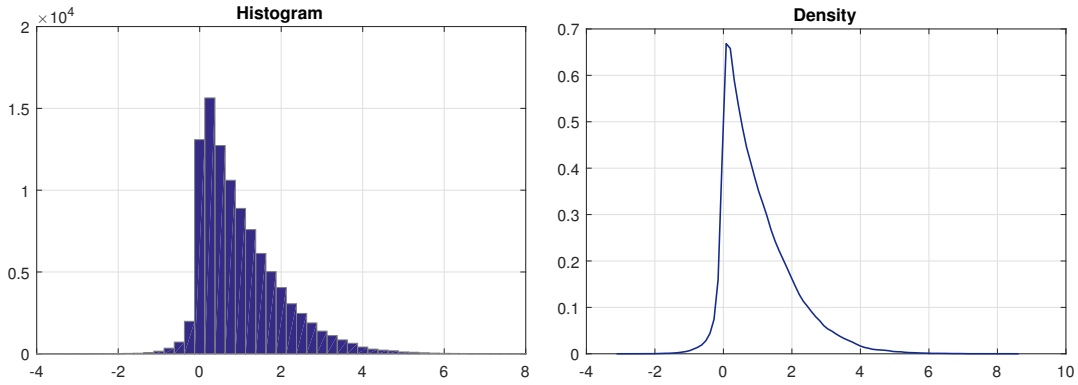

Figure 3.8: Histogram and Density Plot of Perpetuity X with $Y \sim \text{Normal}(1,1)$.

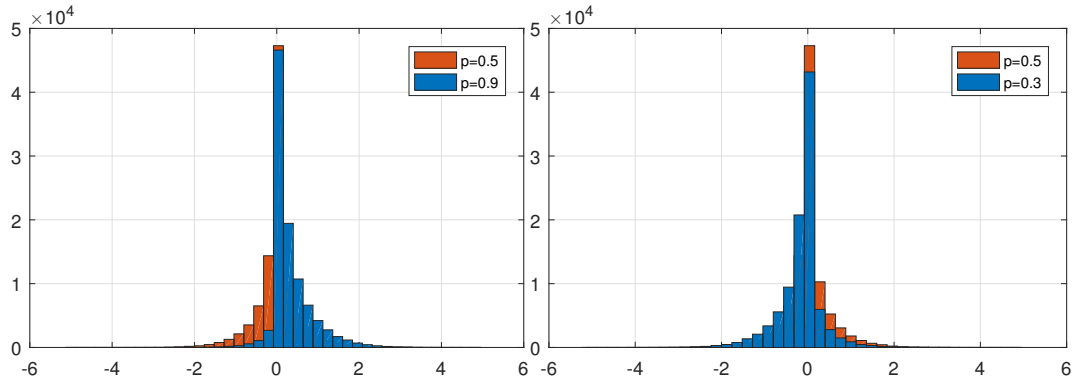

Figure 3.9: Histogram of Perpetuity $\hat{X} = BX_1 - (1-B)X_2$ with $B \sim Bernoulli(p)$ under parameter setting $p = 0.3, 0.5, 0.9$.

Hence, we have that

$$\left(C_t^I, C_t^R\right) \stackrel{\mathcal{D}}{=} \left(Z_t^b + bN_t, \sum_{i=1}^{N_t} Y_i\right),$$

where N_t is a Poisson process with intensity λt, and

$$\lambda := \sqrt{\frac{2}{\pi b}} e^{-\mu b} - \sqrt{2\mu}\,\text{Erfc}(\sqrt{\mu b}),$$

and the jump distribution Y_i has density

$$g_Y(y) = \frac{e^{-\mu(y+b)}}{\lambda\sqrt{2\pi(y+b)^3}}, \quad y > 0,$$

and N_t, Z_t^b and Y_i are all independent from each other. Using the simulation algorithm for Z_t, we can estimate the loss distributions of the insurer for a range of parameters and time horizons. In addition, we can also estimate $\mathbb{P}(C_t^I > x)$ for a given t, μ and truncation level b. Given t, this probability mainly depends on the tilting parameter μ and the truncation level b. Figure 3.10 illustrates how $\mathbb{P}(C_t^I > x)$ varies with the parameters.

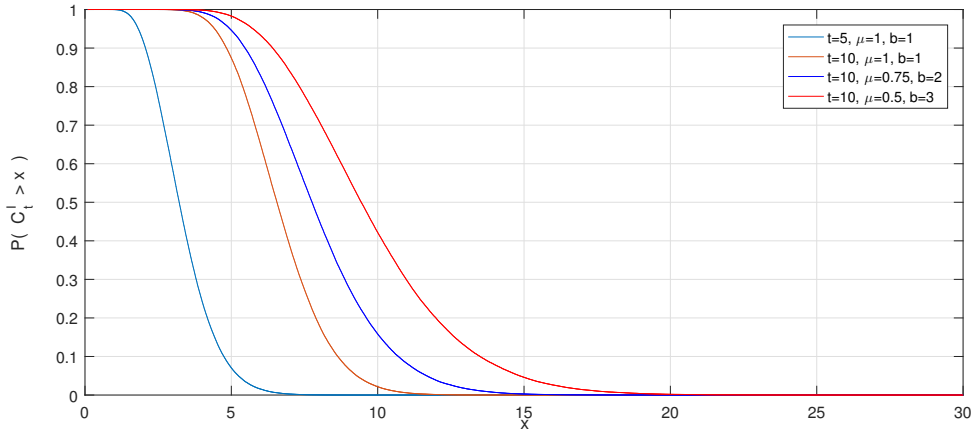

Figure 3.10: $\mathbb{P}(C_t^I > x)$ as a function of x based on parameter settings $t = 5, 10$, $\mu = 0.5, 0.75, 1$, and $b = 1, 2, 3$.

Importance sampling

When x is very large, the event $\{C_t^I > x\}$ is regarded as a rare event. The probability $\mathbb{P}\left(C_t^I > x\right)$ is very small and hence inefficient to estimate using direct Monte Carlo simulation, since the variance is much larger than what we are trying to estimate. We apply importance sampling to reduce the variance by changing the probability measure, such that under the new measure, the rare event happens more often and thus can be more efficiently estimated. Let us denote $l(x) = e^{\xi x}$ for some $\xi \in \mathbb{R}$, and after a change of probability measure, we have

$$\mathbb{E}^*\left[\mathbf{1}_{\{C_t^I > x\}}\right] = \frac{\mathbb{E}\left[\mathbf{1}_{\{C_t^I > x\}} l(C_t^I)\right]}{\mathbb{E}\left[l(C_t^I)\right]},$$

where $\mathbb{E}^*(\cdot)$ denotes the Esscher transform. The Laplace transform of C_t^I under the new measure is

$$\begin{aligned}
\mathbb{E}^*\left[e^{-\beta C_t^I}\right] &= \mathbb{E}\left[\frac{e^{-\beta C_t^I} e^{\xi C_t^I}}{\mathbb{E}\left[e^{\xi C_t^I}\right]}\right] \\
&= \frac{\exp\left(-t\int_0^b (1 - e^{-\beta x} e^{\xi x}) \frac{e^{-\mu x}}{\sqrt{2\pi x^3}} \mathrm{d}x\right) \exp\left(-t\int_b^\infty \left(1 - e^{-\beta b} e^{\xi b}\right) \frac{e^{-\mu x}}{\sqrt{2\pi x^3}} \mathrm{d}x\right)}{\exp\left(-t\int_0^b (1 - e^{\xi x}) \frac{e^{-\mu x}}{\sqrt{2\pi x^3}} \mathrm{d}x\right) \exp\left(-t\int_b^\infty \left(1 - e^{\xi b}\right) \frac{e^{-\mu x}}{\sqrt{2\pi x^3}} \mathrm{d}x\right)} \\
&= \exp\left(-t\int_0^b (1 - e^{-\beta x}) \frac{e^{-(\mu - \xi) x}}{\sqrt{2\pi x^3}} \mathrm{d}x\right) \exp\left(-t\int_b^\infty \left(1 - e^{-\beta b}\right) \frac{e^{-\mu x + \xi b}}{\sqrt{2\pi x^3}} \mathrm{d}x\right).
\end{aligned}$$

According to Asmussen and Glynn (2007) , ξ could be chosen to be the value such that $\mathbb{E}^*[C_t^I] = x$ where

$$\mathbb{E}^*[C_t^I] = \begin{cases} \frac{t\,\mathrm{Erf}(\sqrt{b(\mu-\xi)})}{\sqrt{2(\mu-\xi)}} + te^{\xi b}\left(\sqrt{\frac{2}{\pi b}}e^{-\mu b} - \sqrt{2\mu}\,\mathrm{Erfc}(\sqrt{\mu b})\right), & \mu > \xi, \\ t\sqrt{\frac{2b}{\pi}} + te^{\xi b}\left(\sqrt{\frac{2}{\pi b}}e^{-\mu b} - \sqrt{2\mu}\,\mathrm{Erfc}(\sqrt{\mu b})\right), & \mu = \xi, \\ \frac{t\,\mathrm{Erfi}(\sqrt{b|\mu-\xi|})}{\sqrt{2|\mu-\xi|}} + te^{\xi b}\left(\sqrt{\frac{2}{\pi b}}e^{-\mu b} - \sqrt{2\mu}\,\mathrm{Erfc}(\sqrt{\mu b})\right), & \mu < \xi. \end{cases} \tag{3.7.12}$$

This optimal value of ξ can be computed numerically based on (3.7.12). If $\mu > \xi$, C_t^{I*} remains like the original claim process with parameter $\mu' = \mu - \xi > 0$ under the new probability measure and if $\mu < \xi$, we have $\mu' = \mu - \xi < 0$, in which case we can generate C_t^{I*} based on Algorithm 3.5.6. The estimate for $\mathbb{P}(C_t^I > x)$ based on importance sampling will then be

$$\mathbb{P}^*(C_t^I > x) \approx \frac{1}{n}\sum_{i=1}^{n} \mathbf{1}_{\{x_i^* > x\}} M_{C_t^I}(\xi) e^{-\xi x_i^*}, \tag{3.7.13}$$

where x_i^* are generated under the new probability measure and

$$M_{C_t^I}(\xi) = \begin{cases} e^{-t\left[\sqrt{2(\mu-\xi)}\,\mathrm{Erf}(\sqrt{b(\mu-\xi)}) - \sqrt{2\mu}\,\mathrm{Erf}(\sqrt{b\mu}) + \sqrt{\frac{2}{\pi b}}\left(e^{-(\mu-\xi)b} - e^{-\mu b}\right)\right]} \\ \qquad \times e^{-t\left(1-e^{\xi b}\right)\left[\sqrt{\frac{2}{\pi b}}e^{-\mu b} - \sqrt{2\mu}\,\mathrm{Erfc}(\sqrt{\mu b})\right]}, & \mu > \xi, \\ e^{-t\sqrt{\frac{2}{\pi b}}\left(e^{\xi b} - 1 - \sqrt{b\pi\xi}\,\mathrm{Erfi}(\sqrt{\xi b})\right)} e^{-t\left(1-e^{\xi b}\right)\left[\sqrt{\frac{2}{\pi b}}e^{-\mu b} - \sqrt{2\mu}\,\mathrm{Erfc}(\sqrt{\mu b})\right]}, & \mu = \xi, \\ e^{-t\left[-\sqrt{2|\mu-\xi|}\,\mathrm{Erfi}(\sqrt{b|\mu-\xi|}) - \sqrt{2\mu}\,\mathrm{Erf}(\sqrt{b\mu}) + \sqrt{\frac{2}{\pi b}}\left(e^{|\mu-\xi|b} - e^{-\mu b}\right)\right]} \\ \qquad \times e^{-t\left(1-e^{\xi b}\right)\left[\sqrt{\frac{2}{\pi b}}e^{-\mu b} - \sqrt{2\mu}\,\mathrm{Erfc}(\sqrt{\mu b})\right]}, & \mu < \xi. \end{cases}$$

Hence, with large x, we can apply the importance sampling scheme to estimate $\mathbb{P}(C_t^I > x)$. Table 3.6 reports the estimated probability and estimated standard error based on direct Monte Carlo simulation versus Importance Sampling. We can see that the estimated probabilities under the two methods are very close. However, by using the importance sampling technique, the estimated standard error has been reduced, particularly for a larger x.

Table 3.6: Comparison of estimated $\mathbb{P}(C_t^I > x)$ and estimated standard error (SE) based on $t = 10, \mu = 0.5, b = 3$ via direct simulation under original measure and importance sampling (IS), respectively.

x	10	11	12	13	14	15	16	17	18	19	20
$\mathbb{P}(C_t^I > x)$	0.4203	0.2960	0.1995	0.1268	0.0780	0.0446	0.0261	0.0143	0.0073	0.0038	0.0018
SE($\times 10^{-4}$)	15.61	14.44	12.64	10.52	8.47	6.52	5.04	3.76	2.70	1.95	1.35
$\mathbb{P}(C_t^I > x)$(IS)	0.4208	0.2985	0.1999	0.1272	0.0787	0.0452	0.0256	0.0158	0.0074	0.0038	0.0019
SE($\times 10^{-4}$)	13.13	10.06	7.51	5.30	3.55	2.26	1.38	0.80	0.45	0.24	0.13

3.7.3 Pricing zero coupon Parisian bond

The truncated stable process has a duality relation with the Parisian stopping time of squared Bessel and CIR processes with dimension $\delta \in (0,2)$, see Dassios et al. (2018a). In particular, for a truncated Lévy subordinator Z_t, we have $Z_{\tilde{T}} \overset{\mathcal{D}}{=} \tau$, where τ is the Parisian stopping time and $\tilde{T}$ is an exponential random variable. Hence, one could use our exact simulation scheme to sample Parisian stopping times and thus pricing Parisian zero coupon bonds. Let the dynamics of the interest rate R_t follows a squared Bessel process or a CIR process under the risk-neutral probability measure $\mathbb{Q}$, we introduce a new type of Parisian-type bond, called the Parisian zero coupon bonds, which pays off an amount depending on the final interest rate, when the interest rate remains strictly positive for a consecutive length of time longer than a fixed window length D if this happens before maturity time T. If the interest rate fluctuates around 0 until maturity, the bound expires worthless. The buyer of the bond is thus betting against zero interest rates. Likewise, the seller of the Parisian bond is effectively hedging against a period where interest rates fluctuate around 0. This can be useful when considering interest rates which are bounded by a floor rate away from 0. Let $U_t := t - \sup\{s < t | R_s = 0\}$ be the time elapsed since the last time R_t hits 0 for $R_0 = 0$. Then the Parisian stopping time of R_t starting at 0 is $\tau = \inf\{t > 0 | U_t = D\}$. This is the first time the duration of an excursion exceeds a certain threshold $D > 0$. The payoff of the bond will thus be $h(R_\tau)\mathbf{1}_{\{\tau<T\}}$ at time τ, where τ is the Parisian stopping time, and $h : \mathbb{R}^+ \to \mathbb{R}^+$ is the payoff function. Let $P(r,T)$ be the no-arbitrage price of the bond, we have

$$P(r,T) = \mathbb{E}^r_{\mathbb{Q}}\left[\exp\left(-\int_0^\tau R_s \mathrm{d}s\right) h(R_\tau)\mathbf{1}_{\{\tau<T\}}\right], \tag{3.7.14}$$

where $\mathbb{E}^r_{\mathbb{Q}}$ denotes the expectation under the measure $\mathbb{Q}$, for a process starting at $R_0 = r$.

We obtain the Monte Carlo estimate of (3.7.14) by simulating the Parisian stopping time τ via marked renewal procedure. In Table 3.7, we present numerical examples of the digital zero coupon Parisian bond ($h(x) = 1$) and the zero coupon Parisian call ($h(x) = (x-K)^+$), for a range of parameters α and k. In general, the price for the zero coupon Parisian bond is higher than the zero coupon Parisian call for all α.

3.8 Conclusion

In this chapter, we introduce a new type of Lévy subordinator whose jump sizes are restricted by a certain truncation level. We have derived some important distributional properties of these processes and marked renewal representation which leads to an exact simulation framework in general.

Table 3.7: Price of zero coupon Parisian bond and zero coupon Parisian call with $K = 0.15$ under parameter setting $r_0 = 0.05, 0.2$ and $\alpha = 0.4, 0.6$.

Payoff	$h(x) = 1$			
T	$\delta = 1.2$	$\delta = 1.2$	$\delta = 0.8$	$\delta = 0.8$
	$r_0 = 0.05$	$r_0 = 0.2$	$r_0 = 0.05$	$r_0 = 0.2$
2	0.3318	0.3430	0.1797	0.1937
3	0.4139	0.4241	0.2563	0.2670
4	0.4414	0.4525	0.3018	0.3100
5	0.4493	0.4621	0.3269	0.3328
6	0.4550	0.4627	0.3393	0.3440
7	0.4560	0.4647	0.3458	0.3518
8	0.4566	0.4658	0.3513	0.3565
Payoff	$h(x) = (x-K)^+$			
T	$\delta = 1.2$	$\delta = 1.2$	$\delta = 0.8$	$\delta = 0.8$
	$r_0 = 0.05$	$r_0 = 0.2$	$r_0 = 0.05$	$r_0 = 0.2$
2	0.2675	0.2712	0.1421	0.1519
3	0.3240	0.3405	0.2098	0.2116
4	0.3500	0.3583	0.2330	0.2435
5	0.3536	0.3645	0.2518	0.2605
6	0.3624	0.3658	0.2685	0.2734
7	0.3615	0.3670	0.2699	0.2871
8	0.3658	0.3639	0.2713	0.2824

In particular, we have developed Algorithm 3.4.1 to sample the Dickman process, Algorithm 3.4.2 to sample the truncated gamma process, Algorithm 3.5.3 to sample the truncated stable process, Algorithm 3.5.4 to sample the truncated tempered stable process and Algorithm 3.5.8 to sample the truncated inverse Gaussian process. In addition, we develop an enhanced algorithm, Algorithm 3.5.5, to improve computational speed for the truncated tempered stable with large tilting parameter. Extensive numerical experiments and tests are established in order to demonstrate the accuracy of our results. We also provide applications to finance and insurance, which again demonstrate the applicability and flexibility of our results.

Part II

Exact Simulation on Lévy Based Stochastic Models

Chapter 4

Lévy Driven Ornstein-Uhlenbeck Processes

In this chapter, we study the *Lévy driven Ornstein-Uhlenbeck (OU)* processes. This class of stochastic processes is obtained through replacing the original Brownian motion in the OU process by a general Lévy process. The resulting Lévy driven OU process retains the mean-reverting dynamics, and also possesses some stylised features such as jumps and skewness, which often form the essential components of real financial data. We systematically study distributional properties and design a unique approach to exactly simulate these processes. Our key methodology for simulation design is based on the distributional decomposition of stochastic processes with a minor aid of acceptance and rejection scheme. The results immediately lead to very efficient algorithms without numerical inversion.

4.1 Introduction

A Lévy driven Ornstein-Uhlenbeck process is the analogue of an *ordinary Gaussian OU process* (Uhlenbeck and Ornstein, 1930) with its Brownian motion part replaced by a Lévy process. This class of stochastic processes has been extensively studied in the literature, see Wolfe (1982), Sato and Yamazato (1984), Barndorff-Nielsen (1998), Barndorff-Nielsen et al. (1998), Novikov (2004) and Patie (2005). Comparing with the Gaussian OU processes, the non-Gaussian counterparts offer greater flexibility that can accommodate some crucial distributional features, such as jumps, mean-reverting dynamics, serial dependence and volatility clustering, which are often observed in the real time series data[1]. Nowadays, these processes have been widely used as the continuous-time stochastic models for the observed behaviour of price dynamics in finance and economics. The applicability has been enhanced substantially by Barndorff-Nielsen and Shephard (2001b, 2002).

[1] See empirical evidences in finance from Carr et al. (2002).

They proposed a variety of useful non-negative OU processes for modelling stochastic volatilities. This class of models not only possess mathematically elegant properties, but also has nice economic interpretations for which new information arrives in discrete packets and trades are made in blocks[2]. It has also been widely used for modelling the stylised facts in the financial time series of stock prices, interest rates and stochastic volatilities[3]. In addition, it has also been used in option pricing, see Nicolato and Venardos (2003), Kallsen et al. (2011) and Li and Linetsky (2014), and for describing high-frequency financial data in market microstructure, see Barndorff-Nielsen and Shephard (2003a,b) and Todorov and Tauchen (2006). The process is defined via *stochastic differential equation* as below,

Definition 4.1.1 (Lévy Driven Ornstein-Uhlenbeck Process)**.** *X_t is a Lévy driven Ornstein-Uhlenbeck process that satisfies the stochastic differential equation (SDE)*

$$\mathrm{d}X_t = -\delta X_t \mathrm{d}t + \varrho \mathrm{d}Z_t, \qquad t \geq 0, \tag{4.1.1}$$

where

- $\varrho > 0$ *is a positive constant;*
- $\delta > 0$ *is the constant rate of exponential decay;*
- $Z_t \geq 0$ *with* $Z_0 = 0$ *is a pure-jump Lévy subordinator.*

Equivalently, given the initial level $X_0 > 0$ at time 0, the solution to this SDE (4.1.1) is given by

$$X_t = e^{-\delta t} \mathrm{X}_0 + \varrho \int_0^t e^{-\delta(t-s)} \mathrm{d}\mathrm{Z}_s. \tag{4.1.2}$$

Hence, the resulting process X_t is non-negative, and it is the continuous-time analogue of a discrete-time *autoregression of order* 1 (i.e. *AR(1)*) (Barndorff-Nielsen et al., 1998, p.995). If Z_t is replaced by a standard Brownian motion, then, it returns to the *ordinary Gaussian OU process* (Uhlenbeck and Ornstein, 1930).

4.2 Distributional Properties

In this section, we derive the Laplace transform of Lévy driven OU process for fix time in Theorem 4.2.1, which leads to key results of this chapter.

[2] See empirical evidences from the market microstructure in Easley and O'Hara (1987).
[3] See empirical evidences from Cont (2001).

Theorem 4.2.1. *For a general Lévy driven OU process X_t of Definition 4.1.1, the Laplace transform of $X_{t+\tau}$ conditional on X_t is given by*

$$\mathbb{E}\left[e^{-vX_{t+\tau}} \mid X_t\right] = e^{-vwX_t} \times \exp\left(-\frac{\varrho}{\delta}\int_{vw}^{v}\frac{\Phi(u)}{u}\mathrm{d}u\right), \qquad \tau \in \mathbb{R}^+, \tag{4.2.1}$$

where $w := e^{-\delta\tau}$ and $\Phi(\cdot)$ is the Laplace exponent of Lévy subordinator Z_t.

Proof. Note that, in general, the Laplace exponent for Z_t is

$$\Phi(u) = \int_0^\infty \left(1 - e^{-uy}\right)\nu(y)\mathrm{d}y,$$

where ν is the Lévy measure of Z_t. The infinitesimal generator $\mathcal{A}$ of process (X_t, t) acting on any function $f(x,t)$ within its domain $\Omega(\mathcal{A})$ is given by

$$\mathcal{A}f(x,t) = \frac{\partial f}{\partial t} - \delta x\frac{\partial f}{\partial x} + \varrho\left(\int_0^\infty \left[f(x+y,t) - f(x,t)\right]\nu(y)\mathrm{d}y\right), \tag{4.2.2}$$

see Duffie et al. (2003).

By applying the *piecewise-deterministic Markov processes theory* (Davis, 1984) and martingale approach (Dassios and Embrechts, 1989), we can derive the conditional Laplace transform for X_t. More precisely, set $\mathcal{A}f(x,t) = 0$, we adopt a similar approach as Dassios and Jang (2003) and Dassios and Zhao (2011) to find the martingale solution to $\mathcal{A}f = 0$ for the generator (4.2.2). We try a solution of exponential form $e^{-xA(t)}e^{R(t)}$ where $A(t)$ and $R(t)$ are deterministic and differentiable functions of time t. Then, we get

$$-xA'(t) + R'(t) + \delta xA(t) - \varrho\int_0^\infty \left[1 - e^{-yA(t)}\right]\nu(y)\mathrm{d}y = 0,$$

which implies that,

$$A(t) = ke^{\delta t}, \qquad R(t) = \varrho\int_0^t \Phi\left(ke^{\delta s}\right)\mathrm{d}s, \qquad \forall\, k \in \mathbb{R}^+.$$

Hence, the martingale is of the form

$$\exp\left(-X_t ke^{\delta t}\right)\exp\left(\varrho\int_0^t \Phi\left(ke^{\delta s}\right)\right), \qquad \forall\, k \in \mathbb{R}^+. \tag{4.2.3}$$

Set $k = ve^{-\delta(t+\tau)}$, by martingale property, we obtain

$$\begin{aligned}\mathbb{E}\left[e^{-vX_{t+\tau}} \mid X_t\right] &= \exp\left(-ve^{-\delta\tau}X_t\right)\exp\left(-\varrho\int_t^{t+\tau}\Phi\left(ve^{-\delta(T+\tau-s)}\right)\mathrm{d}s\right)\\ &= \exp\left(-ve^{-\delta\tau}X_t\right)\exp\left(-\frac{\varrho}{\delta}\int_{ve^{-\delta\tau}}^{v}\frac{\Phi(u)}{u}\mathrm{d}u\right).\end{aligned}$$

□

The conditional Laplace transform (4.2.1)[4] in Proposition 4.2.1 is the key tool to develop our exact simulation scheme later in this chapter. It can also be used to obtain an analytical formula for the associated conditional expectation in Proposition 4.2.1.

Proposition 4.2.1. *The expectation of $X_{t+\tau}$ conditional on X_t is given by*

$$\mathbb{E}\left[X_{t+\tau} \mid X_t\right] = wX_t + \frac{\varrho}{\delta}(1-w)\mathbb{E}\left[Z_1\right], \qquad \tau \in \mathbb{R}^+, \tag{4.2.4}$$

where $\mathbb{E}[Z_1] = \int_0^\infty s\nu(s)\mathrm{d}s$.

Proof. Based on Proposition 4.2.1, we have

$$\begin{aligned}\mathbb{E}\left[X_{t+\tau} \mid X_t\right] &= -\frac{\partial}{\partial v}\mathbb{E}\left[e^{-vX_{t+\tau}} \mid X_t\right]\Big|_{v=0}\\ &= e^{-\delta\tau}X_t + \frac{\varrho}{\delta}\lim_{v\to 0}\left(\Phi'(v) - \Phi'\left(e^{-\delta\tau}v\right)\right)\\ &= e^{-\delta\tau}X_t + \frac{\varrho}{\delta}\lim_{v\to 0}\left(\int_0^\infty se^{-vs}\nu(s)\mathrm{d}s - w\int_0^\infty se^{-wvs}\nu(s)\mathrm{d}s\right)\\ &= e^{-\delta\tau}X_t + \frac{\varrho}{\delta}\left(1-e^{-\delta\tau}\right)\int_0^\infty s\nu(s)\mathrm{d}s.\end{aligned}$$

□

4.3 Shot-noise process

Let us start by looking at the simplest Lévy driven OU process, i.e. the shot noise process. The shot noise process $X = \{X_t, t \geq 0\}$ is a positive stochastic process on positive half-line $\mathbb{R}^+$ following

[4] An alternative proof of this result via the characteristic function of stochastic integral for a continuous function proposed by Lukacs (1969) can also be found in Wolfe (1982).

the stochastic differential equation (4.1.1) in Definition 4.1.1, with Z_t being a compound Poisson process. Given the initial level $X_0 > 0$, it is alternatively defined by

$$X_t = X_0 e^{-\delta t} + \sum_{0 \le T_i < t} Z_i e^{-\delta(t-T_i)}, \qquad t \ge 0, \tag{4.3.1}$$

where

- $\{Z_i\}_{i=1,2,\dots}$ is a sequence of i.i.d jump sizes with density f_Z;
- $\{T_i\}_{i=1,2,\dots}$ are the arrival times of a standard Poisson process N_t with rate ρ.

As concluded by Barndorff-Nielsen (1997), the compound Poisson based OU processes are very tractable models that could facilitate many potential applications, see Barndorff-Nielsen and Shephard (2001b, 2002, 2003b); Roberts et al. (2004); Jongbloed et al. (2005); Griffin and Steel (2006); Creal (2008); Frühwirth-Schnatter and Sögner (2009); Schoutens and Cariboni (2010); Bianchi and Fabozzi (2015), for further reference.

4.3.1 Laplace Transform

We derive the conditional Laplace transform of $X_{t+\tau}$ for a fix time $t+\tau$ given X_t in Theorem 4.3.1 below.

Theorem 4.3.1. *The Laplace transform of $X_{t+\tau}$ conditional on X_t is given by*

$$\mathbb{E}\left[e^{-vX_{t+\tau}} \mid X_t\right] = e^{-vwX_t} \times \exp\left(-\frac{\rho}{\delta} \int_0^{\infty} \left(1 - e^{-vs}\right) \int_1^{\frac{1}{w}} f_Z(su)\mathrm{d}u\mathrm{d}s \right), \qquad v \in \mathbb{R}^+, \tag{4.3.2}$$

where $\tau > 0$ is any fixed-length time interval and $w := e^{-\delta\tau}$.

Proof. Based on Theorem 4.2.1, we have

$$\mathbb{E}\left[e^{-vX_{t+\tau}} \mid X_t\right] = e^{-vwX_t} \exp\left(-\frac{\varrho}{\delta} \int_{vw}^{v} \frac{\Phi(u)}{u}\mathrm{d}u \right), \qquad w := e^{-\delta\tau}, \tag{4.3.3}$$

where

$$\Phi(u) = \int_0^{\infty} (1 - e^{-vy}) f_Z(y)\mathrm{d}y,$$

is the Laplace exponent of compound Poisson process. Rewriting the integral term in (4.3.3) as

$$\int_{vw}^{v} \frac{\Phi(u)}{u}\mathrm{d}u \;=\; \int_{vw}^{v} \frac{1}{u} \int_0^{\infty} \left(1 - e^{-uy}\right) f_Z(y)\mathrm{d}y\mathrm{d}u$$

$$= \int_0^\infty \frac{(1-e^{-vs})}{s} \int_s^{\frac{s}{w}} f_Z(y)\mathrm{d}y\mathrm{d}s$$
$$= \int_0^\infty \left(1-e^{-vs}\right) \int_1^{\frac{1}{w}} f_Z(su)\mathrm{d}u\mathrm{d}s,$$

the conditional Laplace transform of X_t can be expressed as (4.3.2). □

4.3.2 Exact Simulation Scheme

The Laplace transform of $X_{t+\tau}$ conditional on X_t in Theorem 4.3.1 implies that $X_{t+\tau}$ has two simple elements, one deterministic trend and one compound Poisson random variable. This result immediately leads to an exact simulation algorithm.

Algorithm 4.3.1 (Exact Simulation of Shot noise Process via Decomposition Approach)**.** *The distribution of $X_{t+\tau}$ conditional on X_t can be exactly decomposed as*

$$X_{t+\tau} \mid X_t \overset{\mathcal{D}}{=} \underbrace{e^{-\delta\tau}X_t}_{\textit{Deterministic trend}} + \underbrace{\sum_{k=1}^{N} S_k}_{\textit{Finite jumps}}, \qquad \tau \in \mathbb{R}^+, \tag{4.3.4}$$

where

- *N is a Poisson random variable ;*
- *$\{S_k\}_{k=1,2,\ldots}$ are i.i.d random variables following a mixture of distributions with density*

$$f_{S_k}(s) \propto \int_1^{\frac{1}{w}} f_Z(su)\mathrm{d}u; \tag{4.3.5}$$

It is well known that there exists a simple alternative algorithm. This is a *path-dependent approach* that is constructed directly based on the definition of shot noise process (4.3.1).

Algorithm 4.3.2 (Exact Simulation of Shot noise process via Path-dependent Approach)**.** *Given the i^{th} jump arrival time T_i and the associated level X_{T_i}, we can exactly simulate the next arrival time T_{i+1} and the associated level $X_{T_{i+1}}$ by the following steps:*

1. *Generate an exponentially distributed random variable $\tau_{i+1}^* \sim \mathrm{Exp}(\rho)$ as the $(i+1)^{\text{th}}$ inter-arrival time;*
2. *Record the next jump arrival time $T_{i+1} = T_i + \tau_{i+1}^*$;*
3. *Record the next pre-jump level $X_{T_{i+1}^-} = X_{T_i}e^{-\delta\tau_{i+1}^*}$;*

Table 4.1: Comparison for Algorithm 4.3.2 vs. Algorithm 4.3.1 for the shot noise process with exponential jumps based on the parameters $(\delta, \rho; \theta; X_0) = (0.5, 1.0; 1.0; 10.0)$ for time intervals $\tau = 0.5, 1$, respectively.

τ	Paths	True	Simulation	Diff	Error %	RMSE	Time	Simulation	Diff	Error %	RMSE	Time
			Algorithm 4.3.2					**Algorithm 4.3.1**				
$\tau = 0.5$	10,000	8.2304	8.2525	0.0221	0.27%	0.0091	0.97	8.2222	-0.0082	-0.10%	0.0087	0.38
	40,000	8.2304	8.2398	0.0094	0.11%	0.0045	3.64	8.2291	-0.0013	-0.02%	0.0044	1.39
	160,000	8.2304	8.2329	0.0025	0.03%	0.0022	14.33	8.2288	-0.0016	-0.02%	0.0022	5.50
	640,000	8.2304	8.2314	0.0010	0.01%	0.0011	59.48	8.2306	0.0002	0.00%	0.0011	21.92
	2,560,000	8.2304	8.2301	-0.0003	0.00%	0.0006	224.03	8.2304	0.0000	0.00%	0.0006	88.48
			Algorithm 4.3.2					**Algorithm 4.3.1**				
$\tau = 1$	10,000	6.8522	6.8621	0.0099	0.14%	0.0111	0.91	6.8418	-0.0104	-0.15%	0.0114	0.38
	40,000	6.8522	6.8559	0.0037	0.05%	0.0056	3.61	6.8543	0.0021	0.03%	0.0057	1.59
	160,000	6.8522	6.8535	0.0012	0.02%	0.0028	14.11	6.8536	0.0014	0.02%	0.0028	5.91
	640,000	6.8522	6.8504	-0.0019	-0.03%	0.0014	55.88	6.8515	-0.0007	-0.01%	0.0014	23.19
	2,560,000	6.8522	6.8521	-0.0001	0.00%	0.0007	240.42	6.8522	-0.0000	0.00%	0.0007	92.81

4. *Generate Z_{i+1} with density f_Z as the $(i+1)^{\text{th}}$ jump size;*

5. *Record the next level $X_{T_{i+1}} = X_{T_{i+1}^-} + Z_{i+1}$.*

An obvious advantage of our decomposition approach (Algorithm 4.3.1) over the traditional path-dependent approach (Algorithm 4.3.2) is that it can generate the distribution directly at the target terminal $t + \tau$ without drawing complete skeletons of the underlying paths from the initial time t to the terminal $t + \tau$.

4.3.3 Simulation Studies

In this section, we illustrate the performance and effectiveness of our algorithm through numerical experiments by assuming Z_i follows an exponential distribution, i.e. the density function or Z_i is

$$f_Z(z) = \theta e^{-\theta u}, \qquad \theta > 0.$$

The parameters were set as $(\delta, \rho; \theta; X_0) = (0.5, 1.0; 1.0; 10.0)$, we conducted a numerical comparison between our decomposition scheme (Algorithm 4.3.1) and the traditional path-dependent scheme (Algorithm 4.3.2) for time intervals $\tau = 0.5, 1$. The detailed numerical results are reported in Table 4.1, where we can see that, for a slightly large number of paths, both algorithms are extremely accurate (in terms of error, error%, and RMSE) by comparing the simulation-estimated means with the associated true values provided by (4.2.4) in Proposition 4.2.1. By comparing the computation time (CPU), we can clearly observe that our new scheme outperforms the traditional approach.

4.4 OU-Γ Process

The *OU-Gamma (OU-Γ) process* $X = \{X_t, t \geq 0\}$ is a positive stochastic process following the stochastic differential equation (4.1.1) in Definition 4.1.1, with Z_t being a gamma process. Unlike the shot noise process, the OU-Γ process has *infinite-activity* jumps (i.e. infinite jumps over any finite time horizon)[5]. Recently, Aït-Sahalia and Jacod (2009, 2011) found that high-frequency stock price data present infinite-activity jumps. Ornthanalai (2014) also provided evidence for infinite-activity jumps in index options and returns from 1996 to 2009, and suggested that infinite-activity jumps, instead of the Brownian increments, should be the default modelling choice in asset pricing models. To develop the exact simulation scheme to sample OU-Γ process, we first derive the Laplace transform of the OU-Γ process.

4.4.1 Laplace transform

The condition Laplace transform of OU-Γ process is given as follows:

Theorem 4.4.1. *The Laplace transform of $X_{t+\tau}$ conditional on X_t can be expressed as*

$$\begin{aligned}
&\mathbb{E}\left[e^{-vX_{t+\tau}} \mid X_t\right] \\
= \;& e^{-vwX_t} \times \exp\left(-\frac{\alpha\varrho}{\delta}\ln w \int_0^\infty \left(1-e^{-vs}\right) s^{-1} e^{-\frac{\beta}{w}s}\mathrm{d}s\right) \\
& \times \exp\left(-\frac{\alpha\varrho}{\delta}\int_0^\infty \left(1-e^{-vs}\right)\int_1^{\frac{1}{w}} \beta e^{-\beta us}\ln u \mathrm{d}u\mathrm{d}s\right), \qquad v \in \mathbb{R}^+. \qquad (4.4.1)
\end{aligned}$$

Proof. The OU-Γ process X_t is driven by a Gamma process Z_t with Laplace exponent

$$\Phi(v) = \alpha \ln\left(1+\frac{v}{\beta}\right), \qquad v \in \mathbb{R}^+,$$

and Lévy measure

$$\nu(s) = \alpha s^{-1} e^{-\beta s}, \qquad \alpha, \beta > 0.$$

According to Theorem 4.2.1, we can express the conditional Laplace transform as

$$\begin{aligned}
\mathbb{E}\left[e^{-vX_{t+\tau}} \mid X_t\right] &= e^{-vwX_t} \exp\left(-\frac{\varrho}{\delta}\int_{vw}^{v} \frac{\alpha}{u}\ln\left(1+\frac{u}{\beta}\right)\mathrm{d}u\right) \\
&= e^{-vwX_t} \exp\left(-\frac{\varrho}{\delta}\int_{vw}^{v} \frac{1}{u}\int_0^\infty \left(1-e^{-uy}\right)\alpha y^{-1} e^{-\beta y}\mathrm{d}y\mathrm{d}u\right), \qquad (4.4.2)
\end{aligned}$$

[5] As the Lévy density of a Gamma process has an infinite integral, the process has infinitely many jumps over any time interval.

where

$$
\begin{aligned}
& \int_{vw}^{v} \frac{1}{u} \int_{0}^{\infty} \left(1-e^{-uy}\right) \alpha y^{-1} e^{-\beta y} \mathrm{d}y \mathrm{d}u \\
= & \int_{w}^{1} \frac{1}{z} \int_{0}^{\infty} (1-e^{-vzy}) \alpha y^{-1} e^{-\beta y} \mathrm{d}y \mathrm{d}z \\
= & \int_{0}^{\infty} \frac{1-e^{-vs}}{s} \int_{s}^{\frac{s}{w}} \alpha y^{-1} e^{-\beta y} \mathrm{d}y \mathrm{d}s \\
= & \int_{0}^{\infty} \frac{1-e^{-vs}}{s} \int_{s}^{\frac{s}{w}} \alpha y^{-1} e^{-\beta \frac{s}{w}} \mathrm{d}y \mathrm{d}s + \int_{0}^{\infty} \frac{1-e^{-vs}}{s} \int_{s}^{\frac{s}{w}} \alpha y^{-1} \left(e^{-\beta y} - e^{-\beta \frac{s}{w}}\right) \mathrm{d}y \mathrm{d}s. \quad (4.4.3)
\end{aligned}
$$

Note that, both of the terms in (4.4.3) are positive, because $e^{-\beta y} \geq e^{-\beta \frac{s}{w}}$ for any $y \in \left[s, \frac{s}{w}\right]$.

1. The first term of (4.4.3) can be expressed as the Laplace exponent of a Gamma random variable, i.e.,

$$
\int_{0}^{\infty} \frac{1-e^{-vs}}{s} \int_{s}^{\frac{s}{w}} \alpha y^{-1} e^{-\beta \frac{s}{w}} \mathrm{d}y \mathrm{d}s = \alpha \ln\left(\frac{1}{w}\right) \int_{0}^{\infty} \left(1-e^{-vs}\right) s^{-1} e^{-\frac{\beta}{w} s} \mathrm{d}s. \quad (4.4.4)
$$

2. The inner integral of the second term of (4.4.3) can be rewritten as

$$
\begin{aligned}
& \frac{1}{s} \int_{s}^{\frac{s}{w}} \alpha y^{-1} \left(e^{-\beta y} - e^{-\beta \frac{s}{w}}\right) \mathrm{d}y \\
= & \alpha \int_{1}^{\frac{1}{w}} \frac{1}{x} \frac{e^{-\beta s x} - e^{-\beta \frac{s}{w}}}{s} \mathrm{d}x \\
= & \alpha \int_{1}^{\frac{1}{w}} x^{-1} \int_{x}^{\frac{1}{w}} \beta e^{-\beta s u} \mathrm{d}u \mathrm{d}x \\
= & \alpha \int_{1}^{\frac{1}{w}} \beta e^{-\beta s u} \ln u \mathrm{d}u. \quad (4.4.5)
\end{aligned}
$$

Finally, we can obtain the conditional Laplace transform (4.4.1) based on the integral representations of (4.4.4) and (4.4.5). □

4.4.2 Exact Simulation Scheme

The distribution of $X_{t+\tau}$ conditional on X_t can be exactly decomposed into three basic components: one deterministic trend, one gamma random variable, and one compound Poisson random variable.

The details are provided in Algorithm 4.4.1.

Algorithm 4.4.1 (Exact Simulation of OU-Γ Process)**.** *The distribution of $X_{t+\tau}$ conditional on X_t can be exactly decomposed as*

$$X_{t+\tau} \mid X_t \overset{\mathcal{D}}{=} \underbrace{e^{-\delta\tau}X_t}_{\textit{Deterministic trend}} + \underbrace{\tilde{\Gamma}}_{\textit{Infinite jumps}} + \underbrace{\sum_{k=1}^{\tilde{N}} S_k}_{\textit{Finite jumps}}, \qquad \tau \in \mathbb{R}^+, \tag{4.4.6}$$

where

- $\tilde{\Gamma}$ *is a gamma random variable of*

$$\tilde{\Gamma} \sim \Gamma\left(\alpha\varrho\tau,\ \beta e^{\delta\tau}\right); \tag{4.4.7}$$

- $\tilde{N}$ *is a Poisson random variable of rate* $\frac{1}{2}\alpha\varrho\delta\tau^2$*;*
- $\left\{S_k\right\}_{k=1,2,\ldots}$ *are i.i.d random variables following a mixture of exponential distributions, i.e.,*

$$S_k \sim \text{Exp}\left(\beta e^{\delta\tau\sqrt{U}}\right), \qquad U \sim \mathcal{U}[0,1], \qquad \forall k = 1,2,.... \tag{4.4.8}$$

Proof. The three components of (4.4.6) correspond to the three terms of the conditional Laplace transform (4.4.1), respectively:

1. The first term of (4.4.1) is the Laplace transform of $e^{-\delta\tau}X_t$.
2. The second term of (4.4.1) is the Laplace transform of a gamma random variable, $\tilde{\Gamma}$, and the corresponding Lévy measure is specified by

$$\nu(s) = \frac{\alpha\varrho}{\delta}\ln\left(\frac{1}{w}\right)s^{-1}e^{-\frac{\beta}{w}s}.$$

3. The Laplace exponent of the third term in (4.4.1) can be rewritten as

$$\frac{\alpha\varrho}{\delta}\int_0^\infty\left(1-e^{-vs}\right)\int_1^{\frac{1}{w}}\beta e^{-\beta us}\ln u\,\mathrm{d}u\mathrm{d}s = \frac{\alpha\varrho}{2\delta}\ln^2 w\int_0^\infty\left(1-e^{-vs}\right)\int_1^{\frac{1}{w}}\beta u e^{-\beta us}f_V(u)\mathrm{d}u\mathrm{d}s, \tag{4.4.9}$$

where

$$f_V(u) = \frac{2}{\ln^2 w}\frac{\ln u}{u}, \qquad u \in \left[1, \frac{1}{w}\right],$$

is the density function of random variable V. This clearly indicates that (4.4.9) is the Laplace exponent of a compound Poisson random variable whose rate parameter is $\frac{\alpha\varrho}{2\delta}\ln^2 w$ and jump

Table 4.2: Comparison between the true mean and the associated simulation results using Algorithm 4.4.1 for the OU-Γ process based on the parameters $(\delta, \varrho; \alpha, \beta; X_0) = (0.5, 1.0; 2.0, 2.0; 10.0)$ for $T = 1, 2, 4, 10$, respectively.

Paths	True	Simulation	Diff	Error %	RMSE	Time	True	Simulation	Error	Error %	RMSE	Time
				$T = 1$						$T = 2$		
10,000	6.8522	6.8471	-0.0051	-0.07%	0.0056	0.48	4.9430	4.9457	0.0026	0.05%	0.0066	0.61
40,000	6.8522	6.8527	0.0005	0.01%	0.0028	1.80	4.9430	4.9422	-0.0008	-0.02%	0.0034	2.16
160,000	6.8522	6.8500	-0.0022	-0.03%	0.0014	7.53	4.9430	4.9424	-0.0007	-0.01%	0.0017	7.94
640,000	6.8522	6.8522	-0.0001	0.00%	0.0007	30.14	4.9430	4.9432	0.0001	0.00%	0.0008	31.44
2,560,000	6.8522	6.8521	-0.0001	0.00%	0.0004	120.41	4.9430	4.9433	0.0003	0.01%	0.0004	126.03
				$T = 4$						$T = 10$		
10,000	3.0827	3.0826	-0.0000	0.00%	0.0093	0.77	2.0539	2.0345	-0.0194	-0.94%	0.0303	1.34
40,000	3.0827	3.0826	-0.0001	0.00%	0.0047	2.88	2.0539	2.0554	0.0015	0.07%	0.0153	4.83
160,000	3.0827	3.0854	0.0027	0.09%	0.0024	11.38	2.0539	2.0545	0.0006	0.03%	0.0076	19.14
640,000	3.0827	3.0812	-0.0015	-0.05%	0.0012	44.47	2.0539	2.0561	0.0022	0.11%	0.0038	77.05
2,560,000	3.0827	3.0836	0.0010	0.03%	0.0006	175.28	2.0539	2.0527	-0.0012	-0.06%	0.0019	305.59

sizes are exponentially distributed with rate βV. Here, V is a well-defined random variable that can be exactly simulated via an explicit inverse transform, as the cumulative distribution function (CDF) of V, i.e.,

$$F_V(u) = \left(\frac{\ln u}{\ln w}\right)^2, \qquad u \in \left[1, \frac{1}{w}\right],$$

can be inverted explicitly as

$$F_V^{-1}(x) = w^{-\sqrt{x}}, \qquad x \in [0, 1].$$

□

For the decomposition specified by (4.4.6), the compound Poisson random variable $\sum_{k=1}^{\tilde{N}} S_k$ can only produce a finite number of (large) jumps. The extra term of the gamma random variable $\tilde{\Gamma}$ in (4.4.6) clearly explains why the OU-Γ process has infinite-activity jumps for any time interval. That is, within any time interval $\tau > 0$, there always exists a gamma random variable $\tilde{\Gamma}$ that produces an infinite number of (small) positive jumps.

4.4.3 Simulation Studies

In this section, we establish various numerical experiments to verify our algorithm. In the numerical implementations, the parameters were set as $(\delta, \varrho; \alpha, \beta; X_0) = (0.5, 1.0; 2.0, 2.0; 10.0)$. for $T = 1, 2, 4, 10$, respectively. The associated numerical results are reported in Table 4.2. The numerical results reported here show that the simulations are very fast and the associated errors (measured in terms of error, error%, and RMSE) are small. Overall, it is evident that our newly developed decomposition approach can achieve high accuracy as well as efficiency.

4.5 OU-TS Process

OU-TS Process is a Lévy driven OU process X_t of Definition 4.1.1 with Lévy subordinator Z_t being a tempered stable process, i.e. $Z_t \sim TS(\alpha, \beta, \theta t)$. As pointed in the concluding remarks of Barndorff-Nielsen and Shephard (2001c, p.19), this type of processes offer great flexibility and are mathematically and computationally tractable, which could lead to a variety of applications, e.g. Barndorff-Nielsen et al. (1998, 2002), Barndorff-Nielsen and Shephard (2001b, 2002, 2003a), Nicolato and Venardos (2003), Gander and Stephens (2007a,b), Andrieu et al. (2010) and Todorov (2015), etc.

4.5.1 Laplace Transform

The conditional distribution of OU-TS process is decomposable, due to the *infinite divisibility* property of TS distribution. We choose a cutting value to break the OU-TS process into several simple elements such that each one can be exactly simulated. Theorem 4.5.1 illustrates the exact distributional decomposition of OU-TS process via integral transforms.

Theorem 4.5.1. *For the OU-TS process X_t, the Laplace transform of $X_{t+\tau}$ conditional on X_t can be expressed by*

$$\begin{aligned}
&\mathbb{E}\left[e^{-vX_{t+\tau}} \mid X_t\right] \\
= \;& e^{-vwX_t} \times \exp\left(-\frac{\varrho\theta(1-w^\alpha)}{\alpha\delta} \int_0^\infty (1-e^{-vs}) \frac{e^{-\frac{\beta}{w}s}}{s^{\alpha+1}} \mathrm{d}s \right) \\
& \times \exp\left(-\frac{\varrho\theta\beta^\alpha\Gamma(1-\alpha)D_w}{\alpha\delta} \int_0^\infty (1-e^{-vs}) \int_1^{\frac{1}{w}} \frac{(\beta u)^{1-\alpha}}{\Gamma(1-\alpha)} s^{(1-\alpha)-1} e^{-\beta us} \frac{u^{\alpha-1}-u^{-1}}{D_w} \mathrm{d}u\mathrm{d}s \right),
\end{aligned}$$

where

$$D_w := \frac{1}{\alpha}\left(w^{-\alpha}-1\right) + \ln w. \tag{4.5.1}$$

Proof. Since the Lévy measure of TS is (2.4.1), the Laplace exponent is specified by

$$\Phi(u) \int_0^\infty (1-e^{-uy}) \frac{\theta}{y^{\alpha+1}} e^{-\beta y} \mathrm{d}y = \frac{\theta\Gamma(1-\alpha)}{\alpha}\left[(\beta+u)^\alpha - \beta^\alpha\right],$$

where $\Gamma(\cdot)$ is *gamma function*, i.e. $\Gamma(u) := \int_0^\infty s^{u-1}e^{-s}\mathrm{d}s$. Based on Proposition 4.2.1, we have

$$\mathbb{E}\left[e^{-vX_{t+\tau}} \mid X_t\right] = e^{-vwX_t} \exp\left(-\frac{\varrho}{\delta} \int_{vw}^{v} \frac{1}{u} \int_0^\infty \left(1-e^{-uy}\right) \frac{\theta}{y^{\alpha+1}} e^{-\beta y} \mathrm{d}y\mathrm{d}u \right),$$

where

$$\begin{aligned}
&\int_{vw}^{v} \frac{1}{u} \int_{0}^{\infty} \left(1-e^{-uy}\right) \theta y^{-\alpha-1} e^{-\beta y} \mathrm{d}y\mathrm{d}u \\
=& \int_{0}^{\infty} \frac{1-e^{-vs}}{s} \int_{s}^{\frac{s}{w}} \theta y^{-\alpha-1} e^{-\beta y} \mathrm{d}y\mathrm{d}s \\
=& \int_{0}^{\infty} \frac{1-e^{-vs}}{s} \int_{s}^{\frac{s}{w}} \frac{\theta}{y^{\alpha+1}} \left(e^{-\beta\frac{s}{w}} + e^{-\beta y} - e^{-\beta\frac{s}{w}}\right) \mathrm{d}y\mathrm{d}s \\
=& \int_{0}^{\infty} \frac{1-e^{-vs}}{s} \int_{s}^{\frac{s}{w}} \frac{\theta}{y^{\alpha+1}} e^{-\beta\frac{s}{w}} \mathrm{d}y\mathrm{d}s + \int_{0}^{\infty} \frac{1-e^{-vs}}{s} \int_{s}^{\frac{s}{w}} \frac{\theta}{y^{\alpha+1}} \left(e^{-\beta y} - e^{-\beta\frac{s}{w}}\right) \mathrm{d}y\mathrm{d}s
\end{aligned} \tag{4.5.2}$$

Since $y < \frac{s}{w}$, the two terms in (4.5.2) are both positive for any $y \in [s, \frac{s}{w}]$. In particular, for the first term of (4.5.2), we have

$$\int_{0}^{\infty} \frac{1-e^{-vs}}{s} \int_{s}^{\frac{s}{w}} \frac{\theta}{y^{\alpha+1}} e^{-\beta\frac{s}{w}} \mathrm{d}y\mathrm{d}s = \frac{\theta(1-w^{\alpha})}{\alpha} \int_{0}^{\infty} \left(1-e^{-vs}\right) \frac{e^{-\frac{\beta}{w}s}}{s^{\alpha+1}} \mathrm{d}s; \tag{4.5.3}$$

for the second term of (4.5.2), we have

$$\begin{aligned}
&\int_{0}^{\infty} \left(1-e^{-vs}\right) \frac{1}{s} \int_{s}^{\frac{s}{w}} \frac{\theta}{y^{\alpha+1}} \left(e^{-\beta y} - e^{-\beta\frac{s}{w}}\right) \mathrm{d}y\mathrm{d}s \\
=& \theta \int_{0}^{\infty} \left(1-e^{-vs}\right) \int_{1}^{\frac{1}{w}} s^{-\alpha} x^{-\alpha-1} \frac{e^{-\beta sx} - e^{-\beta\frac{s}{w}}}{s} \mathrm{d}x\mathrm{d}s \\
=& \theta \int_{0}^{\infty} \left(1-e^{-vs}\right) \int_{1}^{\frac{1}{w}} x^{-\alpha-1} s^{-\alpha} \int_{x}^{\frac{1}{w}} \beta e^{-\beta su} \mathrm{d}u\mathrm{d}x\mathrm{d}s \\
=& \theta \int_{0}^{\infty} \left(1-e^{-vs}\right) \int_{1}^{\frac{1}{w}} s^{-\alpha} \beta e^{-\beta su} \int_{1}^{u} x^{-\alpha-1} \mathrm{d}x\mathrm{d}u\mathrm{d}s \\
=& \frac{\theta\beta^{\alpha}}{\alpha} \Gamma(1-\alpha) D_w \int_{0}^{\infty} \left(1-e^{-vs}\right) \int_{1}^{\frac{1}{w}} \frac{(\beta u)^{1-\alpha}}{\Gamma(1-\alpha)} s^{(1-\alpha)-1} e^{-\beta us} \frac{1}{D_w} \left(u^{\alpha-1} - u^{-1}\right) \mathrm{d}u\mathrm{d}s,
\end{aligned} \tag{4.5.4}$$

where

$$D_w = \int_{1}^{\frac{1}{w}} \left(u^{\alpha-1} - u^{-1}\right) \mathrm{d}u = \frac{1}{\alpha} \left(w^{-\alpha} - 1\right) + \ln w. \tag{4.5.5}$$

□

4.5.2 Exact Simulation Scheme

The exact distributional decomposition of $X_{t+\tau}$ conditional on X_t can be immediately identified from the representation of Laplace transforms in Theorem 4.5.1, and hence implies an exact simulation scheme summarised in Algorithm 4.5.1.

Algorithm 4.5.1 (Exact Simulation of OU-TS Process)**.** *The distribution of $X_{t+\tau}$ conditional on X_t can be exactly decomposed by*

$$X_{t+\tau} \mid X_t \overset{\mathcal{D}}{=} \underbrace{e^{-\delta\tau}X_t}_{\textit{Deterministic trend}} + \underbrace{\widetilde{TS}}_{\textit{Infinite jumps}} + \underbrace{\sum_{k=1}^{N} S_k}_{\textit{Finite jumps}}, \qquad \tau \in \mathbb{R}^+,$$

where

- *$\widetilde{TS}$ is a tempered stable random variable, i.e.*

$$\widetilde{TS} \sim TS\left(\alpha, \frac{\beta}{w}, \frac{\varrho\theta}{\alpha\delta}\left(1 - w^{\alpha}\right)\right); \tag{4.5.6}$$

- *N is a Poisson random variable of rate $\frac{\varrho\theta}{\alpha\delta}\beta^{\alpha}\Gamma(1-\alpha)D_w$ with D_w given by (4.5.5);*

- *$\left\{S_k\right\}_{k=1,2,\ldots}$ are i.i.d random variables of*

$$S_k \sim \Gamma\big(1-\alpha, \beta V\big), \tag{4.5.7}$$

  given that V can be exactly simulated via Algorithm 4.5.2.

Proof. From Theorem 4.5.1, we can see that, the original Laplace transform has been broken into three parts, and each part is a well-defined Laplace transform. In particular, (4.5.3) is the Laplace transform of a tempered stable with Lévy measure

$$\nu(s) = \frac{\theta(1-w^{\alpha})}{\alpha} s^{-\alpha-1} e^{-\frac{\beta}{w}s}.$$

(4.5.4) is the Laplace transform of a compound Poisson random variable with the jump sizes following a gamma distribution of shape parameter $(1-\alpha)$ and rate parameter βV. Here, V is a well-defined random variable with density function

$$f_V(u) = \frac{1}{D_w}\left(u^{\alpha-1} - u^{-1}\right), \qquad u \in \left[1, \frac{1}{w}\right], \tag{4.5.8}$$

with D_w in (4.5.5). This random variable V can be simulated directly via A/R scheme provided in Algorithm 4.5.2. □

Algorithm 4.5.2 (A/R Scheme for V)**.** *The random variable V, defined by its density (4.5.8), can be exactly simulated via the following A/R procedure:*

1. *Set* $C_w := \frac{1}{\alpha}\left(w^{-\frac{\alpha}{2}} - 1\right)^2$,

2. *Generate* $U_1 \sim \mathcal{U}[0,1]$,

3. *Set*
$$V = \left(1 + \sqrt{\alpha C_w U_1}\right)^{\frac{2}{\alpha}}, \tag{4.5.9}$$

4. *Generate* $U_2 \sim \mathcal{U}[0,1]$, *if*
$$U_2 \;\le\; \frac{1}{2}\frac{V^\alpha - 1}{V^\alpha - V^{\frac{\alpha}{2}}},$$
then, accept V; Otherwise, reject this candidate and go back to Step 1.

Proof. Based on the density function (4.5.8), it is easy to derive the CDF of V by

$$F_V(u) := \Pr\{V \le u\} = \frac{1}{D_w}\left[\frac{1}{\alpha}\left(u^\alpha - 1\right) - \ln u\right], \qquad u \in \left[1, \frac{1}{w}\right].$$

However, its inverse function has no explicit form, and the explicit inverse transform is not available. Then, it is natural to consider the A/R scheme for exact simulation. We choose an envelope random variable V' defined by its density function

$$g(u) = \frac{1}{C_w}\left(u^{\alpha-1} - u^{-\frac{\alpha}{2}-1}\right), \qquad u \in \left[1, \frac{1}{w}\right].$$

We can derive its CDF

$$G(u) = \frac{1}{\alpha C_w}\left(u^{\frac{\alpha}{2}} - 1\right)^2, \qquad u \in \left[1, \frac{1}{w}\right],$$

which can be inverted explicitly by

$$G^{-1}(x) = \left(1 + \sqrt{\alpha C_w x}\right)^{\frac{2}{\alpha}}, \qquad x \in [0,1].$$

Hence, V' can be exactly simulated by explicit inverse transform (4.5.9). Obviously, $\frac{u^\alpha - 1}{u^\alpha - u^{\frac{\alpha}{2}}}$ is a strictly decreasing function of $u \in \left[1, \frac{1}{w}\right]$. By L'Hôpital's rule, we can find its upper bound

$$\lim_{u \to 1} \frac{u^\alpha - 1}{u^\alpha - u^{\frac{\alpha}{2}}} = 2.$$

Then, we have

$$\frac{f_V(u)}{g_(u)} = \frac{C_w}{D_w}\frac{u^\alpha - 1}{u^\alpha - u^{\frac{\alpha}{2}}} \le \frac{C_w}{D_w}\lim_{u\to 1}\frac{u^\alpha - 1}{u^\alpha - u^{\frac{\alpha}{2}}} = 2\frac{C_w}{D_w} := \bar{c}_w, \qquad \forall u \in \left[1, \frac{1}{w}\right]. \tag{4.5.10}$$

□

Remark 4.5.1. Note that, $\bar{c}_w$ of (4.5.10) is the expected number of candidates generated until one is accepted, hence, $1/\bar{c}_w$ is the *acceptance probability*, i.e. the probability of acceptance on each attempt. Obviously, it is preferable for us to have $\bar{c}_w$ close to 1. In fact, our Algorithm 4.5.2 is pretty efficient, the acceptance probability is guaranteed to be above 50%. We let $x = \frac{1}{w}$, and then, we have

$$\frac{C_w}{D_w} = \frac{C_{\frac{1}{x}}}{D_{\frac{1}{x}}} = \frac{\frac{1}{\alpha}\left(x^{\frac{\alpha}{2}} - 1\right)^2}{\frac{1}{\alpha}\left(x^\alpha - 1\right) - \ln x}, \qquad x > 1. \tag{4.5.11}$$

Obviously,

$$\frac{\mathrm{d}}{\mathrm{d}x}\left(\frac{C_{\frac{1}{x}}}{D_{\frac{1}{x}}}\right) = \left(x^{\frac{\alpha}{2}} - 1\right)x^{\frac{\alpha}{2}-1}\frac{\frac{1}{\alpha}\left(x^{\frac{\alpha}{2}} - x^{-\frac{\alpha}{2}}\right) - \ln x}{\left[\frac{1}{\alpha}\left(x^\alpha - 1\right) - \ln x\right]^2} > 0, \qquad \forall x > 1,$$

so, $\frac{C_{\frac{1}{x}}}{D_{\frac{1}{x}}}$ in (4.5.11) is a strictly increasing function of $x > 1$. When $w \to 1$ or $x \to 1$, by L'Hôpital's rule, we obtain the lower bound

$$\lim_{x\to 1}\frac{C_{\frac{1}{x}}}{D_{\frac{1}{x}}} = \lim_{x\to 1}\frac{x^{\alpha-1} - x^{\frac{\alpha-1}{2}}}{x^{\alpha-1} - x^{-1}} = \lim_{x\to 1}\frac{(\alpha-1)x^{\alpha-2} - \left(\frac{\alpha}{2} - 1\right)x^{\frac{\alpha}{2}-2}}{(\alpha-1)x^{\alpha-2} + x^{-2}} = \frac{1}{2};$$

when $w \to 0$ or $x \to \infty$, we obtain the upper bound $\lim_{x\to\infty}\frac{C_{\frac{1}{x}}}{D_{\frac{1}{x}}} = \frac{\frac{1}{\alpha}}{\frac{1}{\alpha}} = 1$. Therefore, $\frac{C_w}{D_w} \in \left(\frac{1}{2}, 1\right)$ for $w \in (0,1)$, or, $\bar{c}_w \in (1,2)$ for $w \in (0,1)$, and we have (4.5.12). More precisely, we have $\bar{c}_w \in (1,2)$ and

$$\begin{cases} \bar{c}_w \to 1, & \text{when} \quad w \to 1, \\ \bar{c}_w \to 2, & \text{when} \quad w \to 0. \end{cases} \tag{4.5.12}$$

4.5.3 Enhanced Algorithm for OU-IG Process

We provide an enhanced algorithm for the special case of OU-IG process. The enhancement is mainly achieved by replacing the tempered stable random variable of (4.5.6) in Algorithm 4.5.1 by an inverse Gaussian random variable, and it is well known that inverse Gaussian random variable can be very efficiently simulated without A/R using the classical algorithm developed by Michael et al. (1976).

Algorithm 4.5.3 (Enhanced Exact Simulation of OU-IG Process)**.** *For the OU process X_t with*

Lévy subordinator $Z_t \sim IG\left(\frac{t}{c}, t^2\right)$, $c \in \mathbb{R}^+$, we can exactly simulate $X_{T+\tau}$ conditional on X_t via modifying Algorithm 4.5.1 by

1. *Setting $\alpha = \frac{1}{2}$, $\beta = \frac{1}{2}c^2$ and $\theta = \frac{1}{\sqrt{2\pi}}$;*
2. *Replacing the general tempered stable random variable (4.5.6) by the inverse Gaussian random variable*

$$\widetilde{IG} \sim IG\left(\mu_{IG} = \frac{2\varrho}{\delta c}\left(\sqrt{w} - w\right),\ \lambda_{IG} = \left[\frac{2\varrho}{\delta}\left(1 - \sqrt{w}\right)\right]^2\right),$$

where μ_{IG} is the mean parameter and λ_{IG} is the rate parameter.

Proof. For an inverse Gaussian random variable $IG \sim IG\left(\frac{1}{c}, 1\right)$, the Lévy measure is given by

$$\nu(s) = \frac{1}{\sqrt{2\pi s^3}} e^{-\frac{c^2}{2}s},$$

then, we have

$$IG \sim TS\left(\frac{1}{2},\ \frac{c^2}{2},\ \frac{1}{\sqrt{2\pi}}\right).$$

If we set $\alpha = \frac{1}{2}$, $\beta = \frac{1}{2}c^2$ and $\theta = \frac{1}{\sqrt{2\pi}}$, then, it recovers the special case of OU-IG process. In particular, (4.5.6) turns to be

$$TS\left(\frac{1}{2},\ \frac{c^2}{2w},\ \frac{2\varrho}{\delta\sqrt{2\pi}}(1 - \sqrt{w})\right),$$

with the associated Laplace exponent

$$\int_0^\infty \left(1 - e^{-vs}\right) \frac{\frac{2\varrho\left(1-\sqrt{w}\right)}{\delta}}{\sqrt{2\pi s^3}} e^{-\frac{\left(\frac{c}{\sqrt{w}}\right)^2}{2}s} \mathrm{d}s.$$

Note that, in general, the Laplace exponent of $IG(\mu_{IG}, \lambda_{IG})$ is given by

$$\int_0^\infty \left(1 - e^{-vs}\right) \frac{\sqrt{\lambda_{IG}}}{\sqrt{2\pi s^3}} e^{-\frac{\left(\frac{\sqrt{\lambda_{IG}}}{\mu_{IG}}\right)^2}{2}s} \mathrm{d}s, \qquad \mu_{IG}, \lambda_{IG} \in \mathbb{R}^+. \tag{4.5.13}$$

Under the parameter setting of $\alpha = \frac{1}{2}$, $\beta = \frac{1}{2}c^2$ and $\theta = \frac{1}{\sqrt{2\pi}}$, the general tempered stable random variable in (4.5.6) can be replaced by an inverse Gaussian random variable as

$$TS\left(\frac{1}{2},\ \frac{c^2}{2w},\ \frac{2\varrho}{\delta\sqrt{2\pi}}(1 - \sqrt{w})\right) \overset{\mathcal{D}}{=} IG\left(\frac{2\varrho}{\delta c}\left(\sqrt{w} - w\right),\ \left[\frac{2\varrho}{\delta}\left(1 - \sqrt{w}\right)\right]^2\right).$$

□

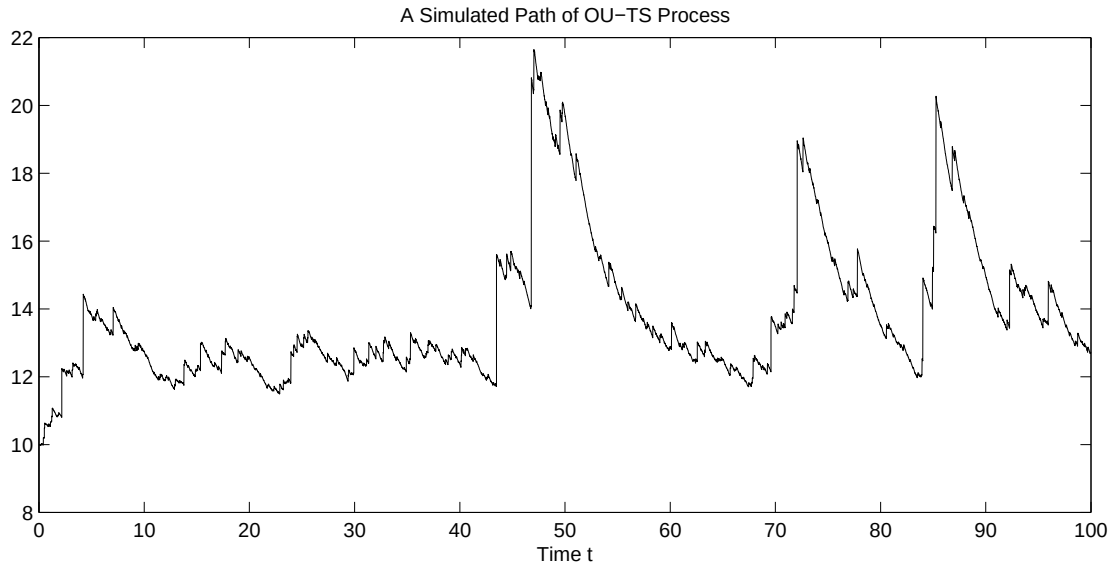

Figure 4.1: A simulated path of OU-TS process by Algorithm 4.5.1, with the parameter setting $(\delta, \varrho; \alpha, \beta, \theta; X_0) = (0.2, 1.0; 0.9, 0.2, 0.25; 10)$ within the time period of $[0, 100]$ and $10,000$ equally-spaced discretisation steps

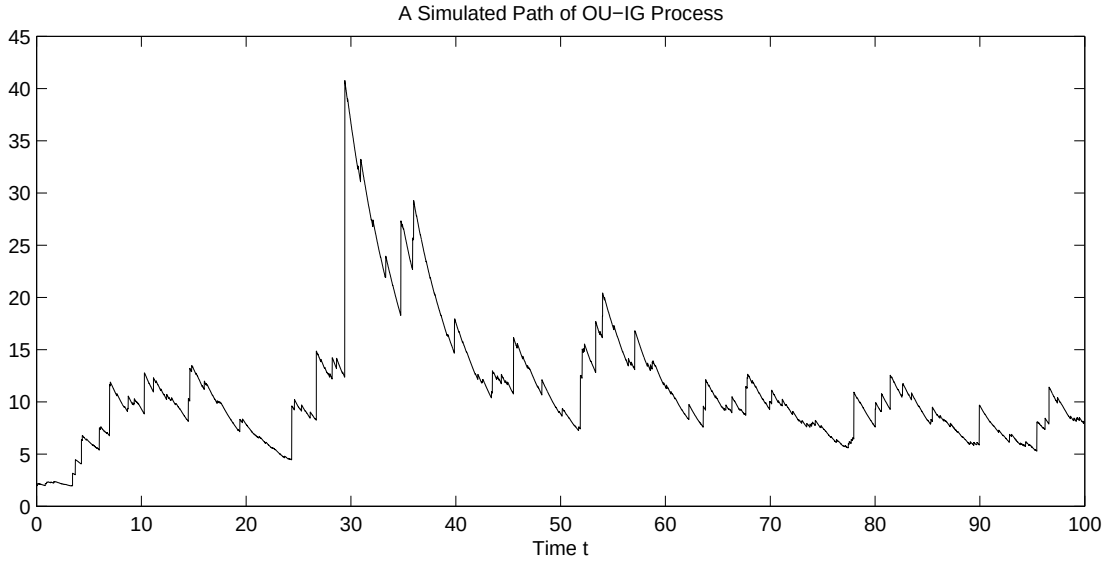

Figure 4.2: A simulated path of OU-IG process by Algorithm 4.5.3, with the parameter setting $(\delta, \varrho; c; X_0) = (0.2, 1.0; 0.5; 2.0)$ within the time period of $[0, 100]$ and $10,000$ equally-spaced discretisation steps

Table 4.3: Comparison between the true means and the associated simulation results for our exact simulation schemes based on the parameter setting $(\delta, \varrho; \alpha, \beta, \theta; X_0; T) = (0.2, 1.0; 0.25, 0.5, 0.25; 10.0; 5.0)$ for OU-TS processes and $(\delta, \varrho; c; X_0; T) = (0.2, 1.0; 1.0; 10.0; 5.0)$ for OU-IG processes, $n_\tau = 1, 2, 5, 10$, respectively.

Paths	True	Simulation	Difference	Error%	RMSE	Time	Simulation	Difference	Error%	RMSE	Time
			OU-TS	$n_\tau = 1$				**OU-TS**	$n_\tau = 2$		
1,000	5.3072	5.3512	0.0440	0.83%	0.0419	2.52	5.3143	0.0071	0.13%	0.0411	0.39
4,000	5.3072	5.3273	0.0201	0.38%	0.0223	10.02	5.2956	-0.0116	-0.22%	0.0208	1.38
16,000	5.3072	5.3044	-0.0028	-0.05%	0.0101	40.28	5.3215	0.0143	0.27%	0.0104	5.33
64,000	5.3072	5.3102	0.0030	0.06%	0.0051	158.95	5.3095	0.0022	0.04%	0.0051	20.84
256,000	5.3072	5.3043	-0.0029	-0.05%	0.0026	634.52	5.3065	-0.0007	-0.01%	0.0026	82.63
			OU-TS	$n_\tau = 5$				**OU-TS**	$n_\tau = 10$		
1,000	5.3072	5.2500	-0.0572	-1.08%	0.0371	0.39	5.2621	-0.0451	-0.85%	0.0390	0.70
4,000	5.3072	5.3153	0.0080	0.15%	0.0209	1.56	5.2977	-0.0095	-0.18%	0.0203	2.72
16,000	5.3072	5.3125	0.0053	0.10%	0.0103	6.09	5.3083	0.0011	0.02%	0.0102	10.63
64,000	5.3072	5.2970	-0.0102	-0.19%	0.0050	24.16	5.3053	-0.0019	-0.04%	0.0051	41.73
256,000	5.3072	5.3101	0.0028	0.05%	0.0025	96.05	5.3066	-0.0006	-0.01%	0.0026	167.44
			OU-IG	$n_\tau = 1$				**OU-IG**	$n_\tau = 2$		
1,000	6.8394	6.8094	-0.0300	-0.44%	0.0454	0.09	6.8100	-0.0294	-0.43%	0.0462	0.14
4,000	6.8394	6.8353	-0.0041	-0.06%	0.0230	0.22	6.8424	0.0030	0.04%	0.0230	0.48
16,000	6.8394	6.8294	-0.0100	-0.15%	0.0117	0.95	6.8335	-0.0059	-0.09%	0.0115	1.66
64,000	6.8394	6.8365	-0.0029	-0.04%	0.0058	3.55	6.8415	0.0021	0.03%	0.0058	6.55
256,000	6.8394	6.8352	-0.0042	-0.06%	0.0029	13.64	6.8425	0.0031	0.05%	0.0029	25.72
			OU-IG	$n_\tau = 5$				**OU-IG**	$n_\tau = 10$		
1,000	6.8394	6.8576	0.0182	0.27%	0.0476	0.25	6.8478	0.0084	0.12%	0.0469	0.50
4,000	6.8394	6.8137	-0.0257	-0.38%	0.0228	0.94	6.8366	-0.0028	-0.04%	0.0236	1.98
16,000	6.8394	6.8637	0.0243	0.36%	0.0117	3.84	6.8491	0.0097	0.14%	0.0116	7.56
64,000	6.8394	6.8374	-0.0020	-0.03%	0.0058	15.02	6.8390	-0.0004	-0.01%	0.0057	29.69
256,000	6.8394	6.8394	-0.0000	0.00%	0.0029	59.80	6.8429	0.0035	0.05%	0.0029	119.45

Table 4.4: Comparison between the true means and the associated simulation results for our exact simulation schemes based on the parameter setting $(\delta, \varrho; c; X_0; T) = (0.2, 1.0; 1.0; 10.0; 5.0)$ for OU-IG process, and each value point is estimated from $100,000$ sample paths.

n_τ	True	Simulation	Difference	Error%	RMSE	Time	Simulation	Difference	Error%	RMSE	Time
			OU-IG	**Algorithm 4.5.1**				**OU-IG**	**Algorithm 4.5.3**		
1	6.8394	6.8423	0.0029	0.04%	0.0047	438.66	6.8393	-0.0001	0.00%	0.0047	5.48
2	6.8394	6.8358	-0.0036	-0.05%	0.0047	34.47	6.8351	-0.0043	-0.06%	0.0046	9.88
3	6.8394	6.8374	-0.0020	-0.03%	0.0046	30.19	6.8400	0.0006	0.01%	0.0046	14.63
4	6.8394	6.8402	0.0008	0.01%	0.0047	33.09	6.8511	0.0117	0.17%	0.0047	18.95
5	6.8394	6.8465	0.0071	0.10%	0.0046	37.52	6.8434	0.0040	0.06%	0.0047	23.75
6	6.8394	6.8403	0.0009	0.01%	0.0046	43.58	6.8310	-0.0084	-0.12%	0.0046	27.97
7	6.8394	6.8373	-0.0021	-0.03%	0.0046	47.80	6.8434	0.0040	0.06%	0.0047	32.83
8	6.8394	6.8246	-0.0148	-0.22%	0.0046	54.41	6.8363	-0.0031	-0.04%	0.0046	37.61
9	6.8394	6.8450	0.0056	0.08%	0.0046	59.55	6.8415	0.0021	0.03%	0.0046	42.80
10	6.8394	6.8385	-0.0009	-0.01%	0.0047	64.58	6.8316	-0.0078	-0.11%	0.0046	48.61

4.5.4 Simulation Studies

In this section, we establish numerical experiments to illustrate the performance and effectiveness of our exact simulation schemes. We have implemented the exact simulation schemes for two cases, OU-TS/OU-IG within the fixed time period $[0, T]$, respectively.

Note that, the choice for the fundamental tempered stable generator is essential as it determines overall simulation efficiency. Since our *two-dimensional Single Rejection Scheme* in Chapter 2 outperforms all the existing algorithms for any parameter settings, we therefore adopt the *two-dimensional Single Rejection Scheme* in Algorithm 2.4.6 to implement Algorithm 4.5.1.

We set the parameters $(\delta, \varrho; \alpha, \beta, \theta; X_0; T) = (0.2, 1.0; 0.25, 0.5, 0.25; 10.0; 5.0)$ for OU-TS process and $(\delta, \varrho; c; X_0; T) = (0.2, 1.0; 1.0; 10.0; 5.0)$ for OU-IG process, and experiment with different numbers of equally-spaced discretisation steps within the period $[0, T]$, i.e. $n_\tau := T/\tau$. Of course, all of our algorithms can be directly applied to the irregularly-spaced time points which may be more useful in practice[6], and the equally-spaced cases here just serve for illustration purpose.

Simulated paths of OU-TS/OU-IG processes have been presented earlier in Figure 4.1 and Figure 4.2, respectively. Convergence analysis for the two cases based on the increasing numbers of sample paths is reported in Table 4.3. The efficiency enhancement for simulating OU-IG process using the enhanced schemes (Algorithm 4.5.3) against the associated general schemes (Algorithm 4.5.1) can be clearly observed through Table 4.4. Overall, from these numerical results reported in this section, it is evident that each algorithm developed can achieve a very high level of accuracy as well as efficiency.

4.6 Conclusion

In this chapter, we have developed an approach to exactly simulate Lévy driven Ornstein-Uhlenbeck processes which are constructed from typical Lévy subordinators, i.e. the compound Poisson process, the gamma process and the tempered stable process. The algorithms are accurate and efficient which have been numerically verified and tested by our extensive experiments. They could be easily adopted for generating sample paths for modelling the dynamics of asset prices, stochastic volatilizes and interest rates to name a few. They would be especially useful for statistical inference, derivative pricing and risk management in practice.

[6]The data in practice, such as trade transactions from market microstructure, are often observed at irregularly-spaced time points, see Engle and Russell (1998).

Chapter 5

Lévy Driven Contagion Models

In this chapter, we introduce a new family of Lévy driven point processes with contagion, by generalising the classical self-exciting Hawkes process and doubly stochastic Poisson processes with non-Gaussian Lévy driven Ornstein-Uhlenbeck type intensities. The resulting framework may possess many desirable features such as skewness, leptokurtosis, mean-reverting dynamics, and more importantly, the contagion or feedback effects, which could be very useful for modelling event arrivals in finance, economics, insurance and many other fields. We characterise the distributional properties of this new class of point processes and develop an efficient sampling method for generating sample paths exactly. Our simulation scheme is based on the distributional decomposition of the point process and its intensity process. Extensive numerical implementations and tests are reported to demonstrate the accuracy and effectiveness of our scheme. Moreover, we apply to portfolio risk management as an example to show the applicability and flexibility of our algorithms.

5.1 Definitions

In this section, we construct a new framework for modelling event arrivals with contagion effects based on Lévy processes. That is, the intensity of the point process is set up to be a non-Gaussian OU process driven by a Lévy subordinator in cooperation with extra self-exciting jumps. Let us first define a simpler version without the self-exciting component:

Definition 5.1.1 (Jump Process with Non-Gaussian Intensity)**. Jump process with non-Gaussian intensity** *is a point process* $N \equiv \left\{T_i\right\}_{i=1,2,\ldots}$ *i.e.* $N_t = \sum_{i\geq 1} \mathbf{1}_{\{T_i \leq t\}}$ *with the stochastic intensity* λ_t *satisfying the stochastic differential equation*

$$\mathrm{d}\lambda_t = -\delta\lambda_t \mathrm{d}t + \varrho \mathrm{d}Z_t, \qquad t \geq 0, \tag{5.1.1}$$

where

- $\varrho > 0$ *is an arbitrary positive constant;*

- $\delta > 0$ *is the constant rate of exponential decay;*

- Z_t*, with* $Z_0 = 0$*, is a Lévy subordinator, which is called the background driving Lévy process (BDLP) of a non-Gaussian OU process.*

This is a special case of Cox point processes. A slightly mathematical generalisation but very useful for applications is to further incorporate a feedback mechanism in the framework by adding a series of self-exciting jumps, i.e. simultaneous jumps (or "*co-jumps*") in the point process and its intensity process. More precisely, this new framework, as a generalised version of the jump process of Definition 5.1.1, is defined via the *stochastic intensity representation* as below:

Definition 5.1.2 (Self-exciting Jump Process with Non-Gaussian Intensity)**.** N_t *is a* **self-exciting jump process with non-Gaussian intensity***, if the intensity process of (5.1.1) is replaced by*

$$\mathrm{d}\lambda_t = -\delta\lambda_t \mathrm{d}t + \varrho \mathrm{d}Z_t + \mathrm{d}J_t, \qquad t \geq 0, \tag{5.1.2}$$

where the extra component J_t *is a pure-jump process specified by*

$$J_t := \sum_{i=1}^{N_t} X_i, \tag{5.1.3}$$

and $\{X_i\}_{i=1,2,\ldots}$ *are non-negative sizes of self-exciting jumps*[1] *with distribution function* $G(z)$*,* $z > 0$*, occurring at the associated (ordered) arrival times* $\{T_i\}_{i=1,2,\ldots}$*, respectively.*

Similar as the *Hawkes process* (Hawkes and Oakes, 1974), N_t in Definition 5.1.2 can be equivalently redefined as a *branching process* via a *cluster process presentation* (Daley and Vere-Jones, 2003, p.175-193). More precisely, N_t is a cluster point process which consists of two types of points: *immigrants* and their *offspring*. The arrivals of immigrants follow a Cox process with Lévy driven OU intensity (5.1.1). Each immigrant generates its offspring, each offspring would further generate offspring, and so on. The generation of any offspring follows a Cox process with exponentially decaying intensity $X^* e^{-\delta(t-T^*)}$, where $X^* \overset{\mathcal{D}}{=} X_i$ and T^* is the arrival (birth) time of its previous generation. The superposition (Daley and Vere-Jones, 2003, Theorem 2.4.VI) of all of these points forms our new self-exciting point process N_t with the stochastic intensity (5.1.2).

Note that, given the initial intensity level $\lambda_0 > 0$, the intensity process (5.1.2) can be alternat-

[1] It is called "self-exciting", as the expression (5.1.3) reveals that the jumps simultaneously occur in the point process N_t and its intensity λ_t, and hence the arrivals of jumps trigger more jumps afterwards.

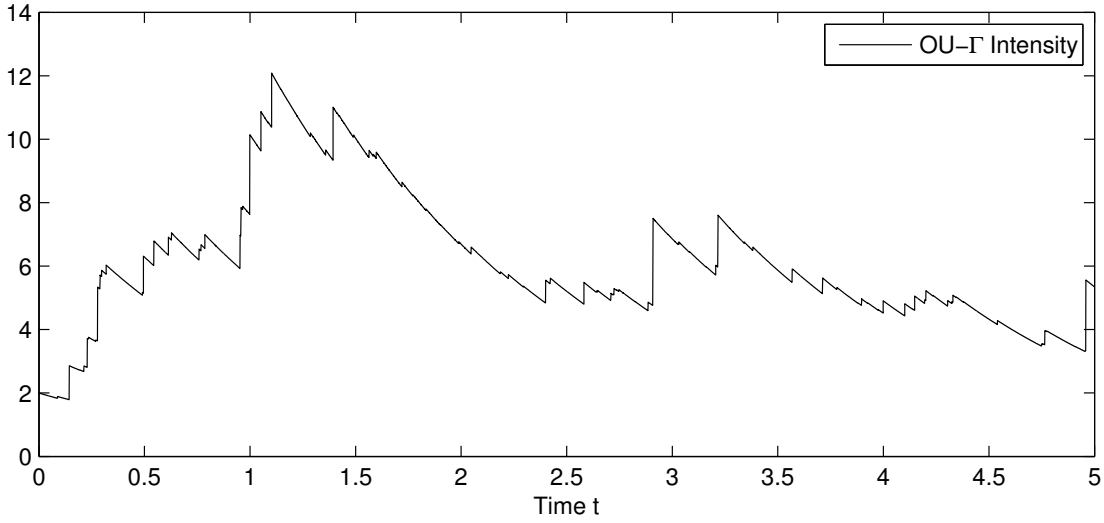

Figure 5.1: A sample path of interarrival intensity process (without self-exciting component) within the time period $t \in [0,5]$ when the BDLP is a Gamma process

ively expressed as

$$\lambda_t = \underbrace{\lambda_0 e^{-\delta t} + \varrho \int_0^t e^{-\delta(t-s)} \mathrm{d}Z_s}_{\text{Exogenous commonly-shared risk}} + \underbrace{\sum_{i=1}^{N_t} e^{-\delta(t-T_i)} X_i}_{\text{Endogenous contagion risk}}, \qquad t \geq 0,$$

which is positive and càdlàg. In fact, this new framework integrates two major types of risk sources. For example, in the context of credit risk or systemic risk, the first part (i.e. the first two terms) is to model the cyclical dependency of companies on some exogenous risk (e.g. movements of interest or FX rates) commonly shared in the entire market, and the cyclical oscillation is captured by the mean-reverting Lévy driven OU process; fundamental common shocks are captured by the pure-jump process Z_t. The second part (i.e. the last term) is to model the endogenous contagion risk due to the local interaction of companies in their business network, without which the overall risk would be underestimated.

The *interarrival intensity process* $\{\lambda_t\}_{T_i \leq t < T_{i+1}}$, for modelling exogenous commonly-shared risk, is defined as the parts of intensity process excluding self-exciting jumps, i.e., (5.1.1), or,

$$\lambda_t = e^{-\delta t}\lambda_0 + \varrho \int_0^t e^{-\delta(t-s)} \mathrm{d}Z_s, \qquad t \in [T_i, T_{i+1}).$$

For instance, a sample path of the interarrival intensity process (without self-exciting component) within the time period $t \in [0,5]$ when the BDLP is a gamma process is represented in Figure 5.1.

This framework is the generalisation of several classical models in the literature: If there is no BDLP Z_t, then, the point process N_t is a generalised *Hawkes process* (Hawkes, 1971a,b) with random marks. If the BDLP Z_t is trivially a subordinator of compound Poisson, then, N_t is a *dynamic contagion process* (Dassios and Zhao, 2011).

For notation simplicity, we denote the Lévy measure of Z_t by ν, the associated Laplace exponent and mean at the unite time by

$$\Phi(u) := \int_0^\infty \left(1 - e^{-uy}\right) \nu(y)\mathrm{d}y, \qquad \mu_Z := \mathbb{E}[Z_1] = \int_0^\infty y\nu(y)\mathrm{d}y, \qquad u > 0,$$

the Laplace transform, mean of self-exciting jump sizes and a constant respectively by

$$\hat{g}(u) := \int_0^\infty e^{-uy}\mathrm{d}G(y), \qquad \mu_G := \int_0^\infty y\mathrm{d}G(y), \qquad \eta := \delta - \mu_G,$$

which are assumed to be finite. In addition, we denote the $(i+1)^{\text{th}}$ interarrival time by

$$\tau_{i+1} := T_{i+1} - T_i, \qquad i = 0, 1, 2, ..., \qquad T_0 = 0,$$

and the *cumulative intensity process* at time t by $\Lambda_t := \int_0^t \lambda_u \mathrm{d}u$.

Since this is a new family of point processes, one may be interested in their basic distributional properties such as means and Laplace transforms. In particular, the conditional expectation of point process is provided here in Proposition 5.1.1, as it will be used later as a simple and general benchmark for numerically validating our newly-developed simulation algorithms.

Proposition 5.1.1 (Conditional Expectation of Point Process)**.** *The expectation of N_{t+s} conditional on N_t and λ_t is given by*

$$\mathbb{E}\left[N_{t+s} \mid N_t, \lambda_t\right] = \begin{cases} N_t + \frac{\varrho\mu_Z}{\eta}s + \left(\lambda_t - \frac{\varrho\mu_Z}{\eta}\right)\frac{1-e^{-\eta s}}{\eta}, & \eta \neq 0, \\ N_t + \lambda_t s + \frac{1}{2}\varrho\mu_Z s^2, & \eta = 0, \end{cases} \qquad s > 0.$$

5.2 General Framework for Exact Simulation

In this section, we outline an exact simulation framework based on exact distributional decomposition for a general point process of Lévy driven OU intensity *with* and *without* self-exciting jumps as defined in Definition 5.1.1 and 5.1.2, respectively. The entire simulation scheme can be

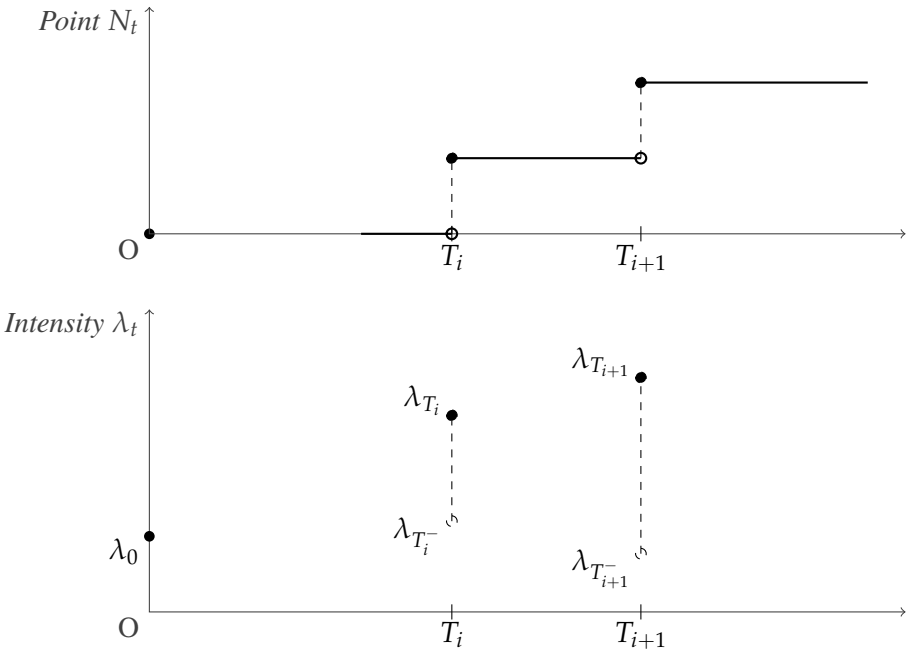

Figure 5.2: Illustration on the exact simulation procedures for a path of point process N_t and the skeleton of its intensity process λ_t around the period $[T_i, T_{i+1}]$

decomposed into three major steps:

1. Conditional on the current arrival time T_i and the associated intensity level λ_{T_i}, generate the next interarrival time τ_{i+1};

2. Further conditional on the realisation of this interarrival time τ_{i+1}, generate the pre-jump intensity level $\lambda_{T_i+\tau_{i+1}^-}$ right before the next arrival time $T_{i+1} = T_i + \tau_{i+1}$;

3. Add a self-exciting jump size X_{i+1} upon the intensity process λ_t and one unit in the point process N_t both at the next arrival time $T_{i+1} = T_i + \tau_{i+1}$.

By recursively implementing the three steps above, a full path of the point process N_t in any time horizon can be exactly produced without bias. A graphical illustration for this proposed algorithm design is provided in Figure 5.2.

The third step indeed is straightforward. In particular, if $X_{i+1} \equiv 0$ for any i, then, it corresponds to the version *without* self-exciting jumps. In order to execute the first two steps, we have first to further investigate the joint distributional properties of the next interarrival time τ_{i+1} and the next pre-jump intensity level $\lambda_{T_i+\tau_{i+1}^-}$, which can be characterised by the conditional joint transform as below.

Theorem 5.2.1 (Joint Laplace Transform of Pre-jump Intensity and Cumulative Intensity)**.** *Conditional on the intensity level λ_{T_i} at the i^{th} arrival time T_i, the joint transform of $\left(\lambda_{T_i+\tau^-}, \Lambda_{T_i+\tau} - \Lambda_{T_i}\right)$*

for any given period $\tau \in (0, \tau_{i+1})$ *is given by*

$$\begin{aligned} & \mathbb{E}\left[e^{-v\lambda_{T_i+\tau^-}} e^{-\left(\Lambda_{T_i+\tau}-\Lambda_{T_i}\right)} \mid \lambda_{T_i}\right] \\ = \quad & \exp\left(-\left[\frac{1}{\delta} + \left(v - \frac{1}{\delta}\right) w\right] \lambda_{T_i} - \varrho \int_{v}^{\frac{1}{\delta}+\left(v-\frac{1}{\delta}\right)w} \frac{\Phi(u)}{1-\delta u} \mathrm{d}u \right), \qquad \tau \in (0, \tau_{i+1}), \end{aligned} \tag{5.2.1}$$

where $w := e^{-\delta\tau}$.

Proof. Given the i^{th} arrival time T_i, the infinitesimal generator of (Λ, λ, t) within the period $t \in [T_i, T_i + \tau_{i+1})$ acting on any function $f(\Lambda, \lambda, t)$ within its domain $\Omega(\mathcal{A})$ is given by

$$\mathcal{A}f(\Lambda, \lambda, t) = \frac{\partial f}{\partial t} - \delta\lambda \frac{\partial f}{\partial \lambda} + \lambda \frac{\partial f}{\partial \Lambda} + \varrho \left\{ \int_0^\infty \Big[f(\Lambda, \lambda + y, t) - f(\Lambda, \lambda, t) \Big] \nu(y) \mathrm{d}y \right\}. \tag{5.2.2}$$

Consider a function

$$f(\Lambda, \lambda, t) = e^{-\tilde{v}\Lambda} e^{-\lambda A(t)} e^{R(t)}, \qquad \tilde{v} \in \mathbb{R}^+, \tag{5.2.3}$$

where $A(t)$ and $R(t)$ are deterministic and differentiable functions with respect to t. Substituting (5.2.3) into (5.2.2) and setting $\mathcal{A}f = 0$, we have

$$-\lambda A'(t) + R'(t) + \delta\lambda A(t) - \tilde{v}\lambda - \varrho\Phi\big(A(t)\big) = 0.$$

Since this equation holds for any λ and Λ, it is equivalent to the equations

$$A'(t) = \delta A(t) - \tilde{v}, \qquad R'(t) = \varrho\Phi\big(A(t)\big).$$

Hence, for any time $t \in [T_i, T_i + \tau_{i+1})$, we have

$$A(t) = ke^{\delta t} - \tilde{v}\frac{e^{\delta t} - 1}{\delta}, \qquad R(t) = \varrho \int_0^t \Phi\left(ke^{\delta s} - \tilde{v}\frac{e^{\delta s} - 1}{\delta} \right) \mathrm{d}s, \qquad k \in \mathbb{R}^+.$$

By the basic property of infinitesimal generator (Dassios and Embrechts, 1989), we have the martingale

$$e^{-\tilde{v}\Lambda_t} \exp\left(-\left(ke^{\delta t} - \tilde{v}\frac{e^{\delta t} - 1}{\delta} \right) \lambda_t + \varrho \int_0^t \Phi\left(ke^{\delta s} - \tilde{v}\frac{e^{\delta s - 1}}{\delta} \right) \mathrm{d}s \right).$$

Setting $\tilde{v} = 1$ and $A\left(T_i + \tau^-\right) = v$ for any $\tau \in (0, \tau_{i+1})$ and using the martingale property, we

have

$$\begin{aligned} & \mathbb{E}\left[e^{-v\lambda_{T_i+\tau^-}} e^{-\left(\Lambda_{T_i+\tau}-\Lambda_{T_i}\right)} \mid \lambda_{T_i}\right] \\ = \; & \exp\left(-\left[\frac{1}{\delta}+\left(v-\frac{1}{\delta}\right)w\right]\lambda_{T_i} - \varrho\int_0^\tau \Phi\left(\frac{1}{\delta}+\left(v-\frac{1}{\delta}\right)e^{-\delta s}\right)\mathrm{d}s\right). \end{aligned}$$

Hence, we can immediately obtain (5.2.1) by the change of variable $u = \frac{1}{\delta} + \left(v - \frac{1}{\delta}\right) e^{-\delta s}$. □

Theorem 5.2.1 provides us with a crucial tool for further investigating the distributional properties of the interarrival time τ_{i+1} and the pre-jump intensity level $\lambda_{T_i+\tau_{i+1}^-}$, jointly and separately, which later leads to their efficient algorithms for exact simulation as follows.

5.2.1 Exact Simulation of Interarrival Time

Let us first outline how to simulate the interarrival time. Given the intensity level λ_{T_i} at the i^{th} arrival time T_i, interestingly, the $(i+1)^{\text{th}}$ interarrival time τ_{i+1} can be exactly expressed as the minimum of two much simpler random variables $V_{T_i}^*$ and V^* where

1. $V_{T_i}^*$ is a defective random variable, which can be directly generated by an explicit inverse transform;

2. V^* is a well-defined random variable, which can be exactly simulated by a simplified version of the classical *thinning scheme* (Lewis and Shedler, 1979).

Algorithm 5.2.1 (Exact Simulation of Interarrival Time)**.** *Conditional on the intensity level λ_{T_i}, the next interarrival time τ_{i+1} can be exactly simulated via*

$$\tau_{i+1} \overset{\mathcal{D}}{=} \begin{cases} V^* \wedge V_{T_i}^*, & D_i > 0, \\ V^*, & D_i < 0, \end{cases} \tag{5.2.4}$$

where

- *D_i is simulated via*
$$D_i := 1 + \frac{\delta}{\lambda_{T_i}} \ln U_1, \qquad U_1 \sim \mathcal{U}[0,1];$$

- *$V_{T_i}^*$ is a simple defective random variable with $P\left(V_{T_i}^* = \infty\right) = \exp\left(-\frac{1}{\delta}\lambda_{T_i}\right)$, i.e.*

$$V_{T_i}^* \overset{\mathcal{D}}{=} -\frac{1}{\delta}\ln D_i; \tag{5.2.5}$$

- *V^* is the first arrival time of a non-homogeneous Poisson process with the rate function*

$$\zeta_t := \varrho\Phi\big(G_0(t)\big), \qquad G_0(u) := \frac{1-e^{-\delta u}}{\delta}, \qquad u \geq 0, \tag{5.2.6}$$

and it can be exactly simulated via the simplified thinning scheme of Simulation Scheme 5.2.2.

Proof. Setting $v = 0$ in (5.2.1) of Theorem 5.2.1, we have

$$P(\tau_{i+1} > \tau \mid \lambda_{T_i}) = \mathbb{E}\left[e^{-\left(\Lambda_{T_i+\tau}-\Lambda_{T_i}\right)} \mid \lambda_{T_i}\right] = P(V^* > \tau) \times P(V^*_{T_i} > \tau),$$

where

$$P(V^* > \tau) = \exp\left(-\varrho \int_0^\tau \Phi\big(G_0(u)\big)\mathrm{d}u\right), \qquad P(V^*_{T_i} > \tau) = e^{-G_0(\tau)\lambda_{T_i}}. \tag{5.2.7}$$

This implies that, the next interarrival time τ_{i+1} conditional on the current intensity level λ_{T_i} can be expressed as the minimum of two independent random variables V^* and $V^*_{T_i}$. Note that, $V^*_{T_i}$ is a defective random variable since the CDF of $V^*_{T_i}$ is

$$F_{V^*_{T_i}}(\tau) = 1 - e^{-G_0(\tau)\lambda_{T_i}},$$

with $F_{V^*_{T_i}}(\infty) = 1 - \exp\left(-\frac{1}{\delta}\lambda_{T_i}\right) < 1$, and the density $f_{V^*_{T_i}}(\tau) > 0$ for any $\tau > 0$. Obviously, if $D_i > 0$, then $V^*_{T_i}$ can be exactly simulated using the explicit inverse transform (5.2.5). Whereas V^* can be interpreted as the first arrival time from a non-homogeneous Poisson process, and it can be exactly simulated via Simulation Scheme 5.2.2 as below. □

Algorithm 5.2.2 (Simplified Thinning Scheme)**.** *V^* can be exactly simulated by the following steps:*

1. *Initialise the candidate time $\tilde{t} = 0$;*
2. *Generate $E^* \sim Exp\,(\zeta_\infty)$ where*

$$\zeta_\infty := \lim_{t\to\infty} \zeta_t = \varrho\Phi\left(\frac{1}{\delta}\right), \tag{5.2.8}$$

   and set $\tilde{t} = \tilde{t} + E^*$;
3. *Generate $U_2 \sim \mathcal{U}[0,1]$,*
   - *if $U_2 \leq \zeta(\tilde{t})/\zeta_\infty$, then, accept this candidate by setting $V^* = \tilde{t}$;*

- *if $U_2 > \zeta(\tilde{t})/\zeta_\infty$, then, reject this candidate, and go back to Step 2 and continue.*

Proof. Since ζ_t in (5.2.6) is a strictly increasing and concave function of time t with the initial value $\zeta_0 = 0$ at time $t = 0$, the maximum level is ζ_∞. Then, the algorithm above actually is a simplified version of the classical *thinning scheme* (Lewis and Shedler, 1979) where only the first arrival time within the period of $[0, t]$ is recorded. □

5.2.2 Exact Simulation of Pre-jump Intensity Level

Conditional the realisation of interarrival time τ_{i+1} as generated by Simulation Scheme 5.2.1, the Laplace transform of the next pre-jump intensity level $\lambda_{T_i+\tau_{i+1}^-}$ is provided as follows.

Theorem 5.2.2 (Laplace Transform of Pre-jump Intensity)**.** *Conditional on the intensity level λ_{T_i} and the $(i+1)^{\text{th}}$ interarrival time τ_{i+1}, the Laplace transform of pre-jump intensity level $\lambda_{T_i+\tau_{i+1}^-}$ is given by*

$$\begin{aligned}\mathbb{E}\left[e^{-v\lambda_{T_i+\tau_{i+1}^-}} \mid \tau_{i+1}=\tau, \lambda_{T_i}\right] &= e^{-vw\lambda_{T_i}} \times \exp\left(-\varrho \int_v^{\frac{1}{\delta}+\left(v-\frac{1}{\delta}\right)w} \frac{\Phi(u)-\Phi\left(u-\frac{u-\frac{1}{\delta}}{v-\frac{1}{\delta}}v\right)}{1-\delta u}\mathrm{d}u\right) \\ &\quad \times \frac{\frac{\varrho}{\delta}\int_0^\infty e^{-vs}\int_s^{\frac{s}{w}} e^{\frac{s}{\delta}}e^{-\frac{y}{\delta}}\nu(y)\mathrm{d}y\mathrm{d}s + w\lambda_{T_i}}{\frac{\varrho}{\delta}\int_0^\infty\int_s^{\frac{s}{w}} e^{\frac{s}{\delta}}e^{-\frac{y}{\delta}}\nu(y)\mathrm{d}y\mathrm{d}s + w\lambda_{T_i}}. \end{aligned} \tag{5.2.9}$$

Proof. Note that, the density function of the $(i+1)^{\text{th}}$ interarrival time conditional on the intensity level λ_{T_i} is

$$P(\tau_{i+1} \in \mathrm{d}\tau \mid \lambda_{T_i}) = \mathbb{E}\left[\lambda_{T_i+\tau^-}\exp\left(-\int_{T_i}^{T_i+\tau}\lambda_u\mathrm{d}u\right) \mid \lambda_{T_i}\right]\mathrm{d}\tau,$$

which implies that,

$$\mathbb{E}\left[e^{-v\lambda_{T_i+\tau_{i+1}^-}}\mathbf{1}_{\{\tau_{i+1}\in\mathrm{d}\tau\}} \mid \lambda_{T_i}\right] = \mathbb{E}\left[\lambda_{T_i+\tau^-}e^{-v\lambda_{T_i+\tau^-}}\exp\left(-\int_{T_i}^{T_i+\tau}\lambda_u\mathrm{d}u\right) \mid \lambda_{T_i}\right]\mathrm{d}\tau.$$

Hence, we have

$$\mathbb{E}\left[e^{-v\lambda_{T_i+\tau_{i+1}^-}} \mid \tau_{i+1}=\tau, \lambda_{T_i}\right] = \frac{\mathbb{E}\left[\lambda_{T_i+\tau^-}e^{-v\lambda_{T_i+\tau^-}}e^{-\left(\Lambda_{T+\tau}-\Lambda_{T_i}\right)} \mid \lambda_{T_i}\right]}{\mathbb{E}\left[\lambda_{T_i+\tau^-}e^{-\left(\Lambda_{T_i+\tau}-\Lambda_{T_i}\right)} \mid \lambda_{T_i}\right]}. \tag{5.2.10}$$

The numerator of (5.2.10) can be obtained by differentiating the joint transform (5.2.1) w.r.t. v, i.e.,

$$\begin{aligned}
& \mathbb{E}\left[\lambda_{T_i+\tau^-} e^{-v\lambda_{T_i+\tau^-}} e^{-\left(\Lambda_{T_i+\tau}-\Lambda_{T_i}\right)} \mid \lambda_{T_i}\right] \\
= & -\frac{\partial}{\partial v}\mathbb{E}\left[e^{-v\lambda_{T_i+\tau^-}} e^{-\left(\Lambda_{T_i+\tau^-}-\Lambda_{T_i}\right)} \mid \lambda_{T_i}\right] \\
= & -\frac{\partial}{\partial v}\left[\exp\left(-\left[\frac{1}{\delta}+\left(v-\frac{1}{\delta}\right)e^{-\delta\tau}\right]\lambda_{T_i}\right)\times\exp\left(-\varrho\int_0^\tau \Phi\left(\frac{1}{\delta}+\left(v-\frac{1}{\delta}\right)e^{-\delta u}\right)\mathrm{d}u\right)\right] \\
= & -\frac{\partial}{\partial v}\left[e^{-G_v(\tau)\lambda_{T_i}}\times e^{-\varrho F_v(\tau)}\right] \\
= & -\left[\varrho\frac{\partial}{\partial v}F_v(\tau)+\frac{\partial}{\partial v}G_v(\tau)\right]\times e^{-G_v(\tau)\lambda_{T_i}} e^{-\varrho F_v(\tau)},
\end{aligned}$$

where

$$G_v(u) := \frac{1}{\delta}+\left(v-\frac{1}{\delta}\right)e^{-\delta u}, \qquad F_v(\tau) := \int_0^\tau \Phi\big(G_v(u)\big)\mathrm{d}u,$$

and

$$\begin{aligned}
\frac{\partial}{\partial v}G_v(\tau) &= -\lambda_{T_i}e^{-\delta\tau}, \\
\frac{\partial}{\partial v}F_v(\tau) &= \int_0^\tau\int_0^\infty y e^{-\delta u} e^{-\left[\frac{1}{\delta}+\left(v-\frac{1}{\delta}\right)e^{-\delta u}\right]y}\nu(y)\mathrm{d}y\mathrm{d}u.
\end{aligned}$$

Note that, ν is the Lévy measure for Z_t, therefore, we have

$$\begin{aligned}
& \mathbb{E}\left[e^{-v\lambda_{T_i+\tau^-_{i+1}}} \mid \tau_{i+1}=\tau, \lambda_{T_i}\right] \\
= & \frac{\left(\varrho\int_0^\tau\int_0^\infty y e^{-\delta u} e^{-\left[\frac{1}{\delta}+\left(v-\frac{1}{\delta}\right)e^{-\delta u}\right]y}\nu(y)\mathrm{d}y\mathrm{d}u + e^{-\delta\tau}\lambda_{T_i}\right)\times e^{-G_v(\tau)\lambda_{T_i}} e^{-\varrho F_v(\tau)}}{\left(\varrho\int_0^\tau\int_0^\infty y e^{-\delta u} e^{-\frac{1}{\delta}\left(1-e^{-\delta u}\right)y}\nu(y)\mathrm{d}y\mathrm{d}u + e^{-\delta\tau}\lambda_{T_i}\right)\times e^{-G_0(\tau)\lambda_{T_i}} e^{-\varrho F_0(\tau)}} \\
= & \frac{\varrho\int_0^\tau\int_0^\infty y e^{-\delta u} e^{-\left[\frac{1}{\delta}+\left(v-\frac{1}{\delta}\right)e^{-\delta u}\right]y}\nu(y)\mathrm{d}y\mathrm{d}u + e^{-\delta\tau}\lambda_{T_i}}{\varrho\int_0^\tau\int_0^\infty y e^{-\delta u} e^{-\frac{1}{\delta}\left(1-e^{-\delta u}\right)y}\nu(y)\mathrm{d}y\mathrm{d}u + e^{-\delta\tau}\lambda_{T_i}} \times \frac{\mathbb{E}\left[e^{-v\lambda_{T_i+\tau^-}} e^{-\left(\Lambda_{T_i+\tau}-\Lambda_{T_i}\right)} \mid \lambda_{T_i}\right]}{\mathbb{E}\left[e^{-\left(\Lambda_{T_i+\tau}-\Lambda_{T_i}\right)} \mid \lambda_{T_i}\right]}. \qquad (5.2.11)
\end{aligned}$$

The first term of (5.2.11) can be calculated more explicitly as

$$
\begin{aligned}
&\frac{\varrho\int_0^{\tau}\int_0^{\infty} ye^{-\delta u}e^{-\left[\frac{1}{\delta}+\left(v-\frac{1}{\delta}\right)e^{-\delta u}\right]y}\nu(y)\mathrm{d}y\mathrm{d}u+e^{-\delta\tau}\lambda_{T_i}}{\varrho\int_0^{\tau}\int_0^{\infty} ye^{-\delta u}e^{-\frac{1}{\delta}\left(1-e^{-\delta u}\right)y}\nu(y)\mathrm{d}y\mathrm{d}u+e^{-\delta\tau}\lambda_{T_i}}\\
=&\frac{\varrho\int_v^{\frac{1}{\delta}+\left(v-\frac{1}{\delta}\right)w}\int_0^{\infty} y\frac{u-\frac{1}{\delta}}{v-\frac{1}{\delta}}e^{-uy}\nu(y)\mathrm{d}y\frac{\mathrm{d}u}{1-\delta u}+w\lambda_{T_i}}{\varrho\int_v^{\frac{1}{\delta}+\left(v-\frac{1}{\delta}\right)w}\int_0^{\infty} y\frac{u-\frac{1}{\delta}}{v-\frac{1}{\delta}}e^{-\left(u-\frac{u-\frac{1}{\delta}}{v-\frac{1}{\delta}}v\right)y}\nu(y)\mathrm{d}y\frac{\mathrm{d}u}{1-\delta u}+w\lambda_{T_i}}\\
=&\frac{\frac{\varrho}{1-\delta v}\int_v^{\frac{1}{\delta}+\left(v-\frac{1}{\delta}\right)w}\int_0^{\infty} ye^{-\left(u-\frac{1}{\delta}\right)y}e^{-\frac{y}{\delta}}\nu(y)\mathrm{d}y\mathrm{d}u+w\lambda_{T_i}}{\frac{\varrho}{1-\delta v}\int_v^{\frac{1}{\delta}+\left(v-\frac{1}{\delta}\right)w}\int_0^{\infty} ye^{-\left(u-\frac{1}{\delta}-\frac{u-\frac{1}{\delta}}{v-\frac{1}{\delta}}v\right)y}e^{-\frac{y}{\delta}}\nu(y)\mathrm{d}y\mathrm{d}u+w\lambda_{T_i}}\\
=&\frac{-\frac{\varrho}{\delta}\int_{1-\delta v}^{(1-\delta v)w}\int_0^{\infty} ye^{\frac{(1-\delta v)zy}{\delta}}e^{-\frac{y}{\delta}}\nu(y)\mathrm{d}y\mathrm{d}z+w\lambda_{T_i}}{-\frac{\varrho}{\delta}\int_{1-\delta v}^{(1-\delta v)w}\int_0^{\infty} ye^{\frac{zy}{\delta}}e^{-\frac{y}{\delta}}\nu(y)\mathrm{d}y\mathrm{d}z+w\lambda_{T_i}}\\
=&\frac{\frac{\varrho}{\delta}\int_0^{\infty}e^{-vs}\int_s^{\frac{s}{w}}e^{\frac{s}{\delta}}e^{-\frac{y}{\delta}}\nu(y)\mathrm{d}y\mathrm{d}s+w\lambda_{T_i}}{\frac{\varrho}{\delta}\int_0^{\infty}\int_s^{\frac{s}{w}}e^{\frac{s}{\delta}}e^{-\frac{y}{\delta}}\nu(y)\mathrm{d}y\mathrm{d}s+w\lambda_{T_i}}.
\end{aligned}
\tag{5.2.12}
$$

As the denominator of the second term of (5.2.11) can be also obtained nicely by setting $v=0$ in the joint transform (5.2.1), i.e.,

$$
\mathbb{E}\left[e^{-\left(\Lambda_{T_i+\tau}-\Lambda_{T_i}\right)}\mid\lambda_{T_i}\right]=\exp\left(-\frac{1-w}{\delta}\lambda_{T_i}-\varrho\int_v^{\frac{1}{\delta}+\left(v-\frac{1}{\delta}\right)w}\frac{\Phi\left(u-\frac{u-\frac{1}{\delta}}{v-\frac{1}{\delta}}v\right)}{1-\delta u}\mathrm{d}s\right).
$$

So, the second term of (5.2.11) can expressed by

$$
\frac{\mathbb{E}\left[e^{-v\lambda_{T_i+\tau^-}}e^{-\left(\Lambda_{T_i+\tau}-\Lambda_{T_i}\right)}\mid\lambda_{T_i}\right]}{\mathbb{E}\left[e^{-\left(\Lambda_{T_i+\tau}-\Lambda_{T_i}\right)}\mid\lambda_{T_i}\right]}
$$

$$
\begin{aligned}
&= \frac{\exp\left(-\left[\frac{1}{\delta}+\left(v-\frac{1}{\delta}\right)w\right]\lambda_{T_i}\right)\exp\left(-\varrho\int_v^{\frac{1}{\delta}+\left(v-\frac{1}{\delta}\right)w}\frac{\Phi(u)}{1-\delta u}\mathrm{d}u\right)}{\exp\left(-\frac{1}{\delta}(1-w)\lambda_{T_i}\right)\exp\left(-\varrho\int_v^{\frac{1}{\delta}+\left(v-\frac{1}{\delta}\right)w}\frac{\Phi\left(u-\frac{u-\frac{1}{\delta}}{v-\frac{1}{\delta}}v\right)}{1-\delta u}\mathrm{d}u\right)} \\
&= e^{-vw\lambda_{T_i}}\times\exp\left(-\varrho\int_v^{\frac{1}{\delta}+\left(v-\frac{1}{\delta}\right)w}\frac{\Phi(u)-\Phi\left(u-\frac{u-\frac{1}{\delta}}{v-\frac{1}{\delta}}v\right)}{1-\delta u}\mathrm{d}u\right). \qquad (5.2.13)
\end{aligned}
$$

Finally, we obtain (5.2.9) immediately by combining the results from (5.2.12) and (5.2.13). □

Apparently, given the i^{th} arrival time T_i and the $(i+1)^{\text{th}}$ interarrival time τ_{i+1}, the pre-jump intensity level $\lambda_{T_i+\tau_{i+1}^-}$ can be simulated by the numerical inversion of Laplace transform (5.2.9) for any Lévy driven contagion process once the associated Lévy measure ν (and Laplace exponent Φ) are specified. Indeed, exact simulation for stochastic processes based on the numerical inversion of Laplace or Fourier transform has been widely adopted in the literature, see Broadie and Kaya (2006), Glasserman and Liu (2010), Chen et al. (2012), Cai et al. (2017) and Kang et al. (2017).

However, for some subclasses such as the very popular specifications of gamma and tempered stable processes, quite remarkably, based on Theorem 5.2.2 the pre-jump intensity level can be exactly decomposed into several simple elements, each of which can be easily simulated exactly without any numerical inversion procedure. In fact, this exact decomposition approach appropriately breaks the Lévy measure of subordinator, and thereby it can be achieved by developing an exact distributional decomposition through Laplace transform representations. In this chapter, our focus is mainly on this decomposition approach, as it leads to a very efficient simulation algorithm for exactly sampling the whole point process, and more importantly, it does not involve additional discretisation or truncation errors which are inevitable in the numerical inversion approach. We will present our discovery based on the decomposition approach in much more details later in Section 5.3.

5.2.3 Exact Simulation of Self-exciting Jumps

Based on our key results of Algorithm 5.2.1 for the interarrival time τ_{i+1} and Theorem 5.2.2 for the associated pre-jump intensity level $\lambda_{T_i+\tau_{i+1}^-}$, now, it is straightforward to further integrate the self-exciting jumps as the final step.

Algorithm 5.2.3 (Exact Simulation of Self-exciting Jumps)**.** *Conditional on (λ_{T_i}, T_i) for any step index $i \in \mathbb{N}^+$, the next self-exciting jumps occurring simultaneously in the intensity process and*

the point process can be exactly simulated via the following steps:

1. *Generate the* $(i+1)^{\text{th}}$ *interarrival time* τ_{i+1} *by thinning via Algorithm 5.2.1;*
2. *Set the* $(i+1)^{\text{th}}$ *arrival time by* $T_{i+1} = T_i + \tau_{i+1}$*;*
3. *Generate the* $(i+1)^{\text{th}}$ *pre-jump intensity* $\lambda_{T_{i+1}^-}$ *with Laplace transform* (5.2.9) *in Theorem 5.2.2;*
4. *Add a self-exciting jump of size* X_{i+1} *to the intensity process at the* $(i+1)^{\text{th}}$ *arrival time* T_{i+1}*, i.e.*
$$\lambda_{T_{i+1}} = \lambda_{T_{i+1}^-} + X_{i+1}. \tag{5.2.14}$$
5. *Add one unit to the point process at the* $(i+1)^{\text{th}}$ *arrival time* T_{i+1}*, i.e.* $N_{T_{i+1}} = N_{T_{i+1}^-} + 1$.

By recursively implementing Algorithm 5.2.3, the skeleton of any Lévy driven OU intensity process λ_t and the associated full path of point process N_t in continuous time can be exactly generated. Moreover, there is almost no restriction on the size of self-exciting jump, X_{i+1}. It is very flexible, as long as it would not overshoot the zero bound: it could be a constant, or, a random variable having a highly general dependency on the past information before and at the arrival time T_i.

Overall, the whole process can be decomposed into interarrival times, pre-jump intensity levels and self-exciting jumps. When specifying the Lévy subordinator Z_t, each of pre-jump intensity levels in Step 3 in Algorithm 5.2.3 allows a further exact distributional decomposition, which leads to an exact simulation algorithm without numerical inversion. The resulting scheme thereby has no bias or truncation errors.

5.3 Typical Examples: Gamma and Tempered Stable Contagion Models

For model implementation, one needs to further specify Z_t in an explicit form. Probably the most widely used and representative Lévy subordinators in the literature are gamma process and tempered stable process. Many scholars adopted these Lévy subordinators as the building blocks to further construct other useful stochastic processes, and there are tremendous relevant papers and work in the literature, see Barndorff-Nielsen and Shephard (2001a,b, 2003a), Cont and Tankov (2004), Schoutens and Cariboni (2010) and Li and Linetsky (2014) to name a few. In this section, we consider two typical examples, i.e. the Gamma Contagion and the Tempered Stable Contagion, and provide applications for these contagion models later in Section 5.5.

Exact Simulation of Interarrival Time

For contagion models driven by the gamma process with shape a and rate b and the tempered stable process with stability α, intensity θ and tilting β, the interarrival time can be simulated via the general algorithm of thinning scheme, Algorithm 5.2.2, by simply calculating ζ_∞ in (5.2.8) from (5.2.6) explicitly as

$$\zeta_\infty \;=\; \begin{cases} \varrho a \ln\left(1+\dfrac{1}{\delta b}\right), & \text{for Gamma,} \\ -\varrho\theta\Gamma(-\alpha)\left[\left(\beta+\dfrac{1}{\delta}\right)^{\alpha}-\beta^{\alpha}\right], & \text{for Tempered Stable.} \end{cases}$$

Exact Simulation of Pre-jump Intensity

The pre-jump intensity level conditional on the realisation of interarrival time is characterised by the Laplace transforms (5.2.9) in Theorem 5.2.2, with Lévy measures ν and Laplace transform specified by (2.3.1, 2.3.2) and (2.4.1, 2.4.2) for the gamma and tempered stable cases, respectively. For both cases, the integral transforms of the pre-jump intensity levels actually can be broken into several simple elements.

The Laplace transform of pre-jump intensity level with three terms in (5.2.9) actually consists two parts: (5.2.12) and (5.2.13). Strikingly, based on Theorem 5.2.2, the first two terms of (5.2.9), i.e., (5.2.13), can be further exactly decomposed for the specified gamma and tempered stable cases respectively as follows.

Algorithm 5.3.1 (Exact Simulation of Pre-jump Intensity Level for Γ-Contagion)**.** *For the* Γ*-contagion, conditional on the intensity level* λ_{T_i} *and the realisation of the* $(i+1)^{\text{th}}$ *interarrival time* $\tau_{i+1} = \tau$*, the distribution of the* $(i+1)^{\text{th}}$ *pre-jump intensity level* $\lambda_{T_i+\tau^-}$ *can be exactly decomposed by*

$$\lambda_{T_i+\tau^-} \mid \lambda_{T_i} \overset{\mathcal{D}}{=} w\lambda_{T_i} + \widetilde{\Gamma} + \widetilde{B} \times S + \sum_{j=1}^{\widetilde{N}} S_j, \tag{5.3.1}$$

where

- $\widetilde{\Gamma}$ *is a gamma random variable of*

$$\widetilde{\Gamma} \;\sim\; \Gamma\left(-\frac{a\varrho}{\delta}\ln w,\; \frac{\vartheta}{w}-\frac{1}{\delta}\right), \qquad \vartheta := b+\frac{1}{\delta}; \tag{5.3.2}$$

- $\widetilde{B}$ *is a Bernoulli random variable taking* 0 *with probability* p_1 *and* 1 *with probability* p_2*, and*

$$p_1 = \frac{w\lambda_{T_i}}{\frac{a\varrho}{\delta}C + w\lambda_{T_i}}, \qquad p_2 = \frac{\frac{a\varrho}{\delta}C}{\frac{a\varrho}{\delta}C + w\lambda_{T_i}}, \qquad C := \delta\ln\left(\frac{b\delta+1-w}{b\delta}\right);$$

- *S is an exponential random variable of $S \sim Exp\left(\vartheta W_0 - \frac{1}{\delta}\right)$ and*

$$W_0 \overset{\mathcal{D}}{=} \left[1 - b\delta\left(e^{\frac{C}{\delta}U_0} - 1\right)\right]^{-1}, \quad U_0 \sim \mathcal{U}[0,1]; \tag{5.3.3}$$

- *$\widetilde{N}$ is a Poisson random variable of rate $\frac{a\varrho}{\delta}\vartheta C_w$ and*

$$C_w := \int_1^{\frac{1}{w}} \frac{\ln u}{\vartheta u - \frac{1}{\delta}} \mathrm{d}u;$$

- *$\left\{S_j\right\}_{j=1,2,\ldots}$ are i.i.d. with $S_j \sim Exp\left(\vartheta W - \frac{1}{\delta}\right)$, and W can be exactly simulated via the A/R scheme of Algorithm 5.3.2.*

Proof. In fact, Algorithm 5.3.1 is only an explicit specification of Theorem 5.2.2. Let us first calculate the first two terms of (5.2.9), i.e., (5.2.13), by

$$\begin{aligned}
&\frac{\mathbb{E}\left[e^{-v\lambda_{T_i+\tau^-}} e^{-\left(\Lambda_{T_i+\tau^-} - \Lambda_{T_i}\right)} \mid \lambda_{T_i}\right]}{\mathbb{E}\left[e^{-\left(\Lambda_{T_i+\tau^-} - \Lambda_{T_i}\right)} \mid \lambda_{T_i}\right]} \\
= \;& e^{-vw\lambda_{T_i}} \times \exp\left(-\frac{a\varrho}{\delta}\ln\left(\frac{1}{w}\right)\int_0^\infty \left(1 - e^{-vs}\right) s^{-1} e^{-\left(\frac{\vartheta}{w} - \frac{1}{\delta}\right)s} \mathrm{d}s\right) \\
& \times \exp\left(-\frac{a\vartheta\varrho}{\delta}\int_0^\infty \left(1 - e^{-vs}\right)\int_1^{\frac{1}{w}} \left(\vartheta u - \frac{1}{\delta}\right) e^{-\left(\vartheta u - \frac{1}{\delta}\right)s} \frac{\ln u}{\vartheta u - \frac{1}{\delta}} \mathrm{d}u\mathrm{d}s\right).
\end{aligned} \tag{5.3.4}$$

Then, by calculating the whole equation (5.2.9) more explicitly, the conditional Laplace transform of the pre-jump intensity level $\lambda_{T_i+\tau^-}$ can be decomposed into four parts:

$$\begin{aligned}
&\mathbb{E}\left[e^{-v\lambda_{T_i+\tau^-_{i+1}}} \mid \tau_{i+1} = \tau, \lambda_{T_i}\right] \\
= \;& e^{-vw\lambda_{T_i}} \times \exp\left(-\frac{a\varrho}{\delta}\ln\left(\frac{1}{w}\right)\int_0^\infty \left(1 - e^{-vs}\right) s^{-1} e^{-\left(\frac{\vartheta}{w} - \frac{1}{\delta}\right)s} \mathrm{d}s\right) \\
& \times \exp\left(-\frac{a\vartheta\varrho}{\delta}\int_0^\infty \left(1 - e^{-vs}\right)\int_1^{\frac{1}{w}} \left(\vartheta u - \frac{1}{\delta}\right) e^{-\left(\vartheta u - \frac{1}{\delta}\right)s} \frac{\ln u}{\vartheta u - \frac{1}{\delta}} \mathrm{d}u\mathrm{d}s\right) \\
& \times \left[\frac{\frac{a\varrho C}{\delta}}{\frac{a\varrho C}{\delta} + w\lambda_{T_i}} \int_0^\infty e^{-vs} \int_1^{\frac{1}{w}} \left(\vartheta u - \frac{1}{\delta}\right) e^{-\left(\vartheta u - \frac{1}{\delta}\right)s} \frac{1}{C\left(\vartheta u^2 - \frac{1}{\delta}u\right)} \mathrm{d}u\mathrm{d}s + \frac{w\lambda_{T_i}}{\frac{a\varrho C}{\delta} + w\lambda_{T_i}}\right].
\end{aligned} \tag{5.3.5}$$

This decomposition of (5.3.5) indicates that the conditional distribution of $\lambda_{T_i+\tau^-}$ is the sum of four independent simple elements of (5.3.1): (1) one deterministic trend, (2) one random variable

$\widetilde{B} \times S$, (3) one gamma random variable, and (4) one compound Poisson random variable. Note that, $\widetilde{B} \times S$ can be alternatively defined as just one single random variable by

$$\widetilde{B} \times S \overset{\mathcal{D}}{=} \begin{cases} 0, & \text{with probability } p_1 = \frac{w\lambda_{T_i}}{\frac{a\varrho}{\delta}C + w\lambda_{T_i}}, \\ S \sim Exp\left(\vartheta W_0 - \frac{1}{\delta}\right), & \text{with probability } p_2 = \frac{\frac{a\varrho}{\delta}C}{\frac{a\varrho}{\delta}C + w\lambda_{T_i}}. \end{cases} \tag{5.3.6}$$

The CDF of W_0 is

$$F_{W_0}(u) = \frac{1}{C_w(a + \frac{1}{\delta})} \ln\left(\frac{\left(a + \frac{1}{\delta}\right)u - \frac{1}{\delta}}{a}\right), \qquad u \in \left[1, \frac{1}{w}\right],$$

which can be inverted explicitly, so we have (5.3.3). The compound Poisson random variable $\sum_{j=1}^{\tilde{N}} S_j$ has the Laplace transform

$$\exp\left(-\frac{a\vartheta\varrho}{\delta}C_w \int_0^{\infty}\left(1 - e^{-vs}\right)\int_1^{\frac{1}{w}}\left(\vartheta u - \frac{1}{\delta}\right)e^{-\left(\vartheta u - \frac{1}{\delta}\right)s}\frac{\ln u}{C_w\left(\vartheta u - \frac{1}{\delta}\right)}\mathrm{d}u\mathrm{d}s\right),$$

so, the Poisson rate is $\frac{a\vartheta\varrho}{\delta}C_w$, and jump-sizes $\left\{S_j\right\}_{j=1,2,\ldots}$ follow an exponential distribution with rate $\vartheta W - \frac{1}{\delta}$. Here, W is a well-defined random variable with density (5.3.7), which can be exactly simulated via the A/R scheme of Algorithm 5.3.2. □

Algorithm 5.3.2 (A/R Scheme for W)**.** *The simulation scheme for W is given as follows:*

1. *Generate $U \sim \mathcal{U}[0,1]$, and set $W = w^{-\sqrt{U}}$,*

2. *Generate $V \sim \mathcal{U}[0,1]$, if*

$$V \leq bW / \left[\vartheta W - \frac{1}{\delta}\right],$$

then, accept W; Otherwise, reject this candidate and go back to Step 1.

Proof. Note that,

$$\vartheta u - \frac{1}{\delta} = bu + \frac{1}{\delta}(u - 1) \geq bu, \qquad u \in \left[1, \frac{1}{w}\right],$$

then, we have

$$f_W(u) = \frac{1}{C_w}\frac{\ln u}{\vartheta u - \frac{1}{\delta}} \leq \frac{1}{C_w}\frac{\ln u}{bu}. \tag{5.3.7}$$

The density function of the envelope W' is

$$f_{W'}(u) = \frac{1}{E_w}\frac{\ln u}{u}, \qquad E_w := \frac{1}{2}\ln^2 w, \qquad u \in \left[1, \frac{1}{w}\right],$$

and with analytic inverse

$$F_{W'}^{-1}(x) = w^{-\sqrt{x}}, \qquad x \in [0,1].$$

Therefore, we have

$$\frac{f_W(u)}{f_{W'}(u)} = \frac{\frac{1}{C_w}\frac{\ln u}{\vartheta u - \frac{1}{\delta}}}{\frac{1}{E_w}\frac{\ln u}{u}} \leq \frac{\frac{1}{C_w}\frac{\ln u}{bu}}{\frac{1}{E_w}\frac{\ln u}{u}} = \frac{1}{b}\frac{E_w}{C_w} = \frac{\ln^2 w}{2bC_w} := \bar{c}_w,$$

and the acceptance condition for the A/R scheme is

$$V \leq \frac{1}{\bar{c}_w}\frac{f_W(W')}{f_{W'}(W')} = b\frac{W'}{\vartheta W' - \frac{1}{\delta}}.$$

□

Algorithm 5.3.3 (Exact Simulation of Pre-jump Intensity Level for TS-Contagion)**.** *For the TS-contagion, conditional on the intensity level λ_{T_i} and the realisation of the $(i+1)^{\text{th}}$ interarrival time $\tau_{i+1} = \tau$, the distribution of the $(i+1)^{\text{th}}$ pre-jump intensity level $\lambda_{T_i+\tau^-}$ can be exactly decomposed by*

$$\lambda_{T_i+\tau^-} \mid \lambda_{T_i} \overset{\mathcal{D}}{=} w\lambda_{T_i} + \widetilde{TS} + \widetilde{B} \times S + \sum_{k=1}^{\widetilde{N}} S_k, \tag{5.3.8}$$

where

- *$\widetilde{TS}$ is a tempered stable random variable of*

$$TS \sim TS\left(\alpha, \frac{\kappa}{w} - \frac{1}{\delta}, \frac{\theta\varrho}{\alpha\delta}\left(1 - w^{\alpha}\right)\right), \qquad \kappa := \beta + \frac{1}{\delta}; \tag{5.3.9}$$

- *$\widetilde{B}$ is a Bernoulli random variable taking 0 with probability p_1 and 1 with probability p_2, and*

$$p_1 := \frac{w\lambda_{T_i}}{\frac{\theta\varrho D}{\delta}\Gamma(1-\alpha) + w\lambda_{T_i}}, \quad p_2 := \frac{\frac{\theta\varrho D}{\delta}\Gamma(1-\alpha)}{\frac{\theta\varrho D}{\delta}\Gamma(1-\alpha) + w\lambda_{T_i}}, \quad D := \frac{\delta}{\alpha}\left[\left(\kappa - \frac{w}{\delta}\right)^{\alpha} - \beta^{\alpha}\right];$$

- *S is a mixture-Gamma random variable of $S \sim \Gamma\left(1-\alpha, \kappa V_0 - \frac{1}{\delta}\right)$ and*

$$V_0 \overset{\mathcal{D}}{=} \left[\delta\beta + 1 - \delta\left(\frac{\alpha D}{\delta}U_2 + \beta^{\alpha}\right)^{\frac{1}{\alpha}}\right]^{-1}, \qquad U_2 \sim \mathcal{U}[0,1]; \tag{5.3.10}$$

- *$\widetilde{N}$ is a Poisson random variable of rate $\frac{\theta\varrho}{\alpha\delta}\kappa\Gamma(1-\alpha)D_w$ and*

$$D_w := \int_1^{\frac{1}{w}} \frac{1 - u^{-\alpha}}{\left(\kappa u - \frac{1}{\delta}\right)^{1-\alpha}}\mathrm{d}u; \tag{5.3.11}$$

- $\left\{S_k\right\}_{k=1,2,\ldots}$ *are i.i.d. with* $S_k \sim \Gamma\left(1-\alpha,\ \kappa V - \frac{1}{\delta}\right)$, *and* V *can be exactly simulated via the A/R scheme of Algorithm 5.3.4.*

Proof. Algorithm 5.3.3 is another explicit specification of Theorem 5.2.2. Similarly as the previous gamma case in Algorithm 5.3.1, given the Lévy measure (2.4.1), we can identify that (5.2.12) is the Laplace transform of $\widetilde{B} \times S$ from the calculation

$$
\begin{aligned}
& \frac{\frac{\varrho}{\delta}\int_0^{\infty} e^{-vs}\int_s^{\frac{s}{w}} e^{\frac{s}{\delta}}e^{-\frac{y}{\delta}}\nu(y)\mathrm{d}y\mathrm{d}s + w\lambda_{T_i}}{\frac{\varrho}{\delta}\int_0^{\infty}\int_s^{\frac{s}{w}} e^{\frac{s}{\delta}}e^{-\frac{y}{\delta}}\nu(y)\mathrm{d}y\mathrm{d}s + w\lambda_{T_i}} \\
= & \frac{\frac{\theta\varrho}{\delta}\int_0^{\infty} e^{-vs}\int_1^{\frac{1}{w}} s^{(1-\alpha)-1}e^{-\left(\kappa u-\frac{1}{\delta}\right)s}u^{-1-\alpha}\mathrm{d}u\mathrm{d}s + w\lambda_{T_i}}{\int_0^{\infty}\int_1^{\frac{1}{w}} s^{(1-\alpha)-1}e^{-\left(\kappa u-\frac{1}{\delta}\right)s}u^{-1-\alpha}\mathrm{d}u\mathrm{d}s + w\lambda_{T_i}} \\
= & \frac{w\lambda_{T_i}}{\frac{\theta\varrho D}{\delta}\Gamma(1-\alpha) + w\lambda_{T_i}} \times 1 \\
& + \frac{\frac{\theta\varrho D}{\delta}\Gamma(1-\alpha)}{\frac{\theta\varrho D}{\delta}\Gamma(1-\alpha) + w\lambda_{T_i}} \times \int_0^{\infty} e^{-vs}\int_1^{\frac{1}{w}} \frac{\left(\kappa u-\frac{1}{\delta}\right)^{1-\alpha}}{\Gamma(1-\alpha)} s^{(1-\alpha)-1}e^{-\left(\kappa u-\frac{1}{\delta}\right)s}\frac{u^{-1-\alpha}}{D\left(\kappa u-\frac{1}{\delta}\right)^{1-\alpha}}\mathrm{d}u\mathrm{d}s \\
= & p_1 \times \mathbb{E}\left[e^{-v0}\right] + p_2 \times \mathbb{E}\left[e^{-vS}\right],
\end{aligned}
$$

where

$$
D = \int_1^{\frac{1}{w}} \frac{u^{-1-\alpha}}{\left(\kappa u-\frac{1}{\delta}\right)^{1-\alpha}}\mathrm{d}u = \frac{\delta}{\alpha}\left[\left(\kappa - \frac{w}{\delta}\right)^{\alpha} - \beta^{\alpha}\right].
$$

So, the outcome of $\widetilde{B} \times S$ is trivially equal to 0 with probability p_1, or, the random variable S with probability p_2. S follows a mixture-gamma distribution with the shape parameter $1-\alpha$ and the rate parameter $\kappa V_0 - \frac{1}{\delta}$. Here, V_0 is a well-defined random variable with density function

$$
f_{V_0}(u) = \frac{u^{-\alpha-1}}{D\left(\kappa u-\frac{1}{\delta}\right)^{1-\alpha}}, \qquad u \in \left[1, \frac{1}{w}\right]. \tag{5.3.12}
$$

It can be directly simulated via the explicit inverse transform (5.3.10), as its CDF is

$$
F_{V_0}(u) = \frac{\delta}{\alpha D}\left[u^{-\alpha}\left(\kappa u - \frac{1}{\delta}\right)^{\alpha} - \beta^{\alpha}\right], \qquad u \in \left[1, \frac{1}{w}\right].
$$

The first two terms of (5.2.9), i.e., (5.2.13), can be expressed by

$$
\begin{aligned}
&\frac{\mathbb{E}\left[e^{-v\lambda_{T_i+\tau^-}}e^{-\left(\Lambda_{T_i+\tau^-}-\Lambda_{T_i}\right)}\mid\lambda_{T_i}\right]}{\mathbb{E}\left[e^{-\left(\Lambda_{T_i+\tau^-}-\Lambda_{T_i}\right)}\mid\lambda_{T_i}\right]}\\
=\;& e^{-vw\lambda_{T_i}}\times\exp\left(-\frac{\theta\varrho}{\alpha\delta}\left(1-w^{\alpha}\right)\int_0^{\infty}\left(1-e^{-vs}\right)\frac{1}{s^{\alpha+1}}e^{-\left(\frac{\kappa}{w}-\frac{1}{\delta}\right)s}\mathrm{d}s\right)\\
&\times\exp\left(-\frac{\theta\varrho}{\alpha\delta}\kappa\Gamma(1-\alpha)\int_0^{\infty}\left(1-e^{-vs}\right)\int_1^{\frac{1}{w}}\frac{\left(\kappa u-\frac{1}{\delta}\right)^{1-\alpha}}{\Gamma(1-\alpha)}s^{(1-\alpha)-1}\frac{1-u^{-\alpha}}{\left(\kappa u-\frac{1}{\delta}\right)^{1-\alpha}}\mathrm{d}u\mathrm{d}s\right),
\end{aligned}
$$

since the Lévy measure ν for the tempered stable subordinator is specified in (2.4.1), and the Laplace exponent of (5.2.13) can be rewritten by

$$
\begin{aligned}
&\varrho\int_v^{\frac{1}{\delta}+\left(v-\frac{1}{\delta}\right)w}\frac{\Phi\left(u-\frac{u-\frac{1}{\delta}}{v-\frac{1}{\delta}}v\right)-\Phi(u)}{1-\delta u}\mathrm{d}u\\
=\;&\frac{\varrho}{\delta}\int_0^{\infty}\left(1-e^{-vs}\right)\frac{1}{s}e^{\frac{s}{\delta}}\int_s^{\frac{s}{w}}\frac{\theta}{y^{\alpha+1}}e^{-\kappa\frac{s}{w}}\mathrm{d}y\mathrm{d}s\\
&+\frac{\varrho}{\delta}\int_0^{\infty}\left(1-e^{-vs}\right)\frac{e^{\frac{s}{\delta}}}{s}\int_s^{\frac{s}{w}}\frac{\theta\left(e^{-\kappa y}-e^{-\frac{\kappa s}{w}}\right)}{y^{\alpha+1}}\mathrm{d}y\mathrm{d}s\\
=\;&\int_0^{\infty}\left(1-e^{-vs}\right)\frac{\theta\varrho}{\alpha\delta}\left(1-w^{\alpha}\right)\frac{1}{s^{\alpha+1}}e^{-\left(\frac{\kappa}{w}-\frac{1}{\delta}\right)s}\mathrm{d}s\\
&+\frac{\theta\varrho}{\alpha\delta}\kappa\Gamma(1-\alpha)\int_0^{\infty}\left(1-e^{-vs}\right)\int_1^{\frac{1}{w}}\frac{\left(\kappa u-\frac{1}{\delta}\right)^{1-\alpha}}{\Gamma(1-\alpha)}s^{(1-\alpha)-1}e^{-\left(\kappa u-\frac{1}{\delta}\right)s}\frac{1-u^{-\alpha}}{\left(\kappa u-\frac{1}{\delta}\right)^{1-\alpha}}\mathrm{d}u\mathrm{d}s.
\end{aligned}
$$

So, for (5.2.13), it consist three components: one deterministic trend, a tempered stable process and a compound Poisson process. In particular, the rate of the compound Poisson process is $\widetilde{N}$ is $\frac{\theta\varrho}{\alpha\delta}\kappa\Gamma(1-\alpha)D_w$, and the jump sizes follow a mixture-Gamma distribution with the shape parameter $(1-\alpha)$ and the rate parameter $\kappa V-\frac{1}{\delta}$. Here, V is a well-defined random variable with density

$$
f_V(u)=\frac{1-u^{-\alpha}}{D_w\left(\kappa u-\frac{1}{\delta}\right)^{1-\alpha}},\qquad u\in\left[1,\frac{1}{w}\right]. \tag{5.3.13}
$$

Overall, we have the conditional Laplace transform of pre-jump intensity level explicitly as

$$
\mathbb{E}\left[e^{-v\lambda_{T_i+\tau_{i+1}^-}}\mid\tau_{i+1}=\tau,\lambda_{T_i}\right]
$$

$$
\begin{aligned}
&= e^{-v w \lambda_{T_i}} \times \exp\left(-\frac{\theta\varrho}{\alpha\delta}\left(1-w^{\alpha}\right) \int_0^{\infty} \left(1-e^{-vs}\right) \frac{1}{s^{\alpha+1}} e^{-\left(\frac{\kappa}{w}-\frac{1}{\delta}\right)s} \mathrm{d}s \right) \\
&\quad \times \exp\left(-\frac{\theta\varrho}{\alpha\delta}\kappa\Gamma(1-\alpha) D_w \int_0^{\infty} \left(1-e^{-vs}\right) \int_1^{\frac{1}{w}} \frac{\left(\kappa u-\frac{1}{\delta}\right)^{1-\alpha}}{\Gamma(1-\alpha)} s^{(1-\alpha)-1} \frac{1-u^{-\alpha}}{D_w\left(\kappa u-\frac{1}{\delta}\right)^{1-\alpha}} \mathrm{d}u\mathrm{d}s \right) \\
&\quad \times \left[\frac{w\lambda_{T_i}}{\frac{\theta\varrho D}{\delta}\Gamma(1-\alpha)+w\lambda_{T_i}} + \frac{\frac{\theta\varrho D}{\delta}\Gamma(1-\alpha)}{\frac{\theta\varrho D}{\delta}\Gamma(1-\alpha)+w\lambda_{T_i}} \times \right. \\
&\qquad \left. \int_0^{\infty} e^{-vs} \int_1^{\frac{1}{w}} \frac{\left(\kappa u-\frac{1}{\delta}\right)^{1-\alpha}}{\Gamma(1-\alpha)} s^{(1-\alpha)-1} e^{-\left(\kappa u-\frac{1}{\delta}\right)s} \frac{u^{-1-\alpha}}{D\left(\kappa u-\frac{1}{\delta}\right)^{1-\alpha}} \mathrm{d}u\mathrm{d}s \right].
\end{aligned}
$$

We can identify from the Laplace transforms above that, the distribution of the $(i+1)^{\text{th}}$ pre-jump intensity level $\lambda_{T_i+\tau^-}$ conditional on λ_{T_i} is exactly equal in distribution to the sum of four simple elements provided in (5.3.8). All these components can be simulated exactly. To simulate the TS random variable, one could use existing algorithm provided in Section 2.4. And to sample the compound Poisson random variable $\widetilde{N}$, one first needs to generate the intermediate random variable V with density (5.3.13). Since there is no closed form for the inverse function of the CDF of V, we have to rely on the A/R scheme of Algorithm 5.3.4. □

Algorithm 5.3.4 (A/R Scheme for V)**.** *The random variable V with density (5.3.13) can be exactly simulated by the following A/R procedure:*

1. *Set* $C_w = \frac{1}{\alpha}\left(w^{-\alpha}+w^{\alpha}-2\right)$,
2. *Generate* $U_1 \sim \mathcal{U}[0,1]$,
3. *Set*
$$V = \left\{ \frac{1}{2}\left[\left(\alpha C_w U_1 + 2\right) + \sqrt{\left(\alpha C_w U_1+2\right)^2 - 4} \right] \right\}^{\frac{1}{\alpha}}, \tag{5.3.14}$$
4. *Generate* $U_2 \sim \mathcal{U}[0,1]$, *if*
$$U_2 \leq \frac{\beta^{1-\alpha}}{V^{\alpha-1}-V^{-1-\alpha}} \frac{1-V^{-\alpha}}{\left(\kappa V-\frac{1}{\delta}\right)^{1-\alpha}},$$
then, accept V; Otherwise, reject this candidate and go back to Step 1.

Proof. The density of V in (5.3.13) can be rewritten by

$$f_V(u) = \frac{1}{D_w}\frac{1}{\kappa^{1-\alpha}} \frac{1-u^{-\alpha}}{\left(u-\frac{1}{\delta\kappa}\right)^{1-\alpha}}, \qquad u \in \left[1, \frac{1}{w}\right].$$

By introducing a constant ξ such that

$$\xi \geq \frac{u^{1-\alpha}}{\left(u-\frac{1}{\delta\kappa}\right)^{1-\alpha}}, \qquad \forall u \in \left[1, \frac{1}{w}\right],$$

we have

$$f_V(u) < \frac{1}{D_w}\frac{\xi}{\kappa^{1-\alpha}}\left[u^{-(1-\alpha)} - u^{-(1+\alpha)}\right], \qquad \forall u \in \left[1, \frac{1}{w}\right].$$

Since the function $\frac{u^{1-\alpha}}{\left(u-\frac{1}{\delta\kappa}\right)^{1-\alpha}}$ is a strictly decreasing function of $u \in \left[1, \frac{1}{w}\right]$, i.e.

$$\frac{\mathrm{d}}{\mathrm{d}u}\left[\frac{u^{1-\alpha}}{\left(u-\frac{1}{\delta\kappa}\right)^{1-\alpha}}\right] = (\alpha-1)\frac{1}{\delta\kappa}u^{-\alpha}\left(u-\frac{1}{\delta\kappa}\right)^{\alpha-2} < 0,$$

we have $\xi \geq \left(\frac{\kappa}{\beta}\right)^{1-\alpha}$ for any $u \in \left[1, \frac{1}{w}\right]$, and then,

$$\xi \geq \max_{1\leq u\leq \frac{1}{w}}\left\{\frac{u^{1-\alpha}}{\left(u-\frac{1}{\delta\kappa}\right)^{1-\alpha}}\right\} = \left(\frac{\kappa}{\beta}\right)^{1-\alpha}.$$

We choose V' to be the envelope random variable with density

$$g(u) = \frac{1}{C_w}\left[u^{-(1-\alpha)} - u^{-(1+\alpha)}\right], \qquad u \in \left[1, \frac{1}{w}\right].$$

Its CDF is

$$G(u) = \frac{1}{\alpha C_w}\left(u^{-\alpha} + u^{\alpha} - 2\right), \qquad u \in \left[1, \frac{1}{w}\right],$$

which has an explicit inverse function

$$G^{-1}(x) = \left\{\frac{1}{2}\left[\left(\alpha C_w x + 2\right) + \sqrt{\left(\alpha C_w x + 2\right)^2 - 4}\right]\right\}^{\frac{1}{\alpha}}, \qquad x \in [0,1].$$

Hence, V' can be exactly simulated via the explicit inverse transform (5.3.14). Setting $\xi = \left(\frac{\kappa}{\beta}\right)^{1-\alpha}$, we have the *acceptance rate* (i.e. the expected number of candidates generated until one is accepted)

$$\bar{c}_w = \frac{\xi}{\kappa^{1-\alpha}}\frac{C_w}{D_w} = \beta^{1-\alpha}\frac{C_w}{D_w} \geq \frac{f_V(u)}{g(u)}.$$

□

We have also carried out some numerical tests for Algorithm 5.3.4 and have found that it can achieve a high level of efficiency and accuracy. For example, it only takes about 7 seconds to gen-

erate $1,000,000$ replications with percentage error 0.1% for the parameter setting $(\delta, \varrho, \alpha, \beta, \theta) = (0.5, 1, 0.9, 0.2, 0.25)$.

Exact Simulation of Self-exciting Jumps

Conditional on the realisations of the interarrival time and pre-jump intensity level as above, the associated self-exciting jump can be easily simulated by just following Algorithm 5.2.3 in general both for Gamma and TS contagion processes.

5.4 Numerical Experiments

In this section, let us take the TS-contagion model as an example, to illustrate the performance of our exact scheme through extensive numerical experiments, and postpone the implementation for the Γ-contagion model later in Section 5.5 with more financial applications. The true value of the conditional expectation of N_T for any fixed time $T > 0$ provided in Proposition 5.1.1 is used to numerically validate and test our algorithms. The associated errors from the true values are reported by three standard measures, we implement Algorithm 5.2.3 for the tempered stable and inverse Gaussian cases in a fixed period of $[0, T]$ *with* and *without* self-exciting jumps, respectively:

Case I: *Jump process with Lévy dirven OU intensity* (of Definition 5.1.1);

Case II: *Self-exciting jump process with Lévy driven OU intensity* (of Definition 5.1.2).

For numerical implementation, we further assume that, the sizes of self-exciting jumps follow an exponential distribution of rate $\gamma > 0$, i.e. $X_i \sim Exp(\gamma)$, and the stable index takes the values of, say, $\alpha = 1/4$ for the tempered stable case. $\widetilde{TS}$ of (5.3.9) is simulated using the *two-dimensional single rejection* scheme in Algorithm 2.4.6 , and the parameters are set by:

1. **TS Case I**: $(\delta, \varrho; \alpha, \beta, \theta; \lambda_0) = (1.0, 0.5; 0.25, 0.2, 0.25; 0.5)$;
2. **TS Case II**: $(\delta, \varrho; \alpha, \beta, \theta; \gamma; \lambda_0) = (1.0, 0.5; 0.25, 0.2, 0.25; 5.0; 0.5)$;
3. **IG Case I**: $(\delta, \varrho; c; \lambda_0) = (1.0, 0.5; 0.5; 0.5)$;
4. **IG Case II**: $(\delta, \varrho; c; \gamma; \lambda_0) = (1.0, 0.5; 0.5; 4.0; 0.5)$.

Simulated sample paths of the point processes within a long period of $t \in [0, 500]$ with the associated histograms are plotted in Figure 5.3, where the cluttering or contagious arrivals of jumps can be clearly presented. Furthermore, to measure the accuracy and efficiency of our scheme, we carry out the convergence analysis: Figure 5.4 presents log-log plots for the RMSE against the CPU time

for each case in two different time horizons $T = 2, 5$, respectively, and the associated results in detail are reported in Table 5.3. Overall, from these numerical results reported in this section, it is evident that our exact scheme can achieve a very high level of accuracy and efficiency.

To be even more prudent, the simulation for the interarrival time based on the *simplified thinning scheme* of Algorithm 5.2.2, as an intermediate step, can be also tested separately. To numerically assess its accuracy and efficiency, we compare the simulated results of V^* with its theoretical tail distribution $P(V^* > \tau)$ as specified in (5.2.7), which can be calculated explicitly by substituting the Laplace exponent Φ from (2.4.2). We set the parameters by $(\delta, \varrho; \alpha, \beta, \theta) = (0.5, 1.0; 0.9, 0.2, 0.25)$, and each estimation is based on $100,000$ replications. Error percentages (*Error%*) for measuring *relative errors* are reported in Table 5.2. The total CPU time for producing the whole Table 5.2 is only 12.64 seconds, and the error percentages are all very tiny.

5.5 Financial Applications: Comprehensive Risk Analysis for A Large Portfolio Facing Contagious Losses

It has now been widely recognised among academics and financial practitioners that, risk spreads through highly interconnected business networks, and defaults could trigger more defaults through a domino effect. The resulting losses presented in financial markets could be amplified. As earlier mentioned in Section 5.3, gamma distribution is a poplar build block in financial applications. Especially, it plays an important role in credit risk modelling. For instance, both the widely-used framework of CreditRisk$^+$ (1997) in the banking industry and influential papers by Gordy (2000, 2003) and Elsinger et al. (2006) in the literature, assumed that, macroeconomic factors are driven by independent gamma-distributed random variables[2]. More recent evidences have been found by Giesecke et al. (2011) that, long periods with relatively few defaults follow by episodes of significant clustering of defaults and the resulting distribution of default rates is highly skewed towards large values. This motivates us to adopt our new model of Γ-contagion as an example for applications in risk management for a portfolio facing domino effect of losses. We assume that exogenous commonly-shared risk is dynamically powered by a gamma process. More precisely, we adopt the gamma distribution as the fundamental driver of randomness (or *Gamma shock*) to construct the *OU*-Γ *interarrival intensity* for a point process N_t in Definition 5.1.2. A simulated path of this interarrival intensity process within the time period $t \in [0, 5]$ based on the parameter setting $(\delta, \varrho; a, b; \lambda_0) = (1.0, 1.0; 4.0, 0.5; 2.0)$ is earlier plotted in Figure 5.1, where we can observe relatively high-frequent and small-size shocks. In fact, it is named as the *OU*-Γ *process* by

[2]Besides, it can be also equipped as a fundamental risk driver for price movements, e.g. the popular *variance Gamma model* (Madan and Seneta, 1990; Madan et al., 1998).

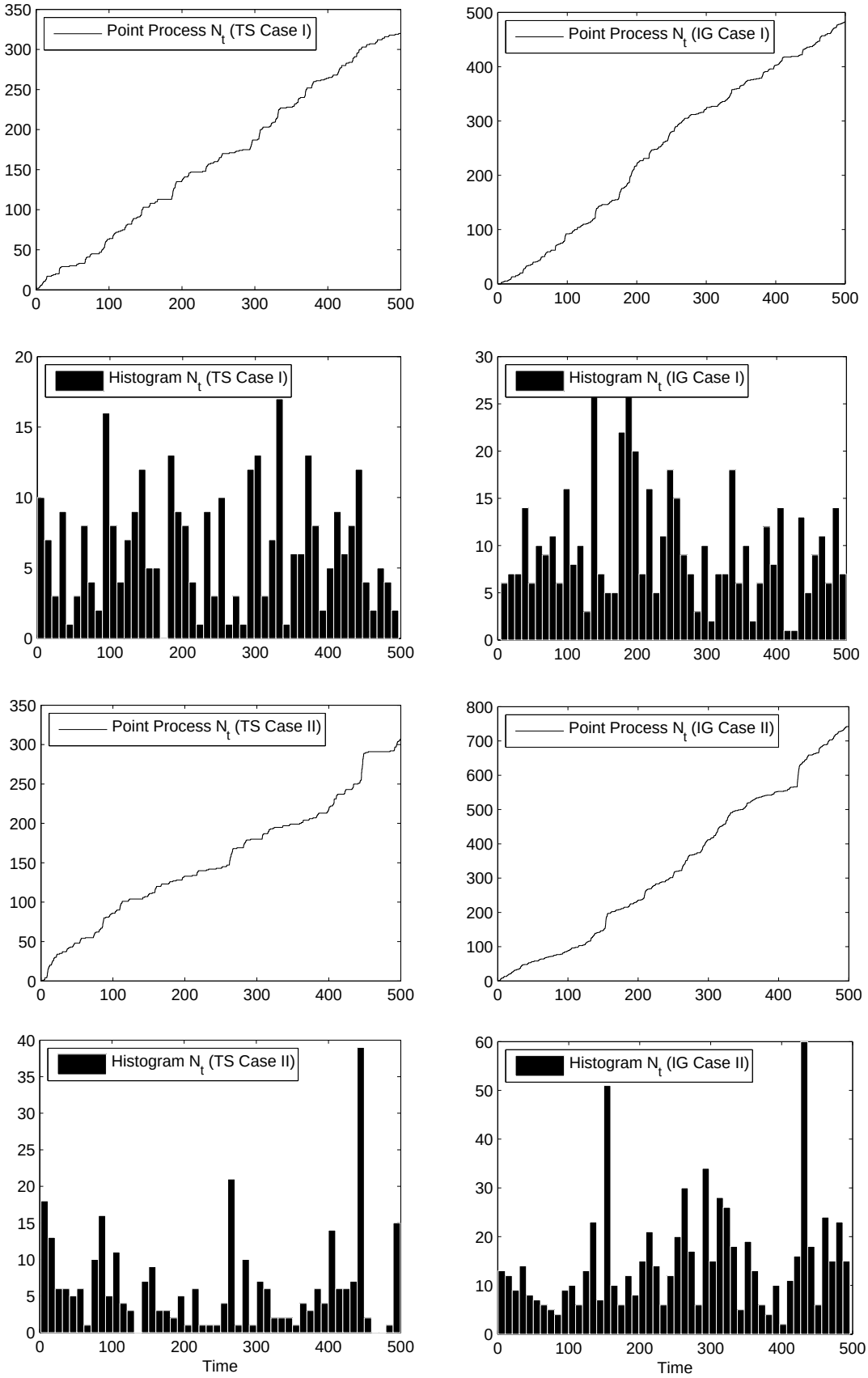

Figure 5.3: Simulated sample paths of the point processes and the associated histogram plots for Case I&II: TS Case I $(\delta, \varrho; \alpha, \beta, \theta; \lambda_0) = (1.0, 0.5; 0.25, 0.2, 0.25; 0.5)$, TS Case II $(\delta, \varrho; \alpha, \beta, \theta; \gamma; \lambda_0) = (1.0, 0.5; 0.25, 0.2, 0.25; 5.0; 0.5)$; IG Case I $(\delta, \varrho; c; \lambda_0) = (1.0, 0.5; 0.5; 0.5)$, IG Case II $(\delta, \varrho; c; \gamma; \lambda_0) = (1.0, 0.5; 0.5; 4.0; 0.5)$

Table 5.1: Simulation results for Case I&II: TS Case I $(\delta, \varrho; \alpha, \beta, \theta; \lambda_0) = (1.0, 0.5; 0.25, 0.2, 0.25; 0.5)$, TS Case II $(\delta, \varrho; \alpha, \beta, \theta; \gamma; \lambda_0) = (1.0, 0.5; 0.25, 0.2, 0.25; 5.0; 0.5)$; IG Case I $(\delta, \varrho; c; \lambda_0) = (1.0, 0.5; 0.5; 0.5)$, IG Case II $(\delta, \varrho; c; \gamma; \lambda_0) = (1.0, 0.5; 0.5; 4.0; 0.5)$

Case	Paths	True	Simulation	Error	Error%	RMSE	CPU Time (sec)
			TS Case				
Case I, $T = 2$	100	1.0138	0.9300	-0.0838	-8.2683%	0.1281	0.11
	400	1.0138	1.0525	0.0387	3.8146%	0.0834	0.36
	1,600	1.0138	1.0363	0.0224	2.2118%	0.0398	1.37
	6,400	1.0138	1.0184	0.0046	0.4548%	0.0208	5.29
	25,600	1.0138	1.0167	0.0029	0.2853%	0.0099	20.53
	102,400	1.0138	1.0133	-0.0005	-0.0509%	0.0049	81.74
	409,600	1.0138	1.0127	-0.0012	-0.1147%	0.0024	321.78
Case I, $T = 5$	100	2.5488	2.5500	0.0012	0.0472%	0.2879	0.22
	400	2.5488	2.4700	-0.0788	-3.0915%	0.1466	0.73
	1,600	2.5488	2.6413	0.0925	3.6274%	0.0815	2.92
	6,400	2.5488	2.5308	-0.0180	-0.7068%	0.0380	11.08
	25,600	2.5488	2.5523	0.0035	0.1361%	0.0190	44.29
	102,400	2.5488	2.5589	0.0101	0.3948%	0.0095	177.92
	409,600	2.5488	2.5437	-0.0051	-0.1998%	0.0048	706.82
Case II, $T = 2$	100	1.1406	1.1500	0.0094	0.8281%	0.1520	0.14
	400	1.1406	1.0925	-0.0481	-4.2133%	0.0909	0.36
	1,600	1.1406	1.1581	0.0176	1.5404%	0.0453	1.48
	6,400	1.1406	1.1233	-0.0173	-1.5145%	0.0228	5.71
	25,600	1.1406	1.1468	0.0062	0.5472%	0.0114	23.21
	102,400	1.1406	1.1305	-0.0101	-0.8835%	0.0056	90.92
	409,600	1.1406	1.1454	0.0049	0.4282%	0.0028	365.82
Case II, $T = 5$	100	3.0290	2.9900	-0.0390	-1.2891%	0.3932	0.23
	400	3.0290	3.0875	0.0585	1.9298%	0.1903	0.87
	1,600	3.0290	3.0413	0.0122	0.4029%	0.0923	3.34
	6,400	3.0290	3.0961	0.0670	2.2135%	0.0491	13.54
	25,600	3.0290	3.0095	-0.0196	-0.6456%	0.0234	52.28
	102,400	3.0290	3.0264	-0.0026	-0.0862%	0.0117	207.73
	409,600	3.0290	3.0308	0.0017	0.0569%	0.0058	831.64
			IG Case				
Case I, $T = 2$	100	1.5677	1.5000	-0.0677	-4.3165%	0.1673	0.06
	400	1.5677	1.6025	0.0348	2.2219%	0.0948	0.19
	1,600	1.5677	1.6431	0.0755	4.8134%	0.0573	0.56
	6,400	1.5677	1.5311	-0.0366	-2.3330%	0.0257	2.17
	25,600	1.5677	1.5745	0.0068	0.4328%	0.0134	8.50
	102,400	1.5677	1.5743	0.0066	0.4229%	0.0068	33.77
	409,600	1.5677	1.5687	0.0011	0.0673%	0.0033	135.05
Case I, $T = 5$	100	4.5034	4.1500	-0.3534	-7.8468%	0.3880	0.11
	400	4.5034	4.3075	-0.1959	-4.3494%	0.2118	0.27
	1,600	4.5034	4.3394	-0.1640	-3.6416%	0.1026	1.06
	6,400	4.5034	4.5084	0.0051	0.1125%	0.0546	4.23
	25,600	4.5034	4.5268	0.0234	0.5202%	0.0272	16.83
	102,400	4.5034	4.5236	0.0203	0.4500%	0.0135	67.08
	409,600	4.5034	4.5037	0.0003	0.0067%	0.0068	268.24
Case II, $T = 2$	100	1.8035	1.7100	-0.0935	-5.1832%	0.21	0.11
	400	1.8035	1.7925	-0.0110	-0.6087%	0.13	0.16
	1,600	1.8035	1.7644	-0.0391	-2.1682%	0.06	0.58
	6,400	1.8035	1.7758	-0.0277	-1.5357%	0.03	2.31
	25,600	1.8035	1.8043	0.0008	0.0454%	0.02	9.31
	102,400	1.8035	1.8025	-0.0010	-0.0569%	0.01	36.07
	409,600	1.8035	1.8039	0.0004	0.0232%	0.00	145.36
Case II, $T = 5$	100	5.5817	5.2400	-0.3417	-6.1216%	0.4584	0.11
	400	5.5817	5.4000	-0.1817	-3.2550%	0.2753	0.34
	1,600	5.5817	5.6300	0.0483	0.8656%	0.1344	1.25
	6,400	5.5817	5.5902	0.0085	0.1517%	0.0698	4.99
	25,600	5.5817	5.5648	-0.0169	-0.3024%	0.0347	19.83
	102,400	5.5817	5.5777	-0.0040	-0.0713%	0.0173	77.70
	409,600	5.5817	5.5738	-0.0079	-0.1419%	0.0087	315.71

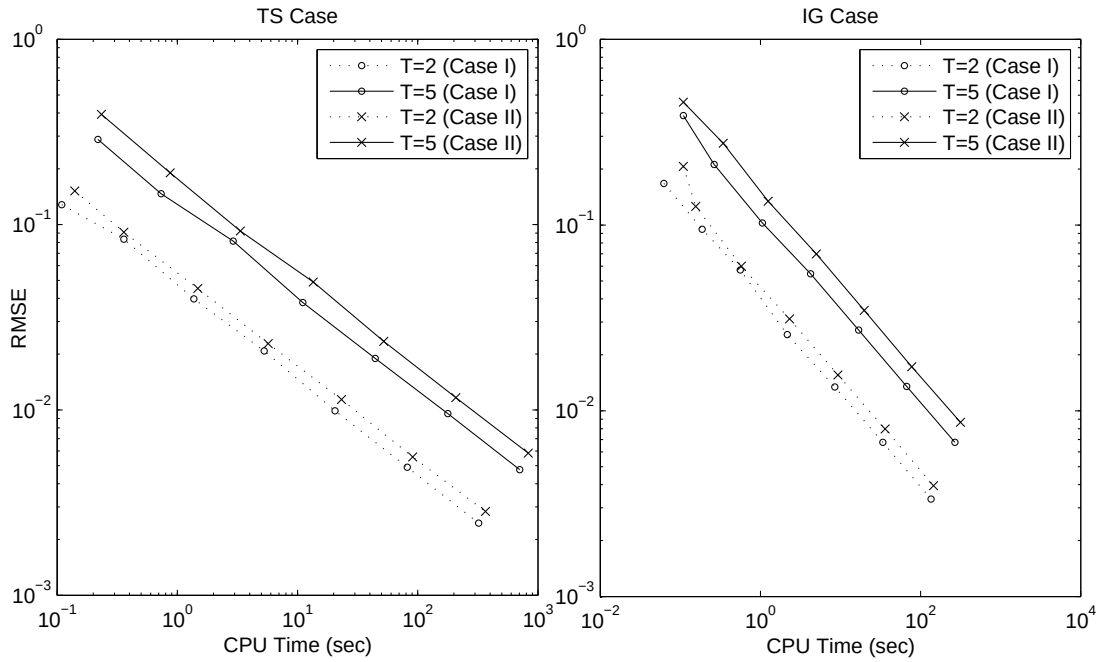

Figure 5.4: Convergence analysis via RMSE v.s. CPU time by log-log plots for Case I&II: TS Case I $(\delta, \varrho; \alpha, \beta, \theta; \lambda_0) = (1.0, 0.5; 0.25, 0.2, 0.25; 0.5)$, TS Case II $(\delta, \varrho; \alpha, \beta, \theta; \gamma; \lambda_0) = (1.0, 0.5; 0.25, 0.2, 0.25; 5.0; 0.5)$; IG Case I $(\delta, \varrho; c; \lambda_0) = (1.0, 0.5; 0.5; 0.5)$, IG Case II $(\delta, \varrho; c; \gamma; \lambda_0) = (1.0, 0.5; 0.5; 4.0; 0.5)$

Table 5.2: Comparison between the theoretical formulas and the associated simulation results for the *simplified thinning scheme* of Algorithm 5.2.2 with each estimation based on 10^5 replications

τ	$\Pr\{V^* > \tau\}$	Simulation	Error%
0.1	98.66%	98.62%	-0.0367%
0.2	94.87%	94.80%	-0.0752%
0.3	89.10%	89.01%	-0.0965%
0.4	81.85%	81.81%	-0.0499%
0.5	73.66%	73.60%	-0.0819%
0.6	65.01%	64.86%	-0.2268%
0.7	56.35%	56.12%	-0.3943%
0.8	48.00%	47.89%	-0.2333%
0.9	40.24%	40.15%	-0.2239%
1.0	33.22%	33.13%	-0.2773%

Barndorff-Nielsen and Shephard (2003a), which has become a very popular tool for modelling stochastic volatilities in a continuous-time setup. Hainaut and Devolder (2008) used it as a special case of Cox processes to model human mortality rates, and applied to actuarial valuation in insurance. Eberlein et al. (2013) treated it as a one-factor model for describing the evolution of instantaneous interest rates.

In reality, contagion may be triggered by losses or defaults of banks or other financial institutions through inter-institutional lendings in the interbank market, or, it may be further amplified due to some common asset holdings of overlapping portfolios (Caccioli et al., 2014). We offer some numerical examples of comprehensive risk analysis for a large portfolio facing contagious

defaults and losses. We construct a simple contagious loss process to capture the propagated defaults for a generic large pool of financial institutions (banks for short)[3] within a financial system. The *aggregate loss process* of this large portfolio by time t is

$$L_t = \sum_{i=1}^{N_t} L_i, \qquad t \geq 0,$$

where N_t is a Γ-*contagion process*, and $L_i \geq 0$ is the absolute value of the loss size for the i^{th} default, of which the mean is denoted by $\mu_L := \mathbb{E}[L_i]$ for any i. We assume that the sizes of self-exciting jumps in (5.1.3) generally satisfy

$$X_i = \varpi_i \times g(H_t), \tag{5.5.1}$$

where

- H_t is the history of the loss path until time t, i.e. $H_t := \{(L_i, T_i)\}_{T_i<t}$;
- $\varpi_i > 0$ is the *amplification multiplier*[4], which might be dependent on the degree of *financial connectivity* of the underlying company i to others, or, the effects of policymakers' interventions to limit the extent of contagion;
- $g(\cdot)$ is a general function of the losses.

In fact, (5.5.1) provides a channel for contagion (or feedback) effects of market participants' reactions to adverse scenarios. The economic interpretation for this model is that, the impacts and the timing of unexpected *exogenic Gamma shocks* acting on the entire portfolio as macroeconomic scenarios are modelled by a mean-reverting OU-Γ process. Each of the shocks may not lead to an immediate default but acts on the underlying intensity via a positive jump, which increases the default probability afterwards. Meanwhile, *endogenous shocks*, i.e. contagious losses due to the propagated defaults, are modelled by self-exciting jumps, and the associated magnitudes can be captured by jump sizes $\{X_i\}_{i=1,2,\ldots}$.

The great flexility of our exact simulation scheme allows us to accurately and efficiently generate highly comprehensive scenarios for risk assessment. In general, our algorithms can simulate sample paths when loss sizes L_i may depend on the entire history of N_t and λ_t before or at time T_i. We discuss several circumstances which can be captured by our models as follows.

[3]The following framework of course would generically work for other types of similar institutions.

[4]The amplification mechanisms in detail were described and analysed in Brunnermeier (2009) and Brunnermeier and Pedersen (2009).

5.5.1 A Simple Benchmark Model

The loss occurred within a financial institution may spread via various business channels and eventually trigger subsequent losses of others in markets. Intuitively, a larger loss may make a larger impact. For illustration convenience, we assume that the sizes of self-exciting jumps satisfy

$$X_i = \bar{\omega} \times L_i,$$

where $\bar{\omega} > 0$ is the *average amplification multiplier*, meaning that each investment has a linear and homogenous amplification effect. We further assume that each loss size is exponentially distributed, i.e. $L_i \sim \mathsf{Exp}(\ell)$, $\ell > 0$ with mean $\mu_L := 1/\ell$. To assess the overall risk of this portfolio, we implement the exact simulation of Algorithm 5.2.3, 5.3.1 *with* (Case I) and *without* (Case II) contagion in the fixed time period $[0, t]$, respectively:

1. *Case I*: $(\delta, \varrho; a, b; \lambda_0) = (0.5, 0.5; 0.5, 2.0; 0.5)$;

2. *Case II*: $(\delta, \varrho; a, b; \ell, \bar{\omega}; \lambda_0) = (0.5, 0.5; 0.5, 2.0; 8.0, 2.0; 0.5)$.

We concentrate on the default number N_t in the system. Case I or II can be considered as a benchmark model, as by Proposition 5.1.1 the expected default number has analytical forms:

Proposition 5.5.1 (Expectation of N_t)**.** *The expected default number until time t is given by*

$$\mathbb{E}[N_t \mid \lambda_0] = \lambda_0 \frac{1 - e^{-\eta t}}{\eta} + \frac{\varrho}{\eta} \left(t - \frac{1 - e^{-\eta t}}{\eta} \right) \frac{a}{b}, \qquad \eta \neq 0, \tag{5.5.2}$$

where

$$\eta = \begin{cases} \delta, & \text{for Case I,} \\ \delta - \bar{\omega}/\ell, & \text{for Case II.} \end{cases}$$

To explore the models, let us first carry out a sensitivity analysis for the expected default number $\mathbb{E}[N_t \mid \lambda_0]$ with respect to (w.r.t.) their key parameters for controlling the external Gamma shocks, a and b, *with* and *without* contagion, and the results are provided respectively in Figure 5.5. Numerical tests for our algorithms are based on the true means (5.5.2). The associated errors are reported by three standard measures are reported in Table 5.3. Convergence analysis via log-log plots of the RMSE against the CPU time for Case I&II and $t = 2, 5$ is presented in Figure 5.6. We can observe that, simulations are pretty fast with very tiny errors, which provides the numerical evidence of accuracy and efficiency for our algorithms.

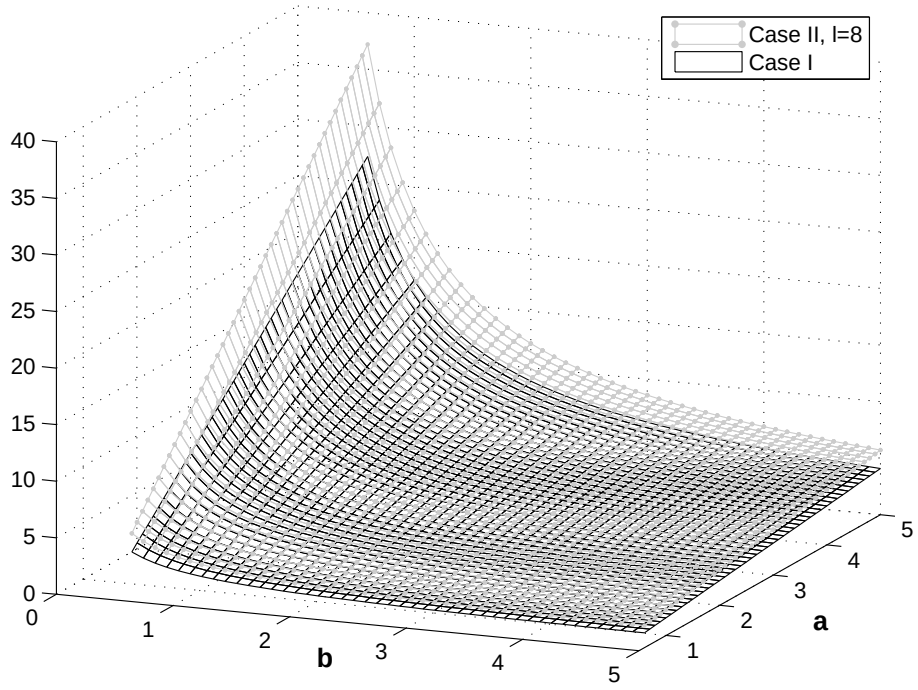

Figure 5.5: Sensitivity analysis for the expected number of defaults $\mathbb{E}[N_{t=5} \mid \lambda_0]$ w.r.t. a and b based on the parameters $(\delta, \varrho; \bar{\omega}; \lambda_0) = (0.5, 0.5; 2.0; 0.5)$

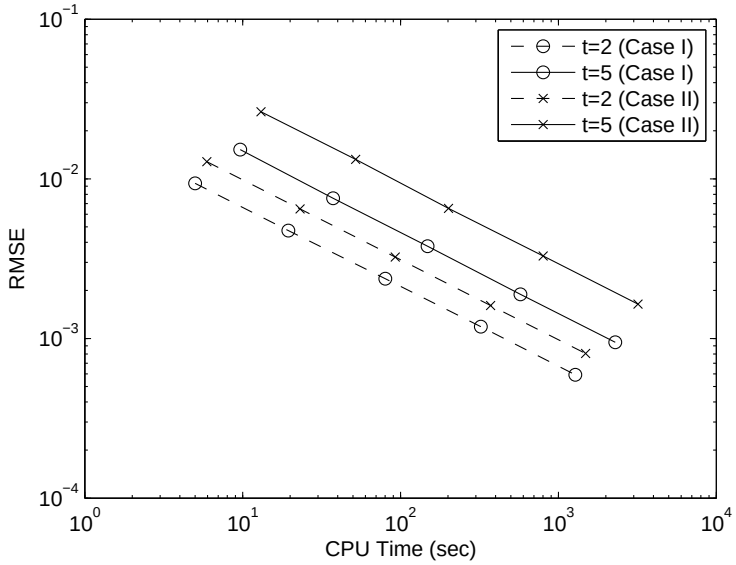

Figure 5.6: Convergence analysis via the log-log plots of the RMSE v.s. the CPU time for Case I&II and $t = 2, 5$: $(\delta, \varrho; a, b; \lambda_0) = (0.5, 0.5; 0.5, 2.0; 0.5)$ for *Case I*, and $(\delta, \varrho; a, b; \ell, \bar{\omega}; \lambda_0) = (0.5, 0.5; 0.5, 2.0; 8.0, 2.0; 0.5)$ for *Case II*

Table 5.3: Simulation results for Case I&II and time $t = 2, 5$: $(\delta, \varrho; a, b; \lambda_0) = (0.5, 0.5; 0.5, 2.0; 0.5)$ for *Case I*, and $(\delta, \varrho; a, b; \ell, \bar{\omega}; \lambda_0) = (0.5, 0.5; 0.5, 2.0; 8.0, 2.0; 0.5)$ for *Case II*

Case	Paths	True	Simulation	Error	Error%	RMSE	CPU Time (sec)
Case I, $t = 2$	10,000	0.8161	0.8154	-0.0007	-0.08%	0.0094	5.00
	40,000	0.8161	0.8151	-0.0010	-0.12%	0.0047	19.50
	160,000	0.8161	0.8135	-0.0026	-0.31%	0.0024	80.13
	640,000	0.8161	0.8159	-0.0001	-0.02%	0.0012	322.89
	2,560,000	0.8161	0.8163	0.0003	0.03%	0.0006	1,280.63
Case I, $t = 5$	10,000	1.7090	1.7297	0.0207	1.21%	0.0152	9.66
	40,000	1.7090	1.6993	-0.0097	-0.57%	0.0076	37.45
	160,000	1.7090	1.7085	-0.0004	-0.02%	0.0038	148.38
	640,000	1.7090	1.7079	-0.0010	-0.06%	0.0019	575.55
	2,560,000	1.7090	1.7083	-0.0006	-0.04%	0.0009	2,291.14
Case II, $t = 2$	10,000	1.0000	0.9983	-0.0017	-0.17%	0.0128	5.94
	40,000	1.0000	1.0054	0.0054	0.54%	0.0065	23.13
	160,000	1.0000	1.0073	0.0073	0.73%	0.0032	92.63
	640,000	1.0000	1.0000	0.0000	0.00%	0.0016	371.98
	2,560,000	1.0000	0.9995	-0.0005	-0.05%	0.0008	1,489.06
Case II, $t = 5$	10,000	2.5000	2.5060	0.0060	0.24%	0.0263	13.06
	40,000	2.5000	2.4964	-0.0036	-0.14%	0.0132	52.00
	160,000	2.5000	2.4882	-0.0118	-0.47%	0.0065	201.44
	640,000	2.5000	2.4972	-0.0028	-0.11%	0.0033	800.75
	2,560,000	2.5000	2.4983	-0.0017	-0.07%	0.0016	3,197.61

5.5.2 A Model with Contagion Threshold

In reality, each loss might not necessarily cause a contagion immediately throughout the entire system. Contagion may be only triggered when the loss surpasses a certain high level, i.e. contagion is likely to occur only in severe scenarios, which has also been reported in Elsinger et al. (2006). This circumstance could be modelled by a mixture of Case I and II, by assuming that the sizes of self-exciting jumps X_i satisfy

$$X_i = \varpi_i \times (L_i - K_i)^+, \tag{5.5.3}$$

where $K_i \geq 0$ is the *contagion threshold* (i.e. the threshold that triggers the contagion effect of the i^{th} loss L_i), and the contagion has been partially capped. When a bank is more vulnerable, its threshold is more easy to be reached. Alternatively, we may interpret K_i as a capital buffer, and it could be a certain quantile of the loss distribution L_i. If we assign the same quantile to all banks, it is equivalently meaning that, an identical economic capital applies to all banks, which is the assumption made by Elsinger et al. (2006, p.1306-1308). If the magnitude of loss overshoots the threshold, the bank may become insolvent, and this risk may then spread to other banks (through the interbank market) resulting in a climb in the default intensity of the entire system (but would not cause other banks default immediately). If the thresholds are very high comparing to the levels of losses, then, it corresponds to a "weak contagion" environment; whereas if the thresholds are very low, then, it is for a "strong contagion" environment.

Table 5.4: Quantiles of the default number $N_{t=5}$, estimated from 10^6 replications based on the parameter setting $(\delta, \varrho; a, b; \ell, \bar{\omega}; \lambda_0) = (0.5, 0.5; 0.5, 2.0; 8.0, 2.0; 0.5)$, with homogenous contagion thresholds $K = \infty, 1/8, 0$, respectively

Quantile / K	5%	25%	50%	75%	95%	Mean	Min	Max
∞	0	1	1	2	5	1.7075	0	17
1/8	0	1	2	3	5	1.9417	0	22
0	0	1	2	4	8	2.5021	0	36

Table 5.5: Quantiles of the default number $N_{t=5}$, estimated from 10^6 replications based on the parameter setting $(\delta, \varrho; a, b; \bar{\omega}; \lambda_0) = (0.5, 0.5; 0.5, 2.0; 2.0; 0.5)$, with $\ell = 8, 4, 2$, respectively

Quantile / ℓ	5%	25%	50%	75%	95%	Mean	Min	Max
8	0	1	2	4	8	2.4969	0	40
4	0	1	2	5	15	4.0628	0	130
2	0	1	4	16	73	15.5662	0	743

With the contagion threshold, contagion could be partially or fully triggered. Here for numerical illustration, we assume that, losses are exponentially distributed and the amplification multipliers and contagion thresholds are homogeneous, i.e. $L_i \sim \mathsf{Exp}(\ell)$, $a_i \equiv \bar{\omega}$ and $K_i \equiv K \geq 0$. The expected default number can hardly capture the full picture of the risk, and we have to look at the entire distribution. We choose $K = \infty, 1/8, 0$ and plot the estimated probability mass function (PMF) of the total default number within the period of $[0, t]$ in Figure 5.7, and the corresponding quantiles are reported in Table 5.4. More specifically, Cases $K = \infty, 1/8, 0$ correspond to the *non-contagion* (i.e. Case I), *partial contagion* and *full contagion* (i.e. Case II), respectively. We can clearly observe that, when K decreases, the contagion would become more pronounced and the tail of losses becomes heavier. The system could be more susceptible to contagion risk when capital buffer K is eroded, and contagion effects magnify the content of risk. As summarised by Eisenberg and Noe (2001, p.1310), bank defaults may be driven by losses from market and credit risk (i.e. fundamental default), and bank defaults may, however, also be initiated by contagion as a consequence of other bank failures in the system (i.e. contagious default). The two types of defaults, under our contagion model (i.e. the self-exciting jump sizes are not all equal to zeros), in fact, are mixed and interacting with each other.

5.5.3 A Model with Explosive Defaults

Contagion or feedback effects could be even further reinforced due to highly leveraged positions (e.g. complicated credit derivatives), and the resulting system thereby becomes explosive, see discussions on the impacts of financial innovations in Corsi et al. (2016, p.1085). This scenario would be extremely severe, rare but possible, i.e. the entire system is not stable and near the boundary of crush. Mathematically, it corresponds to the non-stationary case when $\eta < 0$ in our models. This

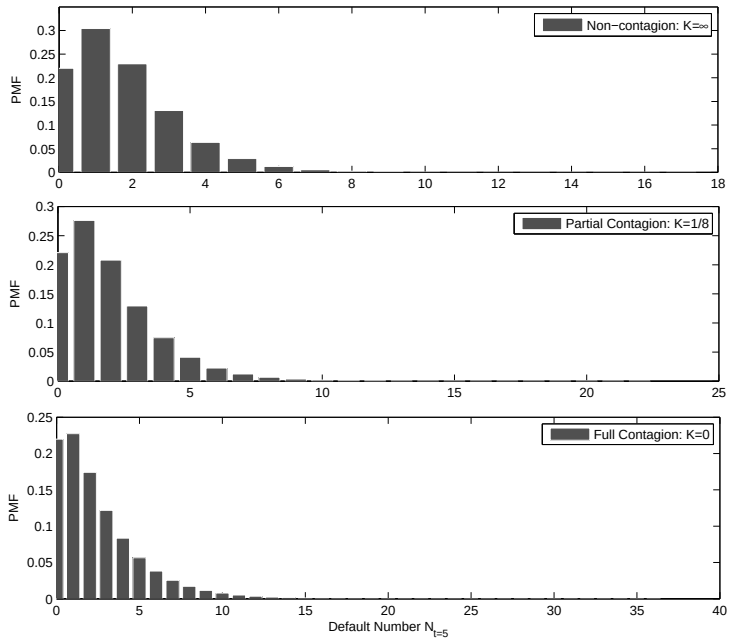

Figure 5.7: Probability mass function (PMF) of the default number $N_{t=5}$, estimated from 10^6 replications based on the parameter setting $(\delta, \varrho; a, b; \ell, \bar{\omega}; \lambda_0) = (0.5, 0.5; 0.5, 2.0; 8.0, 2.0; 0.5)$, with homogenous contagion thresholds $K = \infty, 1/8, 0$, respectively; the associated quantiles are reported in Table 5.4

may due to the "liquidity black holes" when "fire sales" of assets occur: it further depresses prices and leads to a sharp drop in liquidity and may also bring other institutions to fail in a self-reinforcing vicious spiral (Krishnamurthy, 2010; Cont and Wagalath, 2013, 2016). All previous examples were conducted under the stationary condition $\eta > 0$, and in fact our algorithms can also deal with non-stationary cases. In Figure 5.8, we offer three representative examples of $\eta = 1/4, 0, -1/2$ (or $\ell = 8, 4, 2$) for stationary, critical and explosive phases, respectively, and the associated quantiles are reported in Table 5.5. In particular, $\eta = 0$ is the critical level of stability. The resulting loss distributions could present heavy tails, which might be very desirable for many regulators and practitioners.

5.5.4 Other Models

In fact, our models and the associated algorithms could be further extended in several other directions, and we briefly discuss as follows.

- **A model with credit improvement**: In this setup, we allow for the possibility of credit improvement or relief. For example, when a big loss occurs, a rescue plan may be released such as a "bailout" or a large cash injection into the system to ensure liquidity provision. This might significantly enhance the financial system in a relatively short term, and the intensity

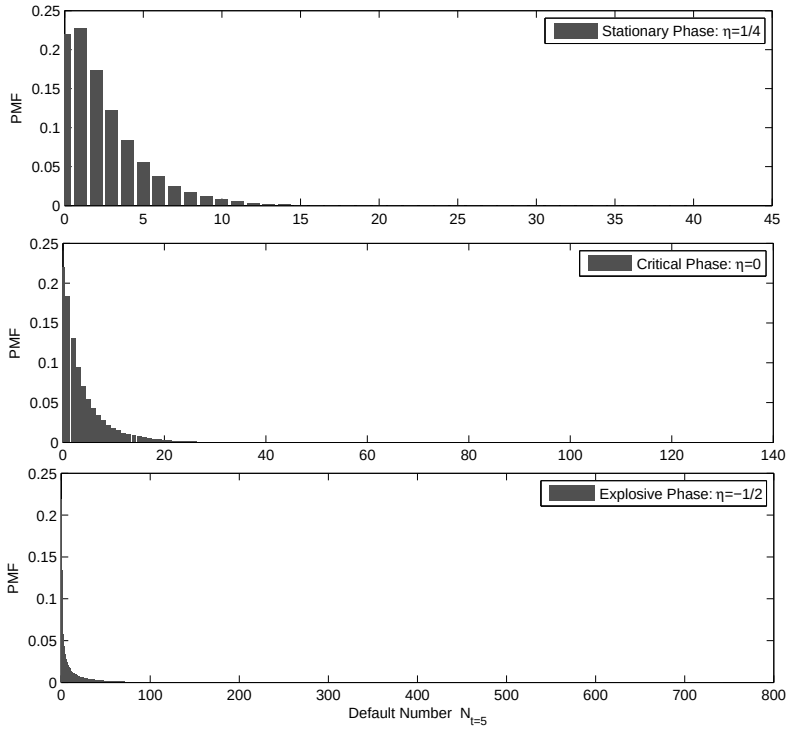

Figure 5.8: Probability mass function (PMF) of the default number $N_{t=5}$, estimated from 10^6 replications based on the parameter setting $(\delta, \varrho; a, b; \varpi; \lambda_0) = (0.5, 0.5; 0.5, 2.0; 2.0; 0.5)$, with $\ell = 8, 4, 2$, respectively; the associated quantiles are reported in Table 5.5

level may have an immediate decline instead of a climb, i.e.,

$$\lambda_{T_i} = d_i \lambda_{T_i^-}, \tag{5.5.4}$$

where $d_i > 0$ is a multiplier (which could be assumed to be a positive random variable). This model allows the intensity to jump in two sides, which can be simply generated by replacing (5.2.14) in the *Step 4* of Algorithm 5.2.3 by (5.5.4).

- **A model with structure breaks**: A severe financial failure could make a large impact to the entire economic environment. For example, the collapse of the U.S. investment banking giant Lehman Brothers in Fall 2008 marked a clear tipping point of the entire financial market around the world. This would immediately act on the default intensity process and cause a structure break for the whole financial system. To model this pattern, we have to go beyond the original definition of the underlying intensity process (5.1.2), but our algorithms still can handle it easily, i.e. after each self-exciting jump, all parameters Θ afterward can be resetted to mimic a structure break. We can assign a new parameter set Θ_i immediately after the i^{th} defaults. Θ_i could depend on the value of the size of the i^{th} self-exciting jump X_i, or, even its whole history. So, the underlying intensity process (5.1.2) should be redefined locally based

on the interarrival intensity (5.1.1) between two successive default times rather than globally throughout the positive real line $t \in \mathbb{R}^+$. Let us illustrate a simple example, say, there are two economic states after each self-exciting jump, one may correspond to a deteriorating economic environment and the other is to an improved one. We can use the parameter settings of Θ_1 and Θ_2 to model these two states respectively. We can choose one to be stable (i.e. stationary case $\eta > 0$) and the other to be unstable (i.e. non-stationary case $\eta > 0$). Then, the entire system could shift between *locally stable* and *locally explosive* phases. Analysis for contagion risk based on the stability of branching processes and allowing for a shift between two phases can also be found in Caccioli et al. (2014) and Corsi et al. (2016).

- **A model with multiple exogenous risk drivers**: In practice, there may be multiple risk factors, such as sector-wide or market-wide events, commonly shared by all institutions. Multi-factor models then are required for modelling intensity processes, see e.g. Duffie and Gârleanu (2001), Das et al. (2007) and Longstaff and Rajan (2008). We could use a superposition of OU intensity processes driven by different Gamma processes to capture the corresponding multiple risk factors[5]. Accordingly, our algorithms may be extendable to this version by using the *superposition theory* of point processes (Daley and Vere-Jones, 2003, Theorem 2.4.VI).

- **A model with multilateral contagion**: Contagion not only occurs within one market (or system, network) but could also spread across different markets. For example, when the loss contagion and investors' fears occur in the options market, it may also spread to the market of the underlying equity or futures on which the options are written. This type of contagion can be captured by adding *mutually-exciting* jumps. Similar as the multivariate Hawkes process, a multi-dimensional Γ-contagion process has to be developed to capture self-contagion effects for each individual, as well as the mutual contagion effects among them.

5.6 Conclusion

In this chapter, we have introduced a new family of self-exciting jump processes whose intensities are driven by Lévy driven OU processes, namely, Lévy driven contagion processes. Backed by the very large family of Lévy subordinators, it indeed offers much richer choices beyond the classical Hawkes process for modelling the contagion of event arrivals in a continuous-time setup in finance, economics and many other fields. We have derived some important distributional proper-

[5]Similarly, the superposition of OU stochastic volatility processes was proposed in Barndorff-Nielsen (2001) and Barndorff-Nielsen and Shephard (2001b, 2002).

ties of these new processes which lead to an exact simulation framework in general. In particular, we have developed exact simulation algorithms by decomposition approach for the Gamma and tempered stable cases as typical examples. The algorithms are accurate and efficient which have been numerically verified and tested by extensive numerical experiments. We also provide applications to portfolio risk management, which again illustrate the efficiency, accuracy, applicability and flexibility of our algorithms. As a class of reduced-form models, it could be easily extended to pricing financial derivatives, particularly multiple-name credit products (e.g. collateralized debt obligations and mortgage-backed securities). It can be employed empirically when input data is available for parameter calibration. Furthermore, it could be widely applied to many other areas, for example, to describe high-frequency trading data in market microstructure, or claim arrivals for an insurance portfolio. Their statistical inference and econometric analysis for this new framework, and further extensions to multidimensional point processes for modelling multilateral contagion, as well as further applications and empirical work for portfolio credit risk analysis, could be very interesting and meaningful topics for future research.

References

Abate, J. and Whitt, W. (1992). The Fourier-series method for inverting transforms of probability distributions. *Queueing Systems*, **10**(1-2):5–87.

Abate, J. and Whitt, W. (1995). Numerical inversion of Laplace transforms of probability distributions. *ORSA Journal on Computing*, **7**(1):36–43.

Abate, J. and Whitt, W. (2006). A unified framework for numerically inverting Laplace transforms. *INFORMS Journal on Computing*, **18**(4):408–421.

Aït-Sahalia, Y., Cacho-Diaz, J., and Laeven, R. J. (2015). Modeling financial contagion using mutually exciting jump processes. *Journal of Financial Economics*, **117**(3):585–606.

Aït-Sahalia, Y. and Jacod, J. (2009). Estimating the degree of activity of jumps in high frequency data. *The Annals of Statistics*, **37**(5A):2202–2244.

Aït-Sahalia, Y. and Jacod, J. (2011). Testing whether jumps have finite or infinite activity. *The Annals of Statistics*, **39**(3):1689–1719.

Aït-Sahalia, Y., Laeven, R. J., and Pelizzon, L. (2014). Mutual excitation in Eurozone sovereign CDS. *Journal of Econometrics*, **183**(2):151–167.

Andrieu, C., Doucet, A., and Holenstein, R. (2010). Particle Markov chain Monte Carlo methods. *Journal of the Royal Statistical Society: Series B (Statistical Methodology)*, **72**(3):269–342.

Arratia, R. (1998). On the central role of scale invariant Poisson processes on $(0,\infty)$. *Microsurveys in discrete probability (Princeton, NJ, 1997)*, pages 21–41.

Asmussen, S. and Glynn, P. W. (2007). *Stochastic Simulation: Algorithms and Analysis*. Springer.

Azizpour, S., Giesecke, K., and Schwenkler, G. (2018). Exploring the sources of default clustering. *Journal of Financial Economics*, **129**(1):154–183.

Bacry, E., Delattre, S., Hoffmann, M., and Muzy, J.-F. (2013). Modelling microstructure noise with mutually exciting point processes. *Quantitative Finance*, **13**(1):65–77.

Barndorff-Nielsen, O. and Shephard, N. (2001a). Modelling by Lévy processess for financial econometrics. In *Lévy Processes*, pages 283–318. Birkhäuser, Boston, MA.

Barndorff-Nielsen, O. E. (1997). Normal inverse Gaussian distributions and stochastic volatility modelling. *Scandinavian Journal of Statistics*, **24**(1):1–13.

Barndorff-Nielsen, O. E. (1998). Processes of normal inverse Gaussian type. *Finance and Stochastics*, **2**(1):41–68.

Barndorff-Nielsen, O. E. (2001). Superposition of Ornstein-Uhlenbeck type processes. *Theory of Probability & Its Applications*, **45**(2):175–194.

Barndorff-Nielsen, O. E., Jensen, J. L., and Sørensen, M. (1998). Some stationary processes in discrete and continuous time. *Advances in Applied Probability*, **30**(4):989–1007.

Barndorff-Nielsen, O. E., Mikosch, T., and Resnick, S. I. (2012). *Lévy Processes: Theory and Applications*. Springer Science & Business Media.

Barndorff-Nielsen, O. E., Nicolato, E., and Shephard, N. (2002). Some recent developments in stochastic volatility modelling. *Quantitative Finance*, **2**(1):11–23.

Barndorff-Nielsen, O. E. and Shephard, N. (2001b). Non-Gaussian Ornstein-Uhlenbeck-based models and some of their uses in financial economics. *Journal of the Royal Statistical Society: Series B (Statistical Methodology)*, **63**(2):167–241.

Barndorff-Nielsen, O. E. and Shephard, N. (2001c). Normal modified stable processes. *Theory of Probability and Mathematical Statistics*, pages 1–19.

Barndorff-Nielsen, O. E. and Shephard, N. (2002). Econometric analysis of realized volatility and its use in estimating stochastic volatility models. *Journal of the Royal Statistical Society: Series B (Statistical Methodology)*, **64**(2):253–280.

Barndorff-Nielsen, O. E. and Shephard, N. (2003a). Integrated OU processes and non-Gaussian OU-based stochastic volatility models. *Scandinavian Journal of Statistics*, **30**(2):277–295.

Barndorff-Nielsen, O. E. and Shephard, N. (2003b). Realized power variation and stochastic volatility models. *Bernoulli*, **9**(2):243–265.

Bertoin, J. (1998). *Lévy Processes*. Cambridge University Press.

Bianchi, M. L. and Fabozzi, F. J. (2015). Investigating the performance of non-Gaussian stochastic intensity models in the calibration of credit default swap spreads. *Computational Economics*, **46**(2):243–273.

Bowsher, C. G. (2007). Modelling security market events in continuous time: Intensity based, multivariate point process models. *Journal of Econometrics*, **141**(2):876–912.

Brémaud, P. and Massoulié, L. (1996). Stability of nonlinear Hawkes processes. *The Annals of Probability*, **24**(3):1563–1588.

Brémaud, P. and Massoulié, L. (2002). Power spectra of general shot noises and Hawkes point processes with a random excitation. *Advances in Applied Probability*, **34**(1):205–222.

Brix, A. (1999). Generalized gamma measures and shot-noise Cox processes. *Advances in Applied Probability*, **31**(4):929–953.

Broadie, M. and Kaya, Ö. (2006). Exact simulation of stochastic volatility and other affine jump diffusion processes. *Operations Research*, **54**(2):217–231.

Brockwell, P. J., Davis, R. A., and Yang, Y. (2007). Estimation for nonnegative Lévy-driven Ornstein-Uhlenbeck processes. *Journal of Applied Probability*, **44**(4):977–989.

Brunnermeier, M. K. (2009). Deciphering the liquidity and credit crunch 2007–2008. *The Journal of Economic Perspectives*, **23**(1):77–100.

Brunnermeier, M. K. and Pedersen, L. H. (2009). Market liquidity and funding liquidity. *The Review of Financial Studies*, **22**(6):2201–2238.

Caccioli, F., Shrestha, M., Moore, C., and Farmer, J. D. (2014). Stability analysis of financial contagion due to overlapping portfolios. *Journal of Banking & Finance*, **46**:233–245.

Cai, N., Song, Y., and Chen, N. (2017). Exact simulation of the SABR model. *Operations Research*, **65**(4):931–951.

Caravenna, F., Sun, R., and Zygouras, N. (2018). The dickman subordinator, renewal theorems, and disordered systems. Working Paper.

Carr, P., Geman, H., Madan, D. B., and Yor, M. (2002). The fine structure of asset returns: An empirical investigation. *The Journal of Business*, **75**(2):305–332.

Carr, P., Geman, H., Madan, D. B., and Yor, M. (2003). Stochastic volatility for Lévy processes. *Mathematical Finance*, **13**(3):345–382.

Cartea, Á. and Jaimungal, S. (2016). A closed-form execution strategy to target volume weighted average price. *SIAM Journal on Financial Mathematics*, **7**(1):760–785.

Cartea, Á., Jaimungal, S., and Penalva, J. (2015). *Algorithmic and High-Frequency Trading*. Cambridge University Press.

Centanni, S. and Minozzo, M. (2006). A Monte Carlo approach to filtering for a class of marked doubly stochastic Poisson processes. *Journal of the American Statistical Association*, **101**(476):1582–1597.

Chandrasekhar, S. and Münch, G. (1950). The theory of the fluctuations in brightness of the milky way, i and ii. *Astrophysical Journal*, **112**:380–398.

Chen, N. and Huang, Z. (2013). Localization and exact simulation of Brownian motion-driven stochastic differential equations. *Mathematics of Operations Research*, **38**(3):591–616.

Chen, Z., Feng, L., and Lin, X. (2012). Simulating Lévy processes from their characteristic functions and financial applications. *ACM Transactions on Modeling and Computer Simulation*, **22**(3):14:1–14:26.

Chhikara, R. and Folks, L. (1988). *The Inverse Gaussian Distribution: Theory, Methodology, and Applications*. CRC Press.

Chi, Z. (2012). On exact sampling of nonnegative infinitely divisible random variables. *Advances in Applied Probability*, **44**(3):842–873.

Cloud, K. and Huber, M. (2017). Fast perfect simulation of vervaat perpetuities. *Journal of Complexity*, **42**:19–30.

Cont, R. (2001). Empirical properties of asset returns: stylized facts and statistical issues. *Quantitative Finance*, **1**(2):223–236.

Cont, R. and Tankov, P. (2004). *Financial Modelling with Jump Processes*. CRC Press.

Cont, R. and Wagalath, L. (2013). Running for the exit: distressed selling and endogenous correlation in financial markets. *Mathematical Finance*, **23**(4):718–741.

Cont, R. and Wagalath, L. (2016). Fire sales forensics: measuring endogenous risk. *Mathematical Finance*, **26**(4):835–866.

Corsi, F., Marmi, S., and Lillo, F. (2016). When micro prudence increases macro risk: The destabilizing effects of financial innovation, leverage, and diversification. *Operations Research*, **64**(5):1073–1088.

Cox, D. R. (1955). Some statistical methods connected with series of events. *Journal of the Royal Statistical Society. Series B (Methodological)*, **17**(2):129–157.

Cox, D. R. (1972). Regression models and life-tables. *Journal of the Royal Statistical Society. Series B (Methodological)*, **34**(2):187–220.

Crane, R. and Sornette, D. (2008). Robust dynamic classes revealed by measuring the response function of a social system. *Proceedings of the National Academy of Sciences*, **105**(41):15649–15653.

Creal, D. D. (2008). Analysis of filtering and smoothing algorithms for Lévy-driven stochastic volatility models. *Computational Statistics & Data Analysis*, **52**(6):2863–2876.

CreditRisk$^+$ (1997). *CreditRisk$^+$: A Credit Risk Management Framework*. Credit Suisse First Boston International.

Daley, D. J. and Vere-Jones, D. (2003). *An Introduction to the Theory of Point Processes: Volume I: Elementary Theory and Methods*. Springer.

Das, S. R., Duffie, D., Kapadia, N., and Saita, L. (2007). Common failings: How corporate defaults are correlated. *The Journal of Finance*, **62**(1):93–117.

Dassios, A. and Embrechts, P. (1989). Martingales and insurance risk. *Communications in Statistics. Stochastic Models*, **5**(2):181–217.

Dassios, A. and Jang, J. (2003). Pricing of catastrophe reinsurance and derivatives using the Cox process with shot noise intensity. *Finance and Stochastics*, **7**(1):73–95.

Dassios, A. and Lim, J. W. (2018). An efficient algorithm for simulating the drawdown stopping time and the running maximum of a brownian motion. *Methodology and Computing in Applied Probability*, **20**(1):189–204.

Dassios, A., Lim, J. W., and Qu, Y. (2018a). Azéma martingales for bessel and cir processes and the pricing of parisian zero-coupon bonds. Working Paper, London School of Economics.

Dassios, A., Qu, Y., and Lim, J. W. (2019). Exact simulation of generalised vervaat perpetuities. *Journal of Applied Probability*, **56**(1):57–75.

Dassios, A., Qu, Y., and Zhao, H. (2018b). Exact simulation for a class of tempered stable and related distributions. *ACM Transactions on Modeling and Computer Simulation*, **28**(3):20:1–20:21.

Dassios, A. and Zhao, H. (2011). A dynamic contagion process. *Advances in Applied Probability*, **43**(3):814–846.

Dassios, A. and Zhao, H. (2017). A generalised contagion process with an application to credit risk. *International Journal of Theoretical and Applied Finance*, **20**(1):1–33.

Davis, M. H. (1984). Piecewise-deterministic Markov processes: A general class of non-diffusion stochastic models. *Journal of the Royal Statistical Society. Series B (Methodological)*, **46**(3):353–388.

De Bruijn, N. (1951). The asymptotic behaviour of a function occuring in the theory of primes. *The Journal of the Indian Mathematical Society*, **15**:25–32.

Devroye, L. (2001). Simulating perpetuities. *Methodology and Computing in Applied Probability*, **3**(1):97–115.

Devroye, L. (2009). Random variate generation for exponentially and polynomially tilted stable distributions. *ACM Transactions on Modeling and Computer Simulation*, **19**(4):1–20.

Devroye, L. and Fawzi, O. (2010). Simulating the Dickman distribution. *Statistics & Probability Letters*, **80**(3):242–247.

Dickman, K. (1930). On the frequency of numbers containing prime factors of a certain relative magnitude. *Arkiv for Matematik, Astronomi och Fysik*, **22**(10):1–14.

Duffie, D., Eckner, A., Horel, G., and Saita, L. (2009). Frailty correlated default. *The Journal of Finance*, **64**(5):2089–2123.

Duffie, D., Filipovic, D., and Schachermayer, W. (2003). Affine processes and applications in finance. *The Annals of Applied Probability*, **13**(3):984–1053.

Duffie, D. and Gârleanu, N. (2001). Risk and valuation of Collateralized Debt Obligations. *Financial Analysts Journal*, **57**(1):41–59.

Easley, D. and O'Hara, M. (1987). Price, trade size, and information in securities markets. *Journal of Financial Economics*, **19**(1):69–90.

Eberlein, E., Madan, D., Pistorius, M., and Yor, M. (2013). A simple stochastic rate model for rate equity hybrid products. *Applied Mathematical Finance*, **20**(5):461–488.

Eisenberg, L. and Noe, T. H. (2001). Systemic risk in financial systems. *Management Science*, **47**(2):236–249.

Elsinger, H., Lehar, A., and Summer, M. (2006). Risk assessment for banking systems. *Management Science*, **52**(9):1301–1314.

Embrechts, P. and Goldie, C. M. (1994). Perpetuities and random equations. *Asymptotic statistics*, pages 75–86.

Embrechts, P., Klüppelberg, C., and Mikosch, T. (1996). *Modelling Extremal Events*. Springer-Verlag.

Embrechts, P., Liniger, T., and Lin, L. (2011). Multivariate Hawkes processes: an application to financial data. *Journal of Applied Probability*, **48A**:367–378.

Engle, R. F. and Russell, J. R. (1998). Autoregressive conditional duration: A new model for irregularly spaced transaction data. *Econometrica*, **66**(5):1127–1162.

Errais, E., Giesecke, K., and Goldberg, L. R. (2010). Affine point processes and portfolio credit risk. *SIAM Journal on Financial Mathematics*, **1**(1):642–665.

Fill, J. and Huber, M. (2010). Perfect simulation of Vervaat perpetuities. *Electronic Journal of Probability*, **15**:96–109.

Frühwirth-Schnatter, S. and Sögner, L. (2009). Bayesian estimation of stochastic volatility models based on OU processes with marginal Gamma law. *Annals of the Institute of Statistical Mathematics*, **61**(1):159–179.

Gander, M. P. and Stephens, D. A. (2007a). Simulation and inference for stochastic volatility models driven by Lévy processes. *Biometrika*, **94**(3):627–646.

Gander, M. P. and Stephens, D. A. (2007b). Stochastic volatility modelling in continuous time with general marginal distributions: Inference, prediction and model selection. *Journal of Statistical Planning and Inference*, **137**(10):3068–3081.

Gaver, J. D. P. (1966). Observing stochastic processes, and approximate transform inversion. *Operations Research*, **14**(3):444–459.

Gençay, R., Dacorogna, M., Muller, U. A., Pictet, O., and Olsen, R. (2001). *An Introduction to High-frequency Finance*. Academic Press.

Giesecke, K., Longstaff, F. A., Schaefer, S., and Strebulaev, I. (2011). Corporate bond default risk: A 150-year perspective. *Journal of Financial Economics*, **102**(2):233–250.

Glasserman, P. and Liu, Z. (2010). Sensitivity estimates from characteristic functions. *Operations Research*, **58**(6):1611–1623.

Goldie, C. M. and Grübel, R. (1996). Perpetuities with thin tails. *Advances in Applied Probability*, **28**(2):463–480.

Gordy, M. B. (2000). A comparative anatomy of credit risk models. *Journal of Banking & Finance*, **24**(1):119–149.

Gordy, M. B. (2003). A risk-factor model foundation for ratings-based bank capital rules. *Journal of Financial Intermediation*, **12**(3):199–232.

Granelli, A. and Veraart, A. E. D. (2016). Modeling the variance risk premium of equity indices: The role of dependence and contagion. *SIAM Journal on Financial Mathematics*, **7**(1):382–417.

Griffin, J. E. and Steel, M. F. (2006). Inference with non-Gaussian Ornstein–Uhlenbeck processes for stochastic volatility. *Journal of Econometrics*, **134**(2):605–644.

Grübel, R. and Rösler, U. (1996). Asymptotic distribution theory for Hoare's selection algorithm. *Advances in Applied Probability*, **28**(1):252–269.

Hainaut, D. and Devolder, P. (2008). Mortality modelling with Lévy processes. *Insurance: Mathematics and Economics*, **42**(1):409–418.

Hawkes, A. G. (1971a). Point spectra of some mutually exciting point processes. *Journal of the Royal Statistical Society. Series B (Methodological)*, **33**(3):438–443.

Hawkes, A. G. (1971b). Spectra of some self-exciting and mutually exciting point processes. *Biometrika*, **58**(1):83–90.

Hawkes, A. G. and Oakes, D. (1974). A cluster process representation of a self-exciting process. *Journal of Applied Probability*, **11**(3):493–503.

Hofert, M. (2011a). Efficiently sampling nested Archimedean copulas. *Computational Statistics & Data Analysis*, **55**(1):57–70.

Hofert, M. (2011b). Sampling exponentially tilted stable distributions. *ACM Transactions on Modeling and Computer Simulation*, **22**(1):1–11.

Hougaard, P. (1986). Survival models for heterogeneous populations derived from stable distributions. *Biometrika*, **73**(2):387–396.

Jongbloed, G., Van Der Meulen, F. H., and Van Der Vaart, A. W. (2005). Nonparametric inference for Lévy-driven Ornstein-Uhlenbeck processes. *Bernoulli*, **11**(5):759–791.

Kallsen, J., Muhle-Karbe, J., and Voß, M. (2011). Pricing options on variance in affine stochastic volatility models. *Mathematical Finance*, **21**(4):627–641.

Kang, C., Kang, W., and Lee, J. M. (2017). Exact simulation of the wishart multidimensional stochastic volatility model. *Operations Research*, **65**(5):1190–1206.

Kanter, M. (1975). Stable densities under change of scale and total variation inequalities. *The Annals of Probability*, **3**(4):697–707.

Krishnamurthy, A. (2010). How debt markets have malfunctioned in the crisis. *Journal of Economic Perspectives*, **24**(1):3–28.

Kyprianou, A. (2006). *Introductory Lectures on Fluctuations of Lévy Processes with Applications*. Springer.

Large, J. (2007). Measuring the resiliency of an electronic limit order book. *Journal of Financial Markets*, **10**(1):1–25.

Lewis, P. A. and Shedler, G. S. (1979). Simulation of nonhomogeneous Poisson processes by thinning. *Naval Research Logistics Quarterly*, **26**(3):403–413.

Li, L. and Linetsky, V. (2013). Optimal stopping and early exercise: an eigenfunction expansion approach. *Operations Research*, **61**(3):625–643.

Li, L. and Linetsky, V. (2014). Time-changed Ornstein-Uhlenbeck processes and their applications in commodity derivative models. *Mathematical Finance*, **24**(2):289–330.

Li, L. and Linetsky, V. (2015). Discretely monitored first passage problems and barrier options: an eigenfunction expansion approach. *Finance and Stochastics*, **19**(4):941–977.

Longstaff, F. A. and Rajan, A. (2008). An empirical analysis of the pricing of collateralized debt obligations. *The Journal of Finance*, **63**(2):529–563.

Lukacs, E. (1969). A characterization of stable processes. *Journal of Applied Probability*, **6**(2):409–418.

Madan, D., Carr, P., and Chang, E. (1998). The variance gamma process and option pricing. *European Finance Review*, **2**(1):79–105.

Madan, D. and Seneta, E. (1990). The variance gamma (V.G.) model for share market returns. *Journal of Business*, **63**(4):511–524.

Mahmoud, H., Modarres, R., and Smythe, R. (1995). Analysis of quickselect: An algorithm for order statistics. *RAIRO - Theoretical Informatics and Applications*, **29**(4):255–276.

Mendoza-Arriaga, R. and Linetsky, V. (2014). Time-changed CIR default intensities with two-sided mean-reverting jumps. *The Annals of Applied Probability*, **24**(2):811–856.

Mendoza-Arriaga, R. and Linetsky, V. (2016). Multivariate subordination of Markov processes with financial applications. *Mathematical Finance*, **26**(4):699–747.

Michael, J. R., Schucany, W. R., and Haas, R. W. (1976). Generating random variates using transformations with multiple roots. *The American Statistician*, **30**(2):88–90.

Nicolato, E. and Venardos, E. (2003). Option pricing in stochastic volatility models of the Ornstein-Uhlenbeck type. *Mathematical Finance*, **13**(4):445–466.

Norberg, R. (2004). Vasiček beyond the normal. *Mathematical Finance*, **14**(4):585–604.

Novikov, A. (2004). Martingales and first-passage times for ornstein–uhlenbeck processes with a jump component. *Theory of Probability & Its Applications*, **48**(2):288–303.

Nyrhinen, H. (2001). Finite and infinite time ruin probabilities in a stochastic economics environment. *Stochastic Processes and their Applications*, **92**(2):265–285.

Ornthanalai, C. (2014). Lévy jump risk: Evidence from options and returns. *Journal of Financial Economics*, **112**(1):69–90.

Patie, P. (2005). On a martingale associated to generalized ornstein–uhlenbeck processes and an application to finance. *Stochastic processes and their applications*, **115**(4):593–607.

Penrose, M. D. and Wade, A. R. (2004). Random minimal directed spanning trees and Dickman-type distributions. *Advances in Applied Probability*, **36**(3):691–714.

Poterba, J. M. and Summers, L. H. (1988). Mean reversion in stock prices: Evidence and implications. *Journal of Financial Economics*, **22**(1):27–59.

Qu, Y., Dassios, A., and Zhao, H. (2019). Efficient simulation of lévy driven point processes. *Advances in Applied Probability*, **51**(4).

Roberts, G. O., Papaspiliopoulos, O., and Dellaportas, P. (2004). Bayesian inference for non-Gaussian Ornstein-Uhlenbeck stochastic volatility processes. *Journal of the Royal Statistical Society: Series B (Statistical Methodology)*, **66**(2):369–393.

Rydberg, T. H. and Shephard, N. (2000). A modelling framework for the prices and times of trades made on the New York stock exchange. In *Nonlinear and Nonstationary Signal Processing*. Cambridge University Press.

Sato, K. (1999). *Lévy Processes and Infinitely Divisible Distributions*. Cambridge University Press.

Sato, K. and Yamazato, M. (1984). Operator-selfdecomposable distributions as limit distributions of processes of Ornstein-Uhlenbeck type. *Stochastic Processes and their Applications*, **17**(1):73–100.

Schoutens, W. (2003). *Lévy Processes in Finance: Pricing Financial Derivatives*. Wiley.

Schoutens, W. and Cariboni, J. (2010). *Lévy Processes in Credit Risk*. John Wiley & Sons.

Stehfest, H. (1970). Algorithm 368: Numerical inversion of Laplace transforms. *Communications of the ACM*, **13**(1):47–49.

Takács, L. (1954). On secondary processes generated by a Poisson process and their applications in physics. *Acta Mathematica Hungarica*, **5**(3-4):203–236.

Takács, L. (1955). On stochastic processes generated by a Poisson process and their applications in physics. *Acta Mathematica Hungarica*, **6**:363–380.

Todorov, V. (2015). Jump activity estimation for pure-jump semimartingales via self-normalized statistics. *The Annals of Statistics*, **43**(4):1831–1864.

Todorov, V. and Tauchen, G. (2006). Simulation methods for Lévy-driven continuous-time autoregressive moving average (CARMA) stochastic volatility models. *Journal of Business & Economic Statistics*, **24**(4):455–469.

Tweedie, M. (1984). An index which distinguishes between some important exponential families. In *Statistics: Applications and New Directions: Proceedings of the Indian Statistical Institute Golden Jubilee International Conference*, pages 579–604.

Uhlenbeck, G. E. and Ornstein, L. S. (1930). On the theory of the Brownian motion. *Physical Review*, **36**(5):823.

Vervaat, W. (1979). On a stochastic difference equation and a representation of non–negative infinitely divisible random variables. *Advances in Applied Probability*, **11**(4):750–783.

Wolfe, S. J. (1982). On a continuous analogue of the stochastic difference equation $x_n = \rho x_{n-1} + b_n$. *Stochastic Processes and their Applications*, **12**(3):301–312.

Zolotarev, V. M. (1964). On the representation of stable laws by integrals. *Trudy Matematicheskogo Instituta imeni VA Steklova*, **71**:46–50.

Zolotarev, V. M. (1986). *One-dimensional Stable Distributions*. American Mathematical Society.